

# **New Ways of Representing Finite Element Results of Shell Structures**

## **Final Report**

Master Graduation Thesis

Commissioner: Delft University of Technology  
Faculty of Civil Engineering and Geo Sciences  
Department of Building and Infra Structure  
Section of Structural Mechanics

Graduate: Paul Schuddeboom  
Student ID: 1394940

Place: Delft  
Date: Thursday, 20 November 2014



**University**

Delft University of Technology  
Faculty of Civil Engineering and Geosciences  
Department of Structural Engineering  
Section of Structural Mechanics

**Visiting address**

Delft University of Technology  
Faculty Civil Engineering and Geosciences  
Stevinweg 1  
2628 CN Delft

**Graduation committee**

Prof. dr. ir. J.G. Rots	CITG, Structural Engineering, Structural Mechanics
Dr. ir. M.A.N. Hendriks	CiTG, Structural Engineering, Structural Mechanics
Dr. ir. P.C.J. Hoogenboom	CiTG, Structural Engineering, Structural Mechanics
Ir. A. Borgart	BK, Architectural Engineering and Technology, Structural Mechanics

**Graduate**

P.D. Schuddeboom  
Bekkumerstraat 36  
7416 ZP Deventer

P.D.Schuddeboom@gmail.com





## ACKNOWLEDGEMENTS

This report is the final product of my graduation thesis at Delft University of Technology regarding the research into new ways of representing finite element results of shell structures. It gives an overview of the activities and results obtained during this graduation project.

I hereby would like to thank the graduation project committee for their guidance during this graduation thesis, for their joined thinking, their discussions during the committee meetings and over the e-mail, their quick responses to my questions and all their other contributions to this graduation thesis.

I especially would like to thank dr. ir. P.C.J. Hoogenboom for all the time he made available for our extended discussions over all of the topics regarding this graduation thesis and for setting up this graduation thesis's main topic with me in the first place.

I also would like to thank Kesio Palacio and Maziar Partovi, co-workers of TNO DIANA, for their quick and elaborate responses during the development of a user supplied subroutine in order to create a post processing tool for the DIANA Finite Element Analysis computer program and for optimising some shell analysis models.

Furthermore I would like to thank my parents for their support and their interest shown during both my graduation thesis and the previous years studying leading up to this point.

Finally I would like to thank my girlfriend, Sanne van Aken, for her support, her motivation and her patience during this graduation thesis. Thank you for keeping asking the right questions and helping me to maintain an overview of this whole graduation thesis when I found myself lost again in some "very important" details.

Paul Schuddeboom  
Deventer, 20 November 2014



## SUMMARY

The Finite Element Method is used in many computer programs to analyse the mechanical behaviour of shell structures. Although this method provides good quantitative insight into the mechanical behaviour of shell structures, it provides little qualitative insight. This master graduation thesis is aimed at expanding Finite Element Analysis (FEA) programs in order to obtain better insight in the qualitative aspect of the mechanical behaviour of shell structures.

A FEA-program can compute and display forces, stresses, strains and displacements in a structure due to a prescribed load or displacement. Based on these quantities (i.e. forces, stresses, strains and displacements), five new quantities have been computed and researched during this thesis. These new quantities are aimed at increasing the insight in the qualitative aspect of the mechanical behaviour of shell structures.

Four shell structures have been modelled in the 3D modelling software package Rhinoceros. The FEA-program TNO DIANA has then been used to obtain the required quantities for computing the five new quantities. This computation of the new quantities has been done with the aid of a self-made post processing tool. This tool has been developed in the Rhinoceros plug-in Grasshopper so that Rhinoceros is also used for displaying the analysis results.

As it turned out, two quantities in particular produced good results. These are the strain energy and the buckling load factor. Strain energy is the energy that is stored in a structure when it deforms due to a load. The buckling load factor is the ratio between the occurring normal forces in a shell structure and the normal force that will cause the shell to fail by buckling. With the aid of strain energy it turned out to be possible to show whether a shell structure is displaying shell or plate behaviour. Furthermore, strain energy combines forces and deformations in all directions, resulting in a single display of analysis results with which a shell structure can be assessed. The buckling load factor shows where and to what extent a shell structure is most likely to buckle.

With the self-made post processing tool it is also possible to display the steepest descends in every part of a shell structure. This provides the tool with opportunities for implementation of the Rain Flow Analogy. The Rain Flow analogy is an alternative method that shows how forces are transferred throughout a shell structure.

Based on the results above it is proposed to implement the strain energy and the buckling load factor in existing FEA-programs. These quantities allow for the design and development of better shell structures by increasing the insight in the mechanical behaviour of these structures.



## SAMENVATTING

De eindige-elementenmethode wordt in veel computerprogramma's gebruikt voor het analyseren van het mechanische gedrag van schaalconstructies. Hoewel deze methode goed kwantitatief inzicht geeft in het mechanische gedrag biedt deze methode minder inzicht in de kwalitatieve aspecten van dit gedrag. Dit afstudeeronderzoek is gericht op het uitbreiden van eindige-elementen-programma's om zo hiermee beter inzicht te krijgen in het kwalitatieve aspect van het mechanische gedrag van schaalconstructies.

Als gevolg van een belasting ontstaan er krachten, spanningen, rekken en verplaatsingen in een constructie die met behulp van een eindig-elementenprogramma kunnen worden berekend en zichtbaar gemaakt. Op basis van deze zogeheten grootheden zijn gedurende dit afstudeeronderzoek vijf nieuwe grootheden berekend en onderzocht die meer gericht zijn op het inzichtelijk maken van het kwalitatieve aspect van het mechanische gedrag van schaalconstructies.

Om deze vijf grootheden te onderzoeken zijn vier schaalconstructies gemodelleerd met behulp van het 3D-ontwerpprogramma Rhinoceros. Vervolgens zijn met behulp van het FEA-programma TNO DIANA de benodigde grootheden berekend waarmee de nieuwe grootheden kunnen worden bepaald. Dit laatste is tenslotte gedaan in Grasshopper waarmee tevens de resultaten worden weergegeven in Rhinoceros.

Tijdens het afstudeeronderzoek bleken vooral de strain energy (de energie die in een constructie wordt opgeslagen doordat een belasting de constructie vervormd) en de buckling load factor (de verhouding tussen de optredende normaalkracht in een constructie en de normaalkracht waarbij de constructie zal bezwijken op knik) goede resultaten op te leveren. Met behulp van de strain energy bleek het mogelijk om aan te tonen waar een schaalconstructie zich vooral als schaal gedraagt (wat wenselijk is bij een schaalconstructie) of waar deze toch meer plaatgedrag vertoont. Tevens combineert de grootheid strain energy zowel kracht als vervorming in alle richtingen waardoor slechts één resultaatplot nodig is om een constructie te beoordelen. De buckling load factor laat vooral zien waar en in welke mate een constructie het meest waarschijnlijk is om te bezwijken op knik.

Verder bleek tijdens de ontwikkeling van de zelfgemaakte post-processor het ook vrij gemakkelijk om de richting van de steilste helling weer te geven wat mogelijkheden biedt voor het implementeren van de Rain Flow Analogy. De Rain Flow Analogy is een alternatieve methode die laat zien hoe de krachten van hun aangrijpingspunt zich richting de oplettingen door de constructie verplaatsen.

Gebaseerd op bovenstaande resultaten wordt aanbevolen om de strain energy en de buckling load factor op te nemen in bestaande eindige-elementenprogramma's. Hiermee kunnen schaalconstructies beter geoptimaliseerd worden en ontstaat er beter inzicht in het mechanische gedrag van de schaalconstructie.



# TABLE OF CONTENTS

LIST OF ABBREVIATIONS AND FILE EXTENSIONS .....	17
NOMENCLATURE .....	19
PREFACE.....	21
<b>1 LITERATURE STUDY.....</b>	<b>25</b>
1.1 INTRODUCTION: THE STRUCTURAL ASSESSMENT OF SHELL STRUCTURES.....	27
1.1.1 Philosophy .....	27
1.1.2 Which types of structural behaviour can be distinguished? .....	27
1.1.3 What makes a well designed shell structure? .....	27
1.1.4 Limitations of the currently available quantities.....	29
1.2 RELATED STUDIES .....	30
1.2.1 Alternative methods in order to gain insight in the mechanical behaviour of plate structures .....	30
1.2.2 Optimising shell structures with the aid of strain energy .....	31
1.2.3 The use of alternative, self-made software tools.....	32
1.3 FINITE ELEMENT ANALYSIS.....	33
1.3.1 Introduction into the Finite Element Method.....	33
1.3.2 Displaying the FEA-program results .....	33
1.3.3 Directional (in)dependency .....	34
1.3.4 Global and local coordinate systems.....	34
1.4 RELATED FIELDS OF RESEARCH.....	36
1.4.1 Evolutionary Structural Optimisation.....	36
1.4.2 Form finding .....	37
1.4.3 Rain Flow Analogy .....	38
1.5 NEW QUANTITIES .....	40
1.5.1 Strain energy .....	41
1.5.2 Eccentricity of the normal force.....	42
1.5.3 Buckling load factor .....	44

1.6	POTENTIALLY SUITABLE SOFTWARE FOR THE DEVELOPMENT OF THE SELF-MADE POST PROCESSOR.....	45
1.6.1	Structural analysis .....	45
1.6.2	Post processing - computing the additional quantities.....	46
1.6.3	Post processing - displaying the results.....	47
1.7	EXISTING OUTPUT OPTIONS OF SOFTWARE PROGRAMS .....	49
1.7.1	Rhinoceros.....	49
1.7.2	DIANA .....	50
1.7.3	Post processors.....	51
<b>2</b>	<b>SELF-MADE POST PROCESSOR.....</b>	<b>55</b>
2.1	DEVELOPMENT OF THE SELF-MADE POST PROCESSOR .....	57
2.1.1	Development of the post processor within DIANA .....	57
2.1.2	Development of the post processor – the alternative way.....	59
2.1.3	General set-up of the used post processing method .....	61
2.1.4	Operation principal of the Grasshopper model .....	62
2.1.5	Limitations of developing a self-made post processing tool.....	68
2.2	THE MECHANICS OF THE NEW QUANTITIES.....	70
2.2.1	Strain energy .....	70
2.2.2	Eccentricity of the normal force.....	71
2.2.3	Buckling load factor .....	72
2.2.4	Out of balance of the in-plane shear force .....	73
2.2.5	Out of balance of the in-plane shear eccentricity of the normal force.....	74
2.2.6	Principal directions .....	75
<b>3</b>	<b>ANALYSIS AND STUDY RESULTS.....</b>	<b>77</b>
3.1	DEFINITION OF SCOPE .....	79
3.1.1	General definition of scope .....	79
3.1.2	Type of structural analysis.....	79
3.1.3	Material usage.....	79
3.1.4	Shell thickness and element type.....	79



3.2	MODEL SET-UP .....	81
3.2.1	Dimensions .....	81
3.2.2	Material properties .....	82
3.2.3	Coordinate systems .....	82
3.2.4	Boundary conditions.....	83
3.2.5	Loads.....	83
3.3	ANALYSIS RESULTS.....	84
3.3.1	Strain energy .....	84
3.3.2	Principal values of the eccentricity of the normal force .....	90
3.3.3	Eccentricity of the normal force in the principal directions of the bending moment 92	
3.3.4	Buckling load factor .....	95
3.3.5	Out of balance of the in-plane shear force .....	100
3.3.6	Out of balance of the in-plane shear eccentricity of the normal force.....	101
<b>4</b>	<b>CONCLUSIONS AND RECOMMENDATIONS .....</b>	<b>105</b>
4.1	CONCLUSIONS .....	107
4.1.1	General conclusions .....	107
4.1.2	Strain energy .....	107
4.1.3	Eccentricity of the normal force.....	108
4.1.4	Buckling load factor .....	109
4.1.5	Out of balance of the in-plane shear force .....	109
4.1.6	Out of balance of the in-plane shear eccentricity of the normal force.....	109
4.2	RECOMMENDATIONS .....	111
4.2.1	Integration of the self-made post processor.....	111
4.2.2	Extension of the curvature analysis tool in Grasshopper and the buckling load factor 111	
4.2.3	Actual improvement of a shell structural design .....	111
4.2.4	Remaining recommendations .....	112
	REFERENCES .....	115

<b>APPENDICES .....</b>	<b>119</b>
APPENDIX A – SET-UP OF A .DCF FILE.....	121
APPENDIX B – ALIGNMENT OF THE LOCAL COORDINATE SYSTEMS .....	123
APPENDIX C – PRINCIPAL DIRECTIONS OF THE DISTRIBUTED BENDING MOMENT .....	133
APPENDIX D - ANALYSIS RESULTS.....	155
APPENDIX E – COMPARISON DISTRIBUTED BENDING SHEAR MOMENT RESULTS .....	209
APPENDIX F – EXAMPLE OF STRAIN ENERGY SUBDIVISION .....	213
APPENDIX G – RAIN FLOW ANALOGY.....	217





# LIST OF ABBREVIATIONS AND FILE EXTENSIONS

## General abbreviations

BLF	-	Buckling Load Factor
ESO	-	Evolutionary Structural Optimisation
FEA	-	Finite Element Analysis
FEM	-	Finite Element Model
RFA	-	Rain Flow Analogy
Rhino	-	Rhinoceros (3D modelling computer program)
USS	-	User Supplied Subroutines (DIANA)

## File extensions

.DAT	-	DATA file
.DCF	-	Document Computation Format file
.IGES	-	Initial Graphics Exchange Specification file
.TB	-	Tabulated file

## Abbreviations used in the result displays

U <sub>in-plane</sub>	-	in-plane strain energy
U <sub>out-of-plane</sub>	-	out-of-plane strain energy
U <sub>total</sub>	-	summation of the in-plane and the out-of-plane strain energy
U <sub>α</sub>	-	ratio of the in-plane and the out-of-plane strain energy according to equation 2-11 (see paragraph 2.2.1)
E <sub>o/t_NF</sub>	-	Eccentricity of the Normal Force
PV1	-	Principal Value 1
αM1	-	Principal direction belonging to the first principal value of the bending moment
dN	-	the difference between $n_{xy}$ and $n_{yx}$ according to equation 2-26 (see paragraph 2.2.4)



# NOMENCLATURE

## Upper case Latin symbols

$E$  = Young's modulus / modulus of elasticity [N/mm<sup>2</sup>]

$M$  = bending moment [Nm]

$N$  = normal force [N]

$U$  = strain energy [Nm]

## Lower case Latin symbols

$a$  = radius of curvature [m]

$c$  = constant [-]

$e$  = eccentricity of the normal force [mm]

$h$  = height [m]

$k$  = principal curvature [m<sup>-1</sup>]

$q$  = shear force [N/mm]

$t$  = shell thickness [mm]

## Lower case Greek symbols

$\gamma$  = shear strain [N/mm]

$\varepsilon$  = strain [-]

$\kappa$  = curvature [m<sup>-1</sup>]

$\lambda$  = buckling load factor [-]

$\nu$  = Poisson ratio [-]

$\rho$  = shear curvature [m<sup>-1</sup>]

$\sigma$  = stress [N/mm<sup>2</sup>]





## PREFACE

This report is the final product of this graduation thesis and consists of four main parts:

- Chapter I – The literature study report;
- Chapter II – The development and set-up of the self-made post processor used during this graduation thesis;
- Chapter III – The actual graduation report containing the results of this thesis;
- Chapter IV – The conclusions and recommendations.

This preface can be used as an introduction to the topic of this graduation thesis.

### Introduction

In order to provide insight into or assess the mechanical behaviour of a structural design, the use of a Finite Element Analysis (FEA) computer program is common practice in the structural engineering community. Most FEA-programs only display quantities such as displacements or stresses with which a structural designer or a civil engineer can assess the structural design.

A special type of structure in the world of civil engineering is the shell structure. This is because of its unique way of remitting the loads to the supports, which in turn allows for very slender structures. This unique way of load transfer makes it hard to assess the mechanical behaviour and the efficiency of the shell structures solely based on quantities such as displacements and stresses. For example, a particular shell design can develop extremely large stresses due to support settlements. The usual stress checks do not give any clue to how the design needs to be improved. The designer then just tries many changes hoping that one of these gives some improvement. Clearly, this is a very time consuming process and success is not guaranteed<sup>1</sup>. Hence, a need exists for additional quantities and/or methods that can be used for better assessment of shell structures.

### Problem definition and objectives formulation

Although the Finite Element Method (FEM) used by FEA-programs provides good insight in the quantitative behaviour of shell structures during loading, it provides very little qualitative insight in their structural behaviour.

This master graduation thesis is aimed at finding additional quantities for FEA-programs in order to obtain better qualitative insight in the structural behaviour of shell structures and to be able to make better assessments of structural designs.

### Graduation assignment description

This master graduation assignment focuses mainly on the additional quantities that can be deduced from and used next to the already existing quantities such as displacements, stresses and strains which are used by most – if not all – Finite Element Analysis programs. In addition to this main focus point some research went into the investigation of different methods – as in opposition to the Finite Element Method – to obtain a better insight in the structural behaviour of shell structures. An example of such a method is the “*Force Flow Method*” or “*Rain Flow Analogy*”.

---

<sup>1</sup> A small physical model of a shell can be of great help. It can be deformed by hand and its behaviour becomes quickly clear.

In order to determine the current state of the use of additional quantities in Finite Element Analysis programs for the structural design of shell structures a literature study has been performed at the beginning of this master graduation thesis. During this literature study it was determined which additional quantities were the most promising to research in the actual research part of this thesis. In this phase of the study it was also determined how to deduce the additional quantities from the existing Finite Element Analysis program quantities. After this a proof of concept was made for three basic types of shell structures: the ellipsoid, the hyperboloid and the hyperparaboloid.

To cope with the large amount of data that is usually generated using FEA-programs some sort of post processor computer program has been made to compute the additional quantities automatically on the basis of the already existing quantities. After finishing the proof of concept a more complex shell design was analysed. The results of both basic and complex shell structure designs are incorporated further on in this report.

### **Activities**

In order to reach the desired end result of this graduation thesis the activities of the thesis have been divided over three milestones:

- Milestone 1: literature study;
- Milestone 2: development proof of concept;
- Milestone 3: the actual graduation research, consisting of creating and analysing miscellaneous shell structural design models and assess the different additional quantities on their eligibility.

Here below each of the activities is individually elucidated.

#### Literature study

The literature study part of the master graduation thesis is used for collecting information regarding the graduation subject in order to prepare for the actual graduation research. In order to fulfil this, the following activities were completed:

- Reading up into the already existing research about assessing the mechanical behaviour of shell structures;
- Collecting information about alternative methods for assessing the structural behaviour of shell structures;
- Collecting information about combining additional quantities with the Finite Element Method;
- Reading up into the mechanics of shell structures and into the Finite Element Method with reference to shell structures;
- Determining which additional quantities will be researched and how they can be computed;
- Determining which software is most suited for the creation of self made post processor;
- Collecting existing models and calculation examples in order to check the results.

The results of these activities will be discussed in chapter 1 of this graduation report.

#### Development of the proof of concept of the self-made post processor

After completing the literature study a proof of concept was developed for the self-made post processor. For this development a simple geometry was analysed in a FEA-program. Based on the geometry and the analysis results the additional quantities were determined and displayed. After verifying the results the use of the self-made post processor was extended to the remaining analysed shell structures. The main advantage of first developing

a proof of concept is that not only can be shown that the basic ideas work, but it also allows for encountering and fixing issues before analysing all the models. This results in only having to fix just one program model instead of having to fix it for all shell structures to be analysed.

#### Creating the design and the structural models

The original intent was to start developing a few basic types of shell structures and expand them with some more complex shell geometries. The geometry of each structure had to be set up in a parametric way in order to be able to quickly vary some main design parameters. In this way several variations of different designs could be analysed. However, due to some change in plans involving the automation of the structural analyses and post processing of the results, only four structural designs were analysed and researched. More about this change of plan can be read about in paragraph 2.1 of this graduation thesis.

#### Analysing the modelled shell structures with the aid of additional quantities

The developed structural models were analysed with the aid of a FEA-program after which a number of additional quantities have been analysed with the aid of the self-made post processor.

#### **Definition of scope**

The definition of scope was expanded due to several reasons during the course of the thesis. An overview of the additions to the definition of scope can be found in paragraph 3.1 of this graduation report.

#### **Resulting products**

The products of this graduation report are described as:

- The literature study report;
- The self-made post processor needed for computation of the additional quantities;
- The analysed design models, in parametric format so that changing of these parameters in case of a work-up to this graduation thesis is possible;
- The final graduation report containing the results of the graduation thesis.

During the thesis it was decided to combine the literature study report with the final graduation thesis report into one report with addition of a brief description of the development and the inner workings of the self-made post processor. Due to a change in set-up the creation of the different parametric design models had to be withdrawn.

#### **Quality control**

In order to guarantee the quality of the graduation research several intermediate presentations were added to the planning. These presentations were planned at the end of milestone 2 and 3. They serve the goal of informing the graduation committee about the state of development and to obtain feedback for the graduate. Next to these presentations multiple progress discussions were organised with the direct supervisor.



# **1 LITERATURE STUDY**



# 1.1 INTRODUCTION: THE STRUCTURAL ASSESSMENT OF SHELL STRUCTURES

## 1.1.1 Philosophy

This graduation thesis is aimed at developing additional quantities that can be used to assess the qualitative structural behaviour of shell structures in a better way. Before these additional quantities can be assessed on their suitability and usefulness it is important first to determine what structural behaviour of shell structures is desirable. Additional questions related to this topic that can be asked are:

- Which types of structural behaviour can be distinguished?
- What makes a well designed shell structure?
- Why is it that the quantities currently available (i.e. stresses and displacements) do not provide a good insight in the structural behaviour of shell structures?

These additional questions will be answered individually here below before answering the big question: What structural behaviour of shell structures is desirable and what does this mean for the assessment of the additional quantities?

## 1.1.2 Which types of structural behaviour can be distinguished?

All structures are assessed for three main aspects: sturdiness, stiffness and stability. These aspects are also known in the civil engineering world as the three Ss. The sturdiness is a parameter related to the strength of the structure or – to be more precise – to the material strength and the load acting on the structure. The stiffness is a parameter that is related to the amount of deformation due to a certain load; a structure with a higher stiffness will deform less than a structure with a lower stiffness. The stability at last is a parameter that assures that a loaded structure does not collapse while it is undergoing certain deformations influencing the flow of forces inside the structure. When the occurring values for each of these parameters are less than the values the structure and material are able to handle then the design is considered structurally safe.

The quantities sturdiness, stiffness and stability are – as their name already indicates – quantitative values, i.e. they indicate whether a structure is safe or not but they only provide limited insight in the structural behaviour itself. For this more qualitative quantities are needed.

## 1.1.3 What makes a well designed shell structure?

From previous theses it was found that there were several “dos and don’ts” regarding the design of shell structures:

- The first regards in-extensional deformation which has to be avoided due to (in)stability issues. In-extensional deformation occurs when the internal forces consist of bending forces only, i.e. no membrane forces occur that consequently would lead to extensional deformations of the shell, hence the name in-extensional deformations. Shell structures that have zero Gaussian curvature over large areas are particularly susceptible to in-extensional deformations. A finite element analysis regarding the natural frequencies of a shell structure can be used to indicate possible in-extensional deformations with the use of the governing natural frequencies and their associated normal modes [7].
- Prevention of the occurrence of concentrated shear forces leading to bending moments;

- Adding upward curvature to the shell edges in order to direct the force flow away from the edge to the supports;
- Prevention of cantilever parts allowing the rain to flow over the edge of the shell;
- From a standpoint of material savings it is good to keep the shell thickness to a minimum;
- From a structural standpoint it is good to allow as much membrane forces in comparison to the out-of-plane bending and shear forces as possible. These latter forces have to be kept to a minimum in order to maintain the desired shell structural behaviour;
- To maintain structural effectiveness and efficiency shell deformations should be minimised as shell structures with a higher stiffness usually show a better load carrying behaviour and therefore have an improved critical load [5].

One can argue that each of these dos and don'ts limits the freedom of the design of a shell in some way in order to obtain a well designed shape. The discussion to what limits this is acceptable is a whole other one that is not the topic of this graduation research. It is however more than imaginable that shape and effectiveness of a shell structural design are closely linked together. The amount of architectural freedom an architect and a structural designer are prepared to sacrifice in order to obtain a better structural shape is something for them to decide. This graduation thesis is only aimed at providing new tools that provides better insight and can help them make a better decision.

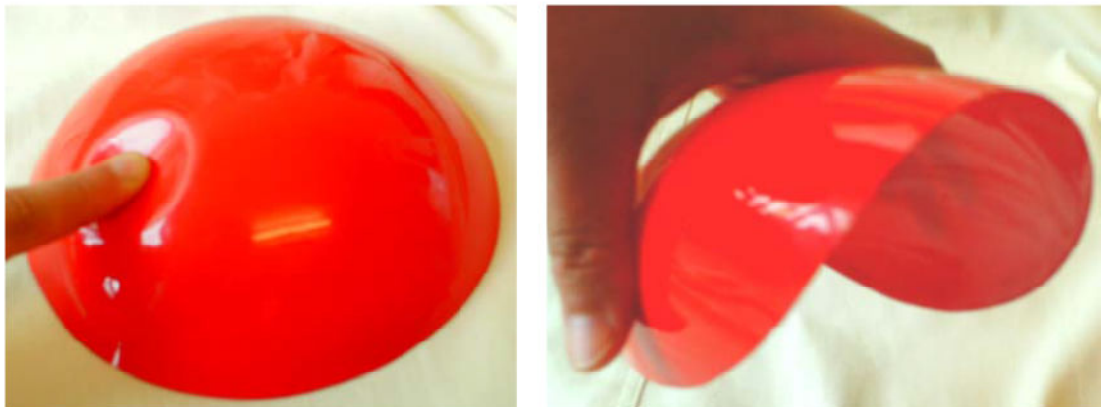


Figure 1.1 – On the left an example of extensional deformation, on the right an example of in-extensional deformation [10].

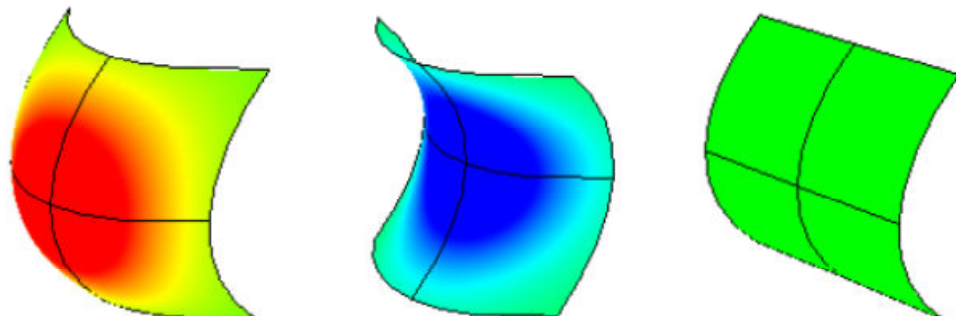


Figure 1.2 – From left to right: displays of positive, negative and zero Gaussian curvature in Rhino [8].



#### **1.1.4 Limitations of the currently available quantities**

One of the limitations of currently available quantities used for assess a shell's structural behaviour is that these quantities such as forces, stresses and strain are all tensor quantities. This means that they have both a value and a direction. Since their directions and the shell geometry rarely coincide it is rather difficult to use them in order to assess the structural design of a shell structure. For this it would be better if scalar quantities could be used since they only have a value and therefore are directionally independent.

Another currently available quantity not mentioned yet is the displacement. Other than for edges where the shell is supported or where a facade is made, the displacement of a shell is less important as for other types of structures. In contradiction with arch type structure it is not necessary for the membrane forces to stay in the middle third of the shell's thickness as they will be pulled back by the hoop forces [8]. At the other hand, the maximum allowable displacement of – for example – a building floor is determined from a practical standpoint instead of that it is based on an aesthetic or structural requirement. This is less of an issue for shell structures apart from the aforementioned limited edge displacements due to the addition of supports and facades.

## 1.2 RELATED STUDIES

In order to gain insight in the current state of shell structural analysis tools and research, this graduation thesis started with the collection of and reading into various (graduation) studies and publications that could be found in the repository of the TU Delft and on the internet. Although over 160 interesting documents and reports were found, none of them discusses exactly this graduation thesis's topic. There were however several documents and reports that treated part of the subjects of this graduation thesis. In this set of subjects, the following distinction can be made:

- The use of alternative methods in order to gain insight in the mechanical behaviour of plate structures;
- The optimisation of shell structures with the aid of strain energy;
- The use of alternative, self-made computer programs in order to develop structural designs.

For each of the three subjects mentioned above, the most important results and conclusions will be discussed here below.

### 1.2.1 Alternative methods in order to gain insight in the mechanical behaviour of plate structures

Regarding this subject a number of graduation reports can be found. One of the more interesting reports is written by Oosterhuis in 2010 [3]. Although these graduation theses treat plate structures instead of shell structures, their tendency is largely the same as this graduation thesis. In Oosterhuis's graduation thesis several (combinations of) methods for the assessment of plate structures are used and assayed in order to obtain better insight in the mechanical behaviour of these plate structures. The list of methods used includes:

- Differential equations (for thin plates);
- Elastic membrane analogy;
- Force Density method;
- Rain Flow Analogy;
- Curvature ratio method;
- Finite difference method;
- Sand hill analogy.

A various number of combinations of these methods were used in order to create parametric design tools for which the results are subsequently compared with the output of an existing structural analysis program (SCIA). Whereas Oosterhuis's thesis focuses on alternative methods that can be used instead of or next to a FEA-program, this graduation thesis focuses more on the additional quantities that can be used within a FEA-program. The main goal of both theses however is to obtain better insight in the qualitative behaviour of structural behaviour although the contribution of the gained insight remains somewhat unclear in Oosterhuis's thesis.

One of the more important outcomes with relation to this thesis is how well the combination of Rhino and Grasshopper is suited for the creation of a parametric framework. Different structures can be created with the use of a couple of Grasshopper components and analysed by a self-made Grasshopper tool. This has the advantage that no structural analysis data or design geometry data has to be converted from one program to another which saves the time and effort in either doing this by hand or by having to create a small program that does this automatically. Furthermore, Grasshopper allows for additional functionality by

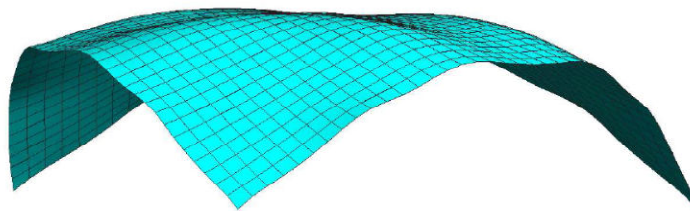
supporting the use of scripts (little pieces of program code) which can be written in different programming languages such as Visual Basic or C#.

Further specifics about the most important alternative methods to the finite element method that were encountered during this thesis are stated in paragraph 1.4.

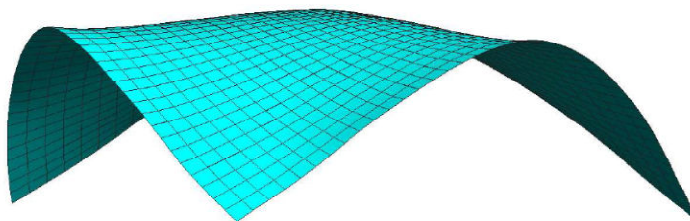
### 1.2.2 Optimising shell structures with the aid of strain energy

A master graduation thesis regarding this topic was performed by Firl in 2010 [5]. Although the optimisation of shell structures is not the same as gaining better qualitative insight in the mechanical behaviour of shell structures, these two subjects do have similarities. With better insight in the mechanical behaviour, a structure could not only be assessed in a better way but possibly this information can also be used to indicate where and how the structure has to be altered in order to obtain a better structural design. A second reason why this master graduation report is interesting is that it uses strain energy for optimising the shell structures.

Strain energy is one of additional quantities that was labelled as very interesting in at the start of the thesis. Amongst others, one of the interesting results of Firl's report is the different optimised shapes for the Kresge Auditorium of the Massachusetts Institute of Technology between the linear and non-linear analyses. The results show that the optimised shape for the non-linear shape is much more realisable and aesthetically more pleasing than the optimised shape obtained with the linear analysis.



(a) Linear strain energy



(b) Nonlinear strain energy

*Figure 1.3 – Optimal shapes for the Kresge Auditorium as analysed by Firl [5]. The upper display shows the optimal shape obtained by performing an analysis where the strain energy is computed in a linear way, the bottom display shows the optimal shape obtained by performing a non-linear strain energy analysis.*

A similar study regarding the optimisation of shell structures is the graduation thesis of Matthijs van den Dool from 2012 [2]. He uses complementary energy instead of strain energy for the optimisation process (see figure 1.4). The main difference between Van den Dool's research and this research is that Van den Dool uses the complementary energy to determine the optimal shape of a structure for different load cases by minimising the amount of complementary strain energy whereas this thesis tries to determine whether strain energy

is a suitable additional quantity for obtaining better insight in the mechanical behaviour of shell structures.

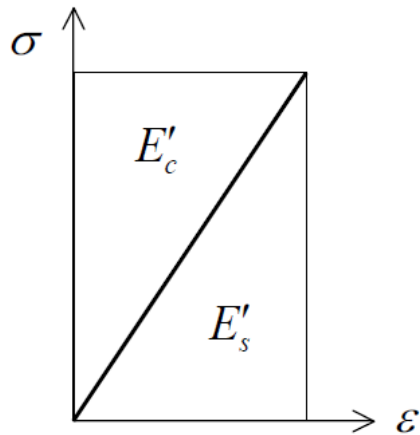


Figure 1.4 – Where the strain energy is the area under the line representing the stress-strain relationship, the complementary energy is the area above this line [6].

An important lesson that can be learned from Van den Dools work is that the use of a self-made analysis tool limits the research possibilities. Next to the fact that developing such a tool is precious, its capabilities are limited in comparison with existing FEA-programs and just for analysis causes, the tool has to be so much more complex in order to obtain the same quantitative results that creating such a tool would be a graduation thesis by itself, as Van den Dools tool is developed on the more simplified Thrust Network Analysis and the Force Density Method in comparison to the Finite Element Method that is fully developed in most FEA-programs nowadays.

More about the quantity strain energy and the other quantities labelled interesting for this graduation thesis can be found in paragraph 1.5.

### 1.2.3 The use of alternative, self-made software tools

During the literature study of this graduation thesis numerous examples have been found of self-made software tools. Most of them are aimed at designing structures, whether or not with some structural mechanics for guidance to the aimed – or “optimal” – result. Only a few used an existing FEA-program, mostly for checking of the results. One exception to this is the work of Van Asselt [1] from 2007. He uses experimental test results to create a user defined stress-strain relationship with the aid of the User Programmable Feature of ANSYS. The main difference with self-made software tools is that in this thesis an existing FEA-program is extended whereas the use of self-made software tools usually is limited in one or more ways.

Regarding the examined literature, one of the main aspects which has to be taken into account regarding the developing of a self-made software tool is that one has to be careful not to spend too much time in the development. Developing a complete FEA-program is obviously far too complex and even the development of the more or less limited tools appeared to be very time consuming. Therefore, one should anticipate for the amount of time it could take of developing such a self-made software tool and the limitations that such a tool might have.

More about self-made software tools can be found in paragraph 1.6.

## 1.3 FINITE ELEMENT ANALYSIS

### 1.3.1 Introduction into the Finite Element Method

Before listing and discussing alternative fields of research next to the finite element method (FEM) a more detailed description of what the finite element method exactly is will be given, along with an evaluation of the limitations of the finite element method that led to the subject of this graduation thesis.

The finite element method is a numerical method to solve partial differential equations [11]. In practice the finite element method comes down to dividing a computer model into a finite number of elements. By applying the differential equations that describe the relation between the load and the resulting stresses and displacements to each element, a large system (matrix) that represents normal equations is created. By applying the proper boundary conditions the discretized differential equations now can be solved.

The finite element method is mostly suited for structures with a complex geometry. Applied in the structural mechanics the finite element method is closely related to the concepts energy and virtual work [11].

The output of a finite element analysis (FEA) consists of stresses and strains computed at integration points and reaction forces and displacements computed at nodes. Given this quantities structures are being evaluated and assessed. The finite element method thus gives especially a quantitative insight in the mechanical behaviour of structures.

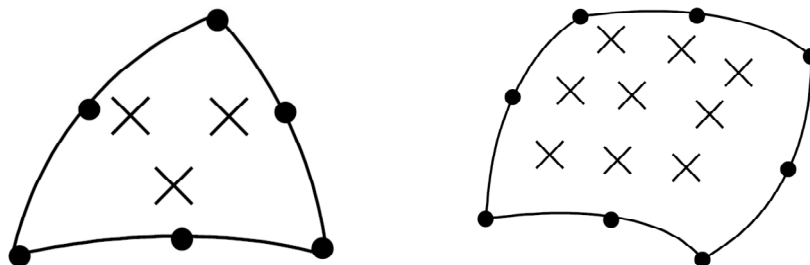


Figure 1.5 - A six-noded triangular element (T6) with 3 integration points [left] and an eight-noded quadrilateral element (Q8) with a (3x3) integration scheme [right] [11].

This master graduation thesis aims at generating and examining alternatives that allow evaluating structures in a more qualitative way. During the literature study the following alternative fields of research were examined:

- Evolutionary Structural Optimisation (ESO);
- Form finding;
- Rain Flow Analogy (RFA).

In the following paragraphs each of these alternative fields of research is discussed individually.

### 1.3.2 Displaying the FEA-program results

There are two essential ways to display the results of a finite element analysis. The first is by means of a contour plot, the second is by means of a vector plot (see figure 1.6).

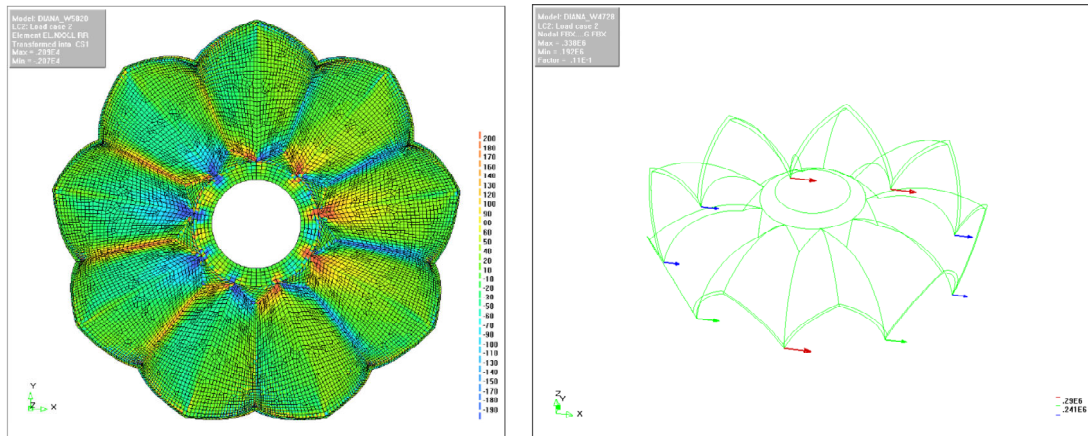


Figure 1.6 – On the left a contour plot of the normal forces  $N_{xx}$ , on the right a vector plot of the reaction forces.

The main difference between these two ways of displaying the results is that a contour plot uses scalar quantities in opposite of a vector plot that uses vector quantities. A scalar quantity only has a magnitude; a vector quantity also has a direction. For the above mentioned alternative quantities it applies that strain energy is a scalar quantity and the eccentricity of the normal force and the buckling load vector both are vector quantities. It is possible to display both scalar quantities as well as vector quantities in a contour plot. In the latter case only the size of the vector is displayed.

### 1.3.3 Directional (in)dependency

In shell structures five directions can be distinguished:

- Principal curvatures  $k_1, k_2$ ;
- Principal normal forces  $n_1, n_2$ ;
- Resulting shear force  $q$ ;
- Principal moments  $m_1, m_2$ ;
- Principal stresses  $\sigma_1, \sigma_2$ .

These five directions do not need to coincide [9]. This poses an additional difficulty in determining the governing value of the before mentioned alternative vector quantities – eccentricity of the normal force and buckling load factor – since they rely on multiple quantities of which the principal directions do not need to coincide.

### 1.3.4 Global and local coordinate systems

FEA-programs distinguish the use of two different coordinate systems, namely the global and the local coordinates system. The geometry of a structure is defined in the global coordinate system. When meshing this geometry, multiple elements are created, each with their own local coordinate system for the sake of simplicity of the FEA-computations. This results therefore in one global coordinate system but in multiple local coordinate systems.

For structural components as beams or plates the results can be displayed in the global coordinate system without a problem because the orientation of such geometry can be aligned in the direction of a rectangular coordinate system. For cylindrical or (partial) spherical structures it is possible to use a global cylindrical or spherical coordinate system for that matter. However, the majority of the geometries of the shell structures modelled in this graduation thesis have a geometry that is not aligned with the direction of any of the aforementioned global coordinate systems. For this reason, it is more convenient to examine the results in the local coordinate systems of each of the different elements since the local

coordinate system is always aligned with the general direction of the element in case of the use of two dimensional shell elements. The problem in this however is that the general direction of different elements can differ from each other. This is due to the shape of each element and the way the meshing program works. When the local coordinate systems are not aligned, a mosaic pattern can occur as can be seen in figure 1.7.

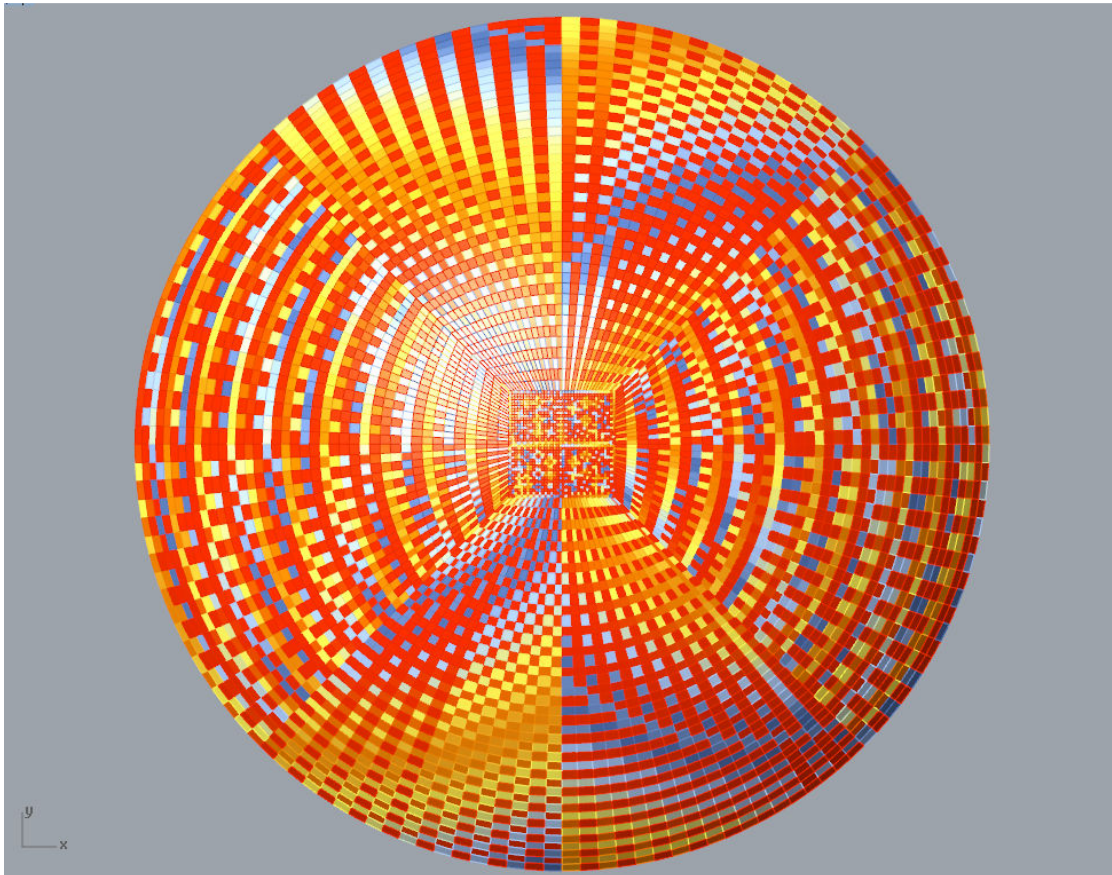


*Figure 1.7 – An example of a mosaic pattern in a dome.*

To prevent such a distorted display of the results the local coordinate systems have to be aligned in some way. For example: in case of the dome, all x-axes point outward in radial direction within the dome's surface, all y-axes point in tangential direction within the dome's surface and the z-axes point upwards perpendicular to the dome's surface. By displaying the results in this way a better image is created of the magnitude of the different quantities all across the structure. A complete overview of the alignment of the local coordinate system for each of the analysed structures can be found in appendix B.



## 1.4 RELATED FIELDS OF RESEARCH

### 1.4.1 Evolutionary Structural Optimisation

Evolutionary structural optimisation is, as can be derived by its name, a method aiming at developing optimal structures. Within the field of computational modelling of structures the following ways of optimisation are being distinguished:

- Optimisation of element size;
- Optimisation of shape;
- Optimisation of topology.

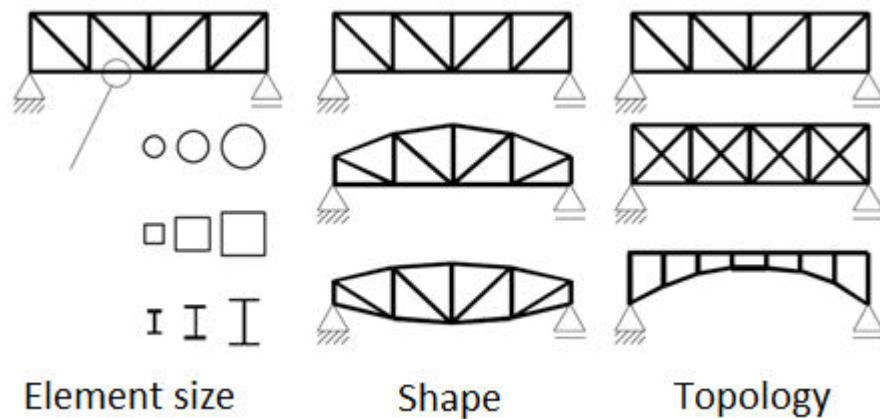


Figure 1.8 – The three distinctive ways of structural optimisation. [15]

At its core evolutionary structural optimisation uses the finite element method but it adds an optimisation algorithm. Evolutionary structural optimisation starts by defining a design space and a number of boundary conditions like supports and a load case. Then the finite element method is used where the design space is meshed and a finite element analysis is run. Subsequently the elements with – for example – the lowest stress are removed and the resulting structure is being analyzed again. This process repeats itself until some stop criterion is met, for example: the lowest stress is higher than some value  $\sigma_{lower bound}$ .

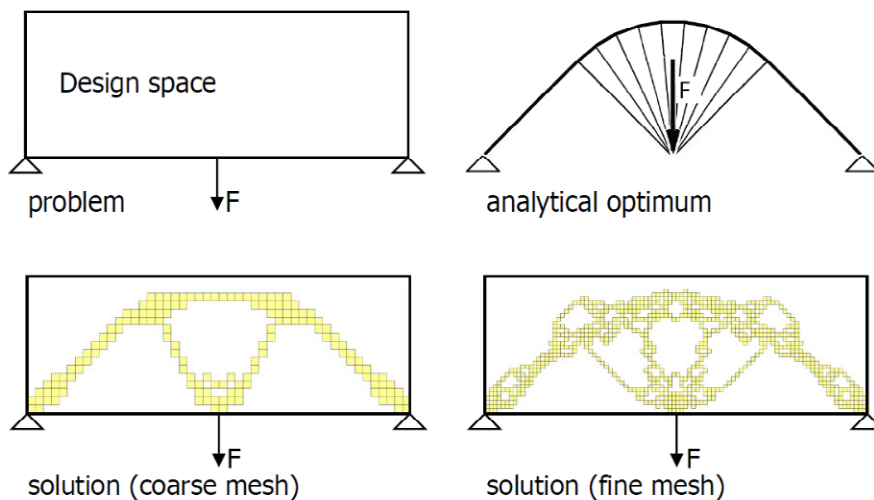


Figure 1.9 - Evolutionary Structural Optimisation [15].



Instead of using the lowest stress as a criterion for determining which elements are being removed some other quantities can be used, for example the eigen-frequency or buckling load. Besides this description of ESO there are some other variants like AESO (Additive Evolutionary Structural Optimisation) and BESO (Bi-directional Evolutionary Structural Optimisation). Where AESO adds elements to a structure, BESO is a combination of both ESO and AESO.



*Figure 1.10 - Evolutionary Structural Optimisation of a shell structure by sequentially removing elements of low stress [13].*

#### **1.4.2 Form finding**

Another method used for creating an optimal structural design is form finding. This method is suited for shell structures in particular because this type of structures is largely loaded by membrane forces and little loaded by bending moments.

There are different ways of form finding, some use real life models (e.g. hanging chain models, soap film models and wet cloth models) and some use computer models. Within computer aided form finding another distinction can be made between different methods:

- The Force Method/ Differential Equations;
- Elastic Membrane Analogy/ Soap Film Analogy/ Minimal Surface Area;
- Force Density Method / Dynamic Relaxation / Particle-Spring Method / Graphic Statics;
- Finite Difference Method;
- Transient Stiffness Method;
- Force Network Analysis/ Thrust Network Analysis;
- Complementary Energy.

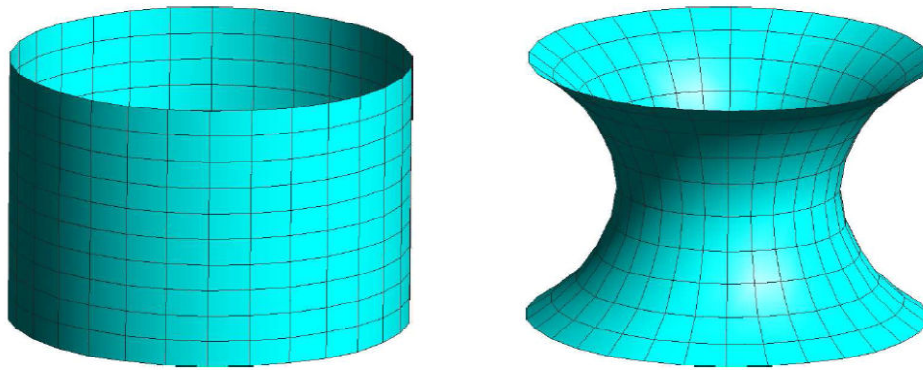


Figure 1.11 - Form finding of a hyperboloid shape. On the left the initial shape and on the right the final shape [5].

A significant difference between form finding and FEM is in the goal each method tries to accomplish. Form finding is all about finding an optimal shape for a certain type of structure with certain boundary conditions and a certain load case. By definition, form finding will lead to a certain optimal shape for a given set of BC's and load case. This means there is little to no architectural freedom. The finite element method preserves this freedom by its quantitative nature. It only computes stresses and displacements; there is no judging how good a shape of the structure is.

Next to the incapability of modelling free form architecture with the form finding method, there is another drawback to this method. A certain form found shape is only optimal for a given set of boundary conditions and load case. If either of these change, due to settlement of (one of) the supports or due to a variable loading condition, the shape of the structure isn't optimal anymore. Due to their great slenderness, shell structures have a relative small self weight/ variable load ratio. This attributes additionally to this disadvantage of the form finding method.

### 1.4.3 Rain Flow Analogy

*Like a rain flow loads will flow along curves with the steepest ascent on the shell surface to its supports.*

This hypothesis is the basis for the rain flow analogy method [6].

The idea of the Rain Flow Analogy originates from the year 1976 by emeritus professor W.J. Beranek of the section structural mechanics from the architectural department of Delft University of Technology [1]. Since then the Rain Flow Analogy has been the subject of several master theses and researches. Ir. A. Borgart from the Faculty of Architecture and the Built Environment is momentarily the driving force behind this method.

The method of Rain Flow Analogy has been developed to obtain a good qualitative insight in the mechanical behaviour of shell structures without having to use computer-power-demanding programs that use the finite element method.

In principle Rain Flow Analogy is a standalone method. Over the last few years however there have been developments of integrating Rain Flow Analogy within FEM computer programs. Within most of today's FEM programs it is possible to plot the principle directions in every element of a shell. Plotting the trajectories however is a scientific problem waiting to be solved [9].

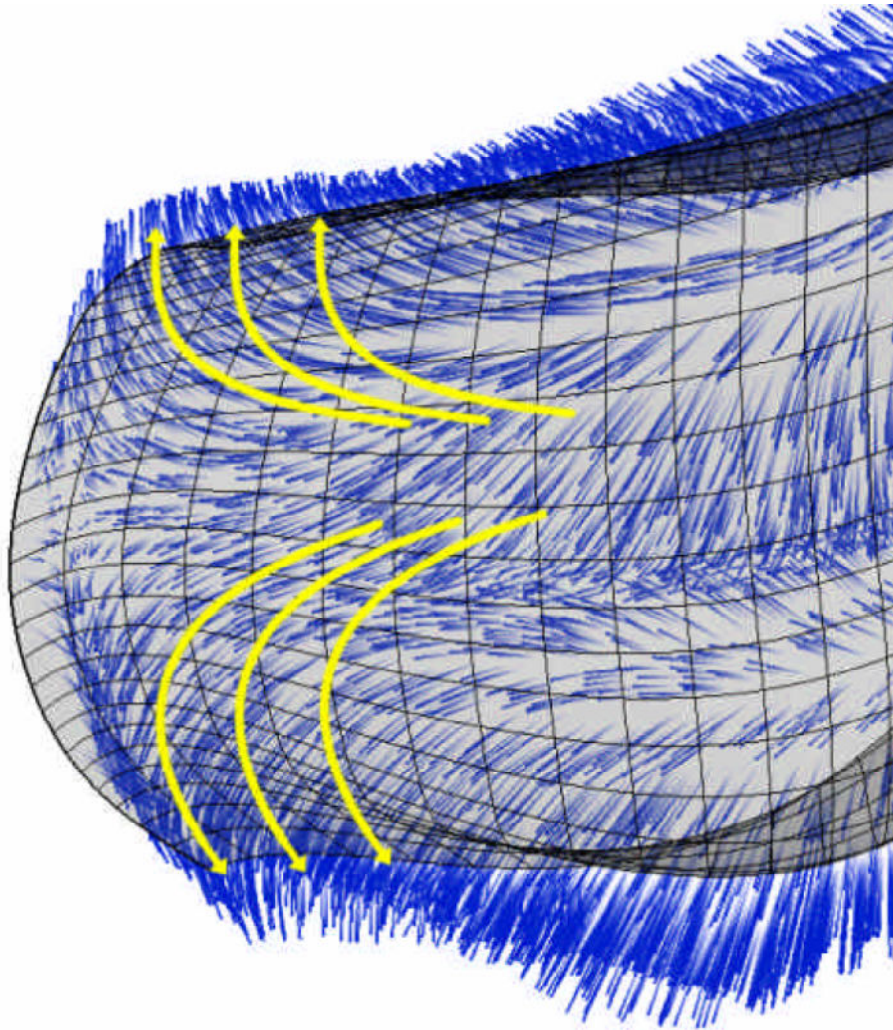


*Figure 1.12 - Rain Flow Analogy. The blue lines are the trajectories, the yellow arrows indicated the flow of forces [3].*

## 1.5 NEW QUANTITIES

Current quantities that are used as output by current FEA-programs are stresses, strains, forces and displacements. Some other quantities that might give more qualitative insight in the mechanical behaviour of shell structures are:

- Strain energy;
- The eccentricity of the normal force;
- The buckling load factor;
- The change of curvature;
- The degree of being a shell or a plate structure;
- The flow of forces;
- The amount of fixing at the supports.

Here below it will be explained why each of these quantities might be a valuable addition to the already existing quantities.

Strain energy is an interesting quantity since it is directional independent. This means that a contour plot suffices to display this quantity's results. Another advantage of the formulation of strain energy is that it combines information from all directions, including shear forces, and combines them into a single display.

The eccentricity of the normal force is expected to be a valuable quantity as it possibly can provide the designer with information on how to improve a shell's geometry. By shifting the shell's neutral line in the direction of its eccentricity the bending forces should theoretically be reduced.

The buckling load factor can be used to indicate where a shell is most likely to buckle and where it is not. In this way it serves as a guide to where to increase or decrease the thickness of a shell.

The change of curvature may be a valuable additional quantity as the change of curvature is important for how the forces are distributed within a shell. Large curvature changes may lead to shear forces and bending moments whereas large flat surfaces with little to no curvature change may be sensitive for buckling. It will however be more difficult to implement this quantity in an existing FEA-program since most FEA-programs cannot even display the curvature of a shell itself, let alone the change of curvature.

The degree of being a shell or a plate structure should indicate whether the designed structure is behaving more like a shell or more like a plate. It should consist of a ratio of the in-plane and the out-of-plane forces so that a large value for example indicates shell behaviour and a lower value indicates plate behaviour, much like as is depicted in figure 1.15. The degree of being a shell or plate structure should result in a scalar quantity that can be computed either by the ratio of the in-plane and the out-of-plane strain energy or by the ratio of the bending moments and normal forces. The first ratio is more preferable since the strain energy itself is already scalar quantity.

The flow of forces might be interesting to research as it would provide the designer with an image of how the forces are distributed from their point of application to the supports. This is what the rain flow analogy or the force flow method tries to accomplish. Since the path of each force would probably cross multiple elements it can be questioned if a FEA-program

that discretises the differential equations that describe a shell's load case is the best software program that can be used for this type of analysis. Maybe a tool with a more continuous approach is preferable.

The amount of fixing at the supports could be an interesting quantity as shell structures have a high degree of static indeterminacy. Most shell structures experience bending moments near the supports, even though it is not fixed at the supports. This is due to the fact that the shell will deform under its loading but it has to curve back to its supports since they remain in the same place. This induced deformation leads to bending moments in the shell surface near the support. It might be interesting to see what the influence would be if the shell supports would be fixed instead of simply pinned with respect with to the distribution of the in-plane and the out-of-plane forces.

During the second graduation committee meeting it was decided to start with the implementation of the quantities strain energy, eccentricity of the normal force, buckling load factor and the degree of being a shell or a plate structure since these were considered the most promising quantities that could be implemented with relative ease in an existing FEA-program.

For the quantities strain energy, eccentricity of the normal force and buckling load factor a more precise description is presented here below.

### 1.5.1 Strain energy

Strain energy is a quantity that describes the relationship between stresses, strains or deformations, displacements, material properties and external effects in the form of energy or work done by internal and external forces [17]. It is the amount of energy it costs for a certain force to deform a structure over a certain distance. For shell structures two types of deformations can be distinguished: extensional deformation and in-extensional deformation.

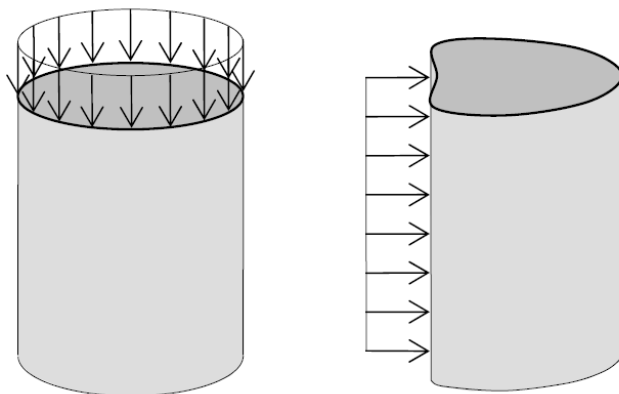


Figure 1.13 - (In-)extensional loading: left extensional loading, right in-extensional loading [10].

In-extensional deformation is caused by out-of-plane loading that doesn't change the Gaussian curvature of the shell. This means that a small force can cause large deformations, resulting in a low amount of strain energy. Because of this, and because large deformations are unwanted in most structures, in-extensional deformations must be avoided when designing shell structures.

Strain energy itself can be divided into two parts: strain energy caused by in-plane loading and strain energy caused by out-of-plane loading.

In-plane strain energy:

$$U_{in-plane} = \frac{1}{2} n_{xx} \varepsilon_{xx} + \frac{1}{2} n_{xy} \gamma_{xy} + \frac{1}{2} n_{yy} \varepsilon_{yy} \quad (1-1)$$

Out-of-plane strain energy:

$$U_{out-of-plane} = \frac{1}{2} m_{xx} \kappa_{xx} + \frac{1}{2} m_{xy} \rho_{xy} + \frac{1}{2} m_{yy} \kappa_{yy} + \frac{1}{2} q_x \gamma_{xz} + \frac{1}{2} q_y \gamma_{yz} \quad (1-2)$$

In these definitions of the strain energy it is assumed that the material behaviour is elastic. The strains and curvatures are those of the middle surface [10].

For the use in a FEA-program the strain energy can be converted to a ratio between the in-plane and out-of-plane strain energy or the two parts can be added to one another to get the total amount of strain energy. In the first case, the ratio between in-plane and out-of-plane strain energy can be used in addition to the alternative quantity eccentricity of the normal force (see paragraph 1.5.2). In the latter case the strain energy over the whole structure can be compared to the strain energy of a variant of this structure.

Loading Type	Strain Energy Constant Variables	Strain Energy General Case
Axial	$U = \frac{F^2 l}{2EA}$	$U = \int_0^l \frac{F^2 dx}{2EA}$
Bending	$U = \frac{M^2 l}{2E I}$	$U = \int_0^l \frac{M^2 dx}{2EI}$
Torsion	$U = \frac{T^2 l}{2GJ}$	$U = \int_0^l \frac{T^2 dx}{2GJ}$
Direct Shear	$U = \frac{F^2 l}{2AG}$	$U = \int_0^l \frac{F^2 dx}{2AG}$
Traverse Shear	$U = \frac{K V^2 l}{2GA}$	$U = \int_0^l \frac{KV^2 dx}{2GA}$

Figure 1.14 - Strain energy for different types of loading [20].

### 1.5.2 Eccentricity of the normal force

The eccentricity of the normal force determines the ratio of the stresses due to bending on one hand and the stresses due to axial loading on the other hand. It gives insight in the structural mechanical behaviour, i.e. is the structure behaving more like a plate or more like a shell? A smaller eccentricity of the normal force leads to better shell behaviour, as can be seen in figure 1.15. The bigger the eccentricity, the more undesirable the design of that part of a structure is.



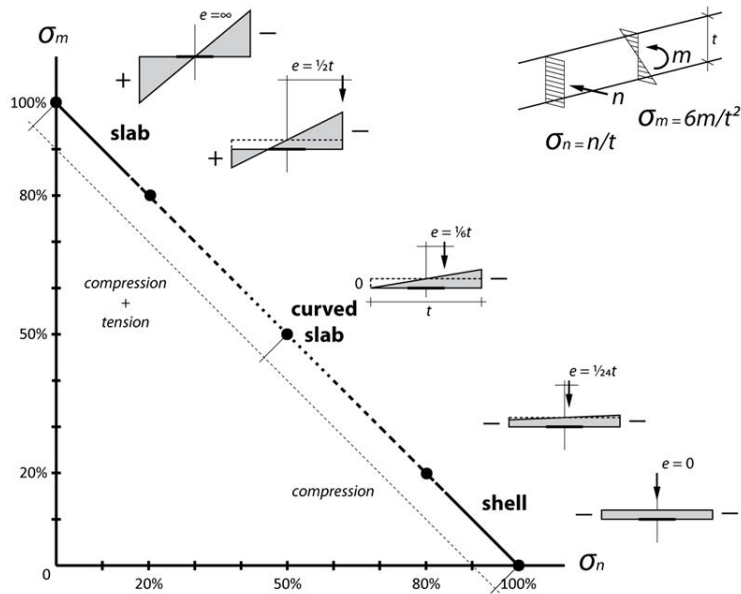


Figure 1.15 - The eccentricity of the normal force gives insight in the structural behaviour [12].

The eccentricity of the normal force can be defined by dividing the bending moment by the normal force. The problem of determining this quantity however is that the eccentricity is a vector quantity and therefore it is directional dependent. This means that if the principal directions of the bending moments and normal forces differ from one another, determining the eccentricity of the normal force is more complicated. It needs to be studied how to determine the normative value of the eccentricity of the normal force that gives the best insight in the structural mechanical behaviour.

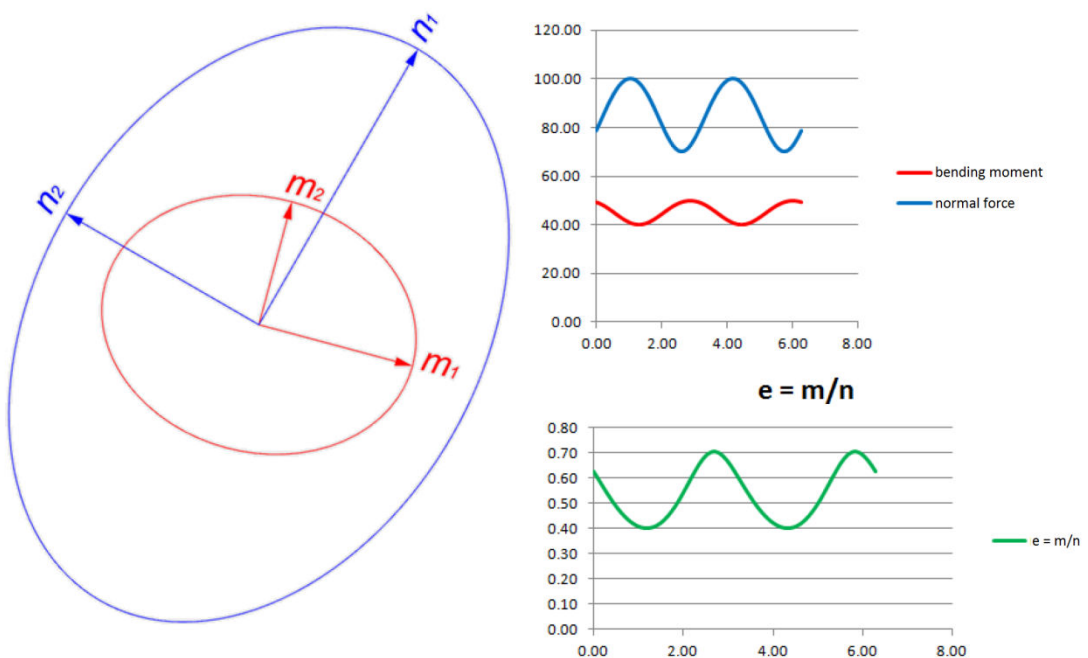


Figure 1.16 – On the left side: a normal force tensor and a bending moment tensor displayed as ellipses, both with different orientations. In the upper right corner: the length of a vector resulting in a sinus function as goes around the edge of the ellipses. In the bottom right corner: the eccentricity of the normal force is also a tensor quantity, again with a different orientation.

### 1.5.3 Buckling load factor

The buckling load factor can be defined by dividing the initial normal force by the critical normal force at which the structure will buckle.

Critical normal stress:

$$n_{cr} = -0.6 \frac{Et^2}{a} \quad (1-3)$$

Buckling load factor:

$$\lambda = \frac{n_{initial}}{n_{critical}} \leq 1 \quad (1-4)$$

As for the eccentricity of the normal force, this alternative quantity is also a vector quantity. Although the initial normal force and the critical normal force have the same direction, the critical normal force is dependent on the curvature perpendicular to its direction ( $1/a$ ). For a structure with an equal curvature in all directions, determining the normative value of the buckling load factor is not a problem. If the curvature is different in different directions, determining the governing buckling load factor is expected to be slightly more complicated. How to determine the governing buckling load factor is an item that needs to be studied during the course of this research, if it is decided to develop the buckling load factor as an alternative output quantity for FEA-programs.

The buckling load factor as presented here is meant only to give a qualitative insight in the structural mechanical behaviour of shell structures and is not supposed to be used as a quantitative check on the buckling behaviour. Comparing the buckling load factor of all the elements of a shell structure with an existing buckling load analysis of a FEA-program however can be used to check the accuracy and the suitability of this alternative quantity.



## 1.6 POTENTIALLY SUITABLE SOFTWARE FOR THE DEVELOPMENT OF THE SELF-MADE POST PROCESSOR

Now that it is clear which additional quantities will be examined and what method will be used, the next step is to figure out how to implement these into a computer program or some piece of software code in order to automate the process of determining the additional quantities. However, first it has to be defined what this piece of software code exactly has to do. For determining the additional quantities from the existing quantities, the following aspects can be distinguished for each of which a choice has to be made:

- Performing the structural analysis: use a FEA-program or develop a self-made analysis tool?;
- Post processing, calculation: what software program or programming language will be used to compute the new quantities from the existing ones?;
- Post processing, displaying the results: what post viewer will be used to display the additional quantities?

Although the choices regarding to these three points are influencing one another in some way, each aspect will be discussed separately down below in order to maintain a clear overview. For each aspect, the advantages and disadvantages of each alternative will be discussed. At the end of each paragraph a founded choice will be made with respect to which programs or programming languages will be used.

### 1.6.1 Structural analysis

For performing a structural analysis, the following alternatives can be distinguished:

- Use an existing FEA-program such as DIANA or ANSYS;
- Create a self-made (simplified) FEA-program;
- Use analytical calculations.

The first alternative is the most suitable for this graduation thesis as both alternatives to the first are too limited in their use. A FEA-program is a very complex piece of software and to create some self-made sort of FEA-program is a task too big to accomplish within the parameters of this graduation thesis. An alternative would be to create a simplified version of a FEA-program, maybe even with different methods for calculating the results. From studies performed earlier (see paragraph 1.2) this most certainly would lead to a computer program that is too limited for its use or would even have deviating results in comparison with a FEA-program structural analysis. Moreover, this would also require the development of a pre processor to, for example, create a mesh. The use of analytical calculations is only suitable for the analysis of the more simple shell structures and can better be used to check the FEA-results of these structures. Further disadvantages of analytical calculations are that they would limit the complexity of the structures to be analysed and they would limit the parametric set-up of the modelling of the shell structures.

Advantages of existing FEA-programs such as DIANA and ANSYS oppose to the above mentioned alternatives are:

- Existing FEA-programs do not have any limitations in boundary conditions or whatsoever as oppose to self-made structural analysis tools;
- No time and effort has to be put into making (the already simplistic) tools adequate for the set-up of this graduation thesis;

- It fits the main purpose of this thesis in a better way;
- Existing FEA-programs correspond in a better way to the additional results as different computer programs or tools correspond in a better way to different analysis methods.

For the implementation of the Rain Flow Analogy a FEA-program may not be the most suitable choice as a FEA-program creates a mesh that divides the structures into many elements in order to perform its structural analysis. Although it might be possible to determine the steepest inclination in a single element, it would be much more difficult to determine the path of a rain flow trajectory coming from one element and passing into another neighbouring element.

A more logical choice would be not to divide the shell surface into elements but keeping it as one continuous surface. This would mean that a tool for the Rain Flow Analogy would not use a FEA-program at all but would be a stand-alone tool. A good program for developing such a tool would be Rhino in combination with Grasshopper as the shell surfaces are being developed with these programs and they have different built-in functionalities for determining all kind of surface properties. More about the available functionalities of Rhino and Grasshopper can be found in paragraph 1.7.

Evident choices for the FEA-program to be used during this graduation thesis are DIANA and ANSYS as both software packages are available. With respect to previous experience with DIANA and with no experience with ANSYS, DIANA would seem to be the first choice. Both FEA-programs seem to have the same analysis functionalities [1], [4], so in this aspect there is no favourite. Also, both FEA-programs have support for user-defined quantities. In DIANA this method of creating your own user variables is called User Supplied Subroutines (USS), in ANSYS it is called User Programmable Feature (UPF).

As it turned out there were problems getting ANSYS to work on the available computers. Two versions of Ansys were tested; the first would not install correctly and the second one had licensing issues. Due to these problems with ANSYS and the previous experience with DIANA, this latter was the FEA-program to use for this master graduation thesis.

The additional quantities that were selected in paragraph 1.5 are all three based on quantities that can be computed based on the existing output results of FEA-programs. The radius of curvature is the only exception in this case but this quantity possibly can be determined with a yet to be developed tool in Rhino/ Grasshopper which later can be combined with the FEA-results.

### **1.6.2 Post processing - computing the additional quantities**

For the post processing part of the structural analysis, the following alternatives can be distinguished:

- Performing both the computation part and the result displaying part of the post processing within the FEA-program (DIANA);
- Performing the computation part within DIANA but displaying the results in a different post viewer (e.g. ParaView);
- Performing the computation part outside DIANA but displaying the results in one of DIANA's post viewers (iDIANA or FX+);
- Performing both the computation part and the result displaying part outside of DIANA.

To make a founded choice, the different alternatives with their advantages and disadvantages as well as the available options of the different already existing post viewers have to be taken into account.

Keeping the calculation part of the post processing within DIANA with the use of User Supplied Subroutines and the result displaying part in either of its post viewers (i.e. iDIANA or FX+) will lead to a work flow that knows little limitations or incompatibility issues and is quite fast in performing structural analyses. In order to set the USS functionality up in a correct way however is not an easy task as can be seen in chapter 2.

The second alternative way, using a different post viewer is only useful if DIANA's own post processors lack certain functionality that is required for this graduation thesis. The third alternative, performing computations based on the existing quantities in order to obtain the additional quantities is a good alternative for computing the buckling load factor, since DIANA does not seem to be able to determine the curvature of a surface, even with the aid of User Supplied Subroutines. The results required for the self-made post processor can be obtained via tabulated files (more about .tb files in paragraph 1.7). Once the existing quantities from these tabulated files are converted into the additional quantities, they can be used as input in one of DIANA's post viewers with the aid of creating FemView neutral files. These files can be imported into iDIANA and allow the user to display quantities computed outside of DIANA.

The fourth alternative can be used if quantities cannot be determined within DIANA and DIANA's post viewers cannot display the result in the desired way. An example of this is the determination of the buckling load factor with the aid of the curvature analysis functionalities in Rhino/ Grasshopper. Instead of converting the computed results into a FemView neutral file as mentioned above, Rhino/ Grasshopper can also be used as a post viewer by directly displaying the results.

### 1.6.3 Post processing - displaying the results

The choice of post viewer is closely interwoven with the choice for one of the four methods mentioned above. The first method seems to suite the best for this graduation thesis but it lacks functionality to compute the buckling load factor. For this some tool has to be created outside DIANA. If this tool is created in Grasshopper, then the logical choice would be to present the results in Rhino. If this tool is created on a standalone basis, then it might be easier and more in line with the other results that the buckling load factor results are also displayed in one of DIANA's post viewers.

Depending on the method of analysis the following post processing options are available for displaying the analysis results:

*iDIANA/FemView*: One of the two available post processors for DIANA. It has disposition over different options for user defined coordinate systems; amongst others cylindrical and spherical coordinate systems which could be convenient for rotation-symmetrical shell structures. It is possible to plot user defined variables with the aid of the aforementioned User Supplied Subroutines. The interface of this post viewer is somewhat outdated and not that user-friendly.

*Midas FX+*: The other of the two available post processors for DIANA. It has a more user-friendly interface but it lacks functionality compared to iDIANA/FemView. For example: it is not possible to create a user defined local coordinate system other

than with the aid of changing the .dat file. It also seems more difficult to display user defined variables with this post processor.

*ParaView*: This post processor is not part of the TNO DIANA software package but it supports user defined quantities. However, it does not seem possible to create a user-defined local coordinate system.

Since the graduate has gained experience with all post processing options the choice for the most suitable post processor depends solely on the available functionality. In this case iDIANA/FemView is the most versatile option. However, it does not have the required functionality for computing the buckling load factor since it lacks any curvature analysis functionality. This functionality could be provided with a self-made tool in Grasshopper. This tool might then also be extended to perform a rain flow analysis.

## 1.7 EXISTING OUTPUT OPTIONS OF SOFTWARE PROGRAMS

The current output options available in the various software programs that are used during the graduation thesis were examined before developing the self-made post processor. These software programs can be divided into the following categories:

- Design software (Rhino);
- Pre processing;
- Structural analysis (DIANA);
- Post processing.

Each of these categories is individually discussed here below.

### 1.7.1 Rhinoceros

Rhinoceros, often abbreviated to Rhino, is a 3D-modeling software program and is the most suitable candidate for creating the design models of the shell structures used in this master graduation thesis. In comparison with CAD software such as AutoDesk's AutoCAD, Rhino supports the .IGES file format. IGES is short for Initial Graphics Exchange Specification and allows for modelling curved surfaces such as shell structures and import them into a pre processor such as FX+. Furthermore, Rhino has the availability of several useful plug-ins. The most important plug-in for this thesis is called Grasshopper. Grasshopper is a graphic algorithm editor which allows the user to combine different components into a parametric model. Each component consist of several lines of code that perform an operation on the input node of that component and put out the result at the output node of the component. In this way, it is very easy and intuitive for a structural engineer to create a computer program without having to write lines of code himself. In addition, Grasshopper allows for extended programming options as it supports the use of self made components that are written in Visual Basic or C#.

Rhino has a built-in function called curvature analysis which allows for checking the design of a shell structure by visualising the curvature of the shell in several ways. It can display the Gaussian curvature, the mean curvature and the maximal and minimal radius of curvature, all with the use of a contour plot.

Next to this Rhino has also a built-in function which allows for visualising changes in the curvature of a curved surface. These functions are called zebra analysis and environment map. The zebra analysis function projects black and white stripes on a surface in a vertical or horizontal pattern. Changes in curvature of the surface can be easily spotted as the width of the stripes changes.



Figure 1.17 – A display of a horizontal zebra analysis in Rhino.

The function environment map lets the user select an image or photo which is projected on and reflected from the surface. Irregularities in the image or photo denote changes in the curvature of the surface.



Figure 1.18 – A display of an environment map in Rhino.

### 1.7.2 DIANA

DIANA has disposition over the following analysis options that are interesting for this graduation research:

- Structural linear static analysis;
- Structural eigenvalue analysis;
- Structural stability analysis;
- Structural nonlinear analysis.

DIANA has the following output options available for post processing:

- Tabulated files (file format .tb);
- Femview (file format .M72 and .V72);
- Midas FX+ for DIANA (file format .dpb).

The first option creates output in text file in a tabulated fashion. The second and third options create output files for respectively iDIANA and FX+.

The following quantities can be computed by DIANA:

- Displacements;
- Forces;
- Strains;
- Stresses.

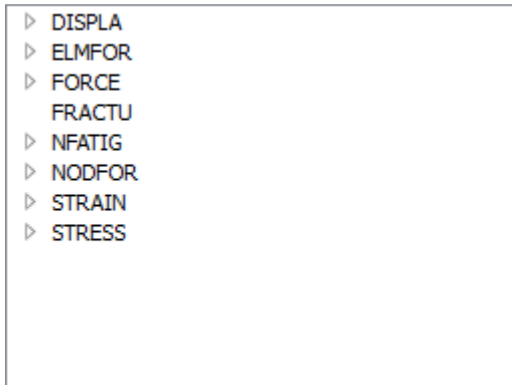


Figure 1.19 – The start of the result tree in DIANA displaying the available output options.

A distinction can be made in the displacements between translational displacements on one hand and rotational displacements on the other hand. The forces distinguish between external, internal, reaction and residual forces. Here also the distinction can be made between translational and rotational forces. The main output results for the stresses and strains are the distributed moments and forces which differentiate in a global or a local coordinate system.

There are two User Supplied Subroutines available that can be used to compute the additional quantities as described in paragraph 1.6. They are called USRMAT and USRSHL. USRMAT is an abbreviation of the words user and material which allows users to define their own stress-strain relationship. However, what makes USRMAT more valuable for this graduation thesis is that user defined quantities can be computed based on the stresses and strains. USRSHL is an abbreviation of the words user and shell and allows users to define new quantities based on the distributed moments and forces. With both User Supplied Subroutines the following quantities can be determined:

- The strain energy, both bending and membrane strain energy;
- The eccentricity of the normal force;
- The initial normal force, needed to compute the buckling load factor.

To compute the buckling load factor itself the surface curvature must also be known. To determine the curvature of a surface is something that cannot directly be done with the aid of User Supplied Subroutines. However, Rhino and Grasshopper have disposition over numeral functions to obtain the surface curvature in a given point. However, this causes the work flow to run out of the DIANA environment.

### 1.7.3 Post processors

For this master graduation research three post processors have been evaluated:

- iDIANA (FemView);
- Midas FX+;
- ParaView.

With all of the three post processors experience was gained in the past few years.

### iDIANA

Although its looks and interface are somewhat outdated, iDIANA is the most versatile of the three post processors. Examples of this versatility are the possibility for the user to create his own coordinate system (e.g. a cylindrical or spherical coordinate system for the rotation symmetric structures) and the ability to adjust the range of the displayed result. More important, it also supports the use of user-defined quantities.

### Midas FX+

Midas FX+ has the most user-friendly interface but it seems to lack support for different coordinate systems (although it supports a cylindrical coordinate system in its pre processor functionality) other than the rectangular one. The lack of supporting different coordinate systems aside from the rectangular coordinate systems might however be obviated by changing the .dat file before the structure analysis is performed. FX+ also does not seem to support other quantities than the already integrated ones.

### ParaView

ParaView supports user-defined quantities but it does not seem to support coordinate systems other than the rectangular coordinate system. However, like with FX+ this issue with the coordinate system might be obviated by changing the .dat file before analysing the structure.







## **2 SELF-MADE POST PROCESSOR**



## 2.1 DEVELOPMENT OF THE SELF-MADE POST PROCESSOR

The self-made post processor developed for this thesis has two main functionalities:

- Reprocessing the existing quantities into the aforementioned additional quantities;
- Displaying the results in a graphic way that is comparable with the graphic results of many other post processors.

The preferable method of post processing was to keep the whole process as much as possible within DIANA with the aid of User Supplied Subroutines. However, after considerable time there still were problems getting the programming environment of DIANA to work properly. At this point, an important choice was made between two different approaches that had a large impact on the remaining part of the graduation thesis, namely:

- Keep on trying getting DIANA's USS-functionality to work correctly, or;
- Switching to one of the different methods of post processing that were mentioned earlier in paragraph 1.6.

Many of the possible causes for the DIANA programming environment not working properly were already examined at the beginning of the development of the proof of concept of the self-made post processor. This made it more difficult to determine the cause of the problems as the list of likely possible causes grew short. A discussion with TNO DIANA in which multiple e-mails have been sent back and forth did solve some part of the problems but it did not manage to let DIANA's USS-functionality perform correctly. Another consideration that was influencing the difficult choice mentioned above was related to time pressure. It was difficult to estimate how much longer it would take in order to get the USS-functionality working properly and the need for showing some results to the exam committee increased over time. For mainly these two reasons it was decided to take a look at an alternative method of post processing to see if this could come up with some results in a shorter time span.

The following part of this chapter is divided into two sections. The first part discusses the problems that were encountered getting DIANA's USS-functionality up and running while it takes a look at possible causes and solutions to these problems. The second part discusses the new approach of post processing the additional quantities that eventually led to the method of post processing that has been used for the remaining part of this graduation thesis.

### 2.1.1 Development of the post processor within DIANA

For the usage of the TNO DIANA's User Supplied Subroutine functionality the following software is needed:

- DIANA itself;
- A license in which User Supplied Subroutine is enabled;
- The Intel Fortran Compiler for compiling User Supplied Subroutines written in Fortran 77 programming code into executable files;
- Microsoft Visual Studio for the integration of the Intel Fortran Compiler.

Because Intel only has a commercial version of their Fortran Compiler available, at first G95 (an open source Fortran 77/95 compiler) has been used instead of the Intel Fortran Compiler. Running the prompt '*diafck*' shows that G95 is recognised by the DIANA Command Box. The first problem that was encountered was related to some incorrect path settings in the installation of DIANA. This problem was caused due to the fact that DIANA was not given

administrator rights during installation. By acknowledging DIANA these rights the problem was resolved.

The second problem, also being the main problem that was never resolved, was related to the creation of object files. This problem resulted in the following error message:

*rcsmake: \*\*\*No rule to make target 'elsgus.obj', needed by 'nl41.exe'.*

To rule out any compatibility issues that might exist due to the use of G95 instead of the Intel Fortran Compiler a 30 day trial version of the Intel Fortran Compiler was installed. This resulted however in the same error message. Running the ifortvars.bat batch file in DIANA's Command Box indicated that the Intel Fortran Compiler was recognised correctly but it did not mention anything about Microsoft Visual Studio. This could denote an improper linkage between DIANA and Visual Studio.

To rule out any problems that could exist due to programming errors a User Supplied Subroutine was used of which it was known that it had worked before. The problems with the creating of the object files remained though. After adding of the associated object file by hand the following error message appeared:

*User supplied subroutine USRMAT not specified.*

On the DIANA support forum it was mentioned to someone who got the same error message that there was some incompatibility between his compiler and the version of DIANA he used. This could indicate to some incompatibility issues between either DIANA and Microsoft Visual Studio or between DIANA and the Intel Fortran Compiler. In the release notes manual belonging to the Intel Fortran Compiler it says that the used version of the compiler is compatible with the used version of Microsoft Visual Studio [21].

Another possible cause of DIANA being unable to generate object files might lay in the difference in age between the DIANA program version (version number 9.4.3) and the Intel Fortran Compiler. To avoid this possible cause a newer version of DIANA (version number 9.5) was installed. Unfortunately, this did not change a thing.

Although more recent versions of the Intel Fortran Compiler are in general backwards compatible with older versions of DIANA, this is not always the case. Due to the traditional method of using User Supplied Subroutines it is necessary that the User Supplied Subroutine is compiled in exactly the same manner as the DIANA program itself. To avoid these incompatibility issues altogether TNO DIANA introduced a newer method which uses Direct Link Libraries (DLL or .dll files). However, when using this method the following error message was displayed:

*error: can't open file uselas.obj for write  
compilation aborted for uselas.f90 (code1)*

It still was not possible to create object files. The latest possible cause suggested when discussing this issue with TNO DIANA was that there might be limitations in the trial version of the Intel Fortran Compiler regarding the creation of object files. Obtaining a fully licensed version just for this graduation thesis was far from realistic and financially feasible. Therefore it was decided to look into different methods of post processing that did not use DIANA's User Supplied Subroutines.

**2.1.2 Development of the post processor – the alternative way**

To quickly obtain some results after the sustaining problems with DIANA’s USS-functionality it was decided to go for a more straightforward approach with a high probability of success. With the aid of Excel it is rather easy to compute the additional quantities from the existing quantities obtained from a tabulated file. The additional quantities could then be displayed in iDIANA following the original plan by creating a FEMVIEW neutral file. Another alternative was to display the results in Rhino with the aid of Grasshopper. Now that it was decided to work around DIANA User Supplied Subroutines it was no longer needed to use one of DIANA’s post viewers to display the results. Furthermore, both Rhino and Grasshopper have a number of ways available for determining the curvature of a surface, an entry needed for the computation of the buckling load factor. By choosing to display the results in Rhino with the aid of Grasshopper, this meant that only one post viewing tool had to be developed.

Within two days such a tool was created and the first results could be displayed in Rhino. For this a square test surface was analysed. The display of the results in Rhino, in this case the displacements due to a distributed load acting on the right hand side of the test surface, were then compared with the display of the results in iDIANA. See figures 2.1, 2.2 and 2.3.

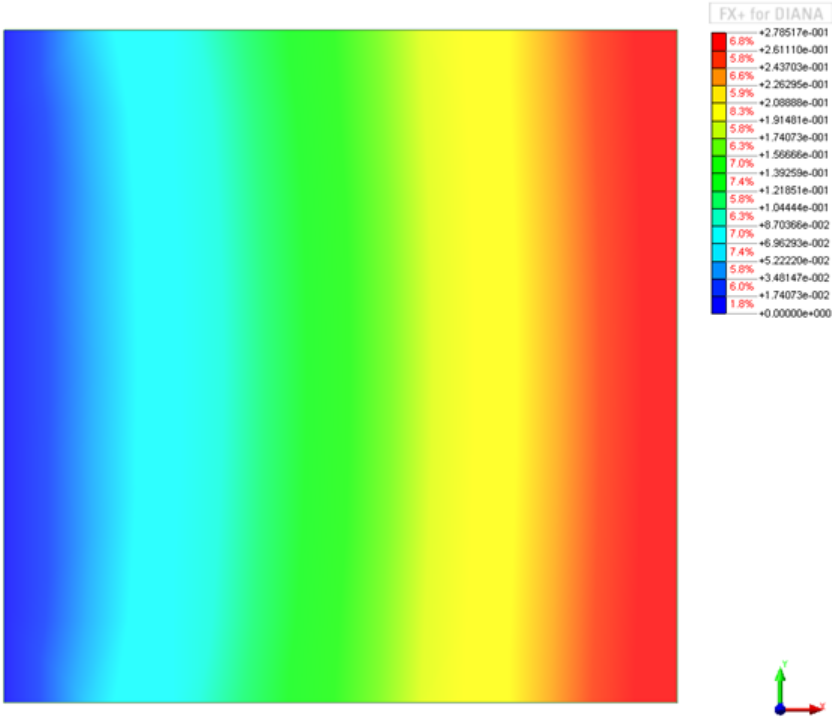


Figure 2.1 – Displacements as displayed by Midas FX+.

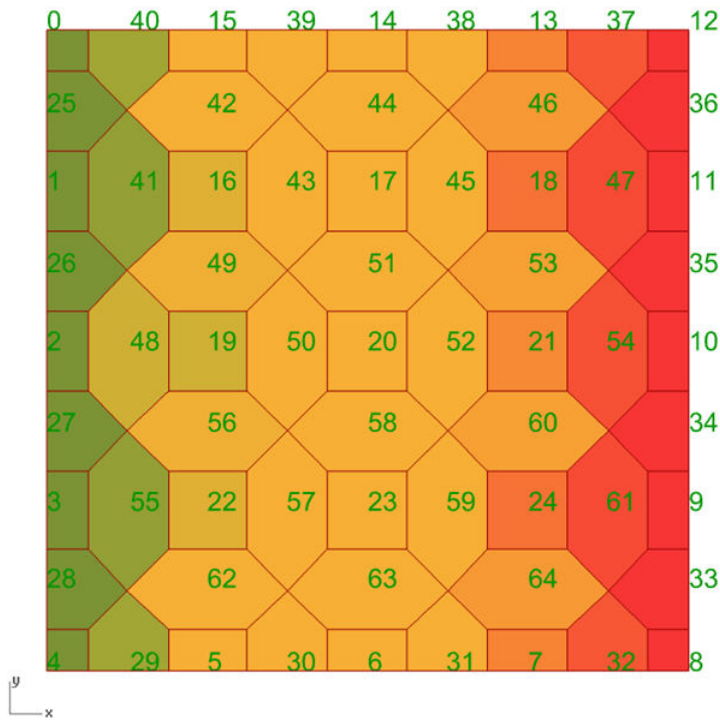


Figure 2.2 – First experimental way of displaying the displacement results by using Voronoi tessellation. The displayed numbers are the node numbers.

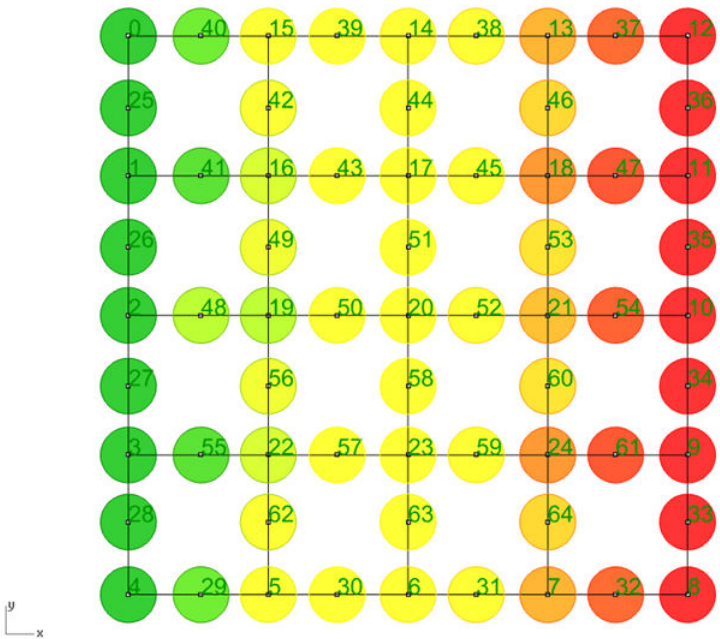


Figure 2.3 – Second experimental way of displaying the displacement results by using colour circles. The numbers displayed are the node numbers.

Figures 2.2 and 2.3 contain experimental ways of displaying the results. First to be used was the Voronoi diagram to display the results. A second way of displaying the results followed the first by using coloured circles. Both ways display the displacements in the nodes of the element. These displays show that the developed post viewing tool in Grasshopper worked correctly but the display of the results itself differed quite a lot from the display of the results in iDIANA. Therefore a third way of displaying the results was developed that uses the actual mesh created by DIANA's pre processor (see figure 2.4). Because DIANA cannot compute the



displacements in the integration points this third way of displaying the results has not been implemented in the square test surface model. The colours used in figure 2.4 have therefore no relations to any values of displacements or whatsoever. The use of the two different colours red and green is simply to illustrate the difference between quadrangular and triangular elements. Eventually this third way was used for displaying all the results for this graduation thesis.

For this final way of displaying the results, every element is divided into three or four sub surfaces, depending on the element being a triangular or a quadrangular one. Subsequently, the values of the different quantities have been determined at the location of the integration points instead of at the nodes. Each of the sub surfaces is then coloured according to the value of the quantity that occurs in the integration point that is contained within that sub surface. Due to this manner, a more similar way of displaying the results in comparison with iDIANA and FX+ is obtained.

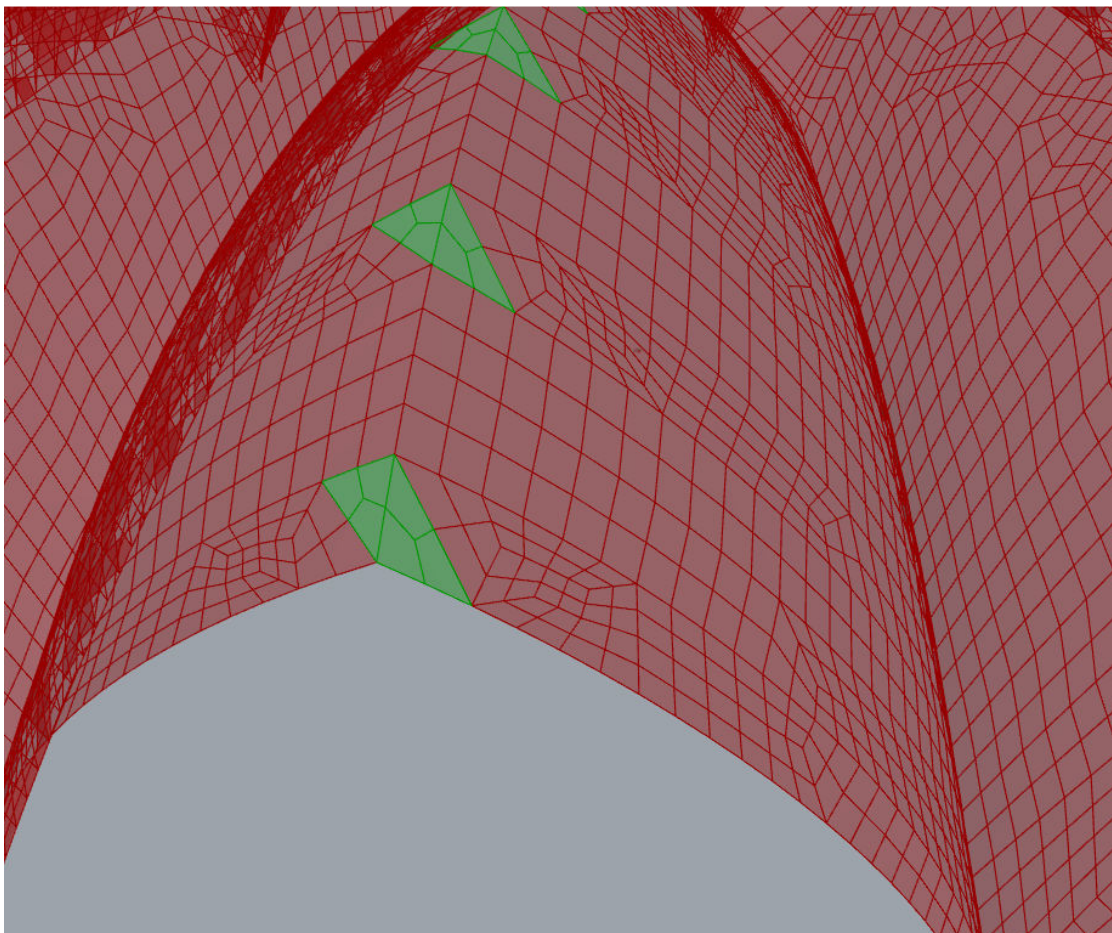


*Figure 2.4 – Different ways of dividing the quadrangular sub surfaces (in four ways, coloured red) and the triangular sub surfaces (in three ways, coloured green). In opposition to the figures with the experimental results mentioned before, the colours in this image do not have any relation to the values of any quantity. The difference in colour is only to be able to distinguish the triangular sub surfaces from the quadrangular sub surfaces.*

### **2.1.3 General set-up of the used post processing method**

The alternative post processing method used during this graduation thesis consists of three main steps. The first step is to compute all the required existing quantities at the location of the integration points and export the results into a tabulated file. This first step is contained in different .dcf files of which an example can be seen in appendix A. Using .dcf files not only

allows for computing the results in integration point instead of in nodes but it also automates and thus speeds up the analysis process. The second and third step consist of copy-pasting the results to Microsoft Excel respectively Grasshopper.

There are two reasons why the results from the tabulated files are copied to Excel first instead of copying them into Grasshopper directly. The first reason is that Excel has a function for converting lines of data into columns. DIANA writes the analysis results into tabulated files in lines in which the results from different quantities are separated by tabs. By using the “text-to-columns” functionality in Excel the lines of data can be separated at each tab and in this way can be converted into columns, each with its own quantity. This makes it easier to sort out the results before copy-pasting them into Grasshopper.

The second reason for using Excel is that it relieves Grasshopper when it is computing the additional results as Excel is much faster in executing the multitude of parametric operations than Grasshopper. Some computations however are more convenient to perform with the aid of Grasshopper. This is because some quantities such as stresses and strains are computed for each of the bottom, middle and top layer whereas other quantities such as the distributed forces and moments are only computed for the middle layer.

#### **2.1.4 Operation principal of the Grasshopper model**

The operation principal of the Grasshopper model consists of the following steps:

- Input of the coordinates of the nodes and integration points and the values of the desired quantity;
- Creating the mesh based on the connected node information;
- Dividing the elements into three or four sub-surfaces, each containing a single integration point;
- Adding values of the existing and some additional quantities and computing the values of the remaining additional quantities;
- Assigning colours to each sub surface corresponding with the value of the quantity in the integration point contained by the sub surface;
- Creating a legend and title for each display of results.

Each step is individually elucidated here below. The Grasshopper model is also prepared for implementation of the Rain Flow Analogy method, mentioned earlier in paragraph 1.4.3. The results of this can be seen in appendix G.

##### **Input of the coordinates of nodes and integration points**

The first step consists of copy-pasting the coordinates of the nodes and integration points from Excel to Grasshopper. Because each number component in Grasshopper containing these coordinates can only hold about 2,500 numbers they are combined in order to form the total list of x-, y- and z-coordinates.

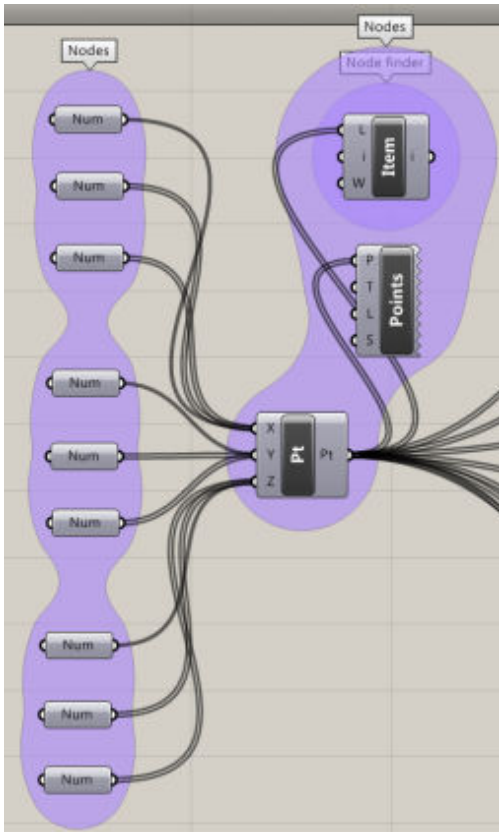


Figure 2.5 – Multiple number components containing the nodal coordinates are combined in a point component which creates the nodes. For the ease of use a point listing component numbering each node and a simple node finder are added.

### Mesh creation

The second step consists of adding the information which nodes are connected to each other to Grasshopper. Based on the nodal coordinates and this information a mesh is created. The mesh itself is based on the corner nodes of each element while the midside nodes are used for the determination of the midpoint of each element that is needed for subdivision of each element as is described in the next step.

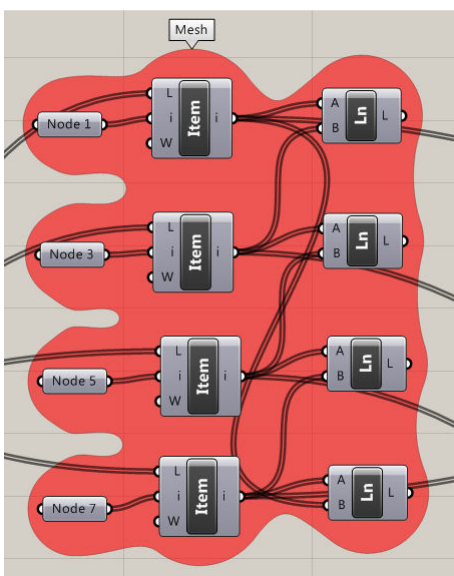


Figure 2.6 – The mesh is created based on the four corner nodes of each element.

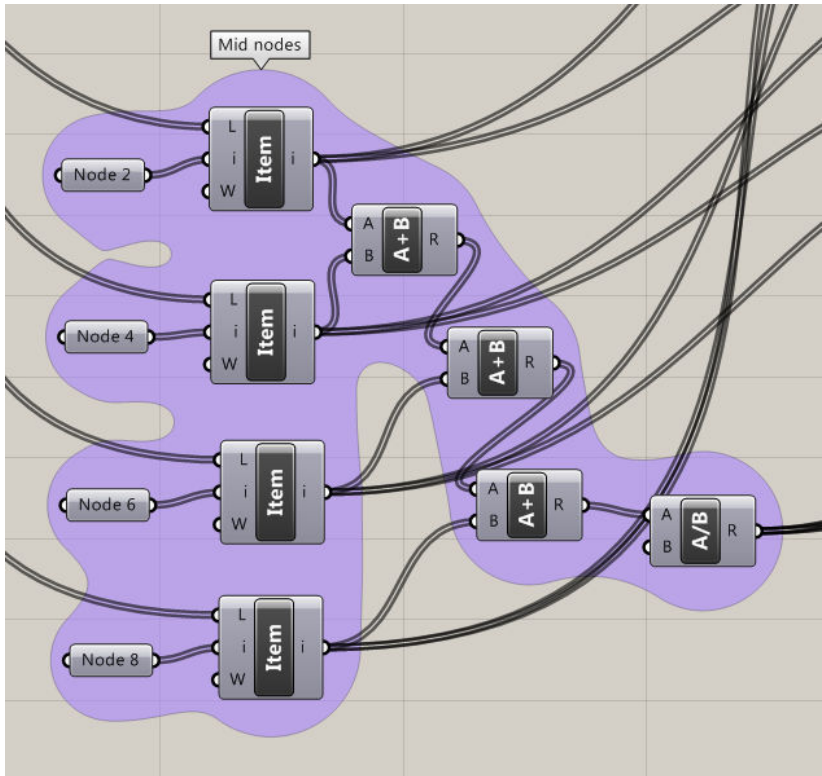


Figure 2.7 – The midside nodes are used in order to create an additional point in the middle of each element that is used to divide every element into sub-elements.

**Element subdivision**

The midpoints created at the second step are used in order to divide each element into sub-surfaces; four sub-surfaces for the quadrangular elements and three sub-surfaces for the triangular elements as can be seen in figure 2.8. In this way every sub-surface will contain exactly one integration point from each of the top, middle and bottom layer.

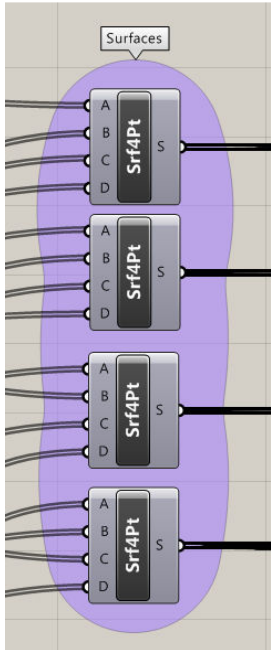


Figure 2.8 – Grasshopper components creating the sub-surfaces based on the corner nodes and the additionally created midpoint of each element.

### Adding of the quantity values

The most time-consuming step is the addition of existing quantities and the calculation of the additional quantities. As with the node and integration point coordinates the values of the different quantities are copy-pasted in multiple number components. These components are then combined into one list that is divided into three or four sub-lists, each containing the values for a specific sub-surface of each element. In order to adjust the range of values displayed the maximum and minimum value of each quantity is determined.

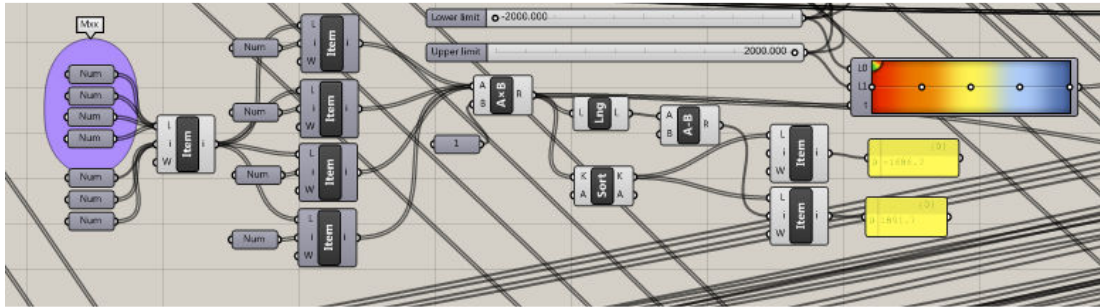


Figure 2.9 – From left to right: the number components containing the values of a quantity, the list component combining all these values, four list components creating sub-list for each specific sub-surface, some components to determine the upper and lower values of the list of quantity values and a colour slider assigning a colour to each value based on the range of values.

### Colouring the sub-surfaces

Based on the value of the different quantities in the integration points each sub-surface is assigned a corresponding colour as can be seen in figure 2.9.

### Creating the legend

In order to assess the different displays of results a legend has to be created indicating which colour is assigned to which value. The components in Grasshopper creating the legend for each quantity consist of two parts. The first part divides the colour slider into a number of ranges. Each colour range is then coupled to a certain value according to the range of the quantity being evaluated by the second part. The reason that this second part is separated from the first is that the value range for each quantity differs from the value ranges for the other quantities.

The most challenging aspect of creating the legend was the fact that it had to be displayed flat on screen in Rhino all of the times. Text components in Grasshopper are programmed in such a way that they do this automatically. When the view of the structure in Rhino is changed due to rotation of the structure the text from Grasshopper will still be displayed flat on screen. The coloured boxes however that indicated which colour represents which value do rotate along with the changed viewing angle of the structure. In order to overcome this issue a sort of control panel was created in the Grasshopper model in order to adjust the rotation and orientation of these coloured boxes according to the viewing angle in Rhino. This control panel consists of a couple of number components for the input of the camera and target coordinates obtained from Rhino by hand. The number of coloured boxes as well as their width and total height can be adjusted by changing a number component or by moving some sliders. With aid of the coordinate input it automatically determined how to rotate the legend's coloured boxes in order to be displayed flat on screen.



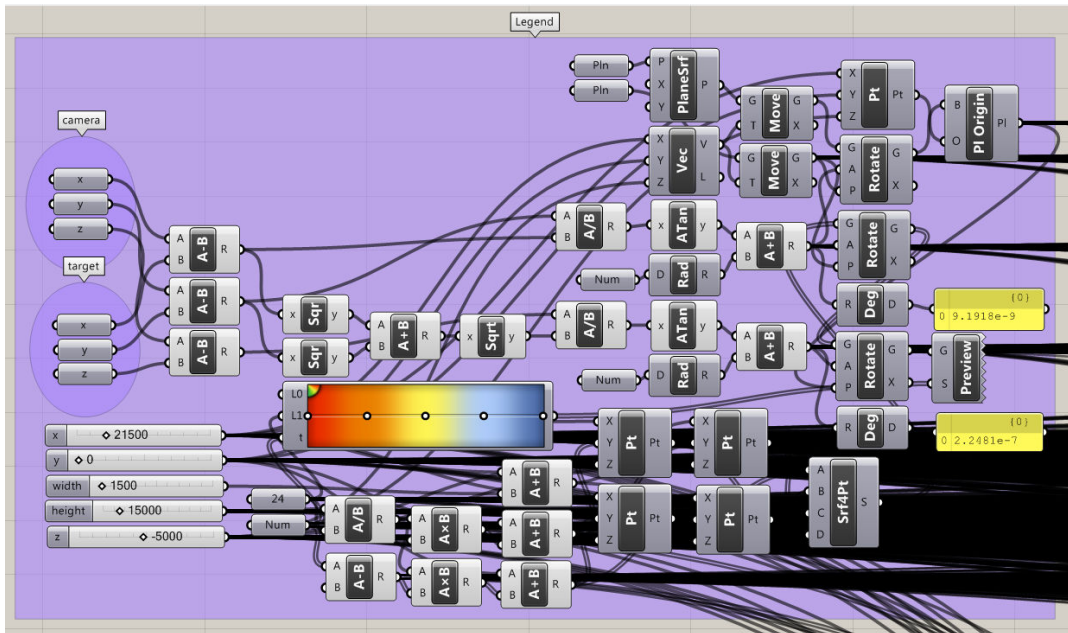


Figure 2.10 – The control panel for the orientation and rotation of the legend’s coloured boxes based on the camera and target location in Rhino is the first part that is needed for the creating of the legend.

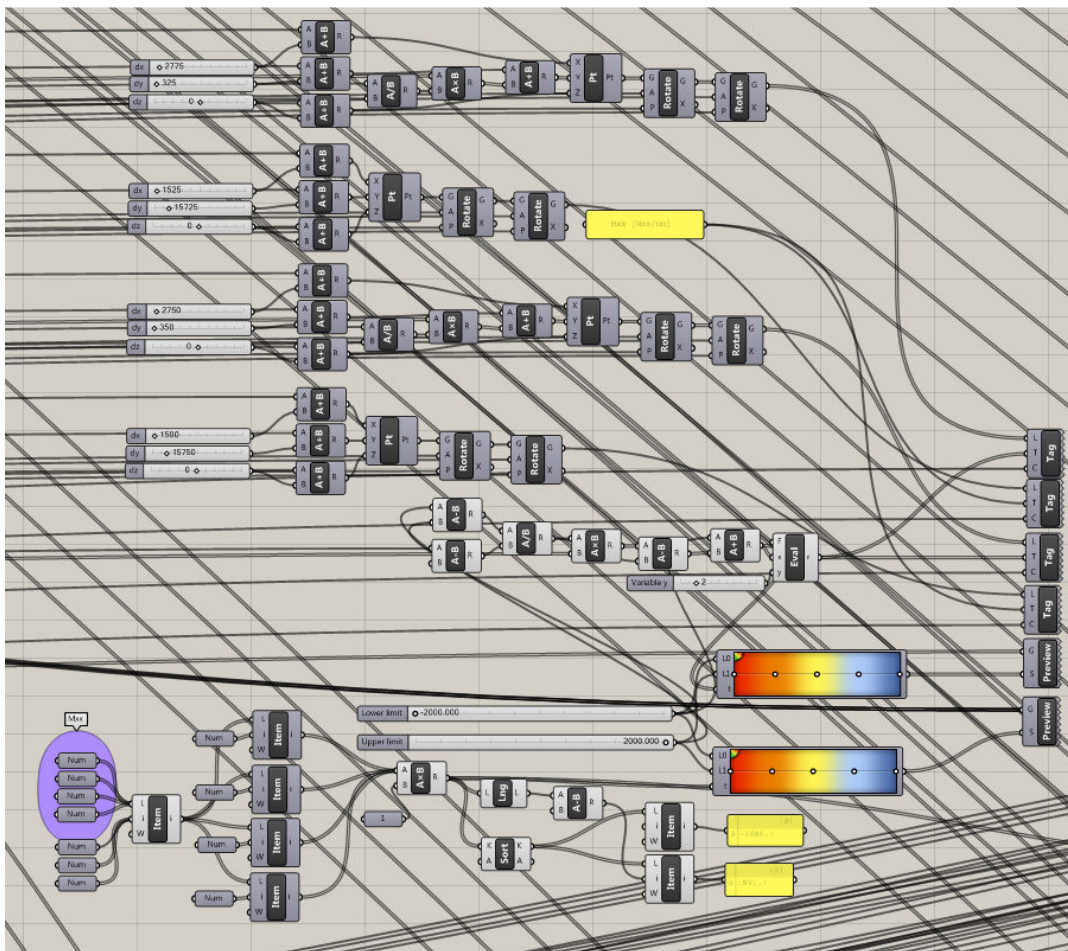


Figure 2.11 – The second part that is added to each quantity displays the title and values for each legend. The upper half is used to alter the display of both title and values. The bottom half processes the quantity itself as can be seen in figure 2.9. The six components at the very right hand side are the actual components that display the results and the legend.

### Vector plot functionality

To be able to create vector plots alongside the contour plots a vector plot functionality was added to the Grasshopper model. This function displays the principal directions by drawing lines in the associated directions through the integration point of each sub-element. The associated principal values are indicated by colouring the lines in the same way that is used for the contour plot functionality.

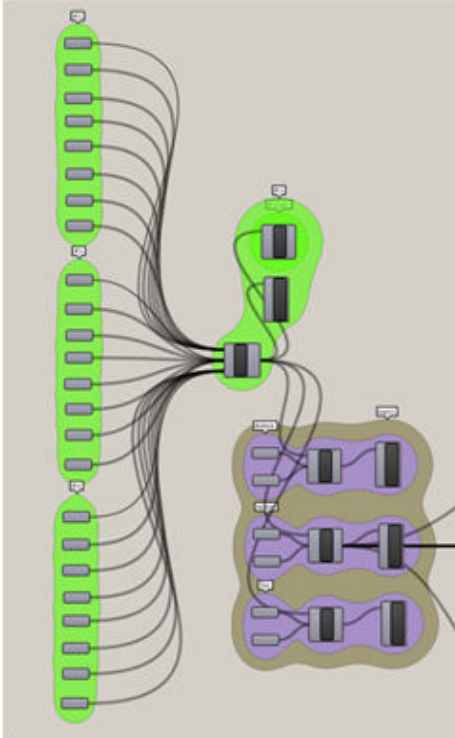


Figure 2.12 – At the left hand side the number components containing the coordinates of the integration points, connected to a point component creating the actual points with the addition of integration point labeller and an integration point finder. The list of integration points is subsequently divided over the bottom, middle and top layer by the components in the bottom right hand side corner.

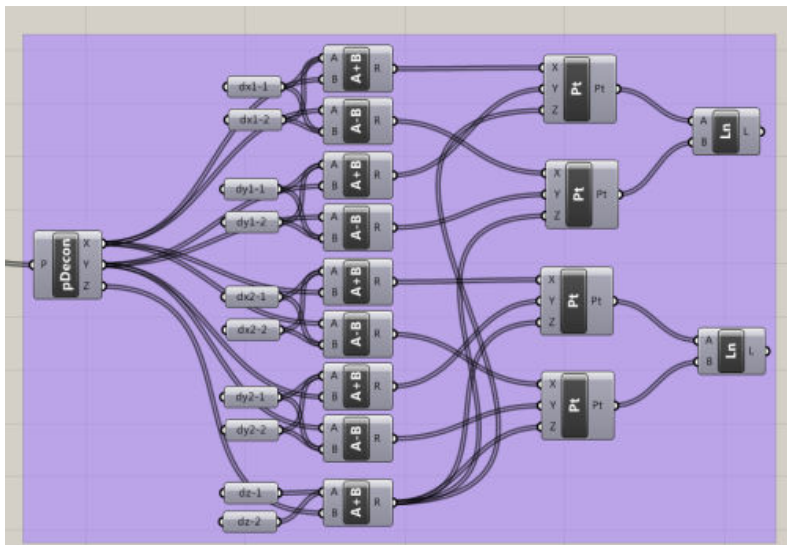


Figure 2.13 – Based on the middle layer of integration points and the principal directions compute in Excel the vector quantities are displayed as lines in the principal directions.

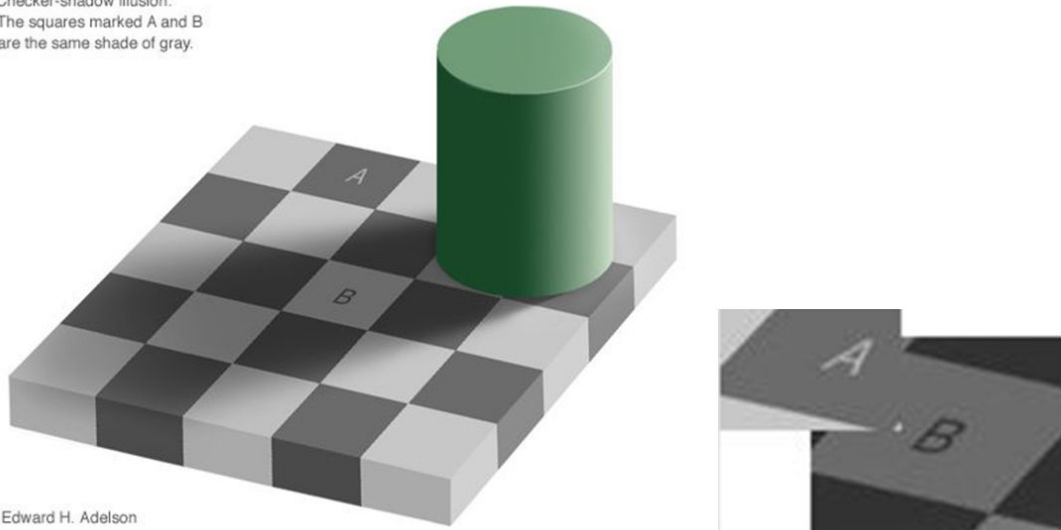
### 2.1.5 Limitations of developing a self-made post processing tool

Next to the limitations of developing a self-made post processor mentioned earlier in paragraph 1.2, using Rhino in combination with Grasshopper turned out to have some other limitations as well that turned up during the development of the Grasshopper post processing tool, namely:

- The amount of items a data component in Grasshopper can contain is limited to approximately 2500 numbers, depending on the number of figures per number. Each of the modelled shell structures contains about 400,000 to 900,000 numbers representing values of various quantities per load case. Due to this, some 320 to 720 sets of numbers had to be copy-pasted from Excel to Grasshopper. This made this particular way of creating a self-made post processing tool very labour intensive, time consuming and sensitive for errors. Furthermore, this prevented setting up a more parametric Grasshopper model in which multiple variations of a structure's design could be analysed, simply because every little change meant that all of the analysis data would have to be manually copy-pasted to Grasshopper again.
- The size of the Grasshopper models eventually grew so big that different loading cases had to be modelled in different Grasshopper files in order to keep the models workable. This prevented the combination of different load cases into load combinations. An extreme situation occurred when it took over half an hour for a Grasshopper model to be loaded into the computer program and for all parametric components to run. This situation occurred on a fairly new desktop computer with a fast quad core processor, 8 GB of ram and an SSD on which Rhino and Grasshopper were installed and from which the program data was loaded and saved to. This limited the productivity of the tool in some way.
- Limitations of the curvature analysis component in Grasshopper allow for only surface to be analysed per component. This means that design models existing of multiple surfaces are more demanding to analyse as each surface has to be manually linked to its associated surface analysis component. Another issue that plays a large part in this is that the linkages of the surfaces to the surface analysis components are not saved in any way. So each time a Grasshopper model is loaded these linkages have to be recreated manually. Not being able to analyse a structure's curvature means that the buckling load factor cannot be computed for this structure. Rhino has a function available for joining multiple surfaces into one surface. However, Grasshopper fails at this point as it still recognises different sub surfaces.
- Rhino is a 3D modelling program that uses a light source to give 3D models a more three dimensional look on the computer screen by creating shadows and thus the sense of dept. This change in the amount of light and also the reflection of the light by the structures lead to a distortion in the display of the colours representing the result values. The apparent difference in colours due to a shadow is called the checker board effect, see figure 2.14. Within Rhino a various number of render options is available from which the best one was selected that caused the least amount of distortion.



Checker-shadow illusion:  
The squares marked A and B  
are the same shade of gray.



Edward H. Adelson

*Figure 2.14 – The checker board effect. Although it looks like square A and B have different colours on the left, their colour is actually the same as can be seen on the right when the squares are put close together [22].*

## 2.2 THE MECHANICS OF THE NEW QUANTITIES

The main goal of this paragraph is to explain how exactly the additional quantities have been determined on the base of the existing quantities. It was decided to determine the degree of being a shell or a plate structure with the aid of the quantity strain energy, as was suggested in paragraph 1.5. Therefore, from this point forward the degree of being a shell or a plate structure is included with the strain energy paragraphs and will be referred to as  $U_\alpha$  (see equation 2-11).

### 2.2.1 Strain energy

From paragraph 1.5, the following definitions of the in-plane and the out-of-plane strain energy are known:

In-plane strain energy:

$$U_{in-plane} = \frac{1}{2} n_{xx} \varepsilon_{xx} + \frac{1}{2} n_{xy} \gamma_{xy} + \frac{1}{2} n_{yy} \varepsilon_{yy} \quad (2-1)$$

Out-of-plane strain energy:

$$U_{out-of-plane} = \frac{1}{2} m_{xx} \kappa_{xx} + \frac{1}{2} m_{xy} \rho_{xy} + \frac{1}{2} m_{yy} \kappa_{yy} + \frac{1}{2} q_x \gamma_{xz} + \frac{1}{2} q_y \gamma_{yz} \quad (2-2)$$

All the quantities at the right hand side of these equations can be extracted from DIANA with the exception of the curvatures. The curvatures are computed in the following manner:

$$\kappa_{xx} = \frac{\varepsilon_{xx,top} - \varepsilon_{xx,bottom}}{t} \quad (2-3)$$

$$\kappa_{yy} = \frac{\varepsilon_{yy,top} - \varepsilon_{yy,bottom}}{t} \quad (2-4)$$

$$\rho_{xy} = \frac{M_{xy}}{D \cdot \frac{1-\nu}{2}} \quad (2-5)$$

with:

$$D = \frac{1}{12} \cdot \frac{E \cdot t^3}{1-\nu^2} \quad (2-6)$$

Based on the in-plane and out-of-plane strain energy multiple combinations have been analysed:

$$\bullet \quad U_{in-plane} + U_{out-of-plane} \quad (2-7)$$

$$\bullet \quad \frac{U_{in-plane}}{U_{out-of-plane}} \quad (2-8)$$

$$\bullet \quad \frac{U_{in-plane}}{U_{total}} \quad (2-9)$$

$$\bullet \quad \frac{U_{out-of-plane}}{U_{total}} \quad (2-10)$$

$$\bullet \quad \frac{U_{in-plane} - U_{out-of-plane}}{U_{total}} \quad (2-11)$$

The first combination is called  $U_{total}$  (or  $U_t$  for short). The latter combination is called  $U_\alpha$  and this represents the degree of being a shell or a plate structure. Absence of out-of-plane strain energy would lead to  $U_\alpha = 1$ ; Absence of in-plane strain energy would lead to  $U_\alpha = -1$ . Values of  $U_\alpha$  close or equal to 1 can then be considered desirable since this means that a shell structure is loaded almost entirely in its plane. Values of  $U_\alpha$  close or equal to -1 on the other hand are undesirable as they indicate that the structure is mainly loaded out of its plane.

### 2.2.2 Eccentricity of the normal force

As was mentioned before in paragraph 1.5 the eccentricity of the normal force is a vector quantity. More to the point, it is a tensor, just like the bending moment and the normal force itself that are required to compute the eccentricity of the normal force.

If the relation between the three different tensors is defined as follows:

$$\underline{M} = \underline{N} \cdot \underline{E} \quad (2-12)$$

then the eccentricity tensor can be computed in the following way:

$$\underline{E} = \underline{M} \cdot \underline{N}^{-1} \quad (2-13)$$

or, in expanded format:

$$\begin{bmatrix} e_{xx} & e_{xy} \\ e_{yx} & e_{yy} \end{bmatrix} = \begin{bmatrix} m_{xx} & m_{xy} \\ m_{yx} & m_{yy} \end{bmatrix} \cdot \frac{1}{\det(\underline{N})} \begin{bmatrix} n_{yy} & -n_{xy} \\ -n_{yx} & n_{xx} \end{bmatrix} \quad (2-14)$$

with:

$$\det(\underline{N}) = n_{xx}n_{yy} - n_{xy}n_{yx} \quad (2-15)$$

All the quantities on the right hand side of these two equations can be derived from the output of DIANA.

If the non-diagonal terms of the eccentricity tensor are expanded (i.e.  $e_{xy}$  en  $e_{yx}$ ), the following is obtained:

$$e_{xy} = m_{xx} \cdot \frac{1}{\det(\underline{N})} \cdot -n_{xy} + m_{xy} \cdot \frac{1}{\det(\underline{N})} \cdot n_{xx} \quad (2-16)$$

$$e_{yx} = m_{yx} \cdot \frac{1}{\det(\underline{N})} \cdot n_{yy} + m_{yy} \cdot \frac{1}{\det(\underline{N})} \cdot -n_{yx} \quad (2-17)$$

It can be seen that these two terms differ from one another. This poses a problem as a non-symmetrical matrix cannot be a tensor. In other words: This would mean that the eccentricity computed in this manner is only a mathematical quantity and not a physical quantity. Tensors are independent of the orientation of the coordinate system which these non-diagonal terms do not seem to be.

Coordinate system dependency can be considered as unwanted as it makes it more difficult to interpret the results for shell structures with a more complex geometry. Therefore, the eccentricity of the normal force is computed in a second way. In this new way, the bending moments and normal forces are taken into account in the principal directions of the bending moments. This leads to the following definitions for the eccentricity of the normal force:

$$e_{\alpha M_1} = \frac{M_1}{N_{\alpha M_1}} \quad (2-18)$$

$$e_{\alpha M_2} = \frac{M_2}{N_{\alpha M_2}} \quad (2-19)$$

where  $\alpha M_1$  and  $\alpha M_2$  are the principal directions belonging to the principal values of the bending moment  $M_1$  respectively  $M_2$ .

### 2.2.3 Buckling load factor

For the four analysed structures, the following definition for the critical membrane force holds:

$$n_{cr} = \frac{-1}{\sqrt{3 \cdot (1 - \nu^2)}} \frac{Et^2}{a} \quad (2-20)$$

With:

$$\nu = 0.2 \quad (2-21)$$

the definition of the critical membrane force simplifies to:

$$n_{cr} = -0.6 \frac{Et^2}{a} \quad (2-22)$$

The buckling load factor is defined for this thesis as:

$$\lambda = \frac{n_{initial}}{n_{critical}} \leq 1 \quad (2-23)$$

where  $n_{initial}$  is the actual membrane force acting within the structure. It is important to stipulate that for the calculation of the critical membrane force, the direction of the curvature of the structure that has to be taken into account is perpendicular to the direction of the membrane force itself. To determine the normative critical membrane force the smaller of the two principal radii has to be used. The determination of the normative buckling load factor is more complicated, since it also depends on the actual membrane force. If the principal directions of the initial membrane force and the surface curvature differ, it is more complicated to determine what the normative value of the buckling load factor is.

Grasshopper, the plug-in for Rhinoceros, has two different components to determine the curvature of a surface. With the first component, the two main principal curvatures can be determined. With the second component, the mean and Gaussian curvature can be determined. For some reason the values obtained with the first component turned out to be wrong. So, in order to determine the principal curvatures, they had to be computed from the mean and Gaussian curvature values. For this, the following formula was used:

$$k_{1,2} = k_M \pm \sqrt{k_M^2 - k_G} \quad (2-24)$$

#### 2.2.4 Out of balance of the in-plane shear force

During one of the meetings with the direct supervisor about the mechanics of shell structure it was discussed how FEA-programs determine the in-plane shear force. Basic structural mechanics assume  $n_{xy}$  to be equal to  $n_{yx}$ . However, there is a small difference between these two. FEA-programs cope with this difference by averaging the two shear components as follows:

$$n_{xy}^* = \frac{n_{xy} + n_{yx}}{2} \quad (2-25)$$

where  $n_{xy}^*$  is used replacing the original  $n_{xy}$  and  $n_{yx}$ .

During this discussion it was suggested to investigate if the difference between the two in-plane shear force components  $n_{xy}$  and  $n_{yx}$  duly was negligible and if it possibly could be used as an indicator for the quality of the structural behaviour. This difference between the two shear components is labelled as the out of balance of the in-plane shear force in this thesis and is discussed in this paragraph.

The following Sanders-Koiter equilibrium equation:

$$k_{xy} (m_{xx} - m_{yy}) - (k_{xx} - k_{yy}) m_{xy} + n_{xy} - n_{yx} = 0 \quad (2-26)$$

can be rewritten to define the difference between the two shear components as follows:

$$dN = n_{xy} - n_{yx} = m_{xy} (k_{xx} - k_{yy}) - k_{xy} (m_{xx} - m_{yy}) \quad (2-27)$$

When analysed in the principal directions of the shell curvature the definition of  $dN$  can be rewritten as:

$$dN = n_{xy}^- - n_{yx}^- = m_{xy}^- (k_1 - k_2) \quad (2-28)$$

where  $n_{xy}^-$ ,  $n_{yx}^-$  and  $m_{xy}^-$  are the shear forces respectively moment in the principal directions of the shell curvature.

When a closer look is taken to the structures to be analysed, it turns out that:

Ellipsoid:	$k_1 = k_2$	$\rightarrow$	$dn = 0$
Hyperboloid:	$k_1 \neq k_2, k_2$ is constant	$\rightarrow$	$dn = h \cdot c \cdot m_{xy}^-$
Hypar:	$k_1 \neq k_2, k_1$ and $k_2$ are not constant	$\rightarrow$	$dn = (\dots) \cdot m_{xy}^-$
Complex geometry:	$k_1 = k_2$	$\rightarrow$	$dn = 0$

When the two principal curvatures are equal to one another the unbalance of the in-plane shear force is zero by definition. For this reason this quantity was only analysed and researched for the hyperboloid and the hypar, since the ellipsoid and the complex geometry consist of spherical parts only.

### 2.2.5 Out of balance of the in-plane shear eccentricity of the normal force

As with the out of balance of the in-plane shear force the two non-diagonal terms of the eccentricity matrix differ from each another, as was seen in paragraph 2.2.2 of this chapter. Subtracting the two non-diagonal terms from one another results in the following equation for the – in this graduation thesis so-called – out of balance of the in-plane shear eccentricity of the normal force:

$$de = e_{xy} - e_{yx} = \frac{m_{xy} (n_{xx} - n_{yy}) + n_{xy} (m_{yy} - m_{xx})}{\det(\underline{N})} = \frac{m_{xy} (n_{xx} - n_{yy}) - n_{xy} (m_{xx} - m_{yy})}{n_{xx} n_{yy} - n_{xy}^2} \quad (2-29)$$

What is noticeable is that the numerator of the right hand side of the equation has a similar form in comparison with the modified Sanders-Koiter equation mentioned in paragraph 2.2.4. It is not clear as what this quantity represents but, because of the aforementioned similarity, it was decided to research this quantity further. In opposition to the coordinate system dependency of the eccentricity of the normal force itself, this new quantity is coordinate system independent.

### 2.2.6 Principal directions

The following formulas have been used for the determination of the principal values and the principal directions. In these equations the quantity distributed bending moment  $M$  is being used:

#### Principal values

$$m_{1,2} = \frac{1}{2}(m_{xx} + m_{yy}) \pm \sqrt{\left[\frac{1}{2}(m_{xx} - m_{yy})\right]^2 + k_{xy}^2} \quad (2-30)$$

#### Principal directions

$$\tan(2\alpha) = \frac{m_{xy}}{\frac{1}{2}(m_{xx} - m_{yy})} \quad (2-31)$$

$$\alpha = \frac{1}{2} \cdot \tan^{-1} \left[ \frac{m_{xy}}{\frac{1}{2}(m_{xx} - m_{yy})} \right] \quad (2-32)$$

#### Rotational matrix

$$\underline{R} = \begin{bmatrix} \cos(\alpha) & \sin(\alpha) \\ -\sin(\alpha) & \cos(\alpha) \end{bmatrix} \quad (2-33)$$





### **3 ANALYSIS AND STUDY RESULTS**



## 3.1 DEFINITION OF SCOPE

Although several project boundaries were set at the start of the thesis, it turned out there were still some variables on which decisions had to be made. This paragraph illustrates the determination process of these variables, which are:

- The type of structural analysis;
- Material usage;
- Shell thickness and element type to be used.

Before these items will be discussed individually, the main goal of this graduation thesis will be reflected upon.

### 3.1.1 General definition of scope

The main focus point of this graduation thesis is to gain insight in the qualitative mechanical behaviour of shell structures. This means that a well defined structural design and an appropriate mechanical model are important to obtain correct and useful results. Matters like building codes which prescribe certain structural thickness for instance are considered to be less important for this thesis.

### 3.1.2 Type of structural analysis

Considering the main focus point of this thesis it was decided to opt for the linear analysis of the structures. Although some research that was found during the literature study suggested different strain energy results between linear and non-linear analysis [5], this would make matters far more complicated. Besides, it was not known how big of an issue this difference might be for assessing the qualitative structural behaviour based on strain energy. In order to keep matters getting too complicated, it was decided to start with linear analysis and if time would let it, some additional research might be put in non-linear analysis.

### 3.1.3 Material usage

The obvious choices for material usage are concrete, steel and possibly timber. Since it was decided to use plain linear analysis and accounting for the fact that this thesis was mainly focussed on the qualitative side of different quantities instead of the quantitative side, the choice for a specific material is less of an influence. So, for this reason the use concrete was chosen as many shells have been built from concrete.

### 3.1.4 Shell thickness and element type

The shell thickness depends on the selected building material and it influences the choice of element type. Regarding the shell thickness the following distinction can be made [4]:

- *Very thick shell*: needs to be modelled three-dimensionally; structurally it is not a shell;
- *Thick shell*: membrane forces, out of plane moments and out of plane shear forces occur; all associated deformations need to be included in modelling its structural behaviour ( $a / t < 30$ );
- *Thin shell*: membrane forces and out of plane bending moments occur; out of plane shear forces occur, however, shear deformation is negligible; bending stresses vary linearly over the shell thickness ( $a / t > 30$ );
- *Membrane*: membrane forces carry all loading; out of plane bending moments and compressive forces are negligible; for example a tent.

The analysed shell structures in this graduation research can be classified as thin shells.

Two different types of elements can be distinguished: 2D shell elements or 3D volume elements (see also figure 3.1). Using shell elements is more straightforward whereas the use of volume elements can lead to more accurate results in some specific cases. Since the shell structures to be analysed are all thin shell structures and because the post processing part for the shell element type is easier to implement, it was decided to perform the analyses with shell elements.

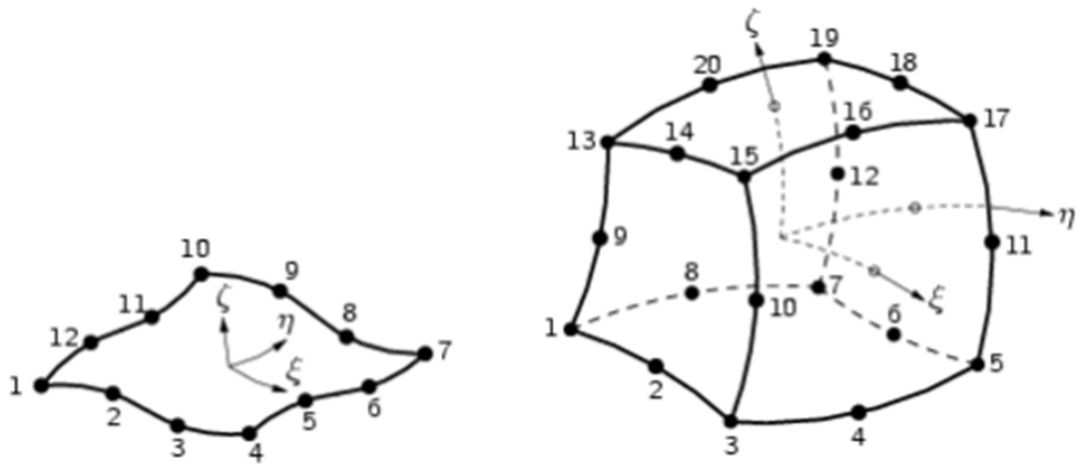


Figure 3.1 – On the left: a shell element; on the right: a 3D volume element [14].

### 3.2 MODEL SET-UP

This paragraph describes the parameters used for all the structures during the analysis research.

#### 3.2.1 Dimensions

The following three basic type of shell structure were the first to be modelled and analysed:

- The ellipsoid;
- The hyperboloid;
- The hypar (hyperbolic paraboloid).

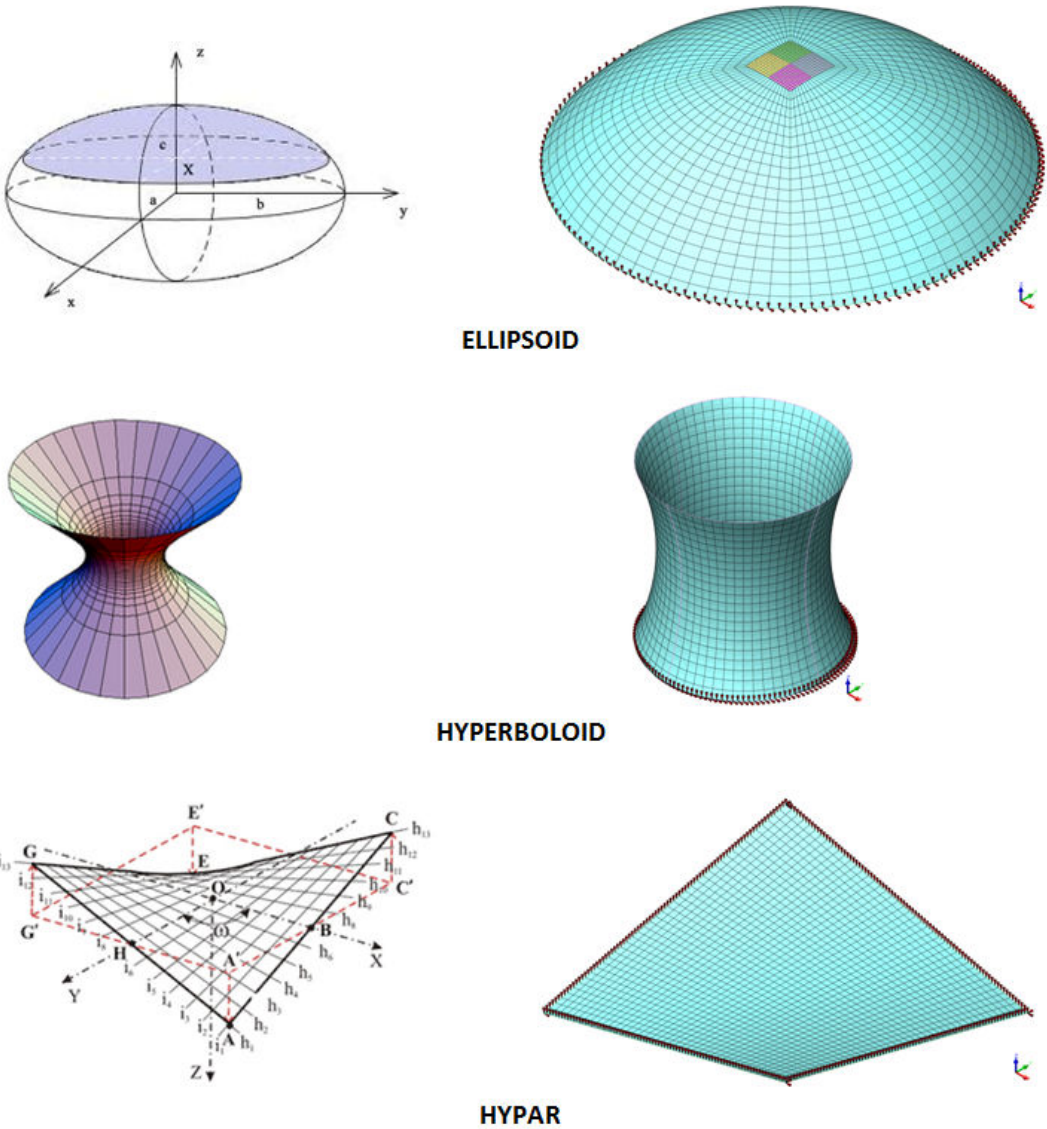


Figure 3.2 – The three basic type of shell structures that were modelled during this graduation thesis. On the left some general images, on the right results after meshing the structures in Midas FX+ [16] [18] [19].

ELLIPSOID			HYPERBOLOID			HYPAR		
Height	10	[m]	Height	20	[m]	Height	5	[m]
Diameter	40	[m]	Diameter	20	[m]	Length	20	[m]
Thickness	100	[mm]	Thickness	100	[mm]	Width	20	[m]
# Elements	16140		# Elements	5084		Thickness	100	[mm]
						# Elements	1681	

Table 3-1 – Dimensions and number of elements for the basic type of shell structures.

Next to these three basic types of shell structures a more complex shell structure has been modelled and analyzed in consequence of the first meeting of the graduation committee. This to map out the existing output options of current FE programs. For this complex shell structure the model was used of a design that was created before this graduation thesis.

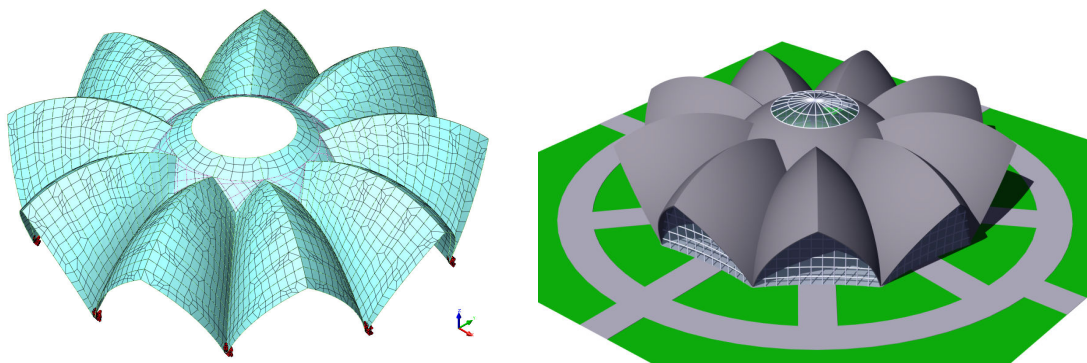


Figure 3.3 – On the left side: the mesh of the complex geometry. On the right side: a rendered image of the complex geometry, complete with roof and side panel windows.

COMPLEX GEOMETRY		
Height	12,5	[m]
Diameter	22,5	[m]
Thickness	200	[mm]
# Elements	13740	

Table 3-2 – The dimensions and number of elements for the complex geometry.

### 3.2.2 Material properties

The following material properties have been used:

#### Concrete C45/55

Elasticity modulus:  $E = 36,000 \text{ [N/mm}^2\text{]}$

Poisson ratio:  $\nu = 0.2$

### 3.2.3 Coordinate systems

The orientation of the coordinates systems in which the results are displayed are the following:

- Ellipsoid - Local cylindrical coordinate system;
- Hyperboloid - Local cylindrical coordinate system;
- Hypar - Local rectangular coordinate system;
- Complex geometry - Local cylindrical coordinate system.

See also appendix B for illustrations.

### 3.2.4 Boundary conditions

The little red arrow heads in figures 3.2 and 3.3 indicate the supports for the analysed structures. The ellipsoid and the hyperboloid are pinned around their bottom edge meaning all translations are equal to zero and all rotations are undetermined. The hyper is only supported in vertical direction around its edges. The four corner nodes however are supported in horizontal direction as well. The complex geometry is pinned at all nine corner points where the geometry touches the ground.

### 3.2.5 Loads

Two different loading conditions can be distinguished:

- Self weight;
- Wind load ( $1 \text{ kN/m}^2$  in global x-axis direction) over the whole body of the structure.

Due to limitations of Grasshopper it was not possible to create a load combination of these loads.

### 3.3 ANALYSIS RESULTS

The following quantities have been analysed during this graduation thesis:

- Strain energy (together with the degree of being a shell or a plate structure);
- Eccentricity of the normal force;
- Buckling load factor.

Next to these quantities, the out of balance of the in-plane shear force and the out of balance of the in-plane shear eccentricity of the normal force were also analysed. Each of these results will be discussed and assessed separately in the following paragraphs. For the ease of reading small thumbnail images of the results have been added to these paragraphs. Full size images can be found in appendix D.

#### 3.3.1 Strain energy

As mentioned before in paragraph 1.5, it is possible to combine the in-plane and out-of-plane strain energy in several different ways in order to obtain better insight in their reciprocal relationship and by doing so obtaining more insight in the efficiency of the shell behaviour of the different analysed structures. It was noticed that two combinations in particular were interesting, namely:

- The total amount of strain energy  $U_t$ ;
- The difference of the in-plane and out-of-plane strain energy divided by the total amount of strain energy, also known as  $U_\alpha$  or the degree of being a shell or a plate structure.

The reason the total amount of strain energy was considered as an interesting quantity was mainly based on the ability to compare different versions of a particular type of structure with each other. Due to a major change in the framework of the post processor as is described in chapter 2 and the additional amount of time and labour that it comes with it, no additional effort was spend in researching the four analysed structures with varying parameters. This means that for each of the four structural types only one version was modelled and analysed which in turn reduces the added value in some extent that the total amount of strain energy otherwise might have contributed to this graduation thesis.

During this graduation thesis all the different combinations of strain energy mentioned in paragraph 1.5 were analysed and researched. However, since none of them seemed to have an added value over the quantities  $U_t$  and  $U_\alpha$  it was decided to incorporate only these latter two quantities in this graduation report.

#### Self weight

The first load case that was analysed was the load case self weight. One striking aspect is that the ellipsoid and the hyperboloid seem to be very efficient shell structures, as can be noticed by extreme high values of  $U_\alpha$ . Near the supports, the value of  $U_\alpha$  reduces slightly. This is due to increasing values of the out-of-plane strain energy near the supports which are caused by hindered deformation due to the support conditions which causes the deformed geometry to bent back to its supports. Regarding the philosophy behind the quantity  $U_\alpha$  both structures could be improved by increasing the shell behaviour near the supports. This would involve allowing the supports to move in a horizontal way in order to prevent hindered deformations. This would however likely be a very expensive and not very practical solution. One could also conclude that, since all values of  $U_\alpha$  are larger than 0.95, these structures are



already as good as can be and that further improvements of the factor  $U_\alpha$  do not outweigh the associated costs.

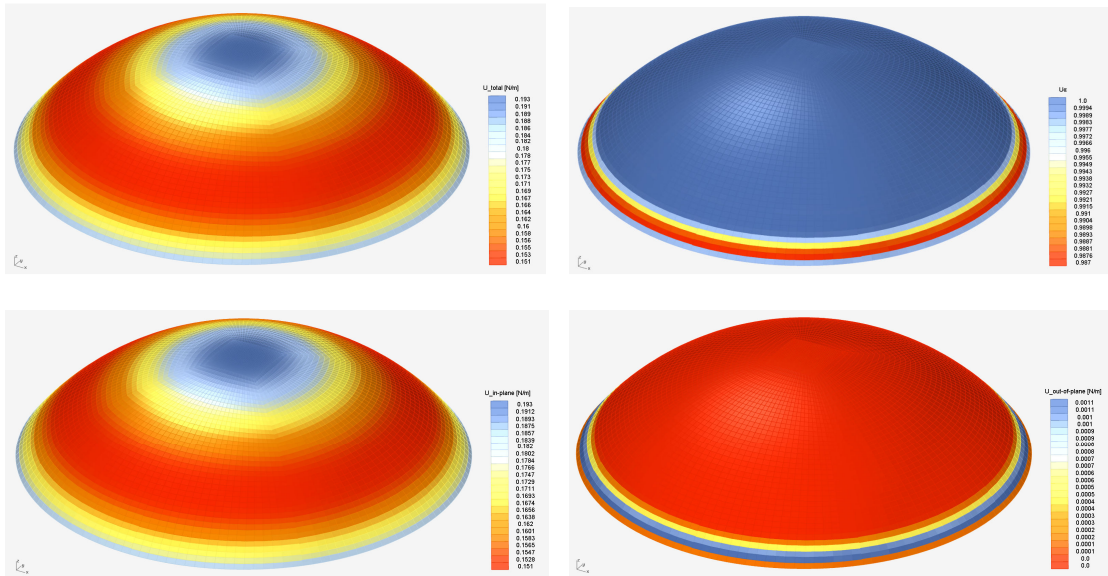


Figure 3.4 – The strain energy results for the ellipsoid for the loading condition self weight.

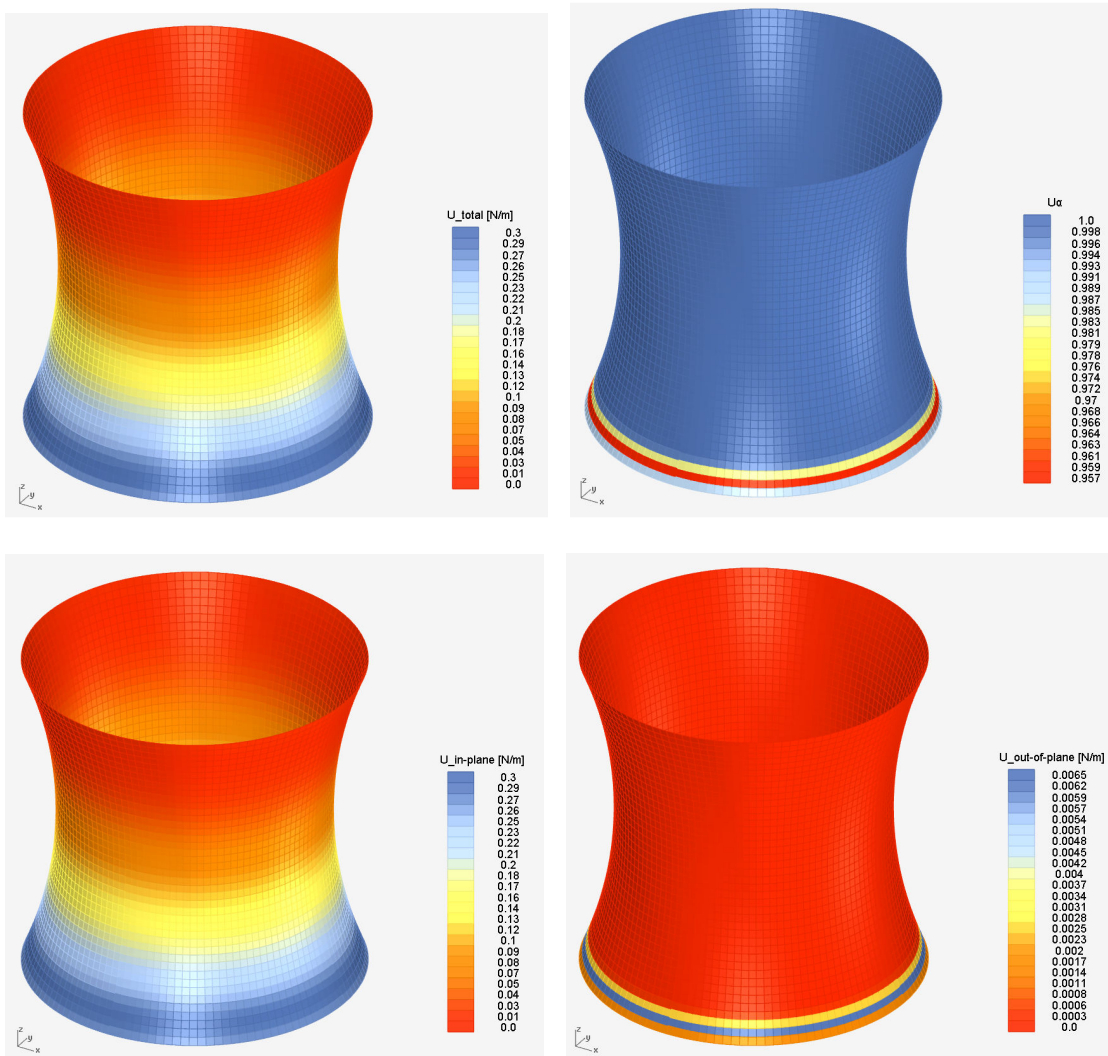


Figure 3.5 – The strain energy results for the hyperboloid for the loading condition self weight.

The lowest value of  $U_\alpha$  occurring in case of the hypar is -0.58. This value occurs in the middle of the edges of the structure. This rather low value of  $U_\alpha$  indicates that the structure is acting more like a plate than a shell in these edge locations. This is mainly due to the large moment near the edges, again caused by hindered deformation of the shell structure, leading to large values of out-of-plane strain energy in combination with low values of in-plane strain energy.

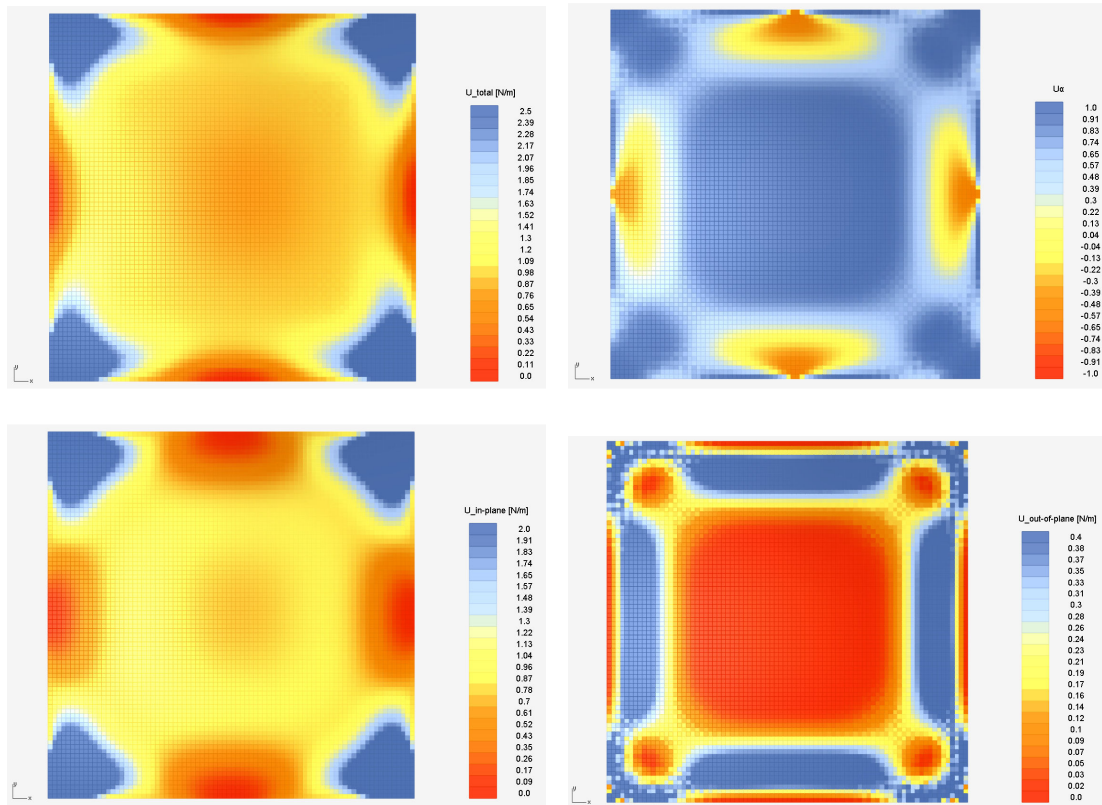


Figure 3.6 – The strain energy results for the hypar for the loading condition self weight.

For the complex geometry the smallest value of  $U_\alpha$  is -1.0. This value occurs at the outer most edges which indicates plate behaviour. Also some outer ring elements have values of  $U_\alpha$  close to -1.0 near the upper ridges as well as some elements near the valleys between the inner and outer parts. These low values probably occur due to a lack of in-plane force in combination with relatively large bending moments.

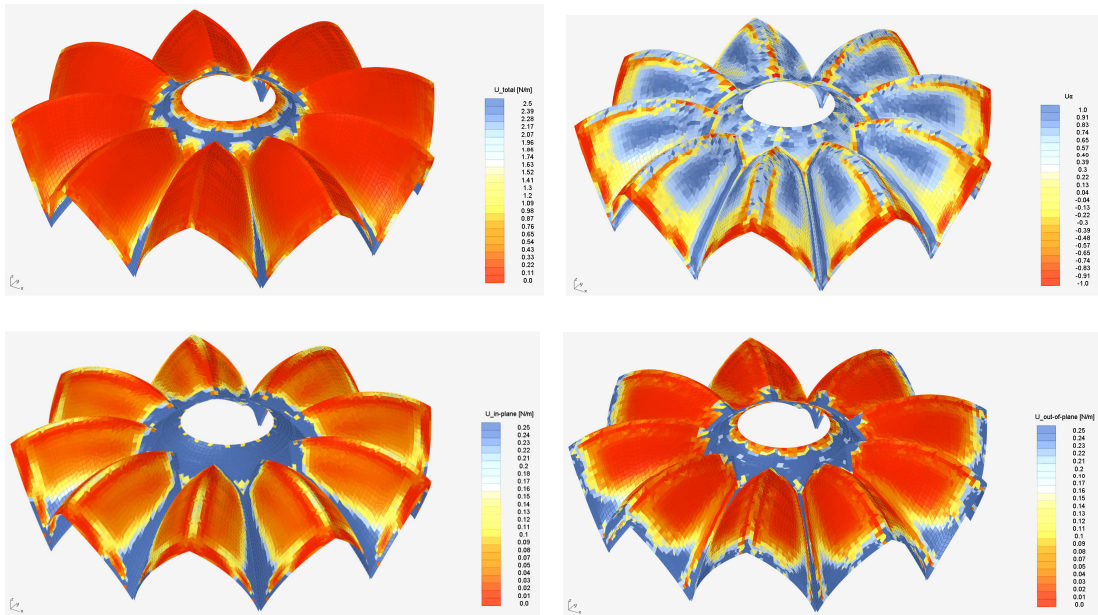


Figure 3.7 – The strain energy results for the complex geometry for the loading condition self weight.

### Wind load

From the values of  $U_\alpha$  it can be seen that the ellipsoid display good shell behaviour for the wind loading condition as well. The factor  $U_\alpha$  locally reduces to a value of 0.5 at two sides of the structure due to an increase of the out-of-plane strain energy in combination with a reduction of the in plane strain energy. From the ratio between the in-plane and out-of-plane strain energy it also can be concluded that – according to this quantity – the ellipsoid is a well formed shell structure. This can also be seen in the display of the total strain energy which is dominated by the in-plane strain energy, as can be witnessed between the similar displays of the in-plane strain energy and the total strain energy.

When the total amount of strain energy is compared for the wind loading condition with the total amount of strain energy, it can be seen that they vary in the same order of magnitude.

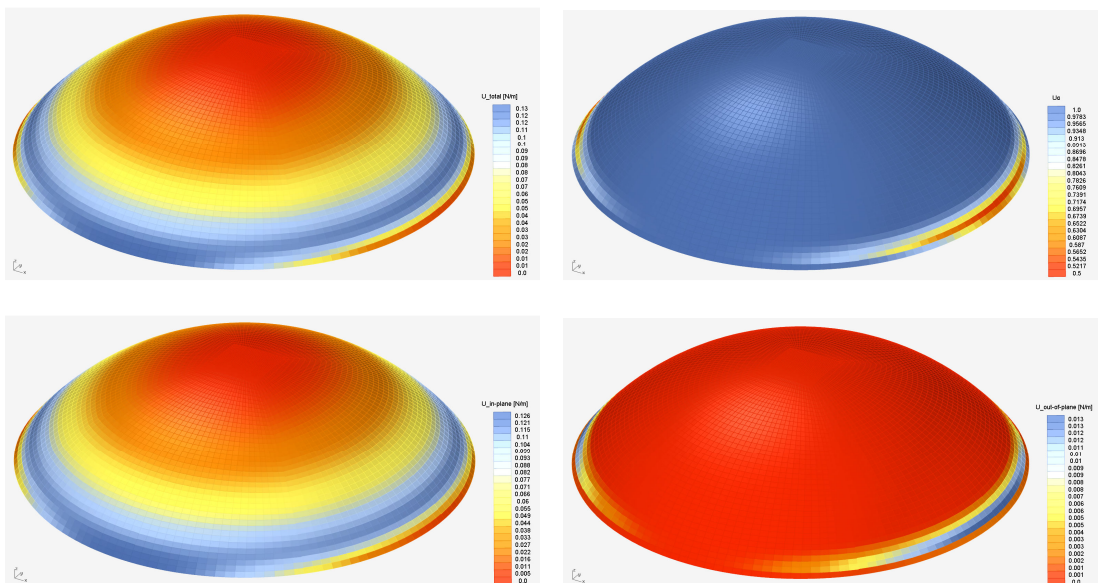


Figure 3.8 – The strain energy results for the ellipsoid for the loading condition wind.



The hyperboloid displays extreme well shell behaviour as well as for self weight as for wind load which is primarily caused by extreme small values of the out-of-plane strain energy. Again the display of the total amount of strain energy is dominated by the in-plane strain energy.

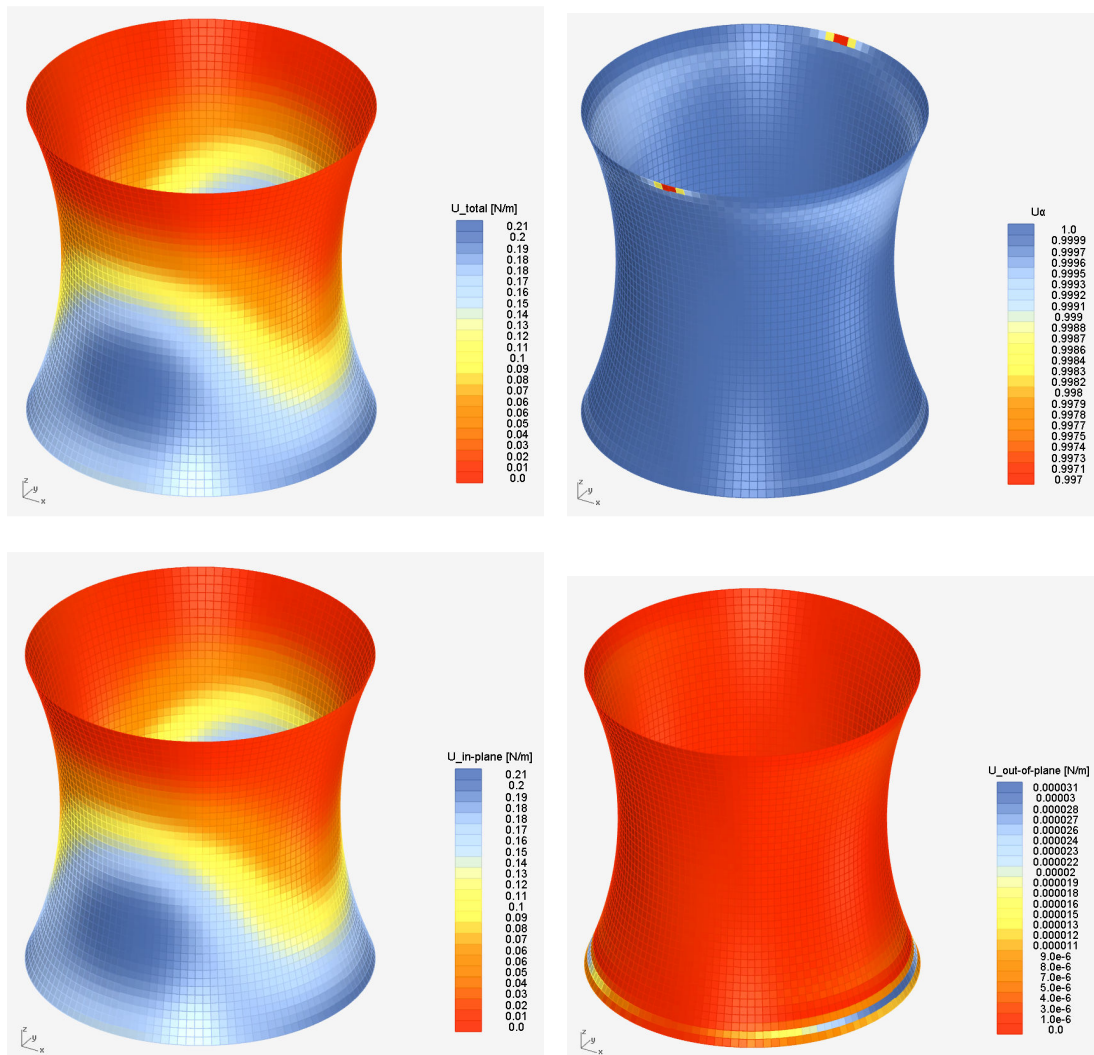


Figure 3.9 – The strain energy results for the hyperboloid for the loading condition wind.

The results for the strain energy for the hyperboloid display considerably smaller values of  $U_\alpha$  in comparison with results for the ellipsoid and the hyperboloid. Some local exceptions to this are the thin edges in the four corners and two spots halfway of the structure oriented in the direction of the wind loading. Again this display is the result of a combination of high respectively low values of the in-plane and out-of-plane strain energy. The hyperboloid is the first structure where the display of the total amount of strain energy is noticeably different from the display of in-plane strain energy, due to values of the out-of-plane strain energy that are larger than their in-plane counterparts. Notice also the arch shaped patterns in the figure displaying the in-plane strain energy results that look as if they are transferring the wind load to the supports.

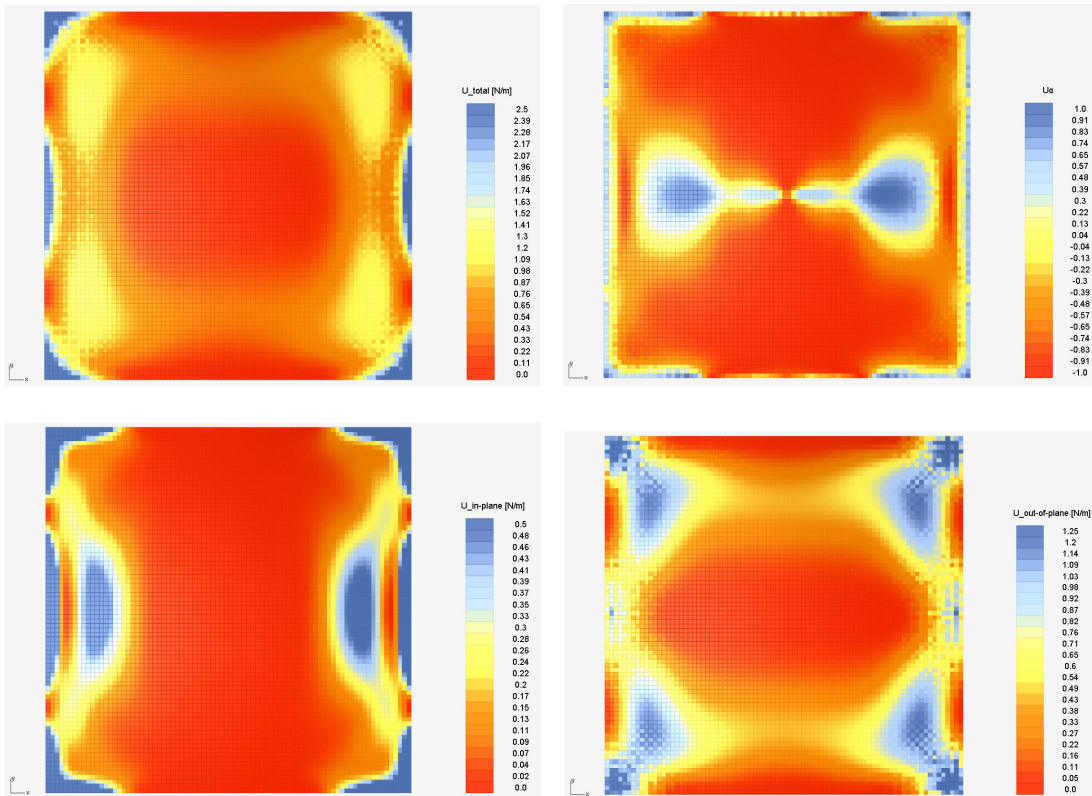


Figure 3.10 – The strain energy results for the hyper for the loading condition wind.

The results of  $U_\alpha$  for the complex geometry seem to display primarily plate behaviour with some exceptions around the top part of the structure. This is due to the considerably large out-of-plane strain energy values in comparison to their in-plane counterparts. The display of the total amount of strain energy shows maximum values at the outer edges of the panels orientated across the wind load direction and in the valleys connecting the outer shell parts with the inner shell part. The firstly mentioned maximum is caused mainly due to out-of-plane strain energy; the latter mainly due to in-plane strain energy. The results of the in-plane energy seem to display some arch action in the outer edges of the structure panels across the wind load direction whereas the maximum values around the inner part of the structure display the importance and effectiveness of the supporting role of this part. All in all this structure seems to display far less shell behaviour as it did when it was loaded by self weight.

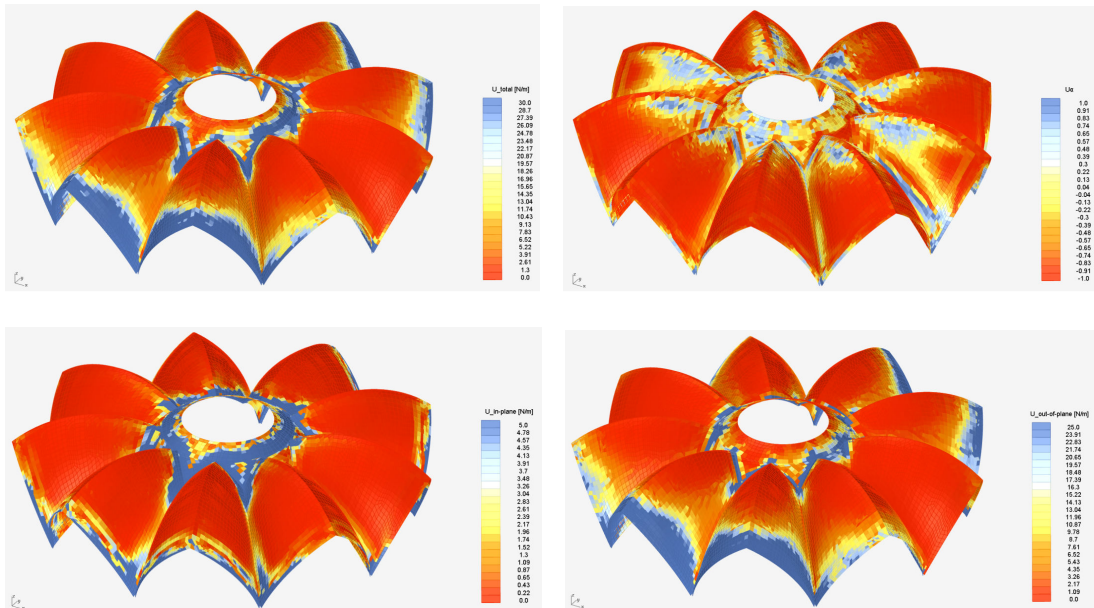


Figure 3.11 – The strain energy results for the complex for the loading condition wind.

### 3.3.2 Principal values of the eccentricity of the normal force

The eccentricity of normal force is computed in two different ways as is described in paragraph 2.2. In this paragraph the principal values of the eccentricity of the normal force and the difference between them is discussed. These principal values are computed in the local coordinate system as is described in appendix B.

#### Self weight

The results for the ellipsoid and the hyperboloid seem to compare to what can be expected for these results, both in shape as well as in values. For both structures it can be clearly seen where the bending moments occur. The ring just below the top of the hyperboloid is a result of the normal force approaching the value zero at this location.

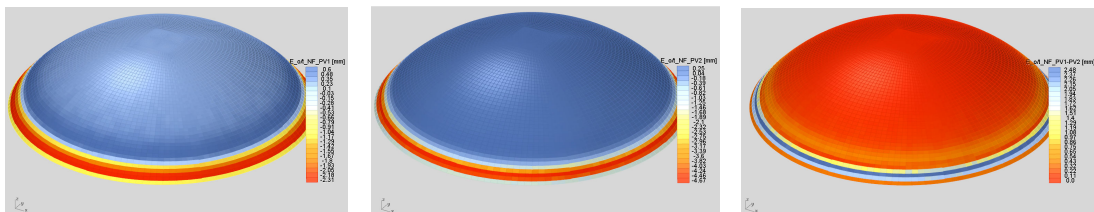


Figure 3.12 – The principal values of the eccentricity of the normal force and the difference between them for the ellipsoid for the loading condition self weight.

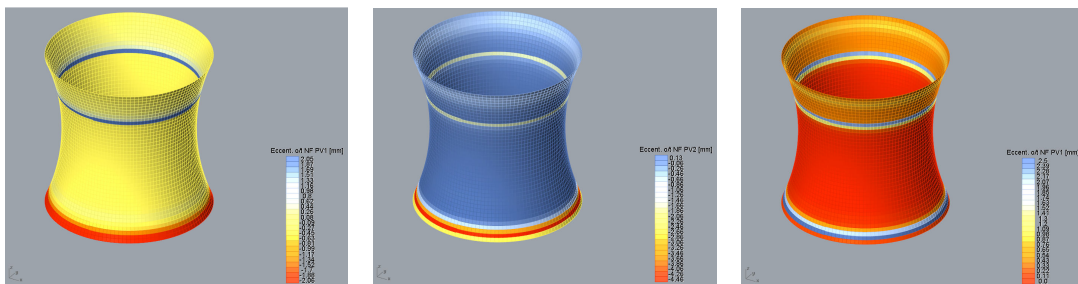


Figure 3.13 – The principal values of the eccentricity of the normal force and the difference between them for the hyperboloid for the loading condition self weight.



The values of the eccentricity for the hypar are remarkable larger although they are not extremely large in comparison to the shell thickness of 100 [mm]. The extreme values of the eccentricity occur at the corners. One conspicuous thing in this is that positive and negative eccentricity values are alternating towards the corners. Maybe this is some damping phenomenon of the bending moments that faint towards the centre of the hypar.

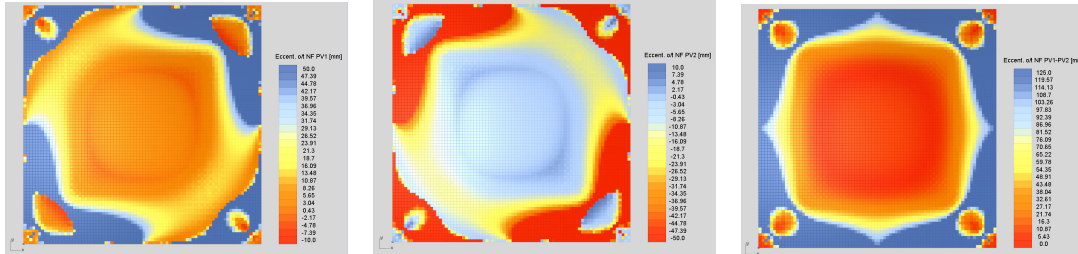


Figure 3.14 – The principal values of the eccentricity of the normal force and the difference between them for the hypar for the loading condition self weight.

The values of the eccentric for the complex geometry are the largest in comparison with the other structures although again they are not extremely large. This is not so difficult to understand because there are many free edges and sharp direction changes in the geometry of this structure. The extreme values of the eccentricity occur at the edges and in the valleys, as can be expected.

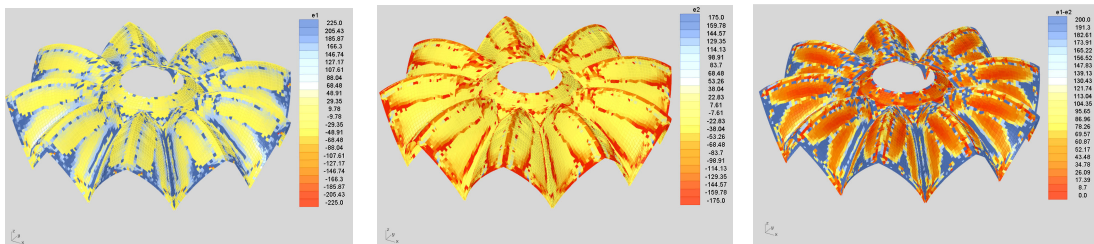


Figure 3.15 – The principal values of the eccentricity of the normal force and the difference between them for the complex geometry for the loading condition self weight.

### Wind load

Looking at the results of the eccentricity of the normal force for the wind loading condition for the ellipsoid it is immediately clear which of the images belongs to the meridional direction and which belongs to the direction of the hoop forces. It is conspicuous that the values belong to the latter direction are relatively larger in comparison with the values belonging to the meridional direction. This could be an indication of good shell behaviour. One other conspicuous thing is that the eccentricity is alternating at the front and backside in the meridional direction. This could be the same damping phenomenon of the bending moments mentioned before with the self weight loading condition of the hypar.

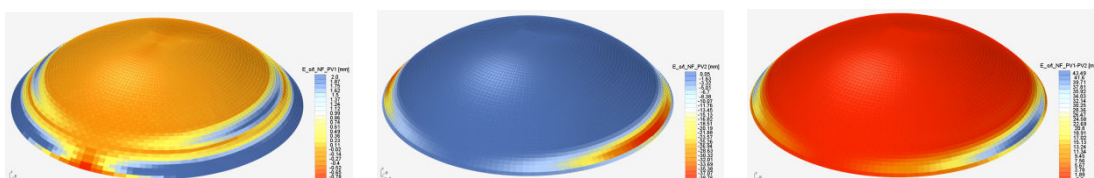


Figure 3.16 – The principal values of the eccentricity of the normal force and the difference between them for the ellipsoid for the loading condition wind load.

The extreme values of the eccentricity for the hyperboloid occur at the upper free edges perpendicular to the wind load direction, which is to be expected. The size of the values itself is relatively small in comparison with the shell thickness. At the bottom of the hyperboloid some sort of parabolic line with extreme values seems to occur. It is however not clear what is causing this pattern at this moment. Some additional research has to be performed in order to explain this phenomenon.

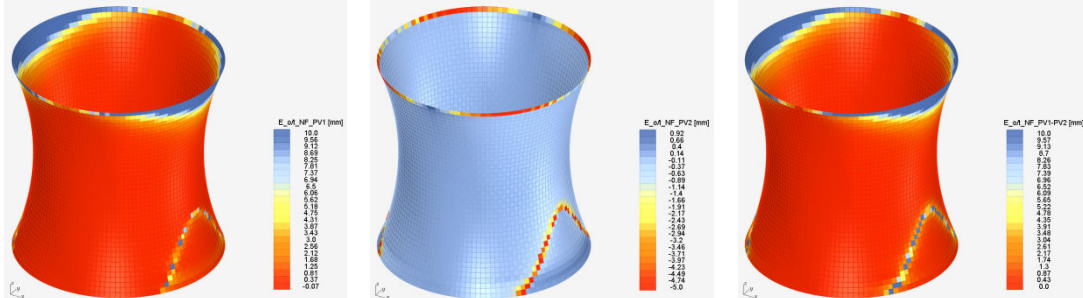


Figure 3.17 – The principal values of the eccentricity of the normal force and the difference between them for the hyperboloid for the loading condition wind load.

The results for the hyper are extremely large in comparison to the thickness and in comparison to the previous results for the wind loading. The extreme values occur in some complex pattern which cannot be explained immediately. It might be that the addition of the principal directions to these figures helps to clarify the results in this matter.

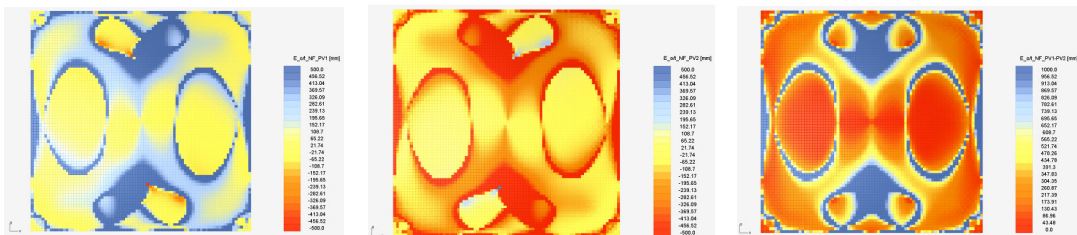


Figure 3.18 – The principal values of the eccentricity of the normal force and the difference between them for the hyper for the loading condition wind load.

The values of the eccentricity for the complex geometry are in the same range as the shell thickness itself. They are somewhat larger as the values for the ellipsoid and the hyperboloid but not as large as the values for the hyper. The extreme values seem to occur at the outer most parts of the shell which are perpendicular to the wind loading direction.

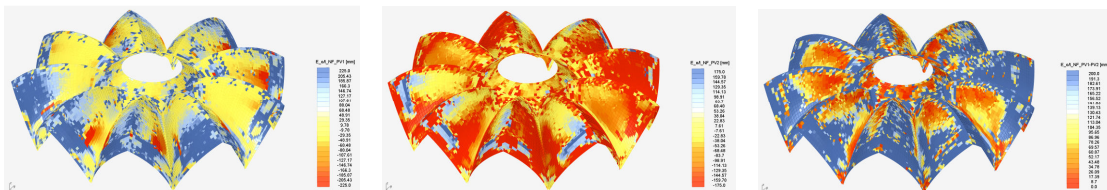


Figure 3.19 – The principal values of the eccentricity of the normal force and the difference between them for the complex geometry for the loading condition wind load.

### 3.3.3 Eccentricity of the normal force in the principal directions of the bending moment

The second way in which the eccentricity of the normal force is computed is described in this paragraph, which is the eccentricity of the normal force in principal directions of the distributed bending moments. These principal directions can be found in appendix C.



### Self weight

The first thing that can be noticed for the results of the ellipsoid is that they are remarkably similar to the results of the principal values of the eccentricity of the normal force. Also the results for the hyperboloid have certain similarities, although it is clear that the results in the principal direction of the bending moments are more orientated in the meridional and hoop force direction.

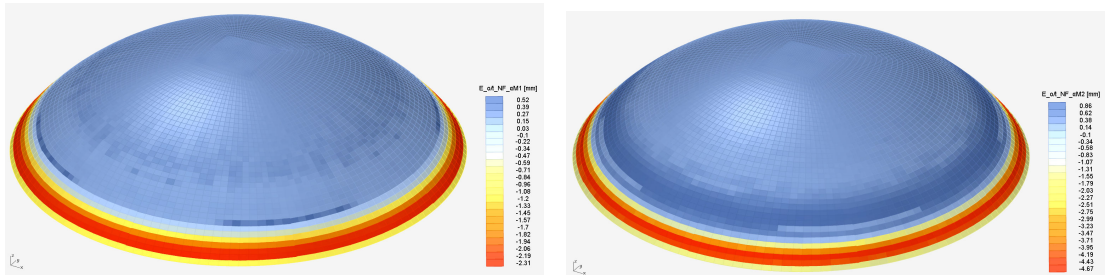


Figure 3.20 – The eccentricity of the normal force results in the principal directions of the distributed bending moments for the ellipsoid for the loading condition self weight.

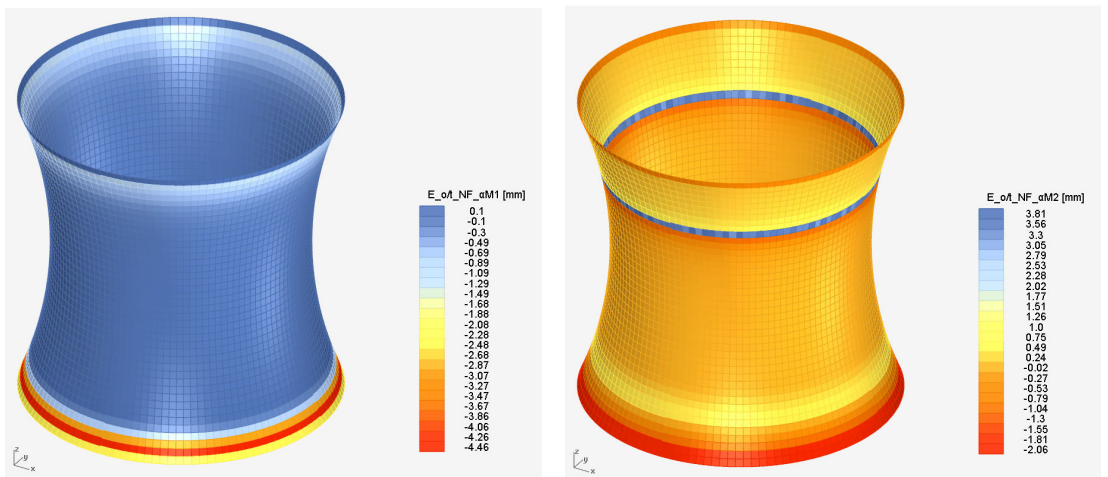


Figure 3.21 – The eccentricity of the normal force results in the principal directions of the distributed bending moments for the hyperboloid for the loading condition self weight.

The results of the eccentricity of the normal force in the principal directions of the bending moments for the hyperboloid are now even larger in comparison to the principal values of the eccentricity. Again a pattern occurs that cannot be immediately explained based only on the values of the eccentricity.

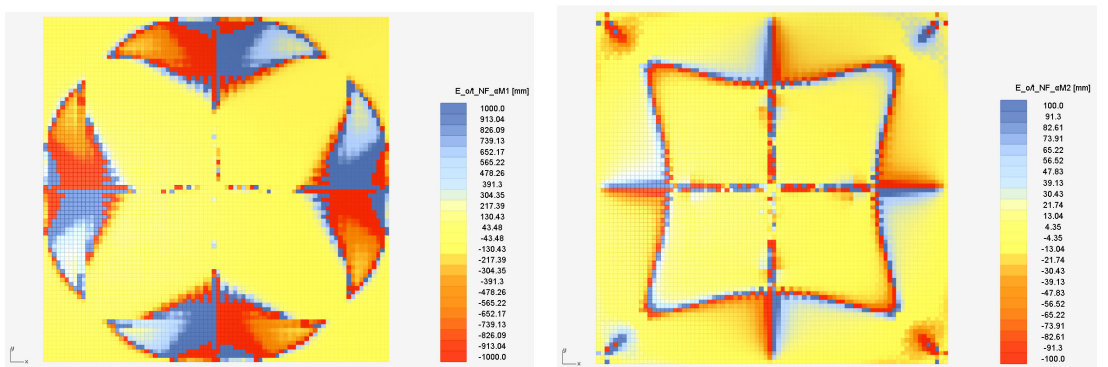


Figure 3.22 – The eccentricity of the normal force results in the principal directions of the distributed bending moments for the hyperboloid for the loading condition self weight.

The results of eccentricity in the principal directions of the bending moments for the complex geometry seem to differ somewhat from the principal values of the eccentricity. However, the extreme values still seem to occur at the free edges and at the valleys and ridges, as can be expected.

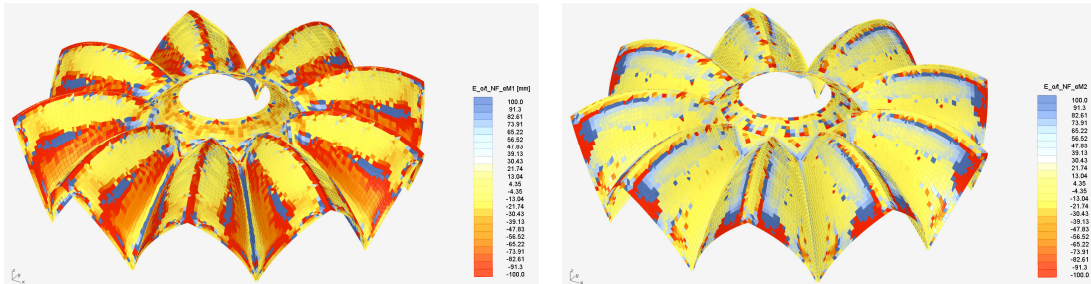


Figure 3.23 – The eccentricity of the normal force results in the principal directions of the distributed bending moments for the complex geometry for the loading condition self weight.

### Wind load

The values and the shape of the eccentricity of the normal force for the ellipsoid and hyperboloid loaded by wind seem to correspond again with what can be expected, although they are somewhat different compared to the principal values of the eccentricity. Also the images of figure 3.24 are not symmetric whereas the figures of the principal directions (see appendix C) do appear to be symmetric.

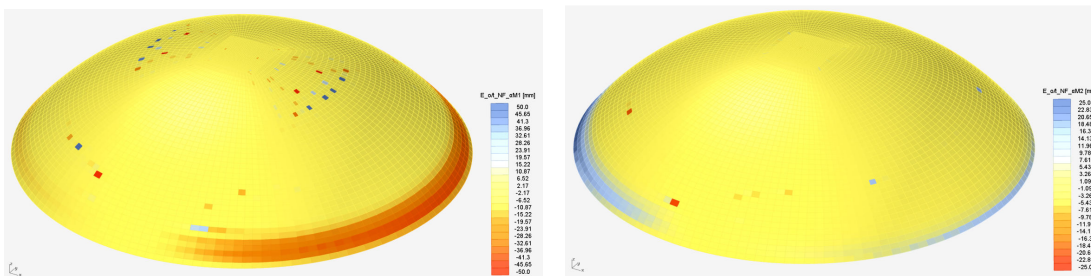


Figure 3.24 – The eccentricity of the normal force results in the principal directions of the distributed bending moments for the ellipsoid for the loading condition wind.

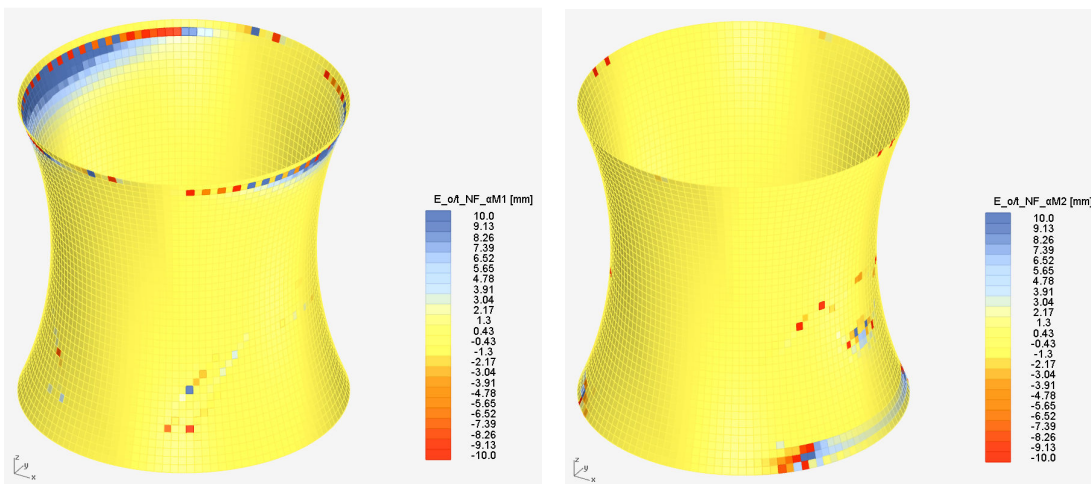


Figure 3.25 – The eccentricity of the normal force results in the principal directions of the distributed bending moments for the hyperboloid for the loading condition wind.

The values of the eccentricity for the hyperboloid are again extremely large. The shape of the results is different from figure 3.18 and is again not immediately explainable.

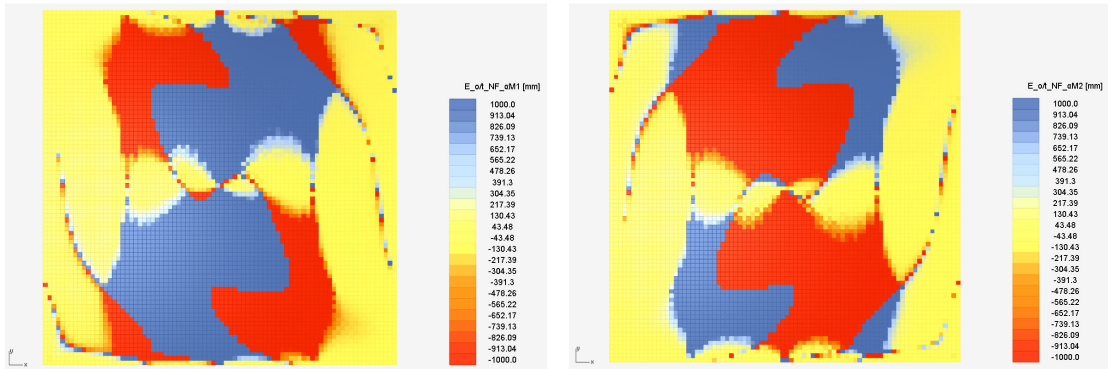


Figure 3.26 – The eccentricity of the normal force results in the principal directions of the distributed bending moments for the hyperboloid for the loading condition wind.

The results of the eccentricity of the normal force in the principal directions of the bending moments for the complex geometry for the wind load are again somewhat different compared to results of the principal values of the eccentricity although the size of the values and the shape of the results do not differ too much from each other.

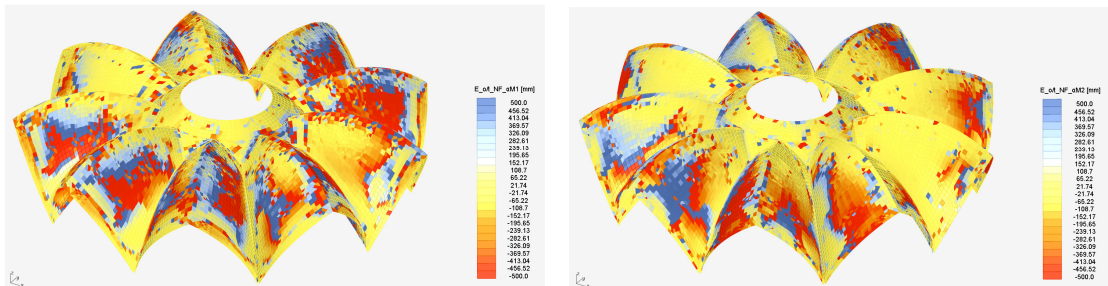


Figure 3.27 – The eccentricity of the normal force results in the principal directions of the distributed bending moments for the complex geometry for the loading condition wind.

### 3.3.4 Buckling load factor

As was mentioned in paragraph 2.2, only the hyperboloid and the hyperboloid have principal curvatures that differ from each other. This poses some additional difficulty in determining the governing value of the buckling load factor for these two structural designs. In order to prevent complications due to this complexity, it was decided to evaluate the buckling load factor in both principal curvature directions. This is why there is only one result for each loading condition for the ellipsoid and two results for both the hyperboloid and the hyperboloid. The results for the complex geometry are also divided over two displays but for another reason. Due to limitations of Grasshopper mentioned before in paragraph 2.1.5, it was decided to compute the buckling load factor for the complex geometry (partially) by hand. This could be done since the complex geometry consists of spherical parts only. Since there are two types of parts, each with a different radius (see figure 3.28), there is a separate figure displaying the correct results for each of these types of parts (see figure 3.32). One figure displays the correct values for the outer ring of parts, the other displays the correct values for the inner ring of parts. The outer ring parts have a radius of 16500 [mm], the inner ring parts have a radius of 24000 [mm].



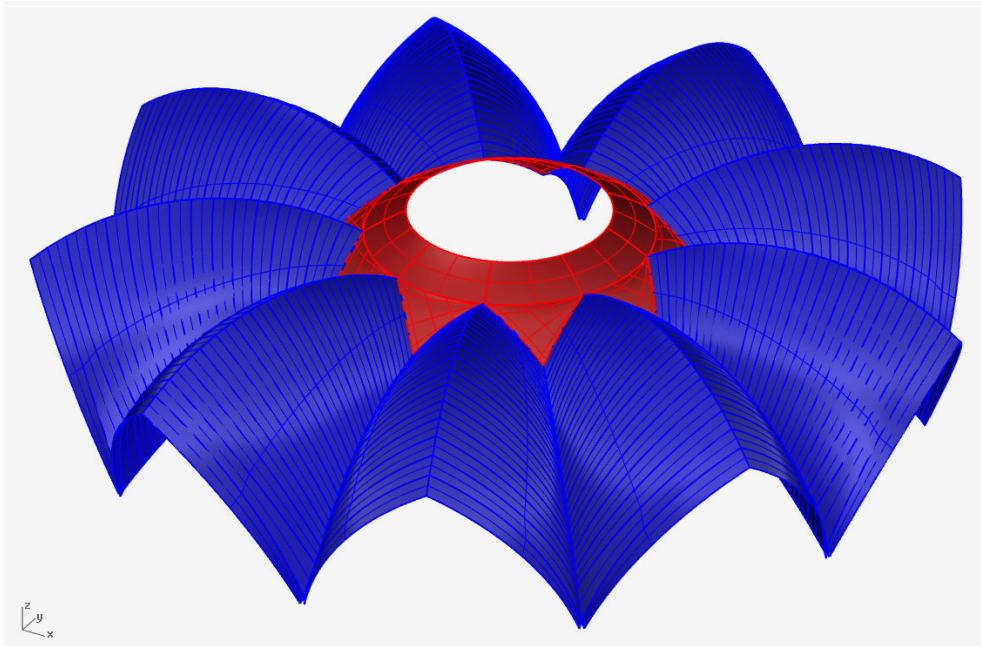


Figure 3.28 – The outside spherical parts (blue) have a radius of 16500 [mm]. The inner spherical part has a radius of 24000 [mm].

Computation of the critical normal force for the inner ring of parts of the complex geometry structure:

$$n_{cr} = -0.6 \frac{Et^2}{a} = -0.6 \frac{36000 \cdot 200^2}{24000} = -36000 [N] \quad (3-1)$$

Computation of the critical normal force for the outer ring of parts of the complex geometry structure:

$$n_{cr} = -0.6 \frac{Et^2}{a} = -0.6 \frac{36000 \cdot 200^2}{16500} \approx -52364 [N] \quad (3-2)$$

During analysis of the results it was noticed that maximum value of the buckling load factor for each structure was far smaller than one. Although this might seem attractive from a quantitative standpoint, this led to result displays of the structure being almost completely coloured red which made it impossible to perform an analysis of the qualitative behaviour. Therefore it was decided to adjust each legend in order to obtain the best insight in the displayed results.

### Self weight

The results of the buckling load factor for the ellipsoid seem to compare well with what can be expected for this structure loaded by self weight. What is noticeable is that the actual values of the buckling load factor are rather small which can be interpreted as an indication for this structure having a good structural design.

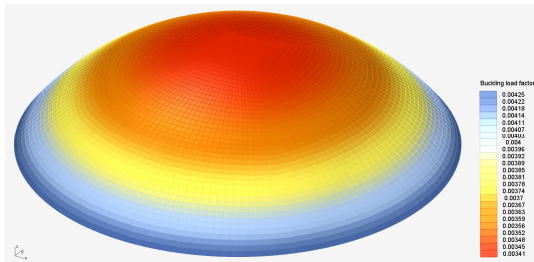


Figure 3.29 – The buckling load factor results for the ellipsoid for the loading condition self weight.

As mentioned before the results of the buckling load factor for the hyperboloid consist of two parts. The first part displays the results of the buckling load factor in the direction of the membrane forces; the second part displays the results in hoop force direction. What is noticeably is that the buckling load force in hoop force direction is actually larger than the buckling load factor in the direction of the membrane forces. The distribution of the results of the buckling load factor for both directions seems to be comparable to what can be expected. Notice how the buckling load factor in the direction of the hoop force displays the change in sign for the normal force in hoop direction.

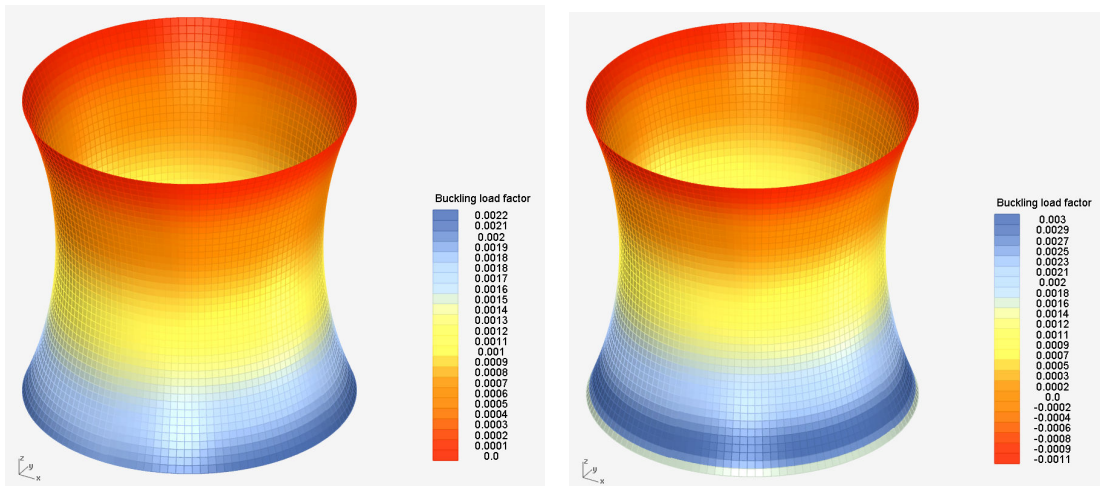


Figure 3.30 – The buckling load factor results for the hyperboloid for the loading condition self weight.

The two main directions for the hyper coincide with the principal directions of the curvature. The general direction of compression runs between the two lowest points of the structure, i.e. from the bottom left hand side to the upper right hand side in figure 3.31. This can also be seen in the results of the buckling load factor. As might be expected, the governing value of the buckling load factor will occur at both supports in the general compression direction.

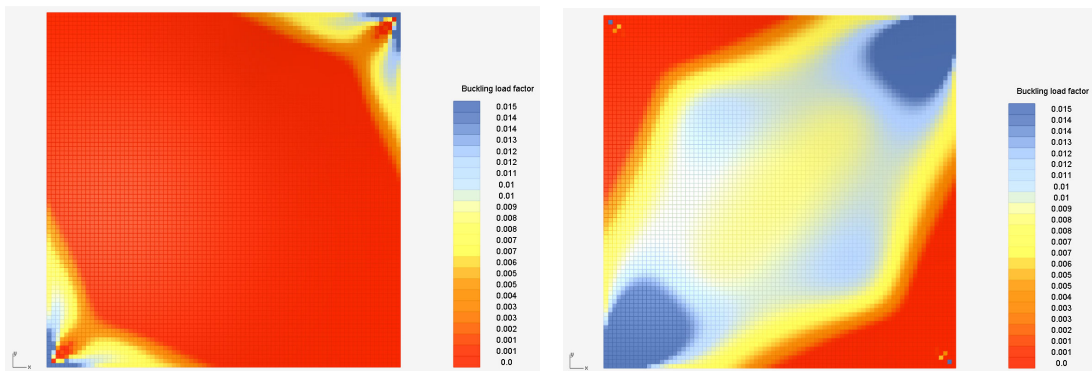


Figure 3.31 – The buckling load factor results for the hyper for the loading condition self weight.

The two figures displaying the results of the buckling load factor for the complex geometry (see figure 3.32) show that the governing values occur in the valleys between the outer parts and in the inner shell part. This latter result can be expected as the structure is designed to lean in somewhat in order to prevent loading the inner shell in tension instead of compression. However, this first result is somewhat unexpected as one might anticipate some strut and tie behaviour within the outer shell parts itself, directing the load of the self weight to the supports in some kind of cantilever like fashion. The outer shell parts however are designed to lean somewhat inwards which causes the compression in the valleys and the tension in the ridges.

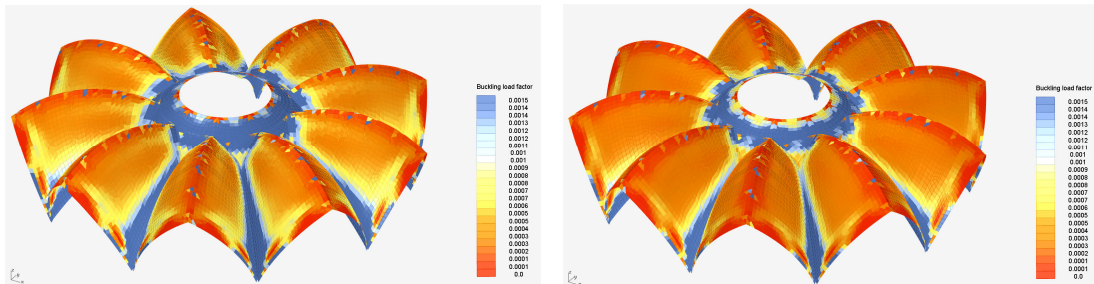


Figure 3.32 – The buckling load factor results for the complex geometry for the loading condition self weight. The image on the left displays the correct values for the inner ring of elements; the image on the right displays the correct values for the outer ring of elements.

### Wind load

The results for the buckling load factor for the wind loading seem to compare well with what can be expected as from all of the displayed results it is fairly easy to tell what direction of the wind load is.

Just as for the strain energy the results of the buckling load factor for the wind load also show the governing hoop force action. Instead of distributing the load over the top of the structure the load is carried by arch action to the supports at both sides of the structure.

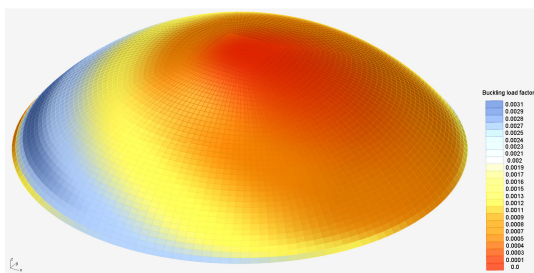


Figure 3.33 – The buckling load factor results for the ellipsoid for the loading condition wind.

As for the self weight loading condition the results for the wind loading condition consist of a part in the membrane force direction and of a part in the hoop force direction. Both results display what would be expected for the buckling load factor in both directions. Looking at the values of the buckling load factor the membrane force direction is governing. This is probably due to the height of the structure.



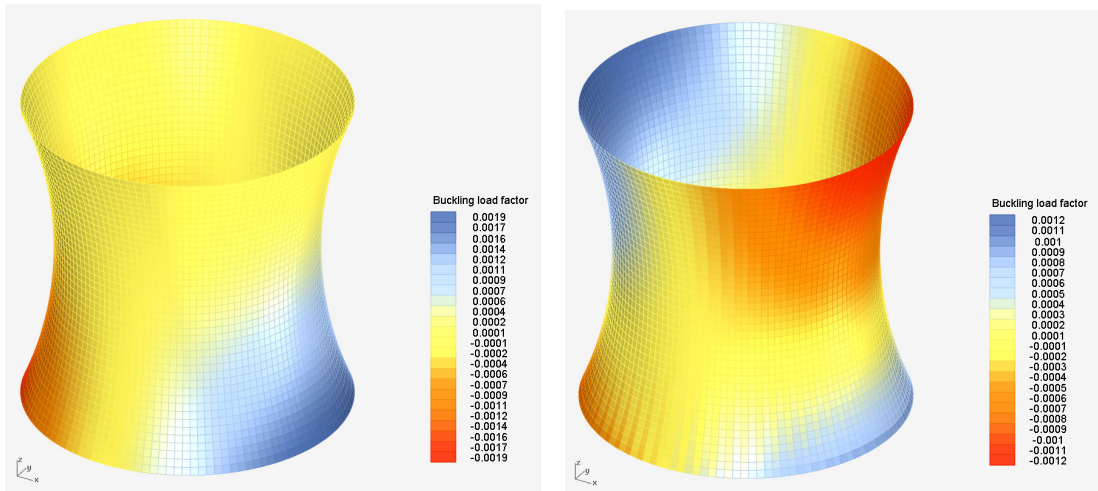


Figure 3.34 – The buckling load factor results for the hyperboloid for the loading condition wind.

Dividing the buckling load factor in two directions gives somewhat difficult to interpret results for the hyper. Looking at each of the results one could distinguish some strut and tie model action. However, it would be considered more convenient for this particular structure and load case if both results could be combined in one figure displaying the results of the governing buckling load factor.

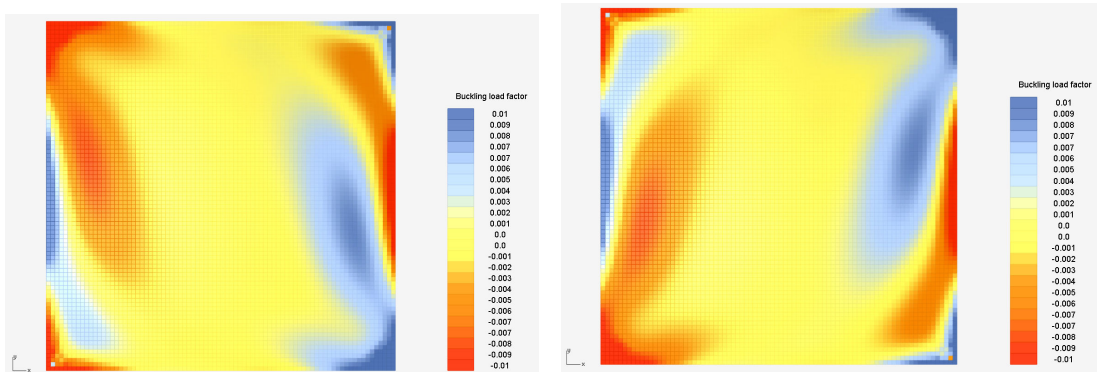


Figure 3.35 – The buckling load factor results for the hyper for the loading condition wind.

The governing buckling load factor for the complex geometry occurs in an arch like shape in the centre piece of the structure guided down to the supports by the valleys and at the very edges of the outer parts of the structure across the direction of the wind load.

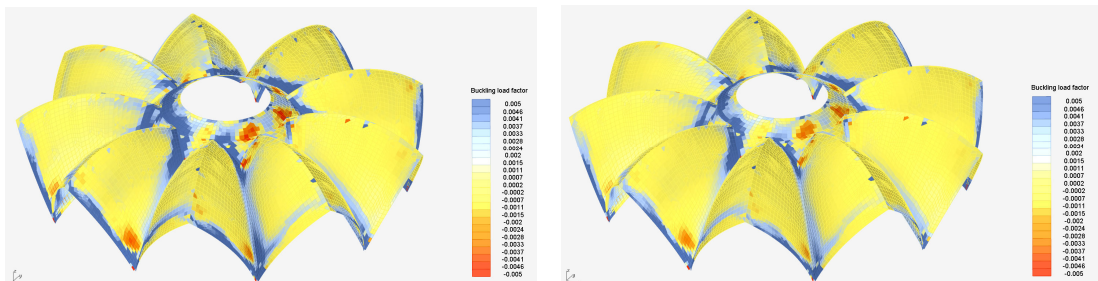


Figure 3.36 – The buckling load factor results for the complex geometry for the loading condition wind. The image on the left displays the correct values for the inner ring of elements; the image on the right displays the correct values for the outer ring of elements.

### 3.3.5 Out of balance of the in-plane shear force

As was mentioned in paragraph 2.2, the out of balance of the in-plane shear force only occurs within the hyperboloid and the hyper. Due to this there are no results for the ellipsoid and for the complex geometry. Bear in mind that the out of balance of the in-plane shear force is the product of the difference of the two principal curvatures  $k_1$  and  $k_2$  and the distributed shear moment  $M_{xy}$  (see paragraph 2.2.4). The blocky results in the figures below are not some programming error made in Grasshopper; this pattern also returns in the DIANA results (see appendix E).

#### Self weight

What is noticeable is the fact that the figures containing the results of the out of balance of the in-plane shear force vary little in comparison with the figures containing the results of the distributed shear moment  $M_{xy}$ . This is the result of the little variation in the difference of the two principal curvatures as the largest value is less than 25% larger than the smallest value for the hyperboloid and less than 12% larger for the hyper. Since the extreme values of the distributed shear moment  $M_{xy}$  occur at the location where the distribution of the difference in principal curvatures is even smaller, this results in almost the same figure for the out of balance of the in-plane shear force in comparison to the distributed shear moment  $M_{xy}$ .

Concerning the size of the out of balance of the in-plane shear force it can be concluded for both the hyperboloid as the hyper that it is negligible compared to the actual in-plane forces.

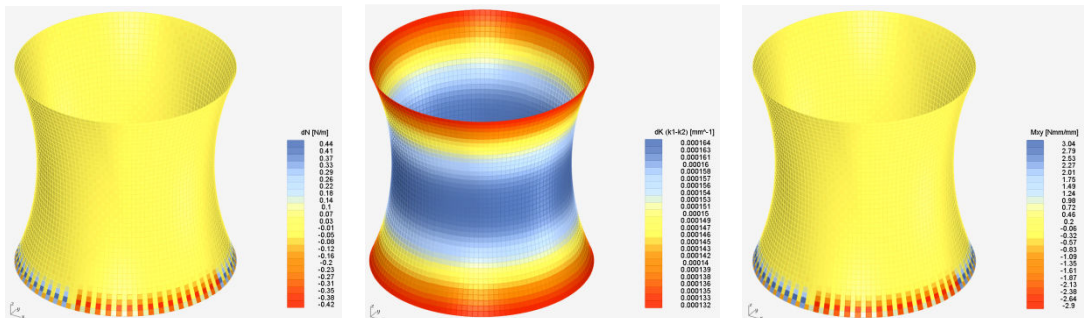


Figure 3.37 – The out of balance of the in-plane shear force results for the hyperboloid for the loading condition self weight.

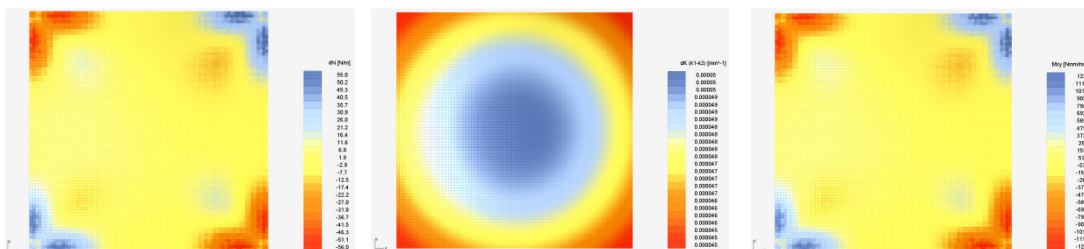


Figure 3.38 – The out of balance of the in-plane shear force results for the hyper for the loading condition self weight.

#### Wind load

For the loading condition wind the same similarities between the results of the out of balance of the in-plane shear force and the distributed bending moment  $M_{xy}$  exists. This is to be expected as the difference of the two principal curvatures has not changed for both structures. The size of the out of balance of the in-plane shear force is again negligible compared to the in-plane forces.



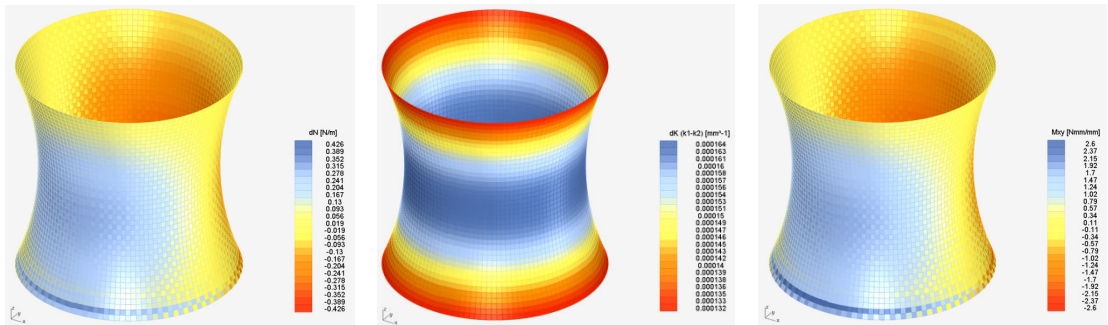


Figure 3.39 – The out of balance of the in-plane shear force results for the hyperboloid for the loading condition wind.

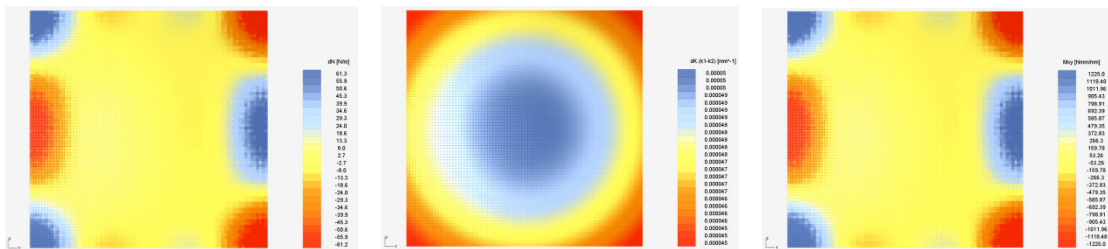


Figure 3.40 – The out of balance of the in-plane shear force results for the hyperboloid for the loading condition wind.

### 3.3.6 Out of balance of the in-plane shear eccentricity of the normal force

During the determination of the eccentricity of the normal force it was discovered that the two non-diagonal matrix elements of the eccentricity tensor differ from one another (see paragraph 2.2.2). This difference is what in this report is called the out of balance of the in-plane shear eccentricity of the normal force. Due to the fact that this unbalance displayed a similar form in comparison to the out of balance of the in-plane shear force it was decided to research if this unbalance was negligible or not.

#### Self weight

Looking at the ellipsoid it is noticeable that the extreme values occur at the bottom edge of the structure (see figure 3.41). This is expectable since the extreme values of the eccentricity itself occur also at this location. Although a clear pattern cannot be distinguished it seems like the maximum and minimum values are in balance for each single element.

For the hyperboloid a similar alternating pattern can be noticed just below the top of the structure where the hoop forces change sign. This causes extreme values for the eccentricity of the normal force which in turn explain the result for the out of balance of the in-plane shear eccentricity of the normal force.

The values of the results for both the ellipsoid and the hyperboloid are rather small compared to the results of the hyperboloid and the complex geometry. For both the hyperboloid and the complex geometry a more uniform pattern can be distinguished. At the hyperboloid the extreme values occur at the edges where the bending moments are extreme. A conspicuous pattern can be noticed in each corner where there seem to be two diagonal lines where the out of balance of the in-plane shear eccentricity of the normal force changes sign. The locations of the extreme values for the complex geometry seem to coincide with the locations of the extreme values of the eccentricity of the normal force itself.

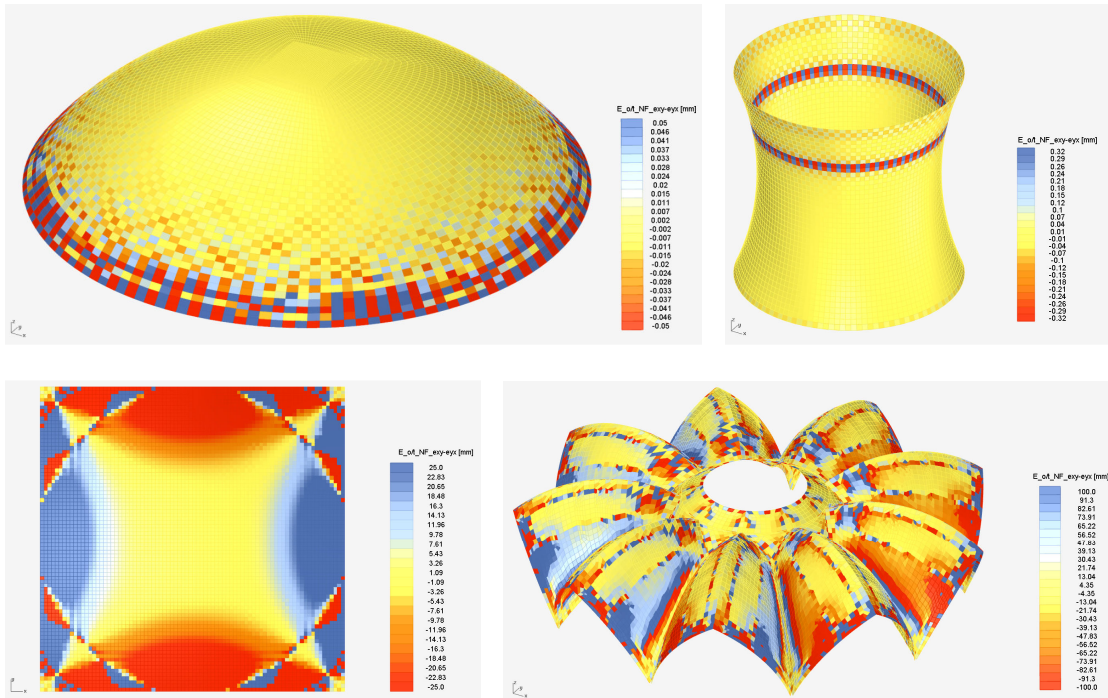


Figure 3.41 – The out of balance of the in-plane shear eccentricity of the normal force results for the loading condition self weight.

### Wind load

The distribution of the values for the ellipsoid and hyperboloid is now clearer in comparison with the self weight loading situation. Extreme values occur for the ellipsoid at the bottom again while the extreme values for the hyperboloid occur at the top edge and at the same parabolic lines at both front and backside that were noticed earlier with the principal values of the eccentricity of the normal force.

The pattern for the hyperboloid is again very distinctive and comparable to the pattern of the principal values of the eccentricity of the normal force itself. The pattern for the complex geometry is also comparable to the results of the principal values of the eccentricity. The absolute values for the hyperboloid and the complex geometry are again much larger than for the ellipsoid and the hyperboloid. However, this has no influence on the accuracy of the principal values of the eccentricity of the normal force itself, since they are computed using both the original non-diagonal shear components  $e_{xy}$  and  $e_{yx}$ .

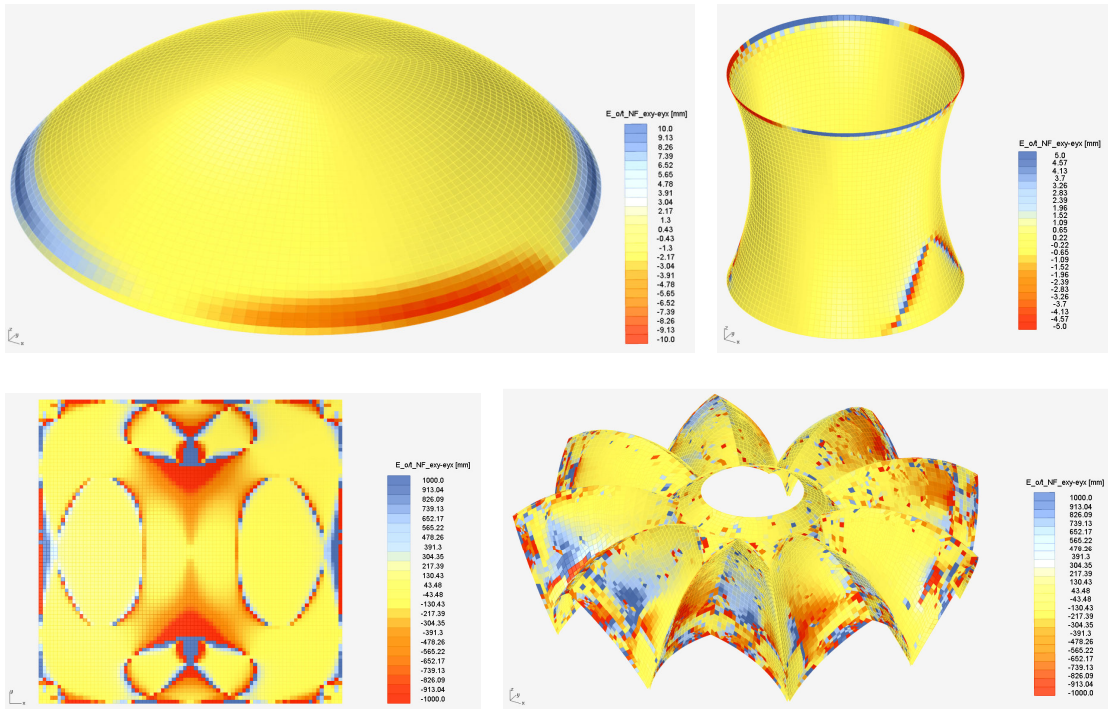


Figure 3.42 – The out of balance of the in-plane shear eccentricity of the normal force results for the loading condition wind.



## **4 CONCLUSIONS AND RECOMMENDATIONS**



## 4.1 CONCLUSIONS

### 4.1.1 General conclusions

Before a shell structure – or any civil engineering structure for that matter – can be build, its design has to be checked for the required strength, stiffness and stability. In order to check these conditions, a Finite Element Analysis (FEA) program is often used to compute the stresses, strains and displacements that will occur. These so-called quantities show whether a shell design can be realised or not but they don't show if, where or how the design can be improved.

This thesis is aimed at finding new quantities that can be used within existing FEA-programs in order to obtain better insight in the structural behaviour of shell structures and to be able to make better assessments of their structural designs.

Using Rhinoceros, a 3D-modelling software program, four shell designs have been created. These shell designs were analysed with the aid of the FEA-program TNO DIANA. Based on the analysis output, new quantities were computed using Grasshopper, a parametric graphic algorithm editor that is used as a plug-in for Rhinoceros. In this way, Rhinoceros is also used for displaying the results on each associated structural design.

A number of quantities proved to be of additional value to the existing quantities, for example: the results for one of the quantities display whether a shell structure is actually behaving like a shell or that it is behaving more like a plate, which clearly is unwanted behaviour for a shell structure. Another result provides additional information to where and how likely a structure will collapse. It is therefore proposed to implement these quantities in existing FEA-programs in order to provide the structural engineer with better insight in the mechanical behaviour of shell structures.

Here below each of the quantities is individually discussed more into detail.

### 4.1.2 Strain energy

When a structure is deformed by a load, this results in energy stored inside the structure. This energy is called strain energy. There are two types of strain energy that can be distinguished: out-of-plane strain energy, which is caused by loading of the structure perpendicular to its surface and in-plane strain energy, which is caused by loading of the structure in its surface. Because shell structures are usually thin structures that cannot coop very well with out-of-plane loading, out-of-plane energy is unwanted.

Different combinations of the out-of-plane and in-plane strain energy have been researched. Two of these combinations led to good results. The first combination is the sum of both out-of-plane and in-plane strain energy, also referred to as the total strain energy. The second combination is the ratio of the out-of-plane and the in-plane strain energy.

The total strain energy shows where the structure is experiencing the largest combination of loading and deformation. With this quantity, different variants of a certain type of structure can be compared in order to determine the preferable variant. The biggest advantage of strain energy is that it is a directional independent quantity. This property is most advantageous for complex free form shell design for which it is difficult to determine the governing geometry directions in which the load is transferred to the supports. This property

also results in one single result plot for assessing a shell structure. This in contrary to the usual quantities, e.g. normal force or bending moment that are tensor quantities for which their value is dependent of the direction in which they are considered.

The ratio of the out-of-plane and the in-plane strain energy can be used to determine whether a structure is behaving like shell or like a plate. For this a relative high value of the in-plane strain energy denotes shell behaviour, which is desirable for a shell structure. A relative high value of the out-of-plane strain energy denotes plate behaviour, which is undesirable. When a structure displays mostly plate behaviour, it can be decided to change the shape of the geometry or to design different supports. In case of local plate behaviour, the curvature of the shell can for example locally be adjusted to obtain better shell behaviour. For the ratio of the out-of-plane and in-plane strain energy it also holds that only one result plot is required.

#### **4.1.3 Eccentricity of the normal force**

When a normal force acts eccentrically in a cross-section, this results in a bending moment. The eccentricity of the normal force can therefore be defined as the ratio of the bending moment and the normal force itself. Shell structures are less suitable to cope with bending moments as their thickness is very small compared to their span and because of their way of internal load transfer. Therefore, the eccentricity of the normal force can be used as an indication of the suitability of a shell structure in coping with and transferring loads to the supports.

The eccentricity of the normal force is, in opposite to the strain energy, not a scalar quantity but a tensor quantity. Each point of a shell contains two principal bending moments and therefore also two principal eccentricities. The difference of these two eccentricities is a measure for the required shell thickness. The sum of the two principal eccentricities is a measure for the shape correction of the shell.

The eccentricity of the normal force is not a physical quantity but just an arithmetic quantity. This means that the eccentricity of the normal force is dependent on the chosen direction of the coordinate system. This makes the eccentricity particularly unsuitable for analysing free form shell structures for which it is difficult to determine suitable directions of the coordinate system. For this reason it was decided to analyse the eccentricity of the normal force also in the direction of the bending moments. In this way, the directions are not depending on the geometry of the shell but on the direction of the internal loading.

At the start of this thesis, it was expected that the results of the eccentricity of the normal force would turn out to be quite similar in comparison to the ratio of the out-of-plane and in-plane strain energy. However, this turned out not to be the case. This is probably due to the fact that the eccentricity of the normal force is not a physical quantity. Some of the results contain extremely large values of the eccentricity of the normal force. These values are the result of very small values of the normal force. An important difference with the strain energy is that, for this latter quantity, the computation only consists of additions and multiplications. Therefore, it will never result in extreme values as a result of dividing by a very small number.

Next to these issues, some visual patterns occurred that are difficult to explain and which certainly do not lead to better insight in the structural behaviour. Furthermore, the principal directions of the eccentricity change quite a lot within and between the different elements. It is therefore recommended to further research the eccentricity of the normal force before it is implemented in an existing FEA-program.



#### 4.1.4 Buckling load factor

The buckling load factor is the ratio between the normal force acting within the structure and the normal force at which the structure will fail due to buckling. Every part of the shell has a different buckling load factor that can be displayed with the aid of a contour plot. The advantage of this method in comparison with a linear buckling load analysis is that the imperfection sensitivity can be applied. The knock down factor on the other hand, which compensates for the difference between the analytical and the experimental results, has not yet been applied.

The buckling load factor can be used as both qualitative as well as quantitative quantity. In the first case shows the buckling load factor were a shell structure is most likely to fail due to buckling. In the latter case can the buckling load factor visualise the buckling load capacity of each part of a shell structure.

The buckling load factor results are a welcome addition to the so-called eigen-frequency analyses which do display the buckling load shape but fail in representing the buckling load sensitivity. This is why it is recommended to implement the buckling load factor in existing FEA-programs as well.

#### 4.1.5 Out of balance of the in-plane shear force

In-plane shear forces in perpendicular cross-sections are equal to one another in plate theory. In shell theory this is not the case because of the curvature of the shell geometry. This results in a small residual force perpendicular to the shell surface which is generally neglected in FEA-programs by averaging the shear forces. The difference between these shear forces is what is labelled as the out of balance of the in-plane shear force.

During this thesis, it has been shown that for the analysed slender shell structures this difference between the shear forces can safely be neglected. The difference has been computed and displayed as a contour plot. The results of these plots show large similarities with the results of the distributed bending shear moment  $M_{xy}$ . This is because of the minor variations in the difference of the two principal curvatures of the analysed structures. It is expected that this difference may play a larger part for the more complex free form shell structures with a greater thickness. This is something however that has to be researched more in to detail.

#### 4.1.6 Out of balance of the in-plane shear eccentricity of the normal force

As is mentioned before, the eccentricity of the normal force is not a physical quantity but an arithmetic quantity. This means that the two non-diagonal terms of the eccentricity tensor differ from one another. This difference is what is labelled as the out of balance of the in-plane shear eccentricity of the normal force.

It was found that this difference is independent of the direction of the coordinate system which is convenient for analysing free form shell structures. Also, some parts of the mathematical definition showed similarities with the rearranged Sanders-Koiter equation that defines the out of balance with the in-plane shear force. Therefore it was decided to analyse this quantity.

The results of this quantity did not lead to new insights in the mechanical behaviour of shell structures. Furthermore, the physical meaning of this quantity remains unclear, what makes it difficult to assess the results. Therefore it is recommended to research different variants of this quantity.



## 4.2 RECOMMENDATIONS

Besides a number of smaller recommendations, three main subjects can be distinguished as recommendations for further analysis and research. These three main subjects will individually be discussed here below. The remaining recommendations will jointly be discussed thereafter.

### 4.2.1 Integration of the self-made post processor

Although the development of the self-made post processor in Grasshopper has proven to be very instructive it became clear that, as the development progressed, this is not the best way to analyse a large number of varying structural designs within a limited amount of time. This is mainly because of three reasons:

- It takes a lot of time copy-pasting the vast amounts of data from Excel to Grasshopper;
- The number of items that can be copy-pasted to a single number component in Grasshopper is limited;
- The processing speed of Grasshopper is limited compared to that of an actual FEA-program such as DIANA or ANSYS.

Although it was known beforehand what the limitations of a self-made post processor would be, it was only during the development of the post processor that the limitations of both DIANA and Grasshopper became clear. This is an additional point of attention regarding further research. The choice for developing the self-made post processor made it unsuitable for the parametric set-up of quickly changing different design models as it was originally intended to do. In case of a follow-up to this graduation research it is therefore highly recommended to try to keep both pre and post processing as much as possible within DIANA or ANSYS. The gained analysing speed would allow for analysing multiple variations of different structures, thereby providing more insight in the influence of each design parameter in the results of the different additional quantities.

### 4.2.2 Extension of the curvature analysis tool in Grasshopper and the buckling load factor

The buckling load factor was analysed in the principal directions of the curvature. This led to two displays of results for the shell design with different principal curvatures what made it more difficult to interpret the actual structural behaviour. For this reason it is recommended to expand the functionality of the Grasshopper model so that it can determine the governing values of the curvature and hence the governing buckling load factor values. The main issue in this is that the resulting inverse product of both the initial normal force vector and the critical normal force vector results in a non-physical quantity as occurred in the computation of the eccentricity of the normal force vector. This is something that has to be accounted for. Other definitions of the buckling load factor could be used to solve this issue. This is why it is recommended to extend the applied formulations of the buckling load factor.

### 4.2.3 Actual improvement of a shell structural design

During the graduation thesis it was suggested to actually improve one of the designs based on the results of the additional quantities in order to confirm if these quantities would actually provide better qualitative insight in the structural behaviour of shell structures. Unfortunately due to the limited time available this idea was never put into action. Therefore it is highly recommended as one of the main focus points for a follow-up.

#### 4.2.4 Remaining recommendations

Finally there are a number of minor recommendations that could be accomplished quite easily, namely:

- Extending the Grasshopper model with the addition of a tool being able of displaying the change in Gaussian curvature in any point of a shell structure;
- Verification of the buckling load factor results with an eigen-frequency analysis for the four analysed structures;
- Adjusting the ambient lighting in Rhino and the colour schemes used in order to prevent the distorting of the display of the results and to make the results from the self-made post processor easier to compare to the results of another post processor;
- Combining both contour plot results and quantity direction plot results in a single results display, using contrasting colours so that they are both clearly visible;
- Adjusting the support conditions of the hypar in a more realistic way so that it actually could be constructed in practice. Due to the design of the current support conditions large tensional forces occur which are undesired in concrete structures;
- Analysing more complex shell structures. For now only one complex shell design has been analysed which makes it difficult to correctly assess the additional quantities for all sorts of complex geometries;
- Analysing more free form shell structures with larger thickness in order to research the results of the out of balance of the in-plane shear force is still negligible;
- Analysing the already designed shell structures under an asymmetric (wind) loading condition. It might be that for the current evenly distributed wind load the analysed shell structures display good shell behaviour while this might not be the case for unevenly distributed loads, considering the sensitivity of shell structures to point loads;
- Reanalysing the already designed shell structures with non-linear analysis and comparing the results for especially the strain energy to the results of the linear analysis and comparing them to the results of *Firl* [2].





## REFERENCES

### Master graduation theses

- [1] Van Asselt, P.H. (2007). *Analysis of stressed membrane structures – Implementation of non-linear material behaviour in structural analysis*. Delft: Delft University of Technology.
- [2] Van den Dool, M. (2012). *Optimising shell structures by calculating the minimum complementary energy*. Delft: Delft University of Technology.
- [3] Oosterhuis, M.R. (2010). *A parametric structural design tool for plate structures*. Delft: Delft University of Technology.
- [4] Voormeeren, L.O. (2011). *Extension and verification of sequentially linear analysis to solid elements*. Delft: Delft University of Technology.

### PhD graduation theses

- [5] Firl, M. (2010). *Optimal Shape Design of Shell Structures*. München: Technische Universität München (TUM).

### Lecture notes

- [6] Blaauwendraad, J. (2002). Reader belonging to the course "CT5141 – Theory of Elasticity, Energy Principles and Variational Methods". Delft: Delft University of Technology.
- [7] Coenders, J.L. (2008). Reader belonging to the course "CIE5251 - Structural Design - Special Structures". Delft: Delft University of Technology.
- [8] Hoogenboom, P.C.J. (2013). Handout 1 belonging to the course "CIE4143 - Shell analysis, Theory and Application". Delft: Delft University of Technology.
- [9] Hoogenboom, P.C.J. (2013). Handout 5 belonging to the course "CIE4143 - Shell analysis, Theory and Application". Delft: Delft University of Technology.
- [10] Hoogenboom, P.C.J. (2013). Handout 7b belonging to the course "CIE4143 - Shell analysis, Theory and Application". Delft: Delft University of Technology.
- [11] Wells, G.N. (2006). *The Finite Element Method: An Introduction*. Delft: Delft University of Technology.

## Lecture sheets

- [12] Borgart, A. (2013). *Shell Structures* belonging to the course "CIE5251 - Structural Design - Special Structures". Delft: Delft University of Technology.
- [13] Rots, J.G. and Hendriks, M.A.N. (2009). Lecture sheet 2 (*Introduction*) belonging to the course "CIE5148 - Computational Modelling of Structures". Delft: Delft University of Technology.
- [14] Rots, J.G. and Hendriks, M.A.N. (2009). Lecture sheet 3 (*Elements*) belonging to the course "CIE5148 - Computational Modelling of Structures". Delft: Delft University of Technology.
- [15] Rots, J.G. and Hendriks, M.A.N. (2009). Lecture sheet 11 (*Structural Optimisation*) belonging to the course "CIE5148 - Computational Modelling of Structures". Delft: Delft University of Technology.

## World Wide Web

- [16] <http://en.wikipedia.org/wiki/Hyperboloid>
- [17] [http://en.wikipedia.org/wiki/Strain\\_energy](http://en.wikipedia.org/wiki/Strain_energy)
- [18] <https://mathspig.wordpress.com/2012/03/>
- [19] <http://mcis2.princeton.edu/candela/paraboloid.html>
- [20] [http://roymech.co.uk/Useful Tables/Beams/Strain Energy.html](http://roymech.co.uk/Useful_Tables/Beams/Strain_Energy.html)
- [21] <https://software.intel.com/sites/default/files/managed/b6/b3/release-notes-f-2013sp1-w-en-u1-o.pdf>
- [22] [http://web.mit.edu/persci/people/adelson/checkershadow\\_illusion.html](http://web.mit.edu/persci/people/adelson/checkershadow_illusion.html)







# **APPENDICES**

**A – SET-UP OF A .DCF FILE**

**B – ALIGNMENT OF THE LOCAL COORDINATE SYSTEMS**

**C – PRINCIPAL DIRECTIONS OF THE DISTRIBUTED  
BENDING MOMENT**

**D – ANALYSIS RESULTS**

**E – COMPARISON DISTRIBUTED BENDING SHEAR  
MOMENT RESULTS**

**F – EXAMPLE OF STRAIN ENERGY SUBDIVISION**

**G – RAIN FLOW ANALOGY**



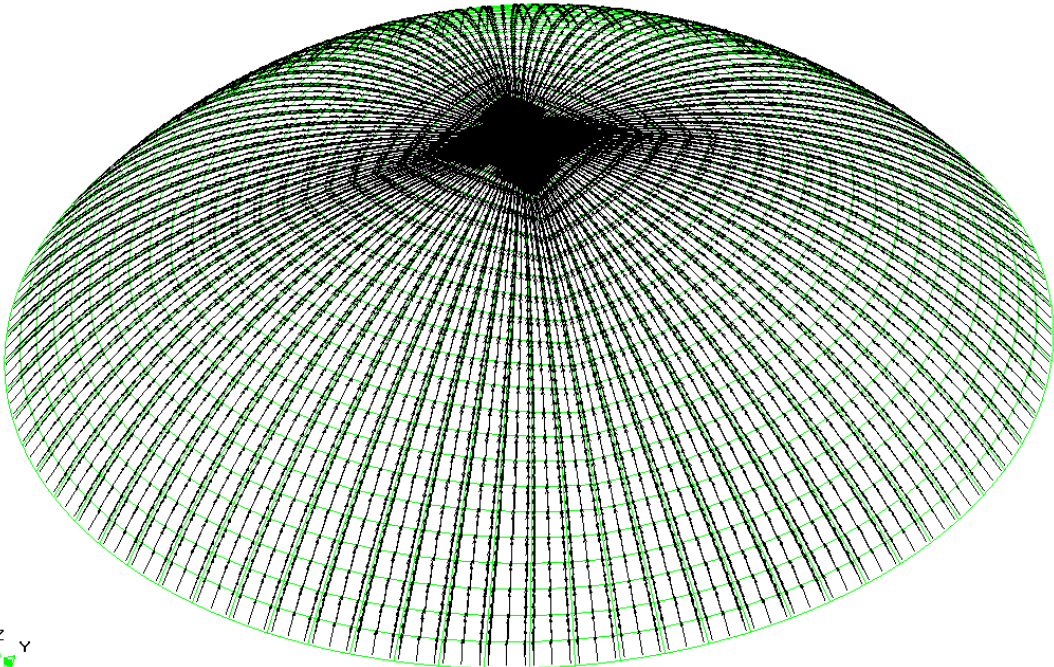
## APPENDIX A – SET-UP OF A .DCF FILE

```
*FILOS
INITIA
:read model data file "Ellipsoid.dat"
*INPUT
:execute the linear static analysis
*LINSTA
:output the analysis results
BEGIN OUTPUT TABULA FILE= "Ellipsoid"
BEGIN LAYOUT
  LINPAG 10000000
  DIGITS RESULT 6
END LAYOUT
  STRESS TOTAL LOCAL INTPNT COOR
  STRAIN TOTAL LOCAL INTPNT COOR
  STRESS TOTAL DISMOM LOCAL INTPNT
  STRESS TOTAL DISFOR LOCAL INTPNT
END OUTPUT
BEGIN OUTPUT FEMVIE
  STRESS TOTAL LOCAL INTPNT
  STRAIN TOTAL LOCAL INTPNT
  STRESS TOTAL DISMOM LOCAL
  STRESS TOTAL DISFOR LOCAL
END OUTPUT
*END
```

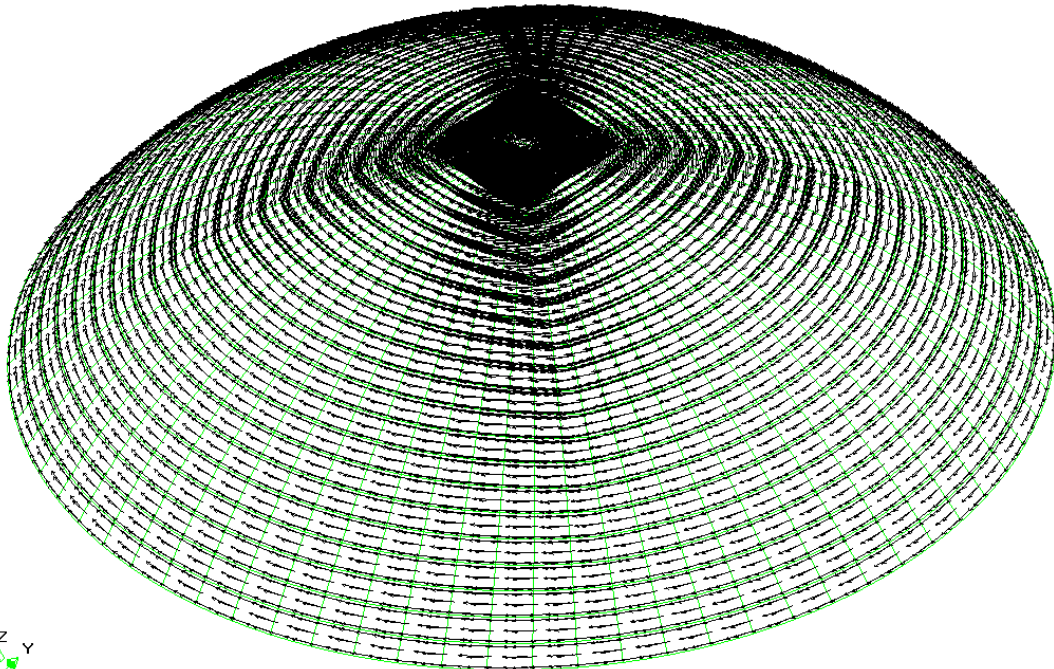


# APPENDIX B – ALIGNMENT OF THE LOCAL COORDINATE SYSTEMS

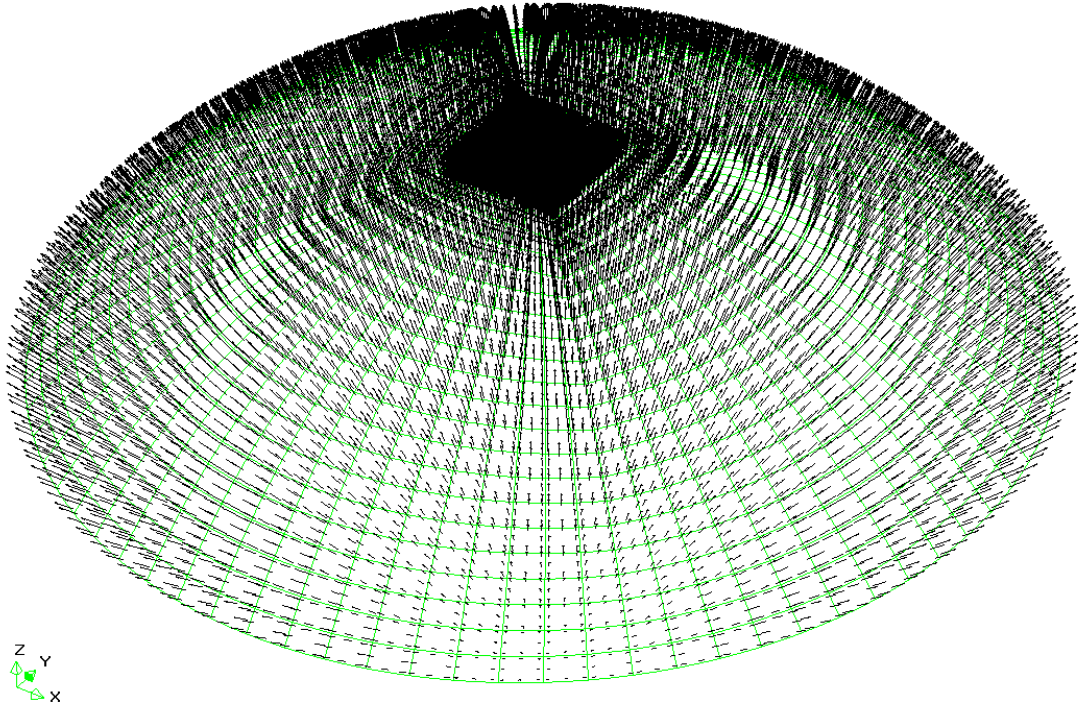
## Ellipsoid



*x-axis: pointing outwards in radial direction, laying in the surface of the shell*



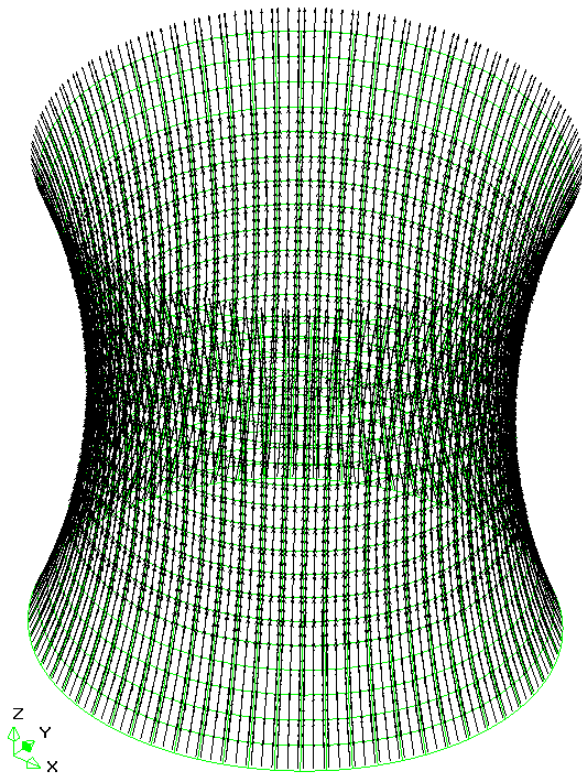
*y-axis: pointing in tangential direction, laying in the surface of the shell*



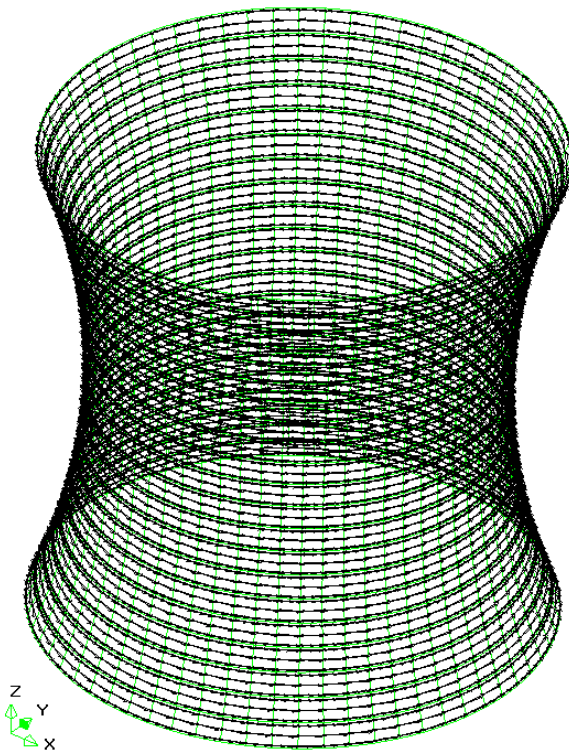
*z-axis: pointing outwards, perpendicular to the surface of the shell*



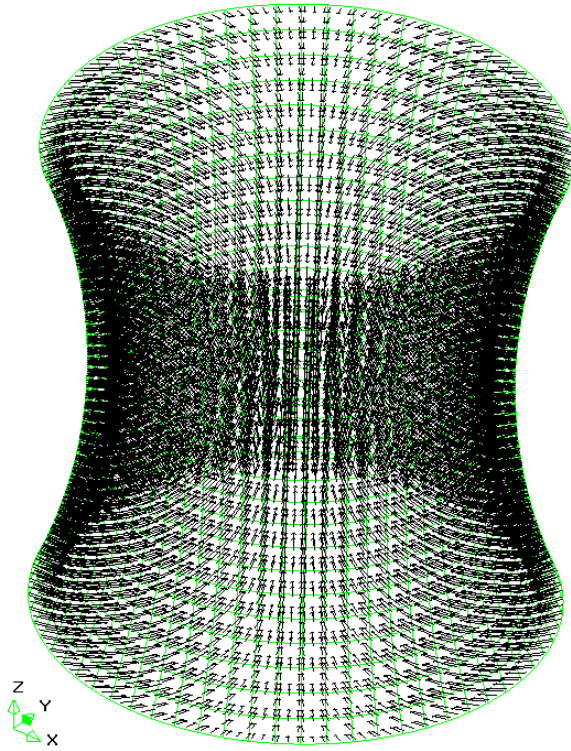
## Hyperboloid



*x-axis: pointing outwards in radial direction, laying in the surface of the shell*

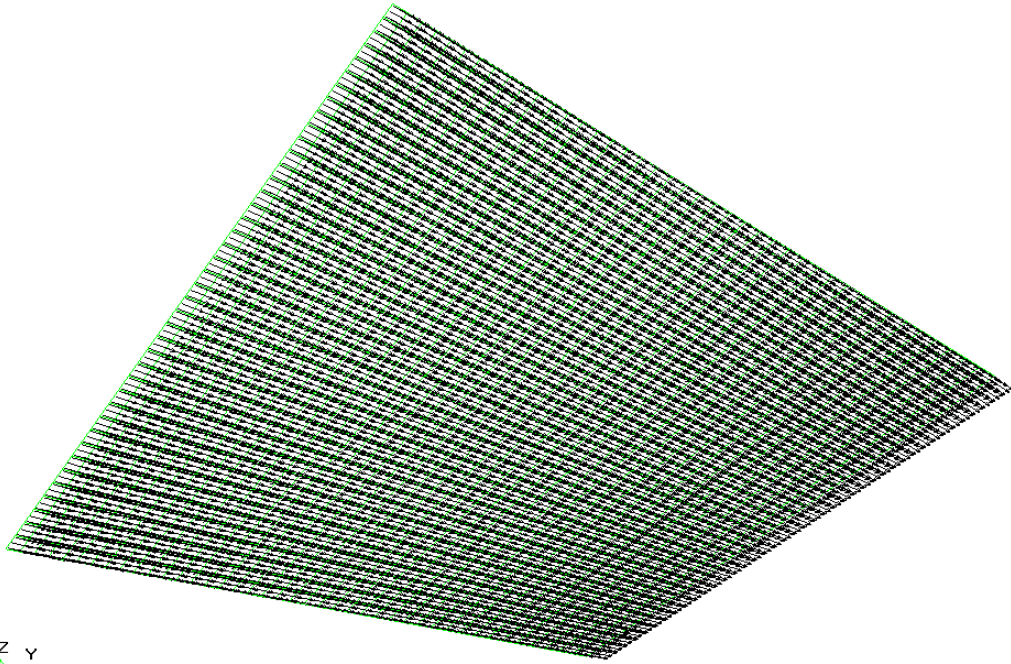


*y-axis: pointing in tangential direction, laying in the surface of the shell*

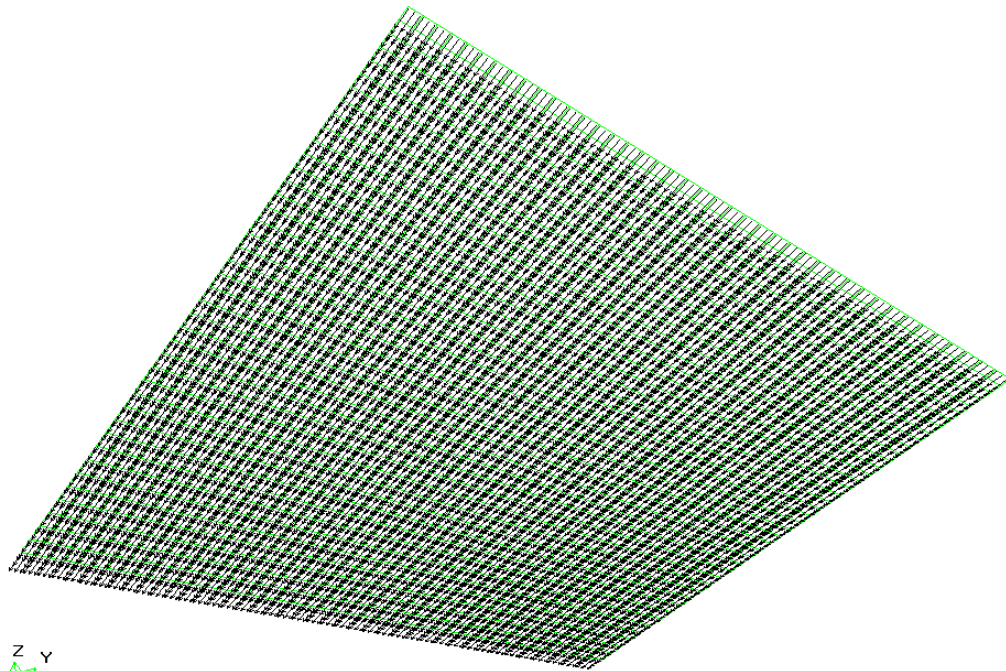


*z-axis: pointing inwards, perpendicular to the surface of the shell*

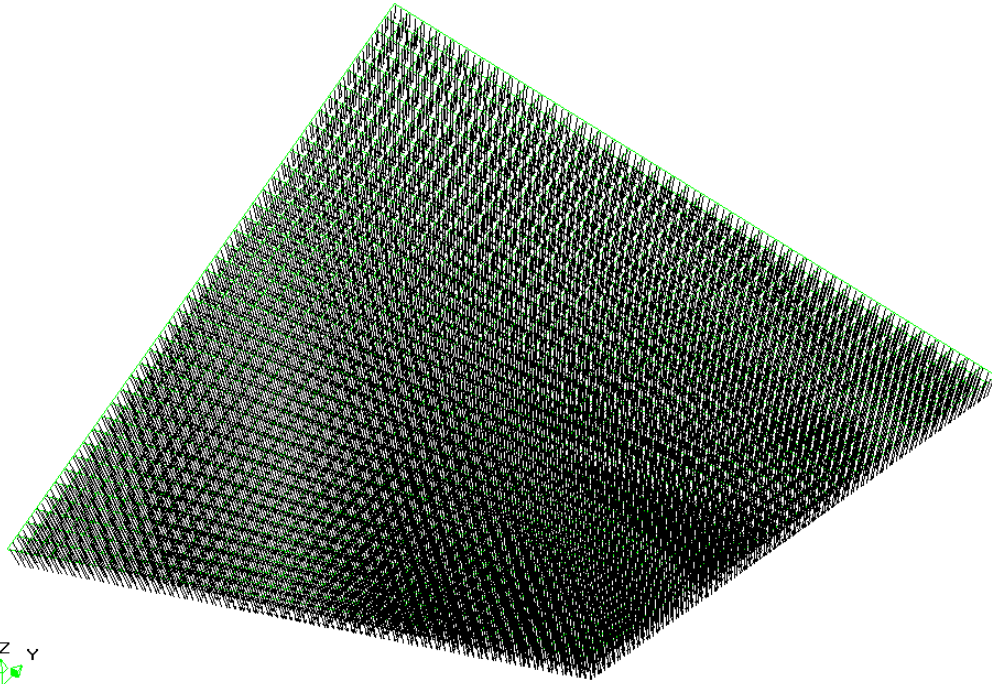
Hypar



*x-axis: pointing in global x-direction but laying in the surface of the shell*



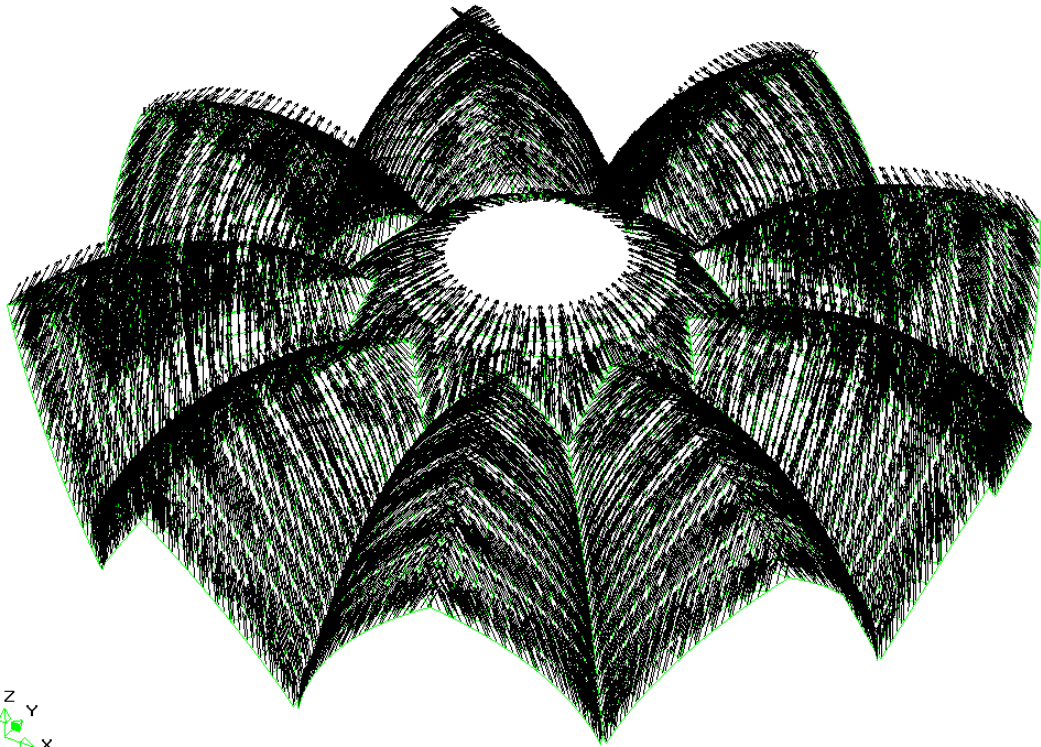
*y-axis: pointing in global y-direction but laying in the surface of the shell*



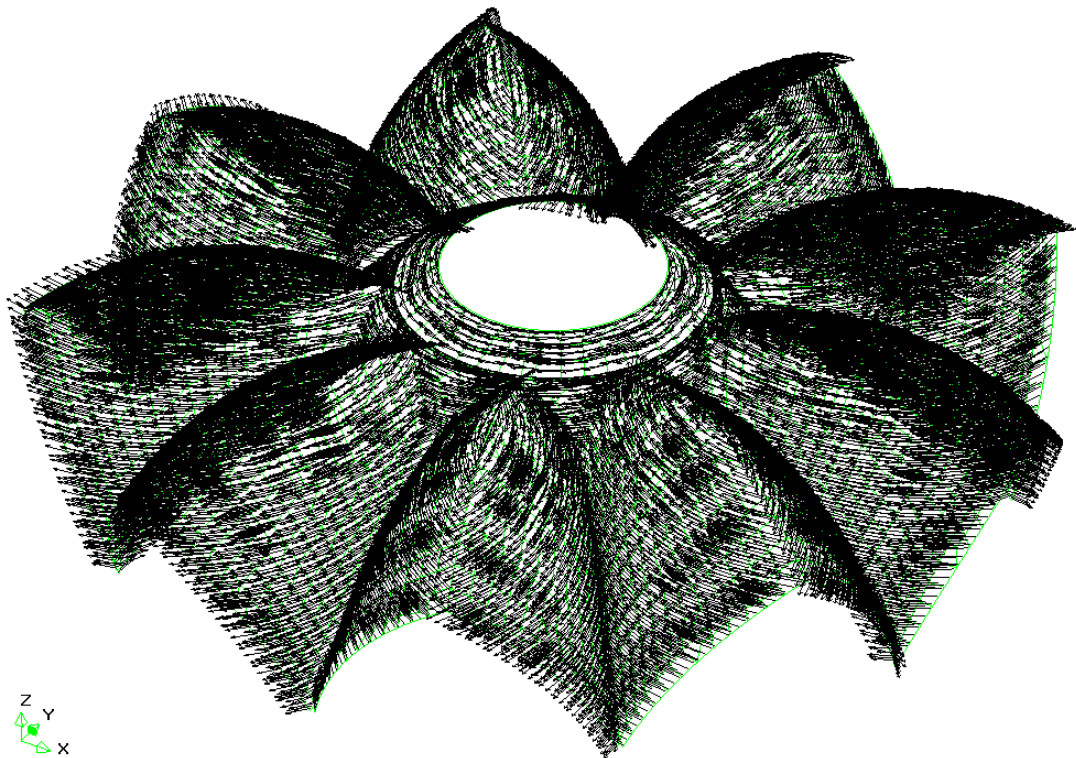
*z-axis: pointing downwards, perpendicular to the shell surface*



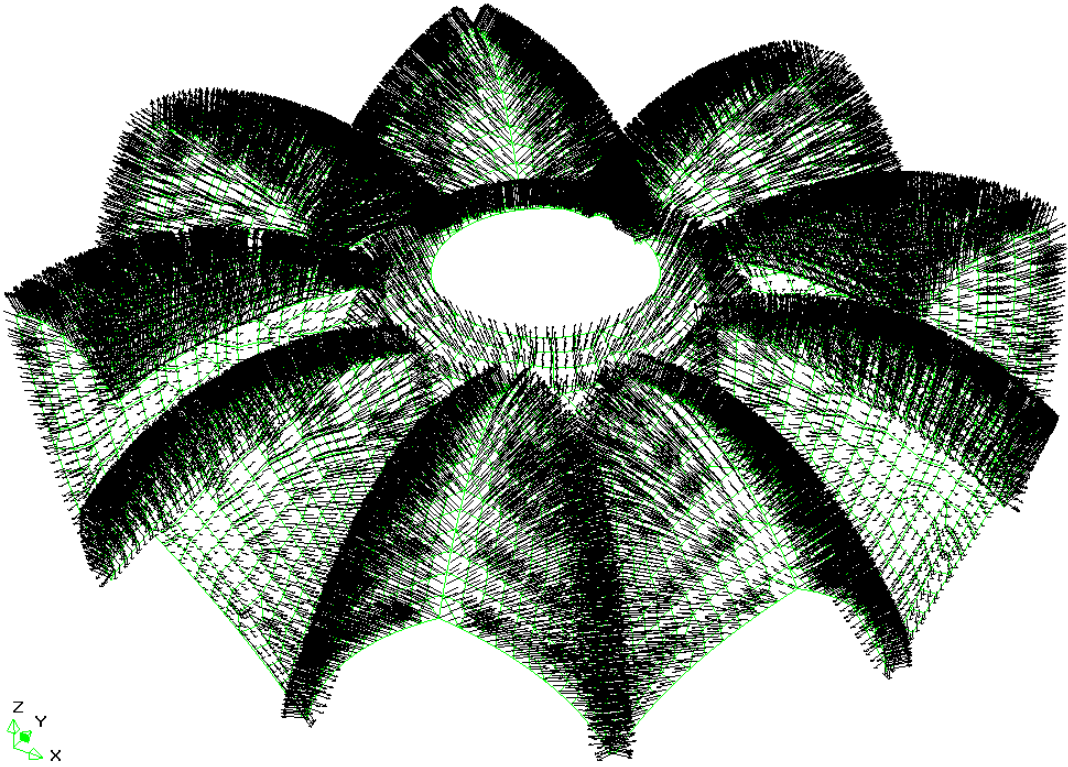
Complex geometry



*x-axis: pointing outwards in radial direction for the inner ring of elements, laying in the surface of the shell*



*y-axis: pointing in tangential direction for the inner ring of elements, laying in the surface of the shell*



*z-axis: pointing outwards, perpendicular to the surface of the shell*



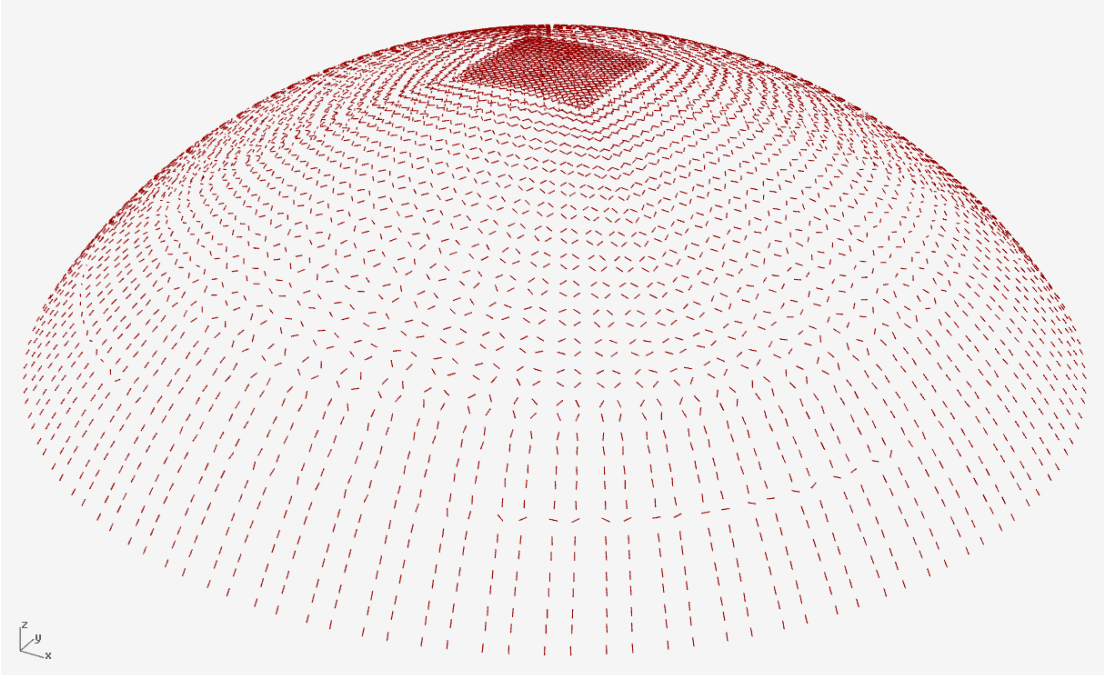




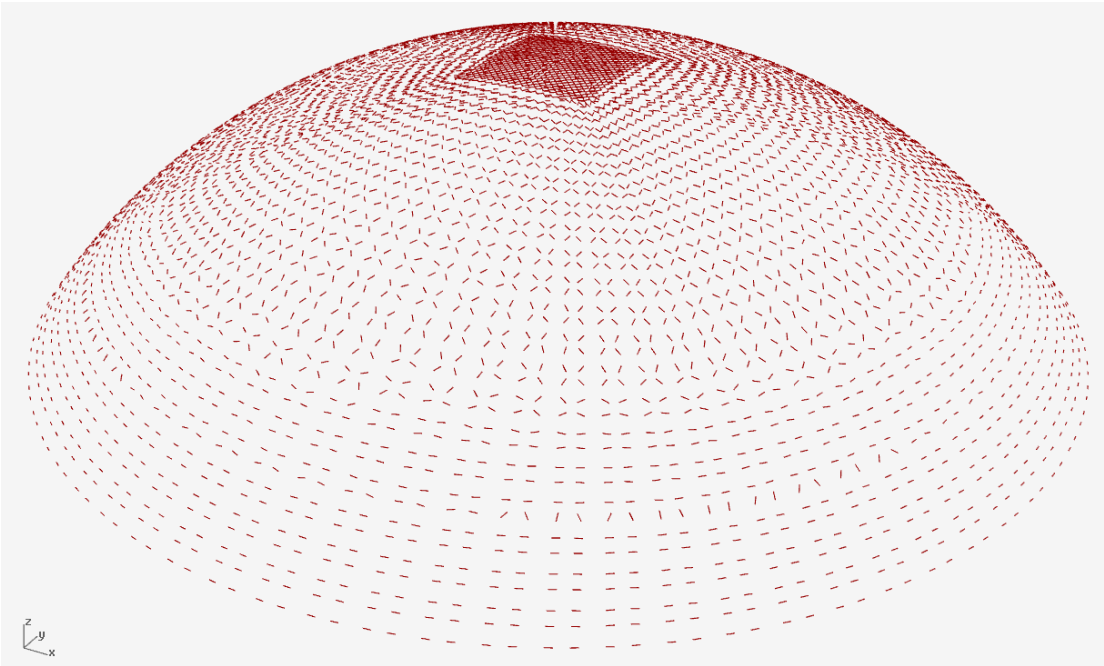
# APPENDIX C – PRINCIPAL DIRECTIONS OF THE DISTRIBUTED BENDING MOMENT

Ellipsoid

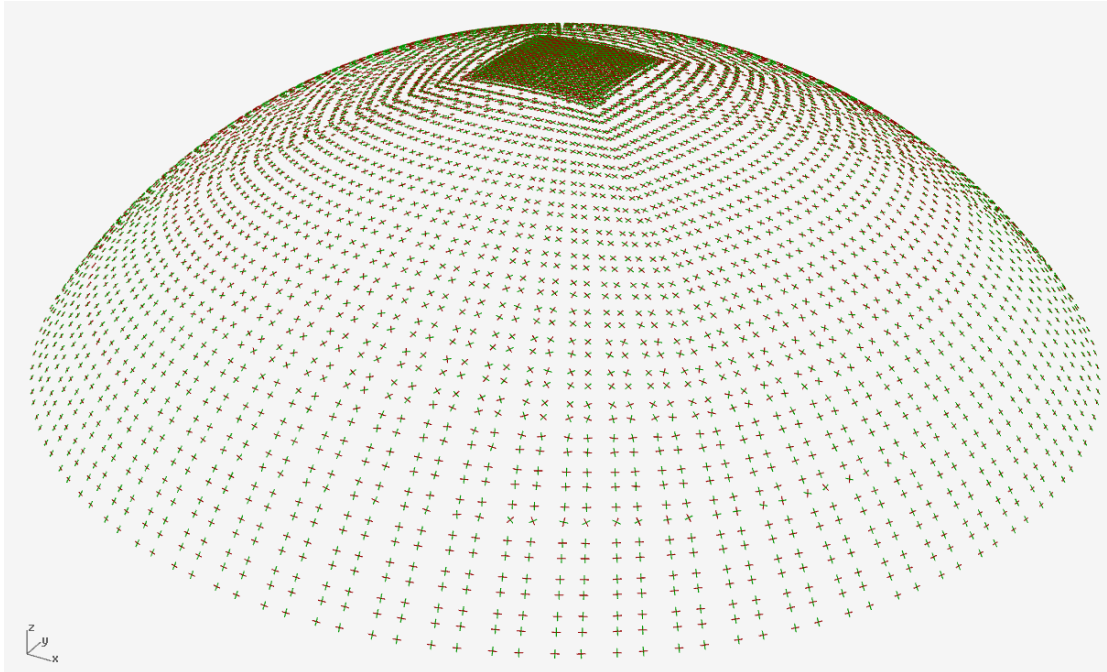
Self weight



*First principal direction of the distributed bending moment.*

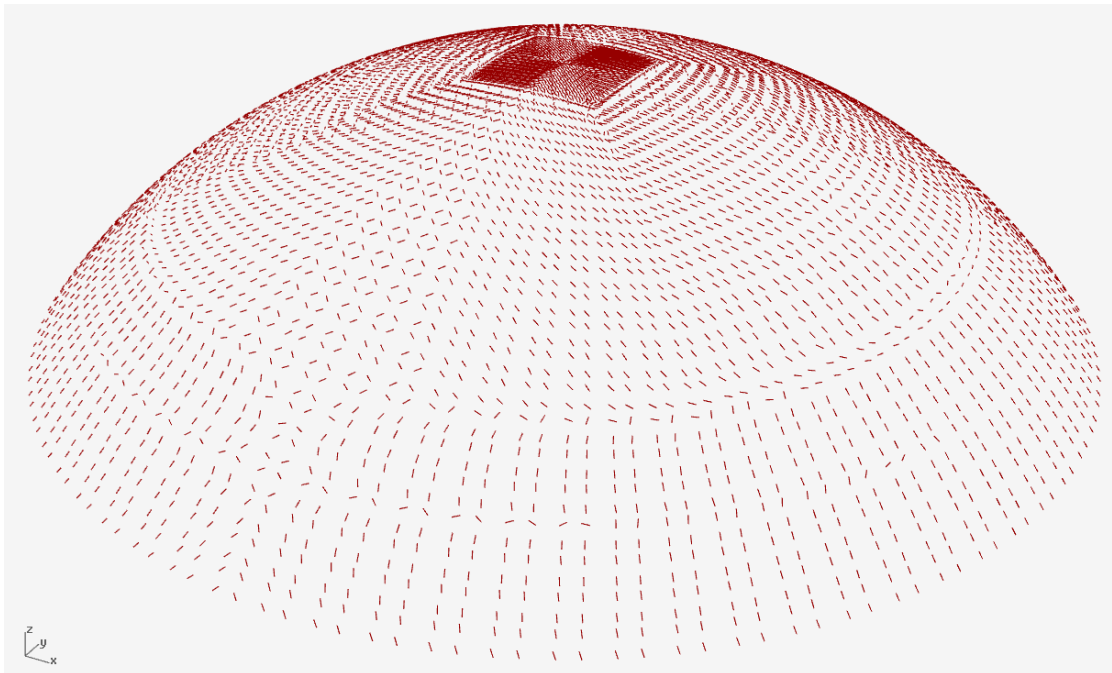


*Second principal direction of the distributed bending moment.*

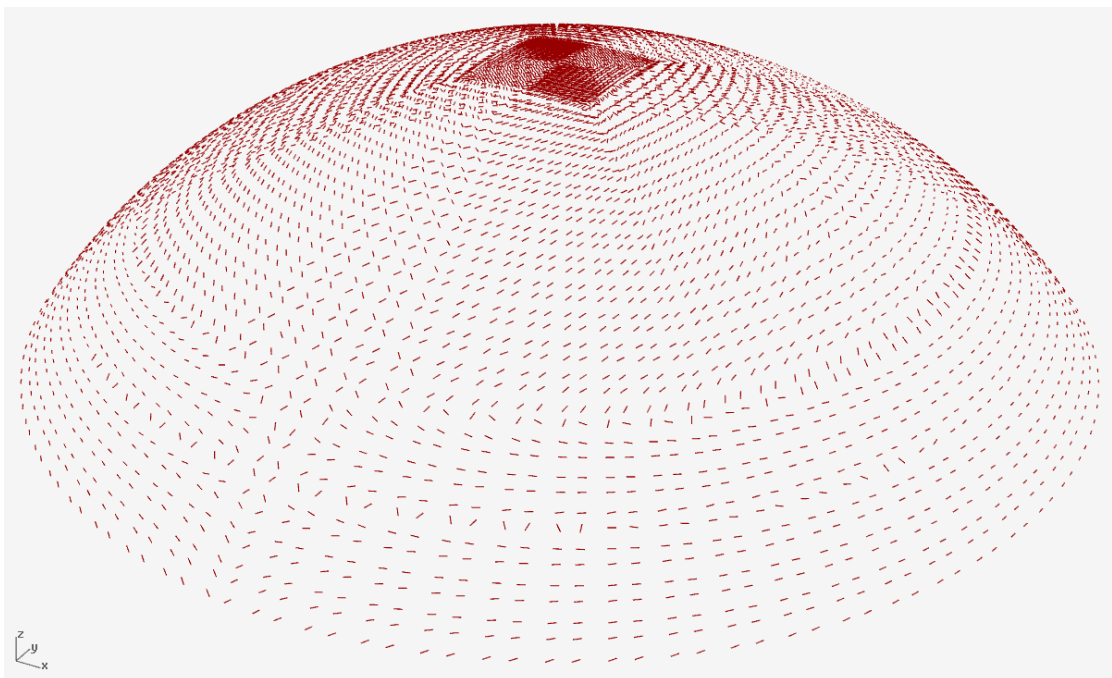


*First (green) and second (red) principal direction of the distributed bending moment.*

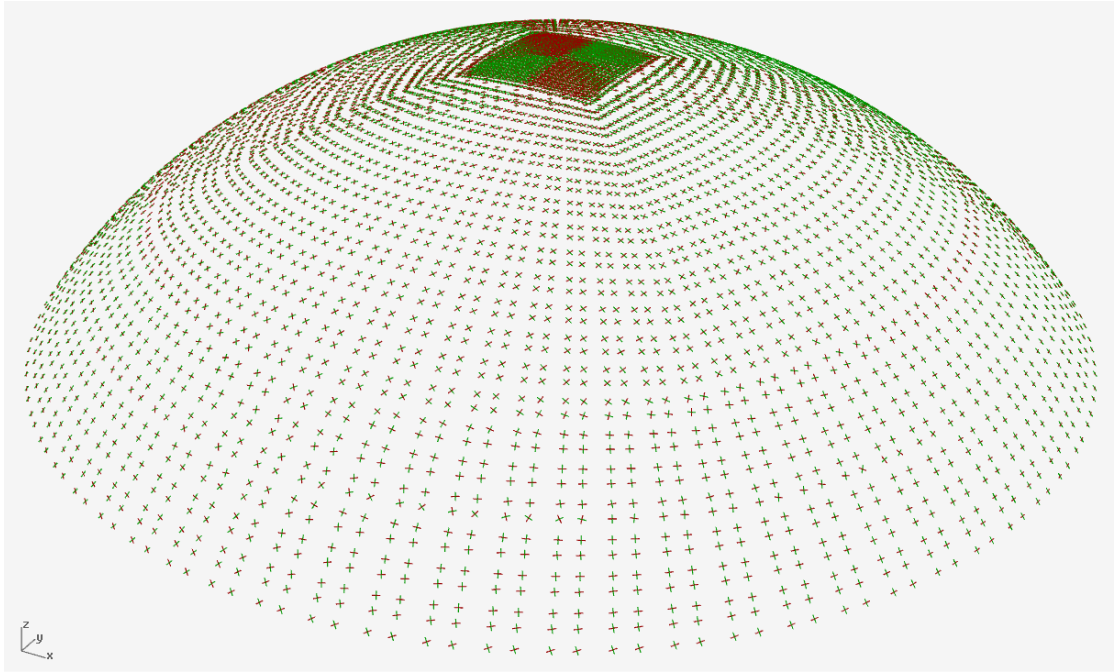
## Wind load



*First principal direction of the distributed bending moment.*



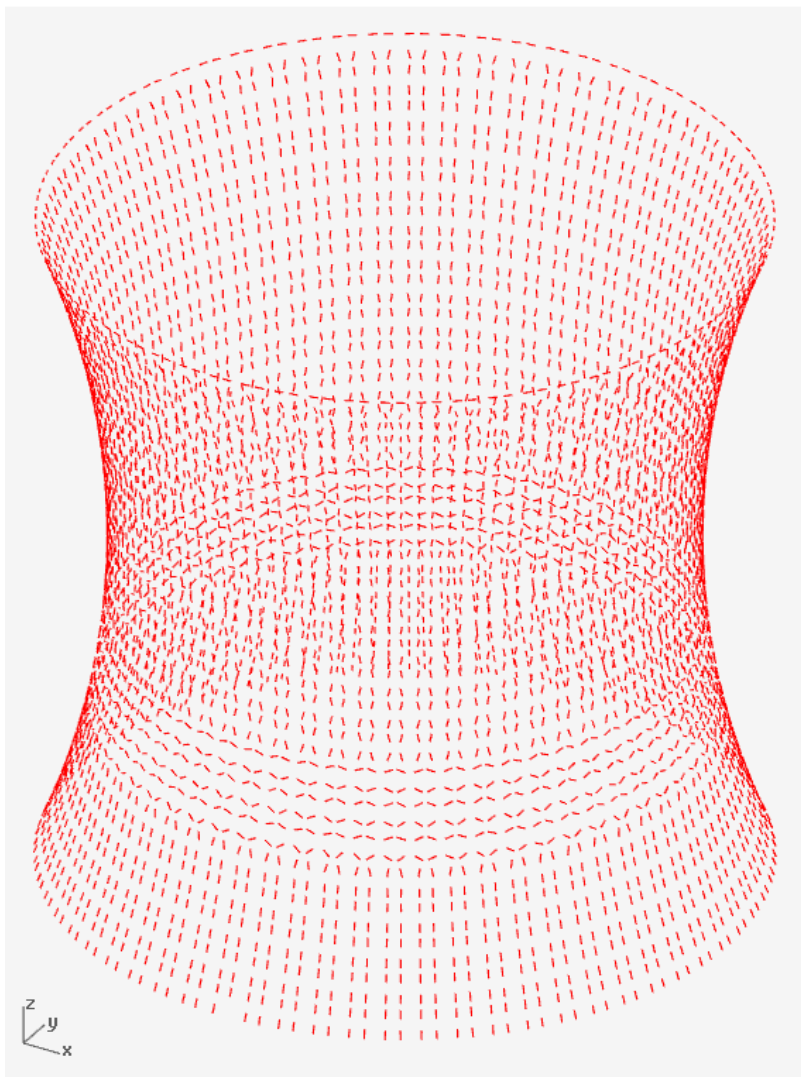
*Second principal direction of the distributed bending moment.*



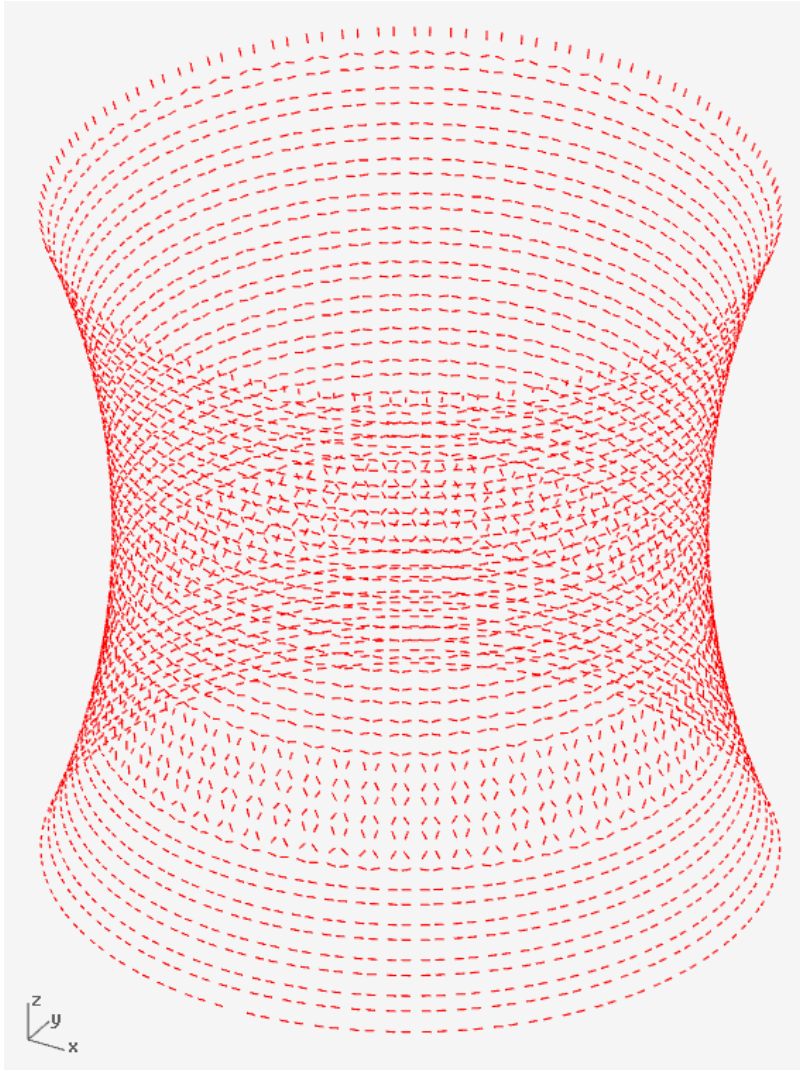
*First (green) and second (red) principal direction of the distributed bending moment.*

## Hyperboloid

Self weight

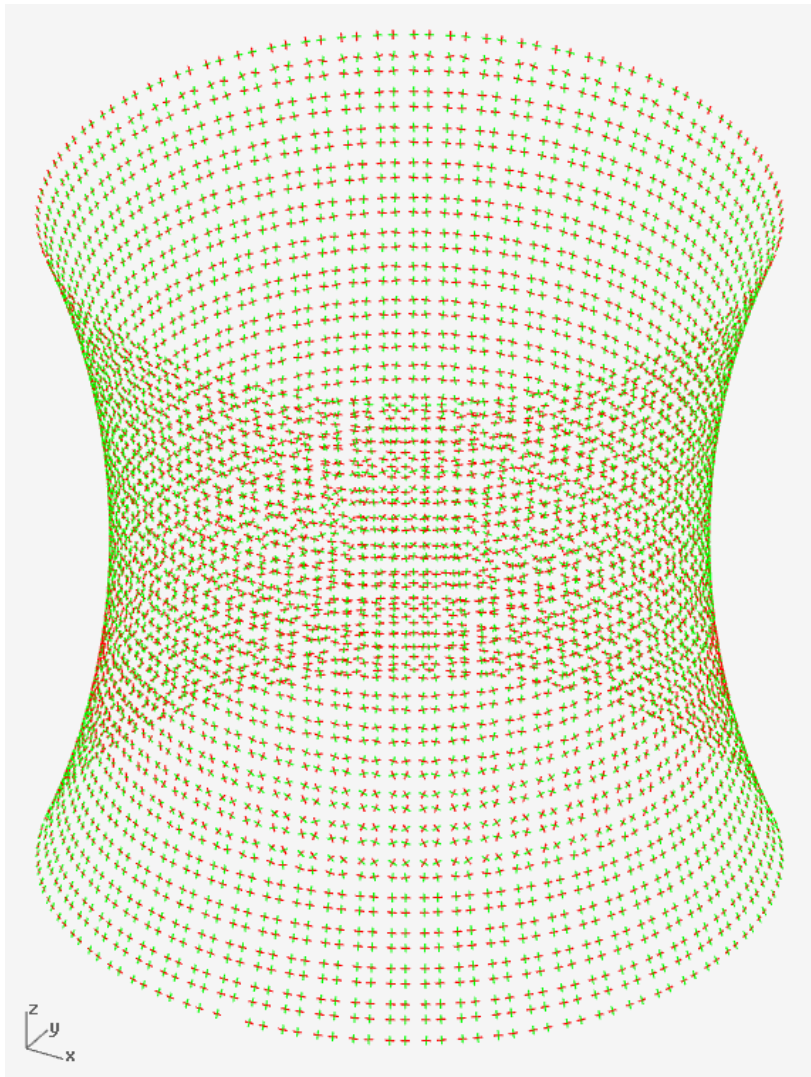


*First principal direction of the distributed bending moment.*



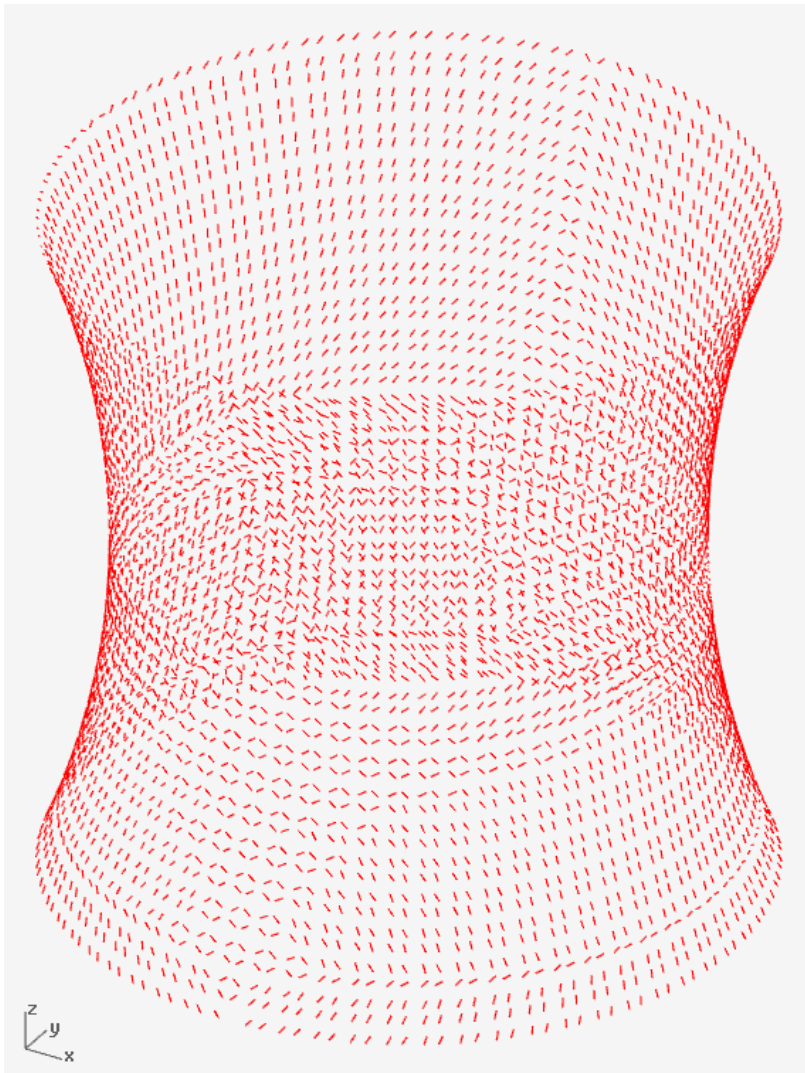
*Second principal direction of the distributed bending moment.*





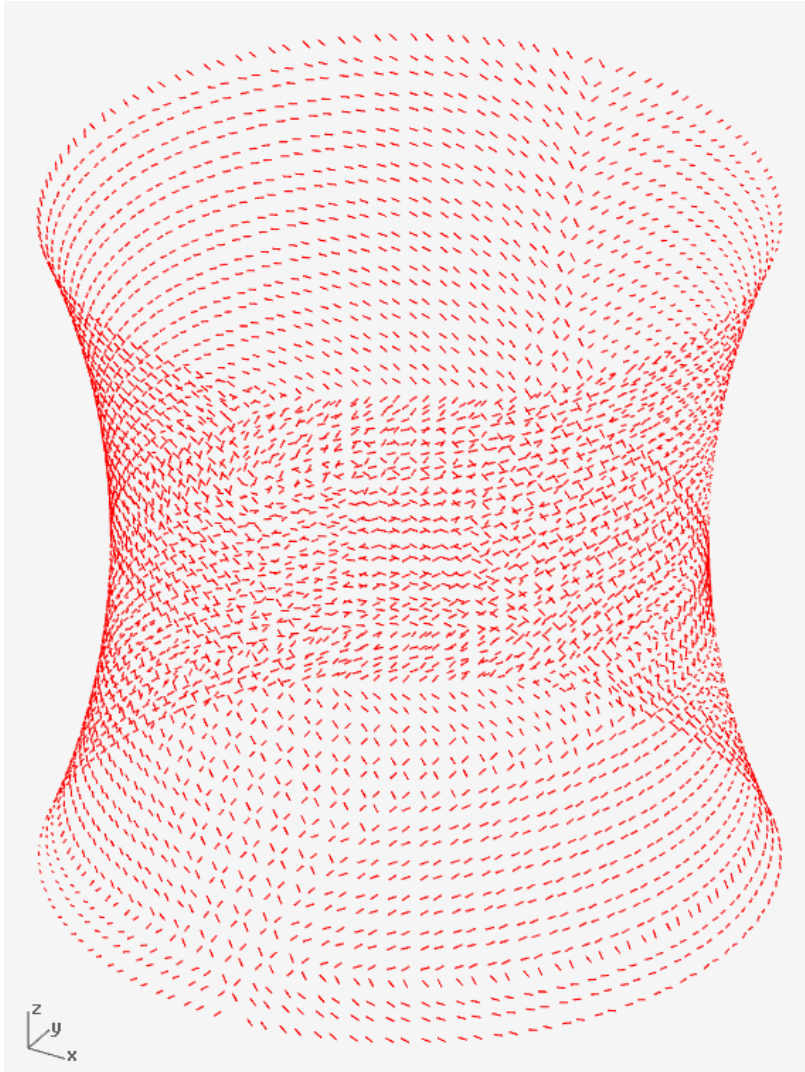
*First (green) and second (red) principal direction of the distributed bending moment.*

## Wind load

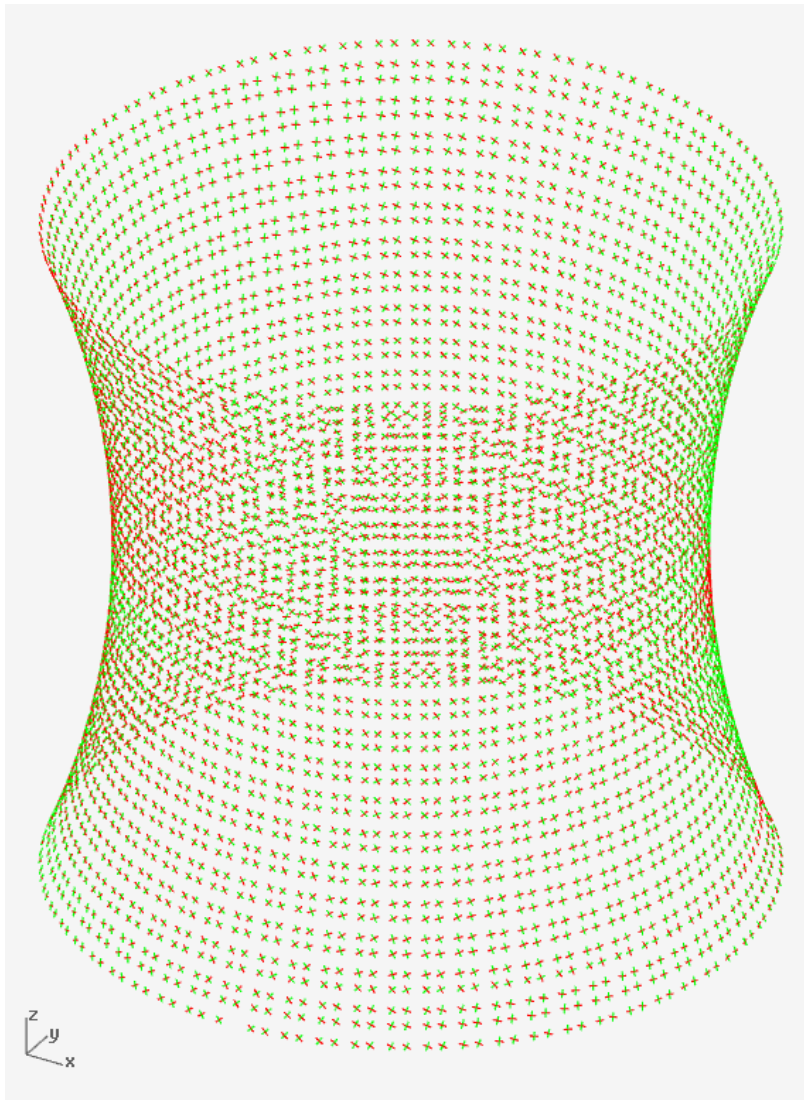


*First principal direction of the distributed bending moment.*





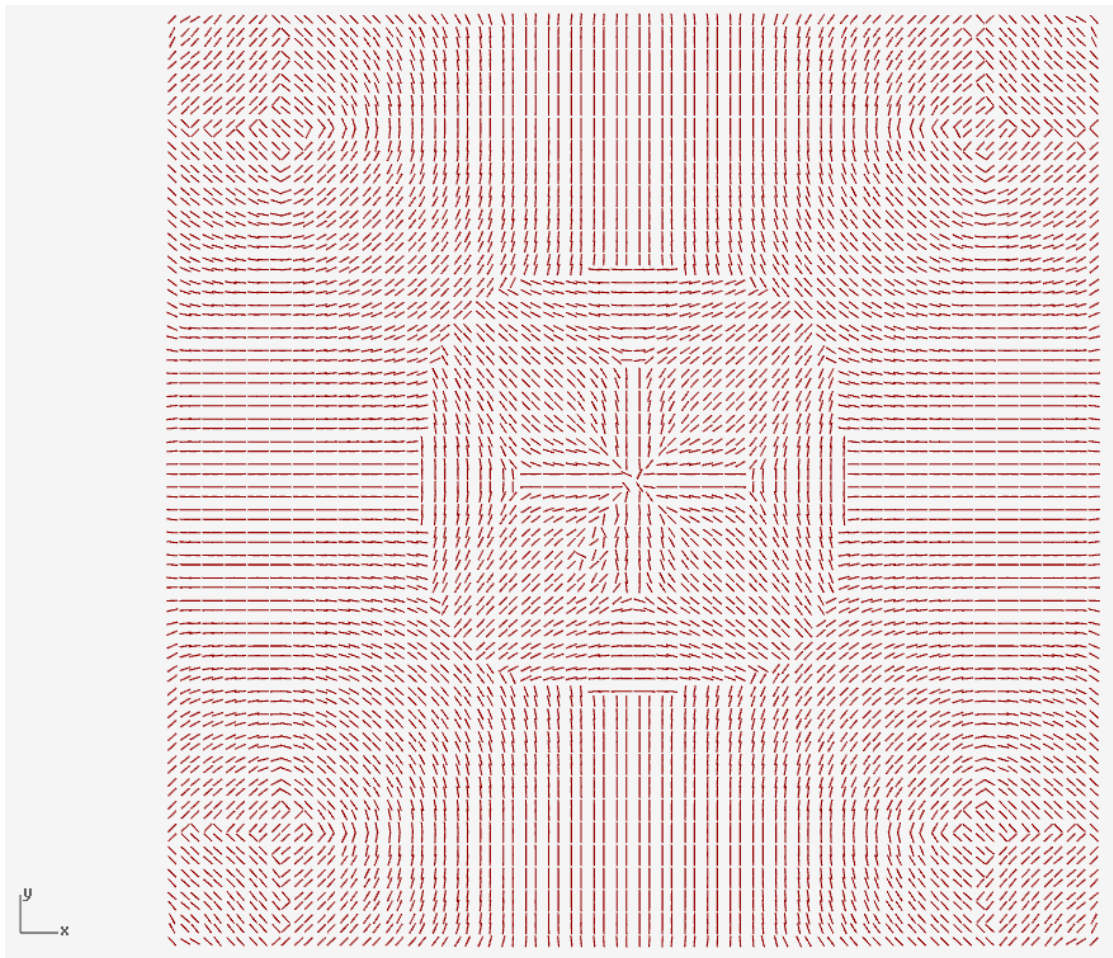
*Second principal direction of the distributed bending moment.*



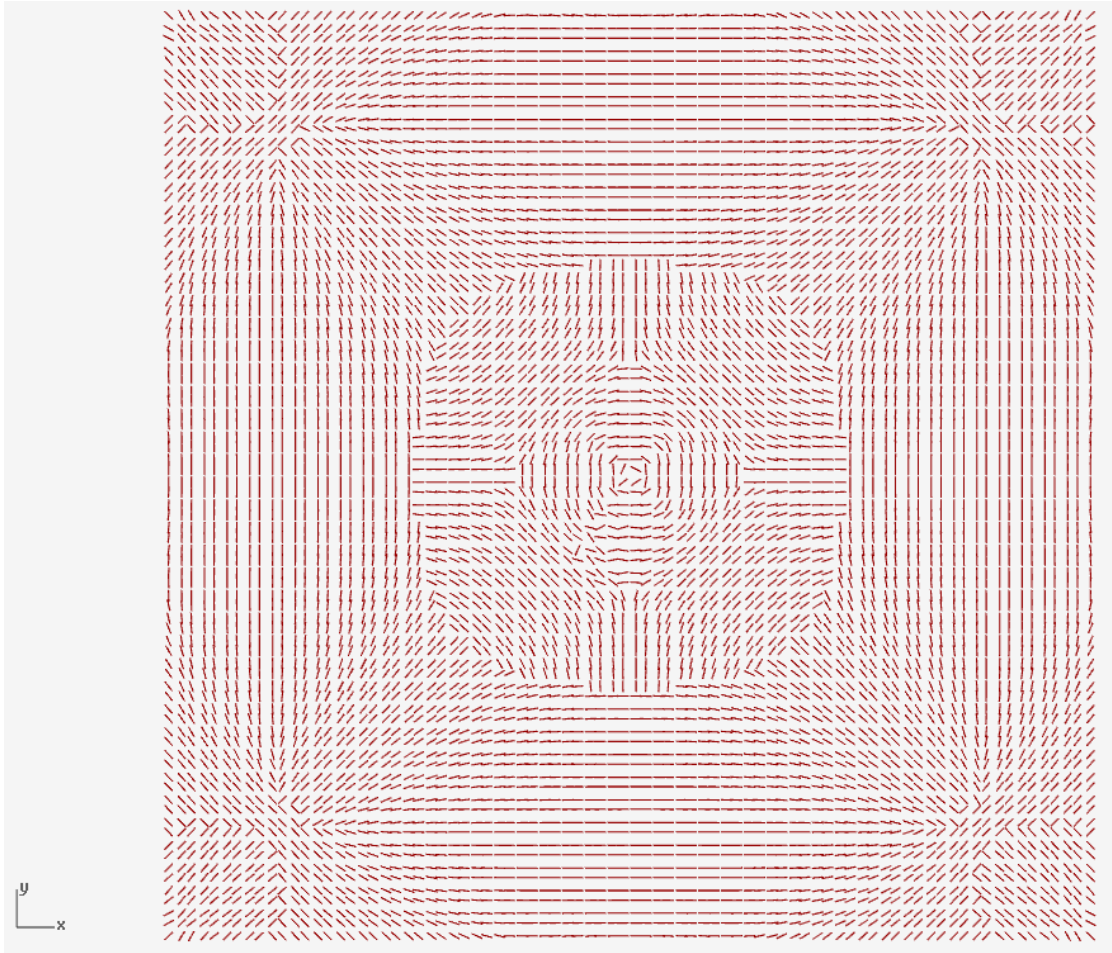
*First (green) and second (red) principal direction of the distributed bending moment.*

**Hypar**

**Self weight**

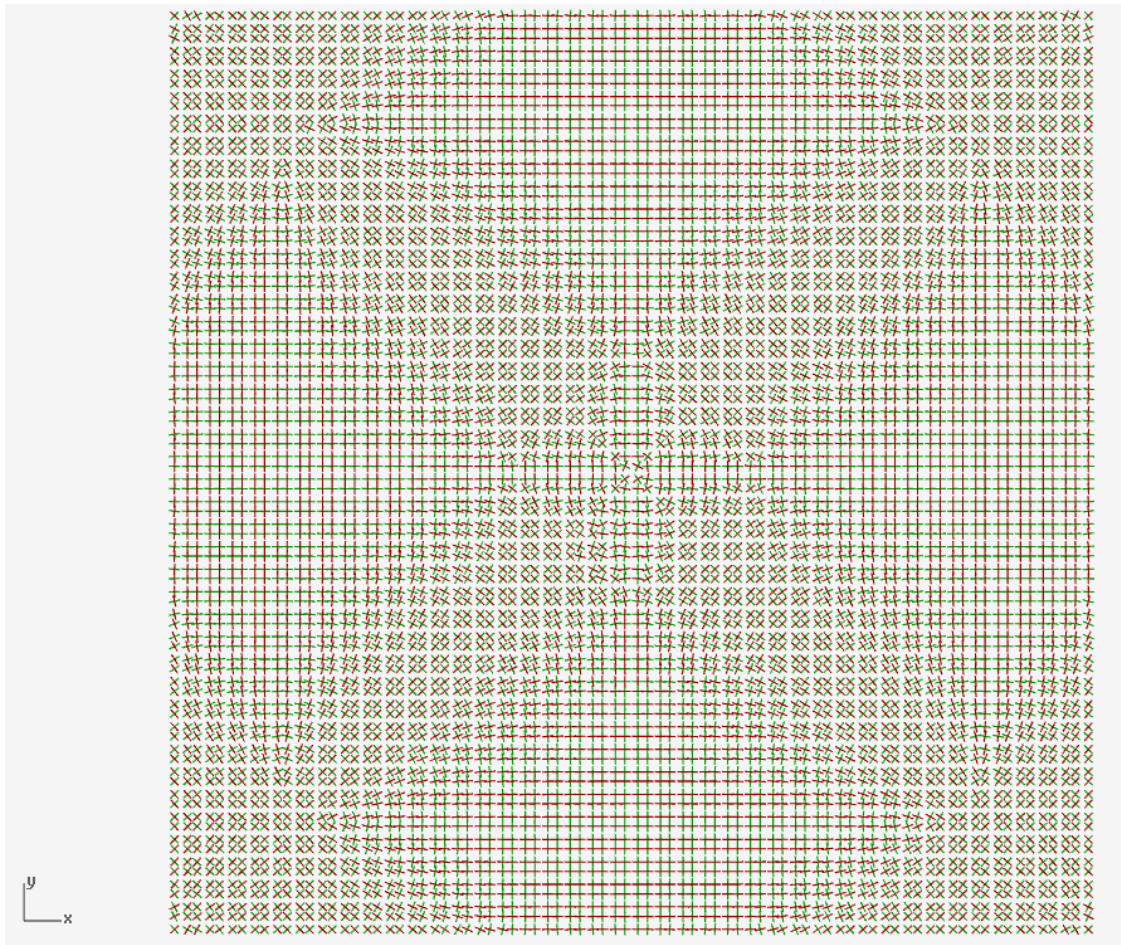


*First principal direction of the distributed bending moment.*



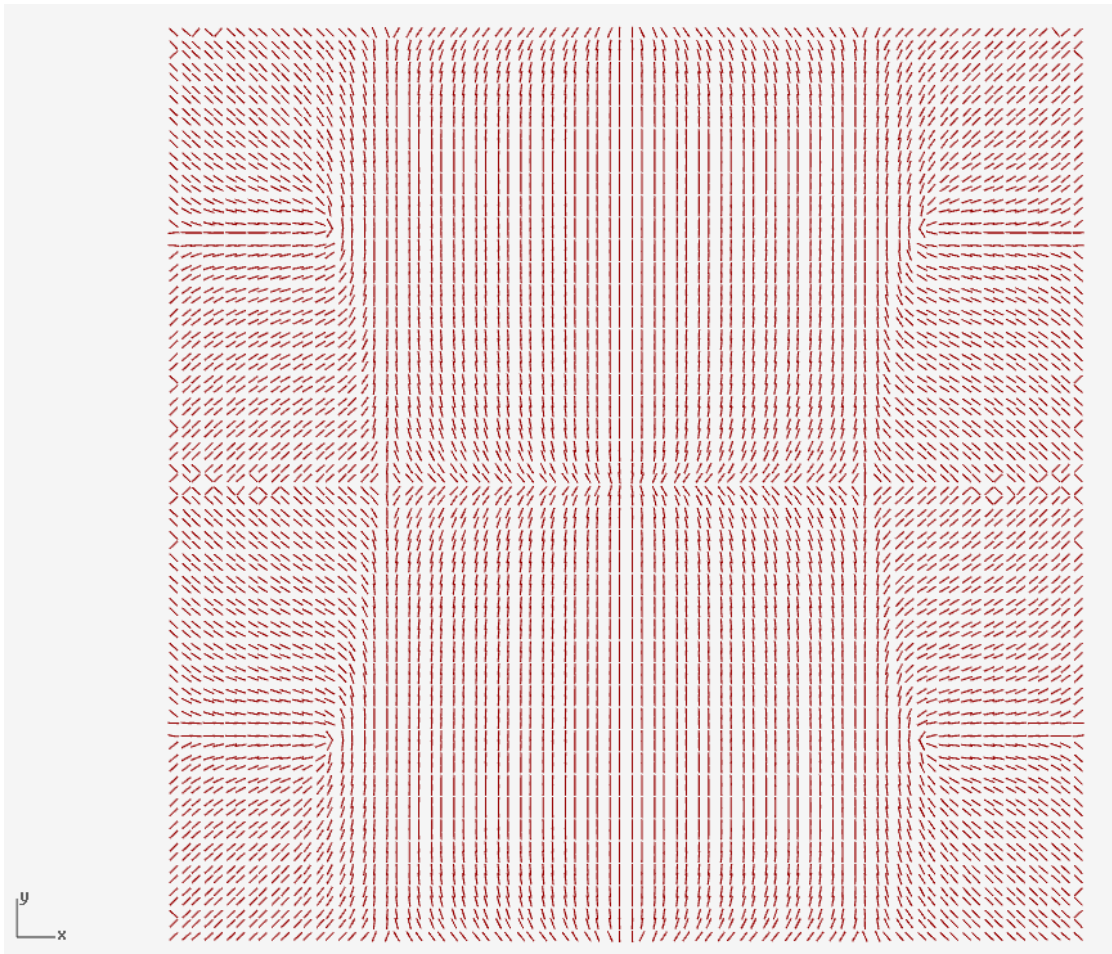
*Second principal direction of the distributed bending moment.*



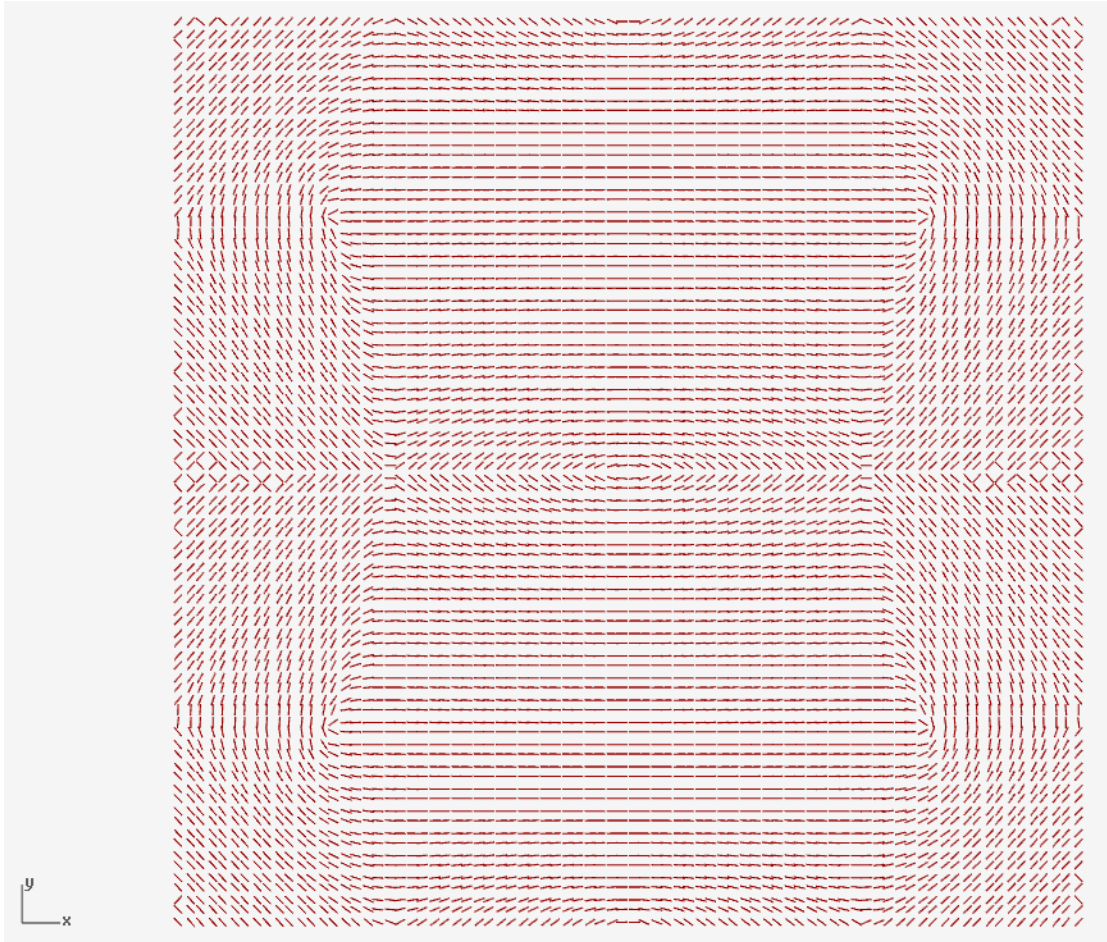


*First (green) and second (red) principal direction of the distributed bending moment.*

## Wind load

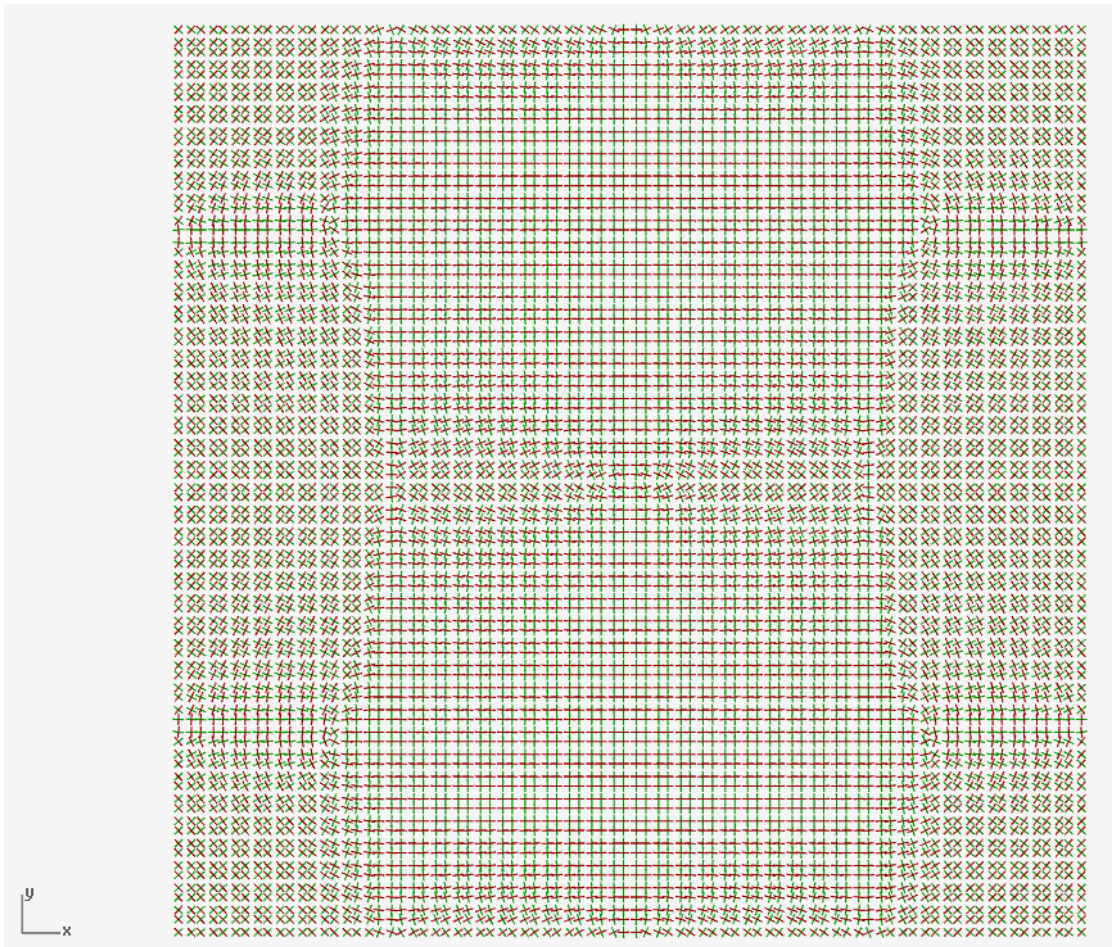


*First principal direction of the distributed bending moment.*



*Second principal direction of the distributed bending moment.*



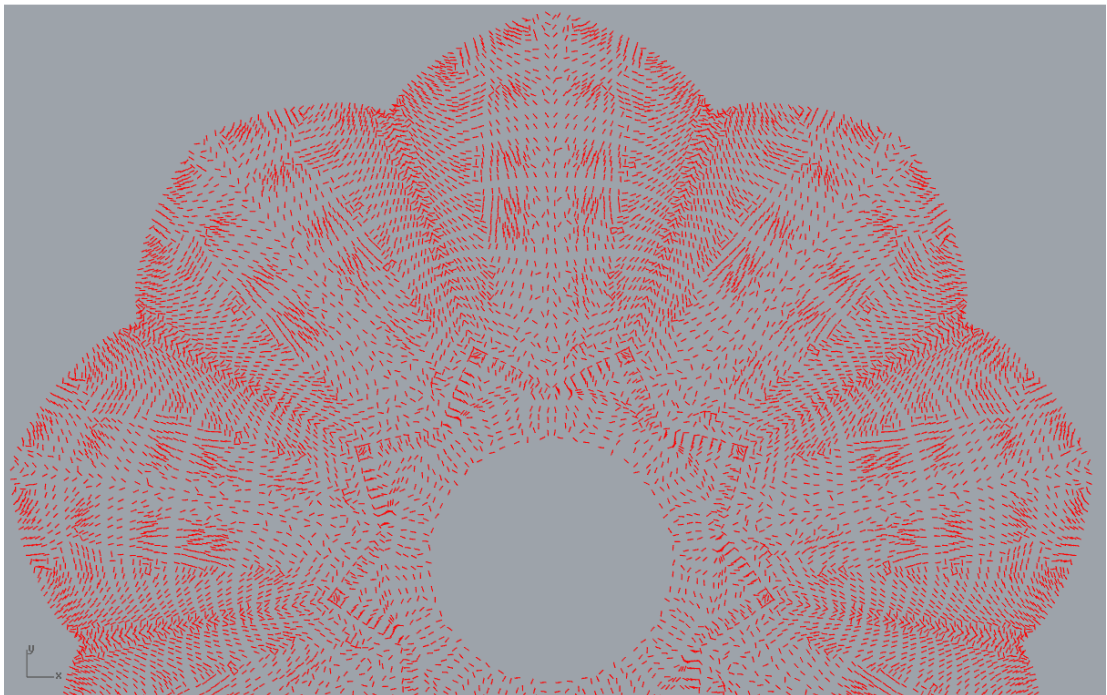


*First (green) and second (red) principal direction of the distributed bending moment.*

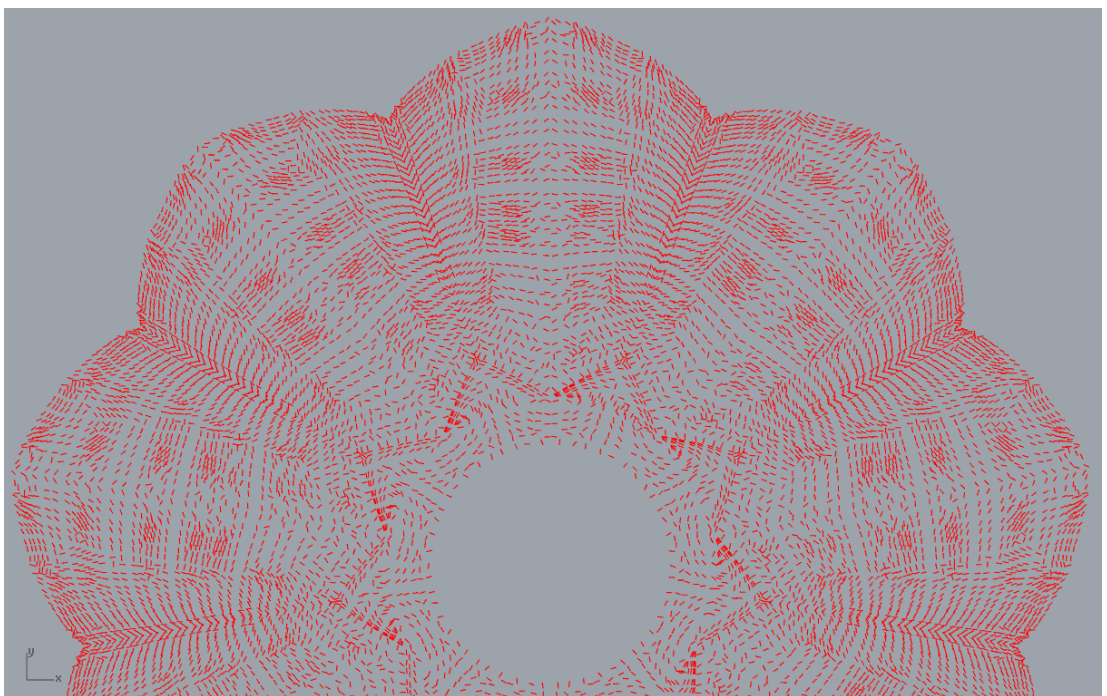


## Complex geometry

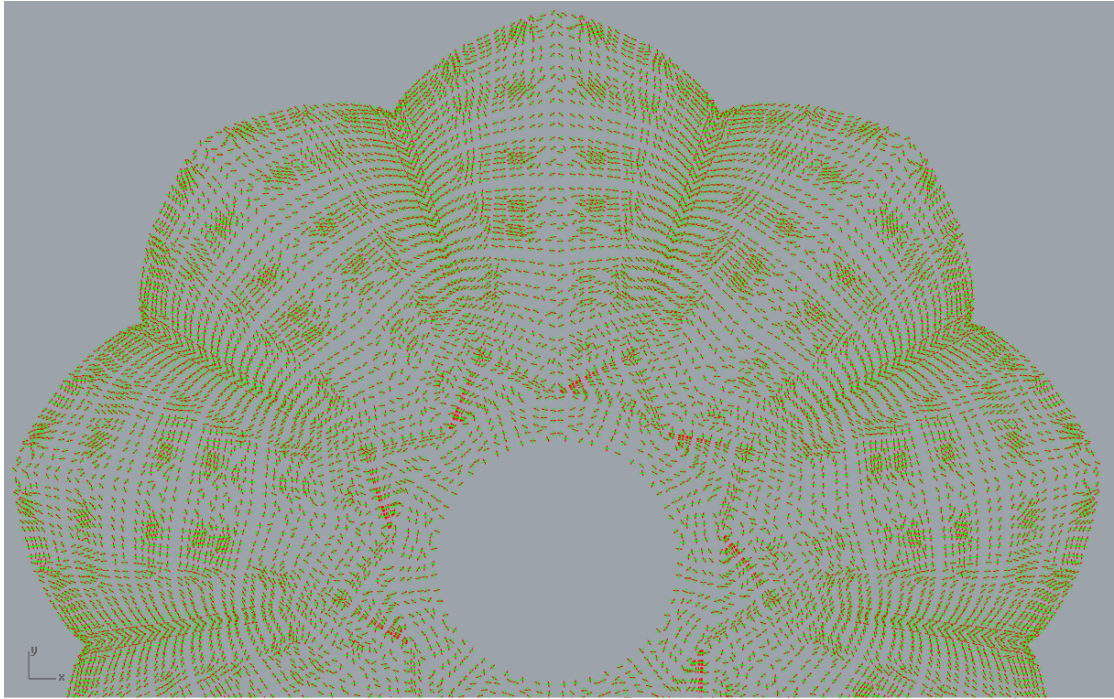
### Self weight



*First principal direction of the distributed bending moment.*

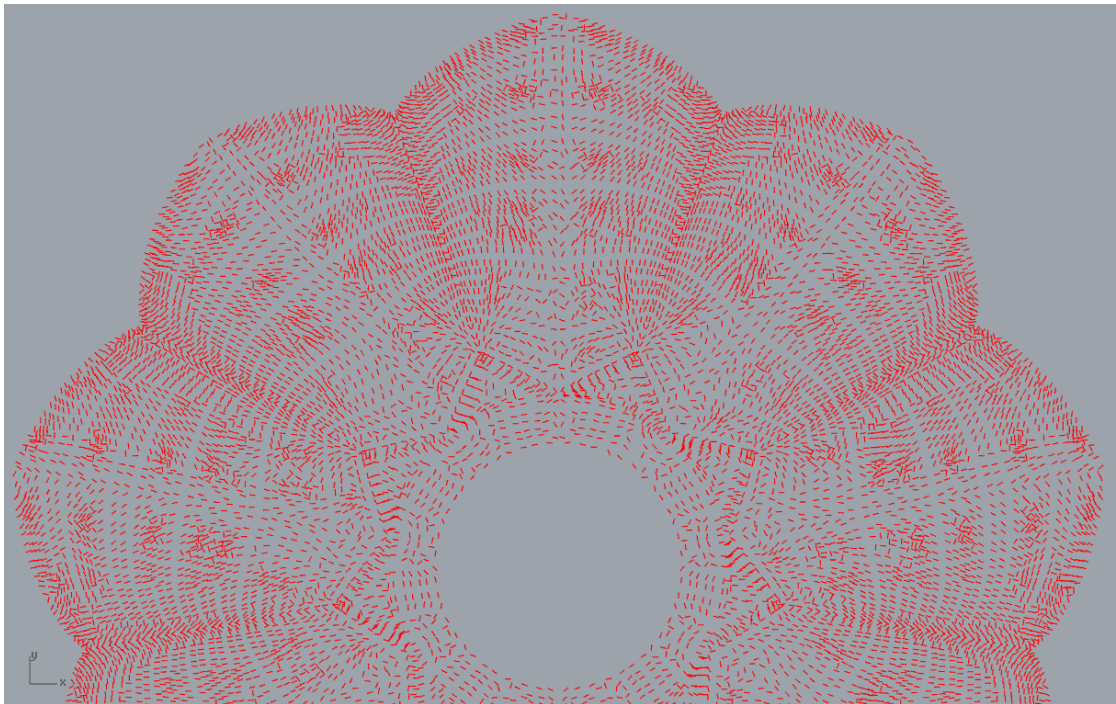


*Second principal direction of the distributed bending moment.*

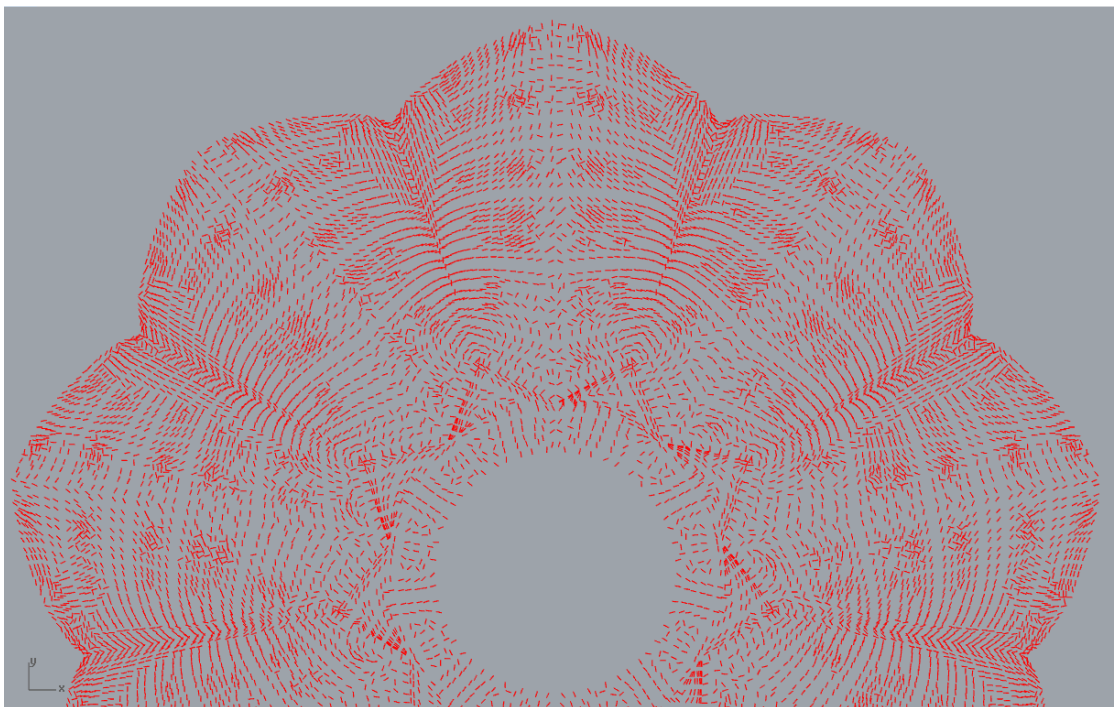


*First (green) and second (red) principal direction of the distributed bending moment.*

**Wind load**

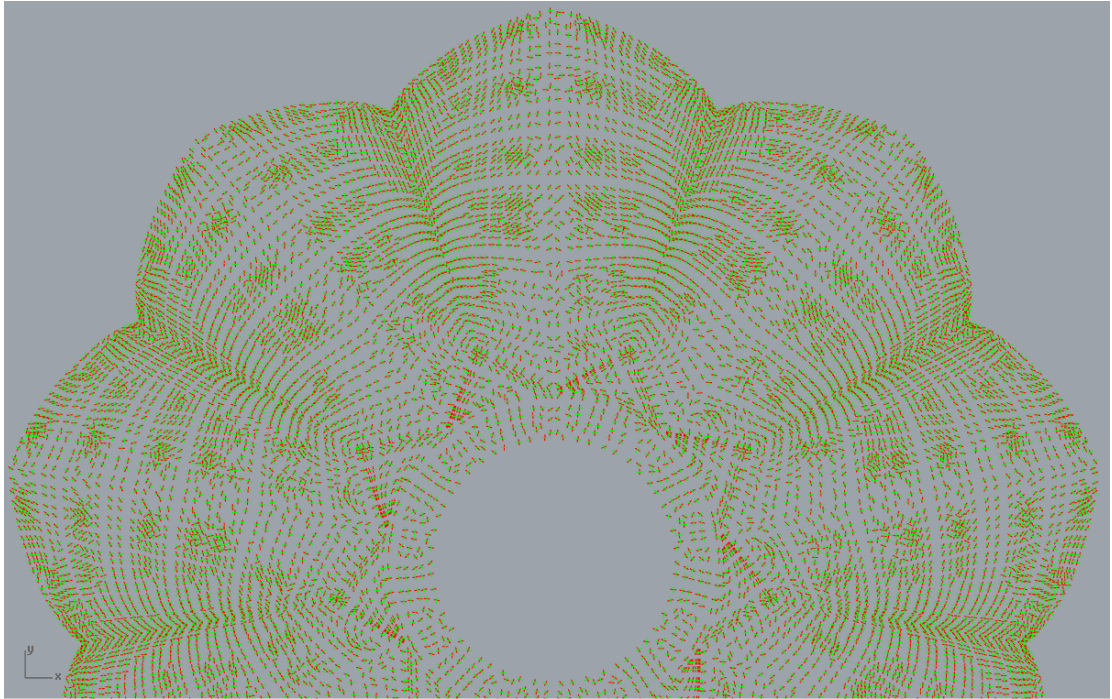


*First principal direction of the distributed bending moment.*



*Second principal direction of the distributed bending moment.*





*First (green) and second (red) principal direction of the distributed bending moment.*



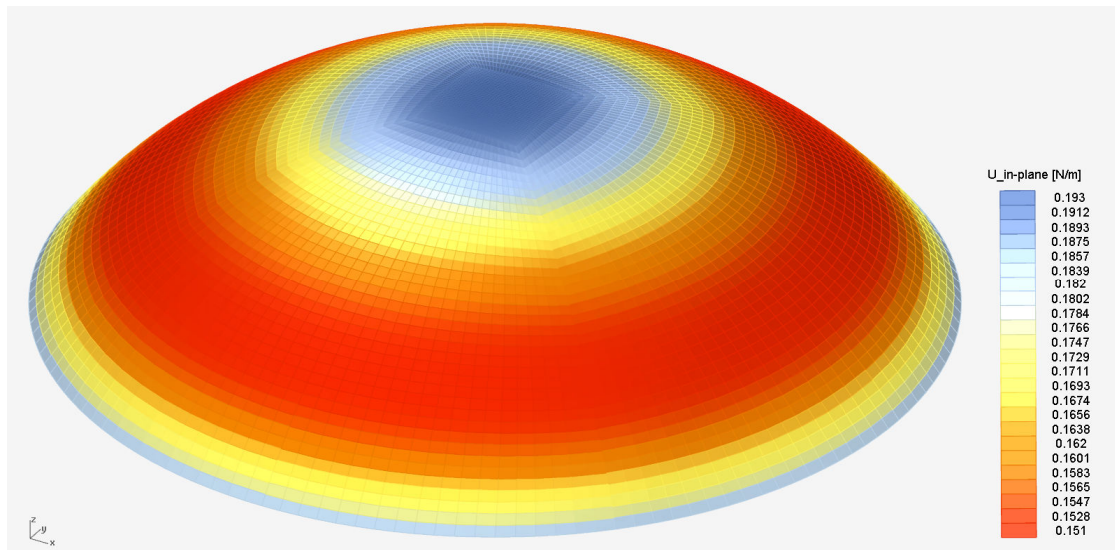


## APPENDIX D - ANALYSIS RESULTS

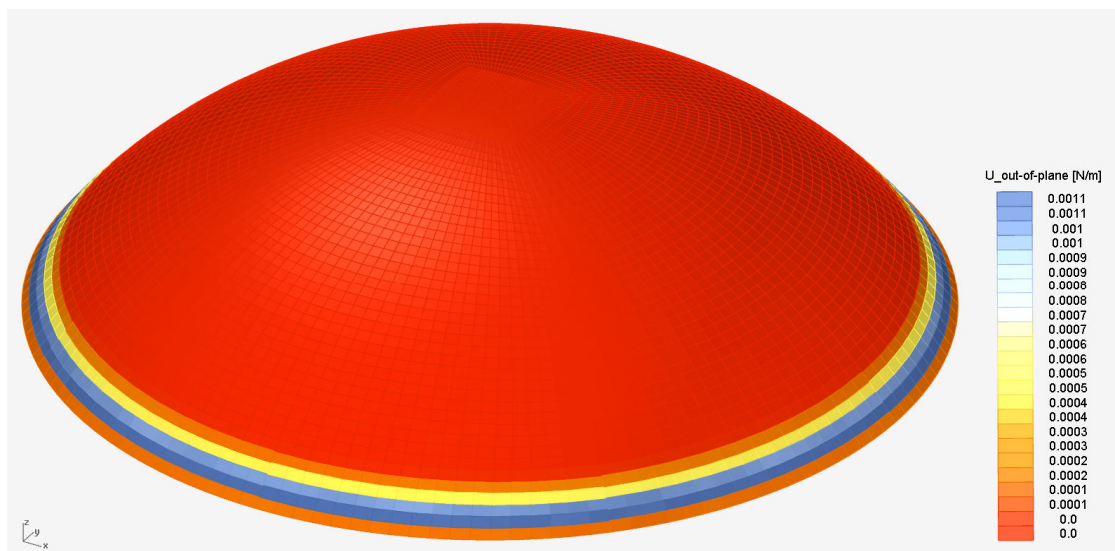
Strain energy

Self weight

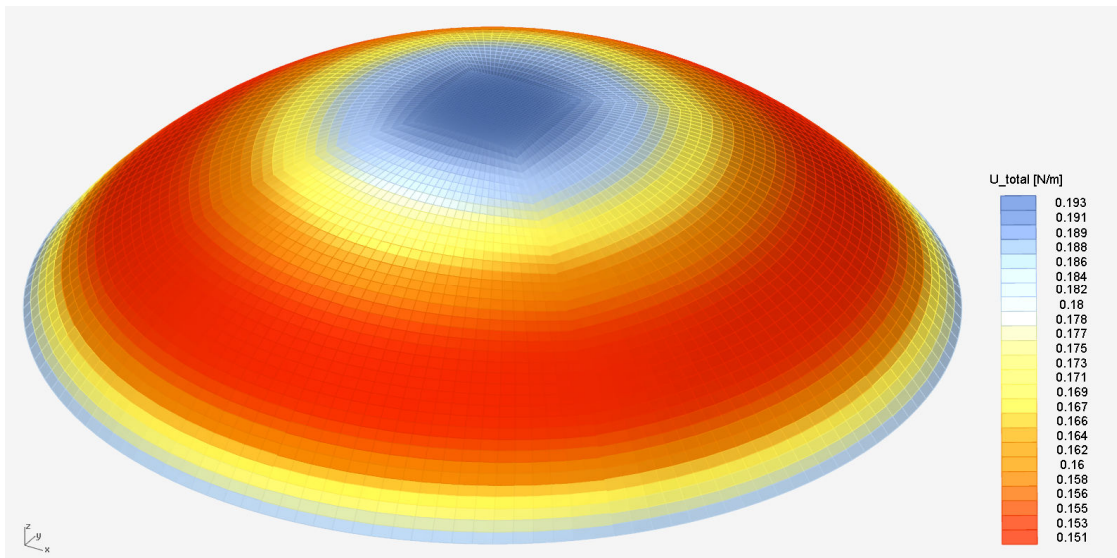
Ellipsoid



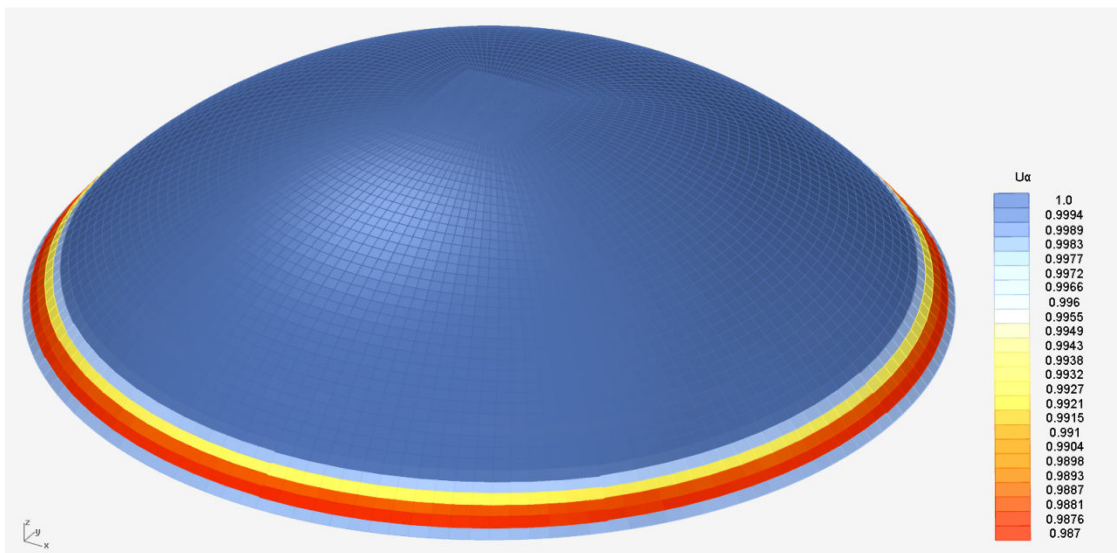
*The in-plane strain energy results for the ellipsoid for the loading condition self weight.*



*The out-of-plane strain energy results for the ellipsoid for the loading condition self weight.*



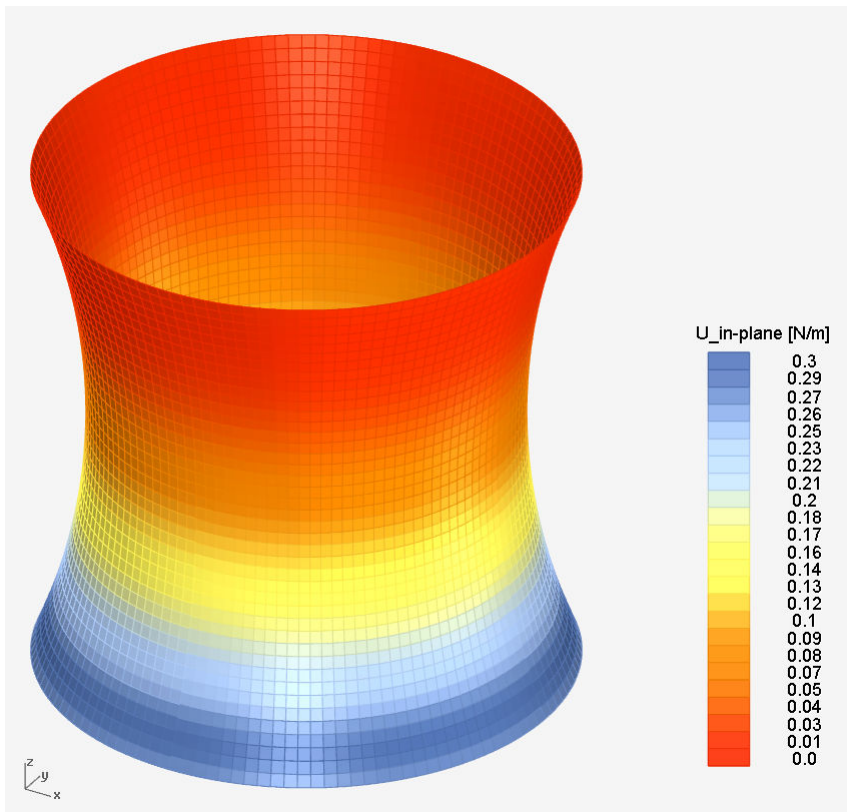
The total strain energy results for the ellipsoid for the loading condition self weight.



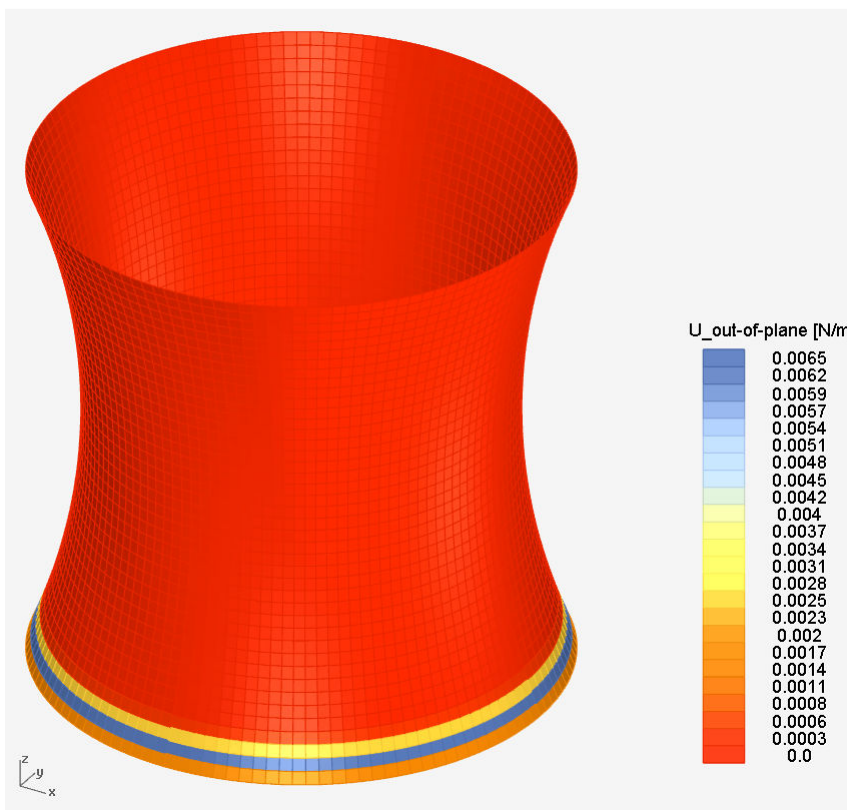
The strain energy results for  $U_\alpha$  for the ellipsoid for the loading condition self weight.



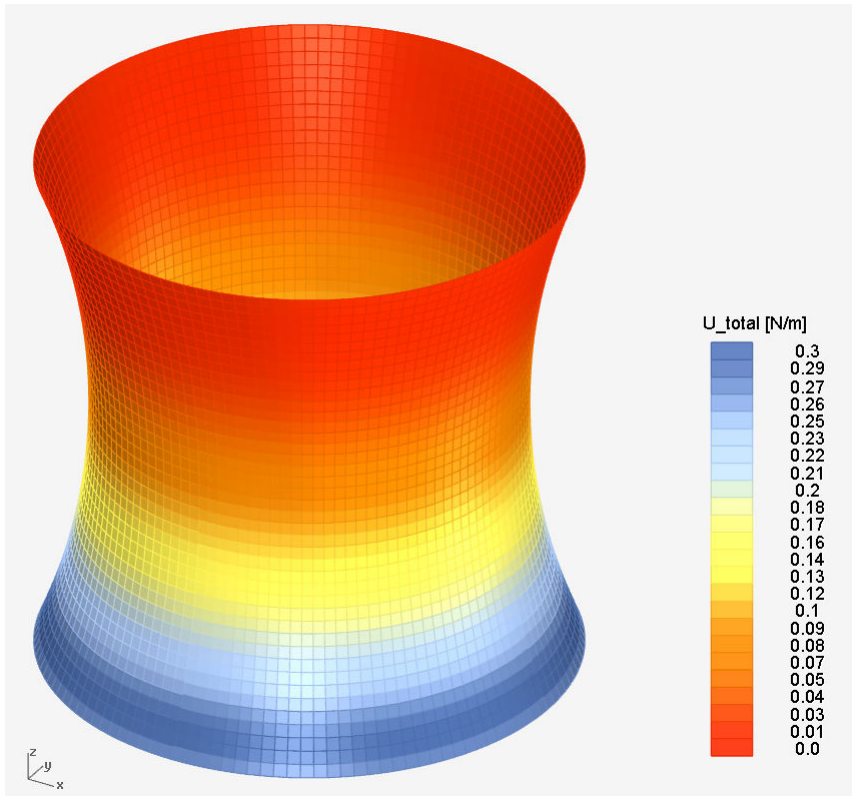
## Hyperboloid



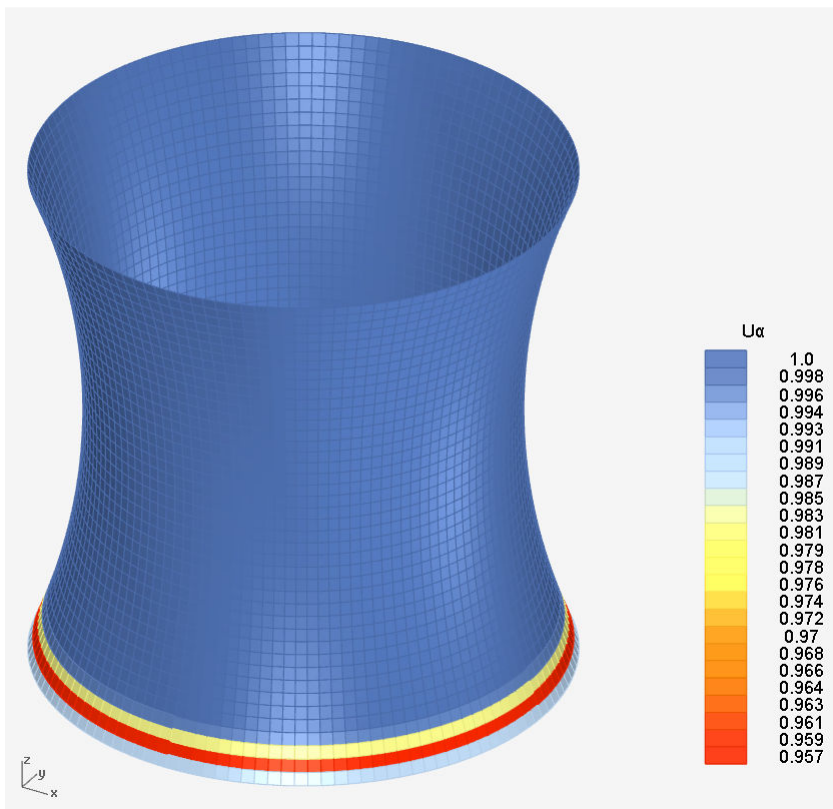
The in-plane strain energy results for the hyperboloid for the loading condition self weight.



The out-of-plane strain energy results for the hyperboloid for the loading condition self weight.

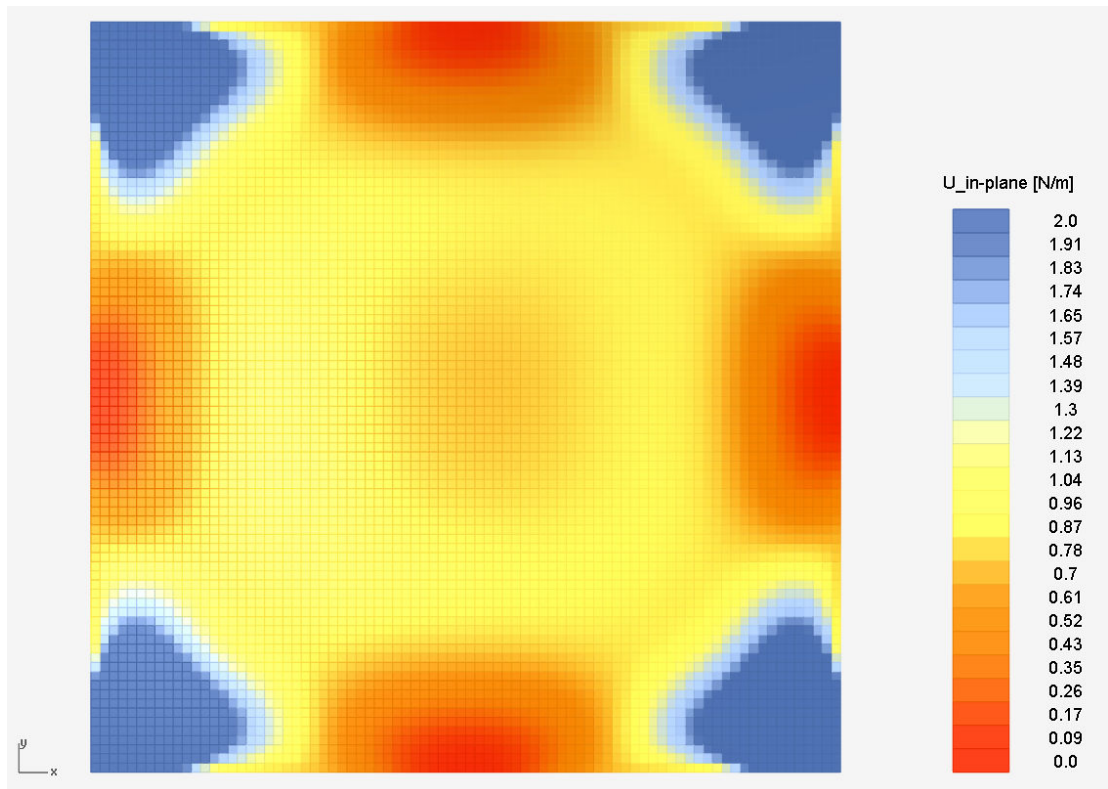


The total strain energy results for the hyperboloid for the loading condition self weight.

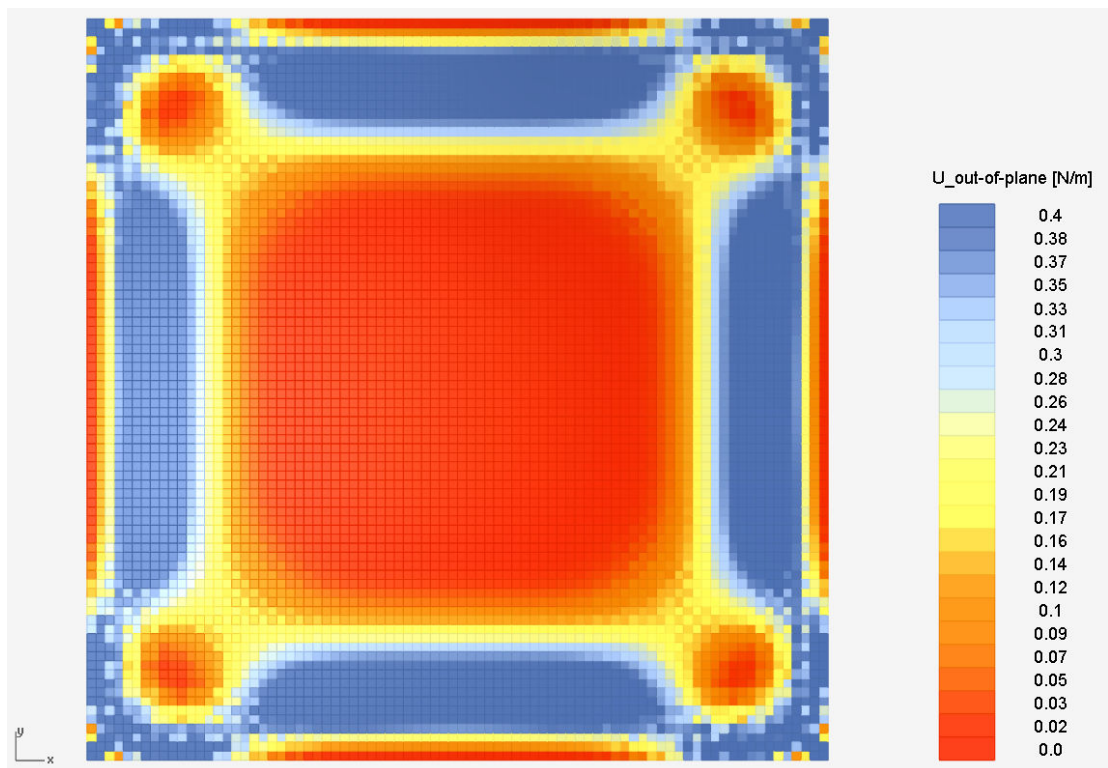


The strain energy results for  $U_\alpha$  for the hyperboloid for the loading condition self weight.

## Hypar

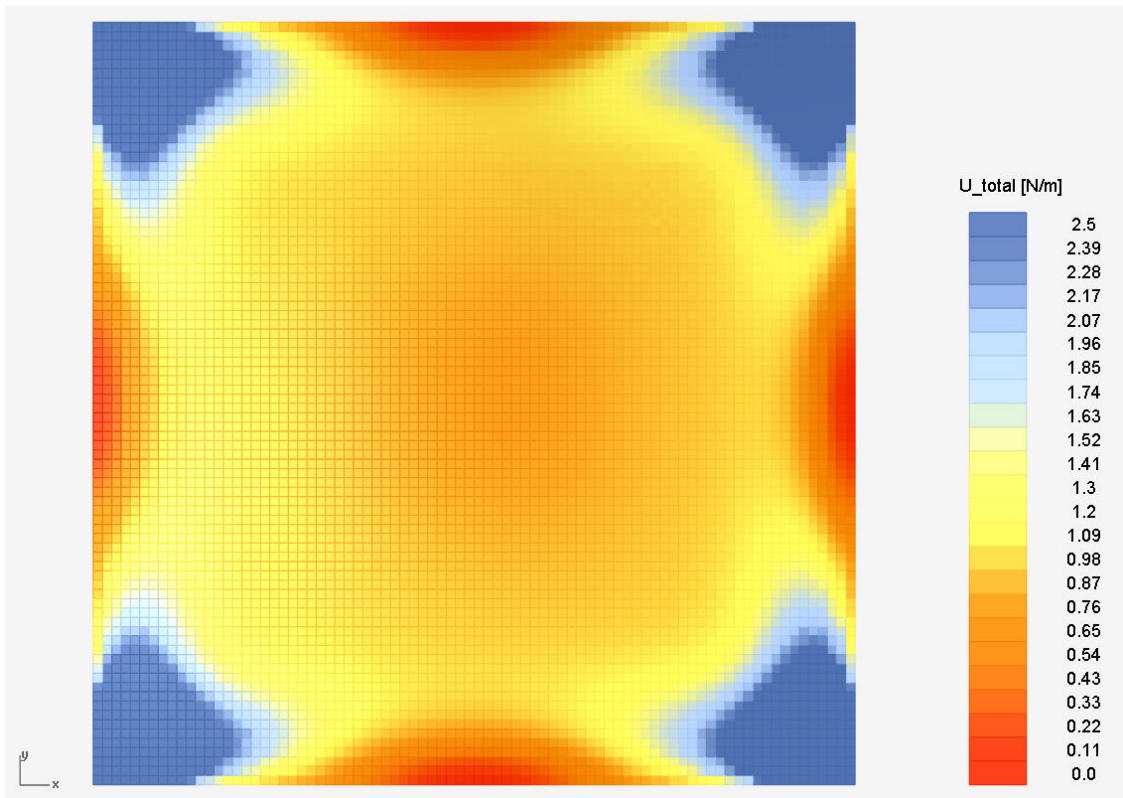


*The in-plane strain energy results for the hypar for the loading condition self weight.*

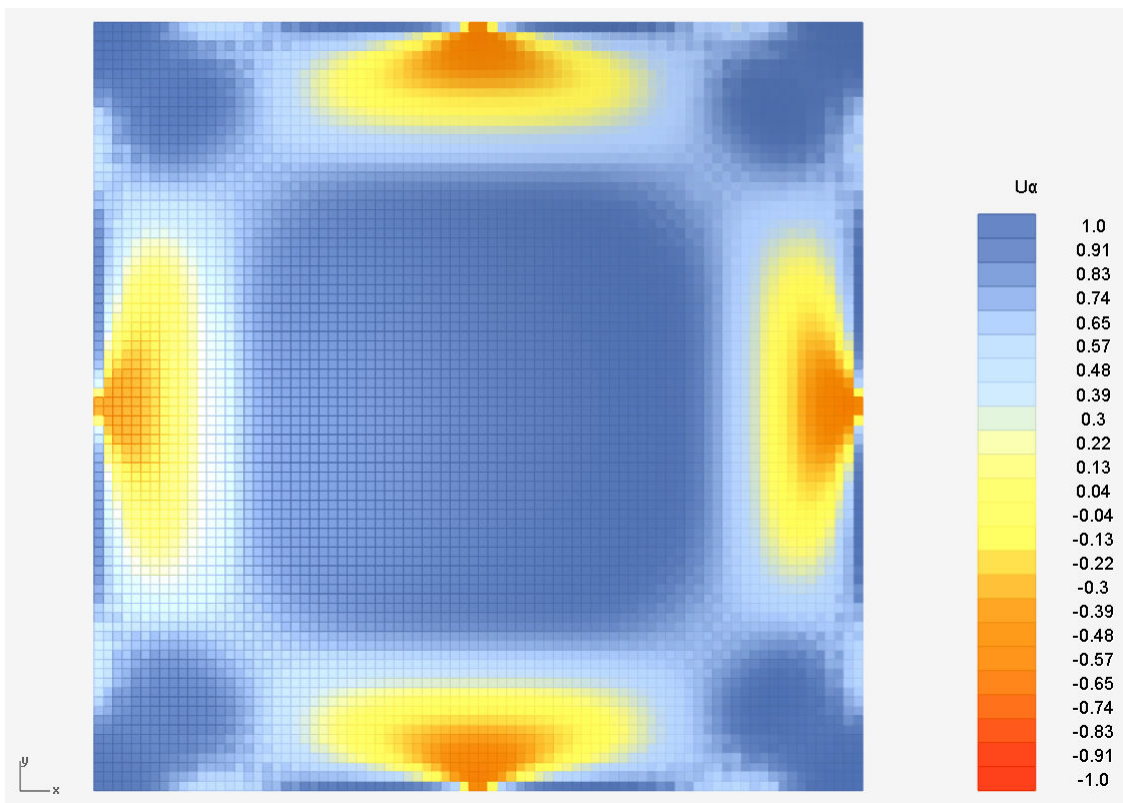


*The out-of-plane strain energy results for the hypar for the loading condition self weight.*



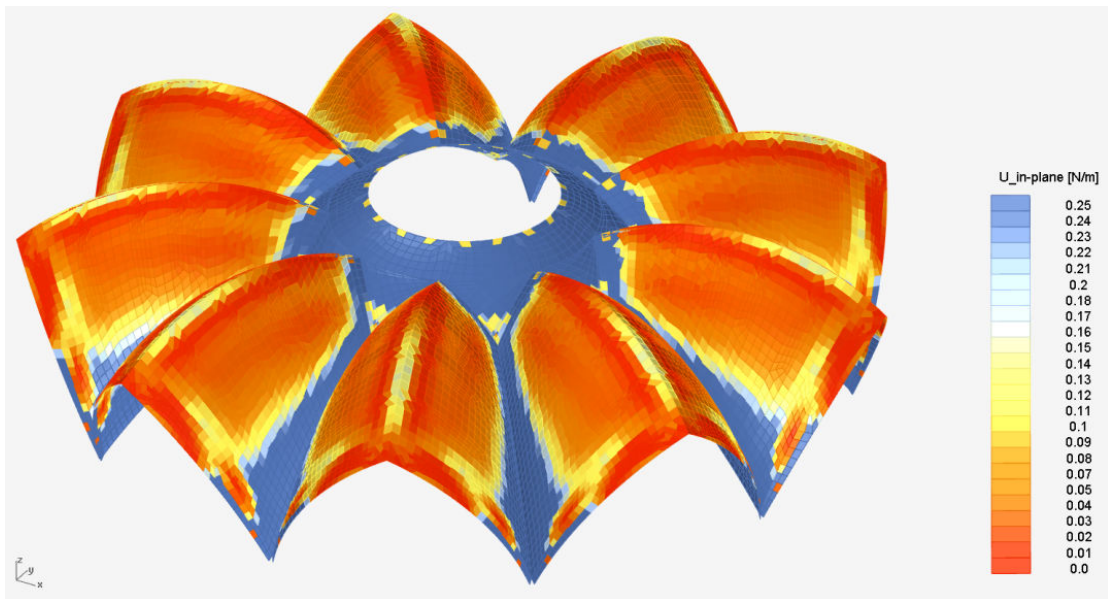


The total strain energy results for the hyperboloid for the loading condition self weight.

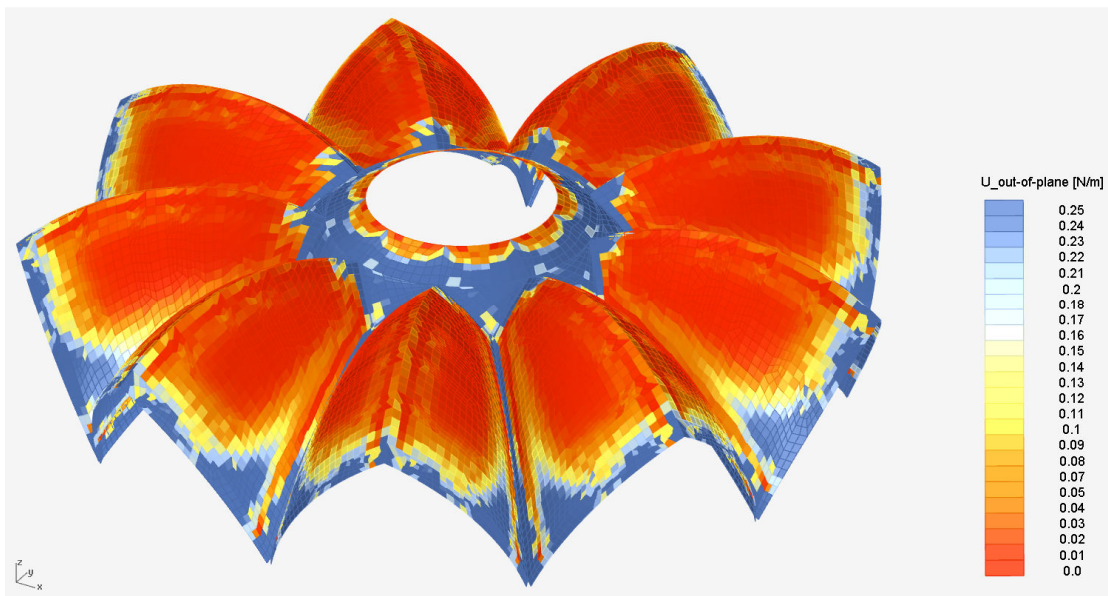


The strain energy results for  $U_{\alpha}$  for the hyperboloid for the loading condition self weight.

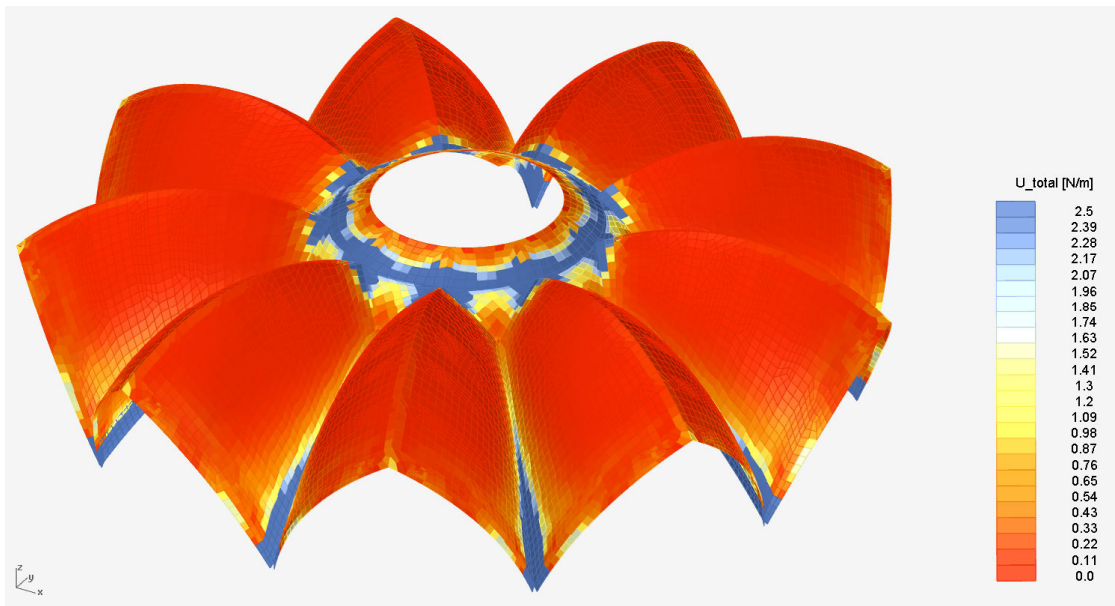
## Complex geometry



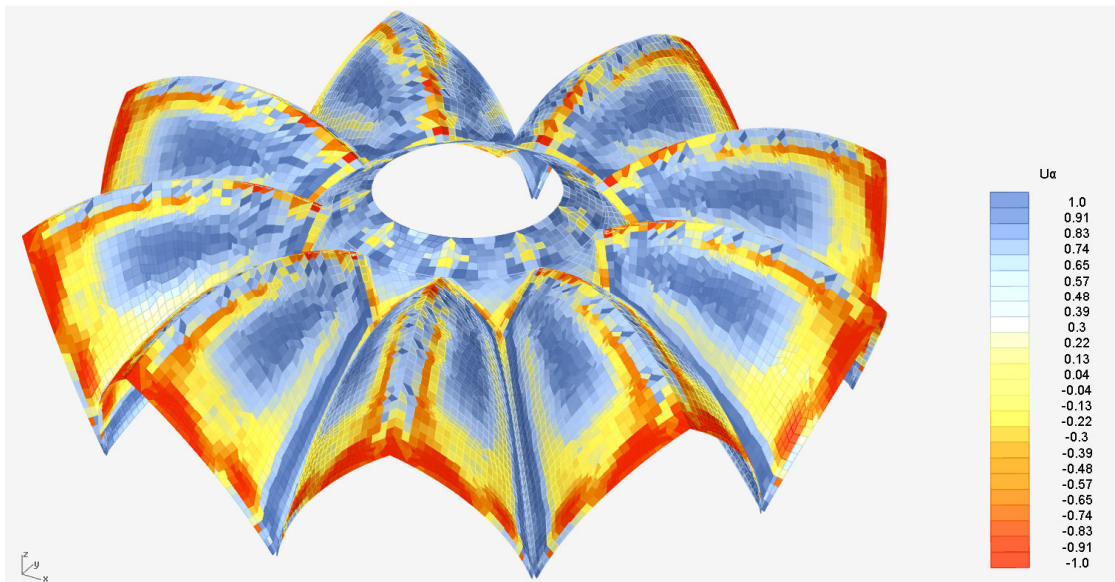
*The in-plane strain energy results for the complex geometry for the loading condition self weight.*



*The out-of-plane strain energy results for the complex geometry for the loading condition self weight.*



The total strain energy results for the complex geometry for the loading condition self weight.

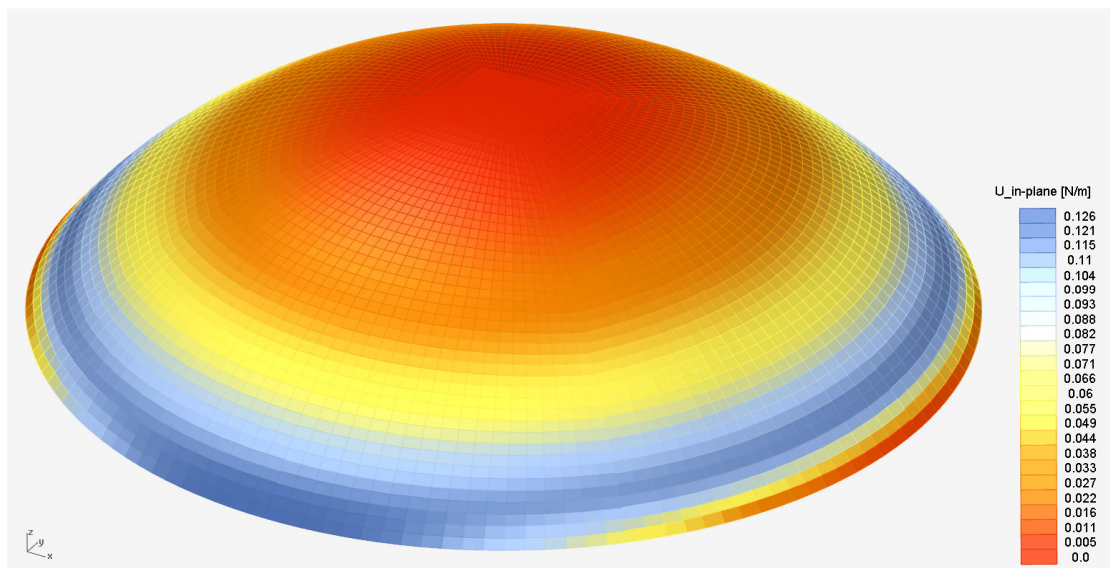


The strain energy results for  $U_\alpha$  for the complex geometry for the loading condition self weight.

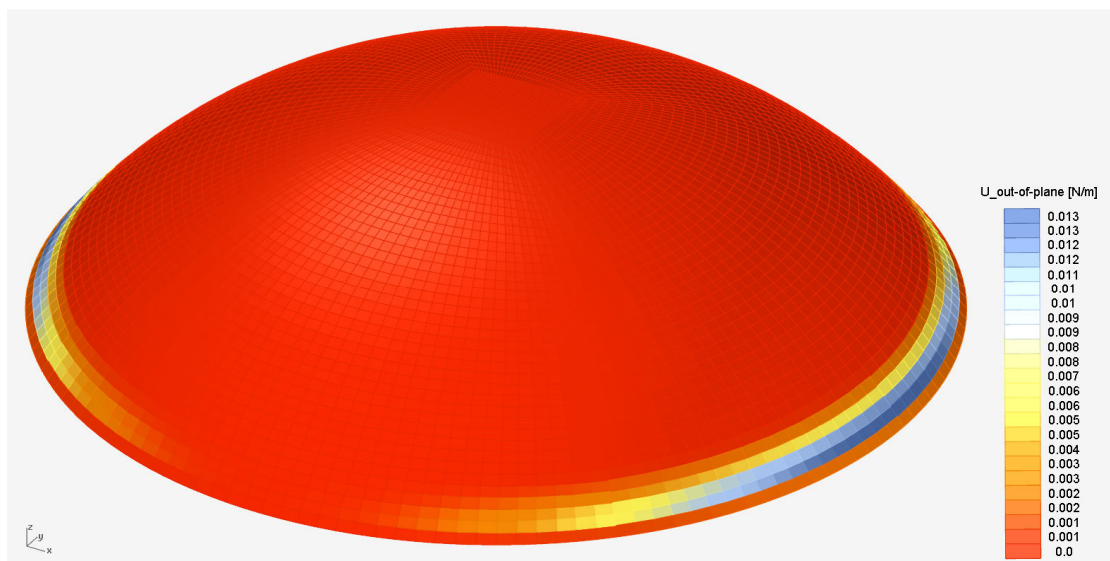


## Wind load

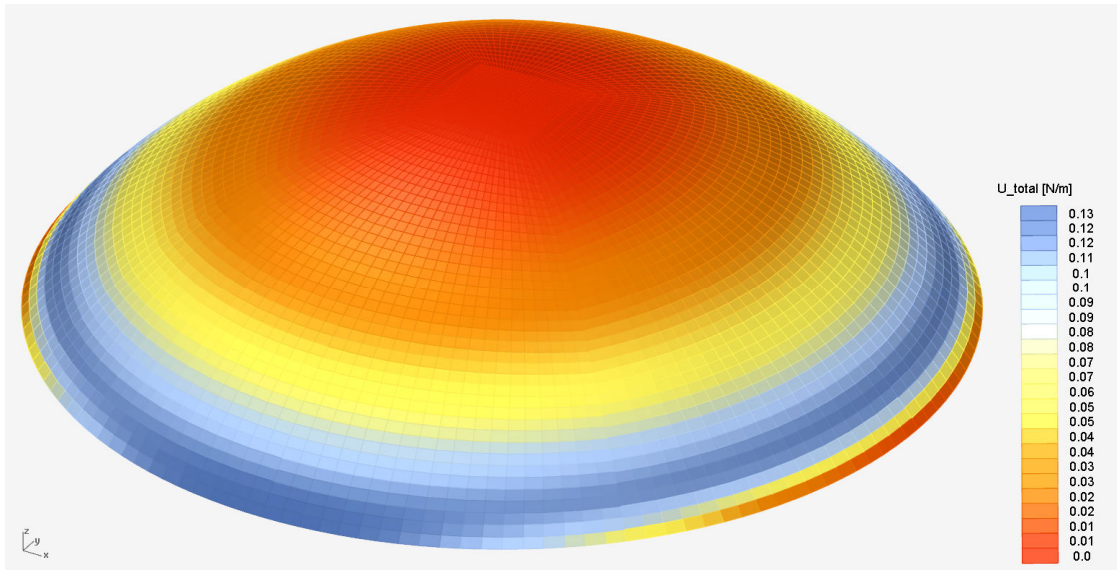
### Ellipsoid



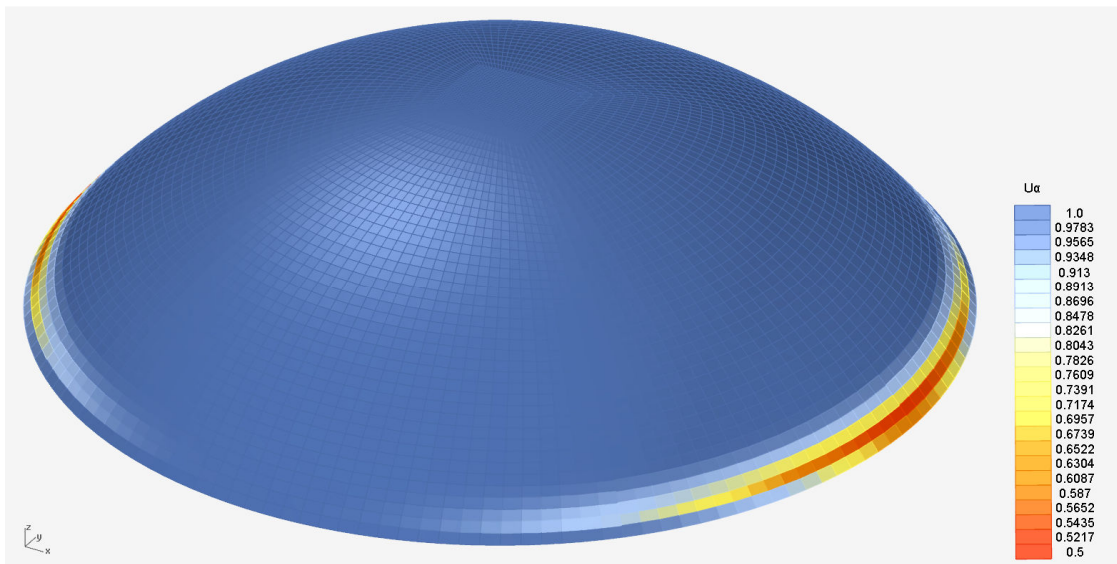
*The in-plane strain energy results for the ellipsoid for the loading condition wind.*



*The out-of-plane strain energy results for the ellipsoid for the loading condition wind.*



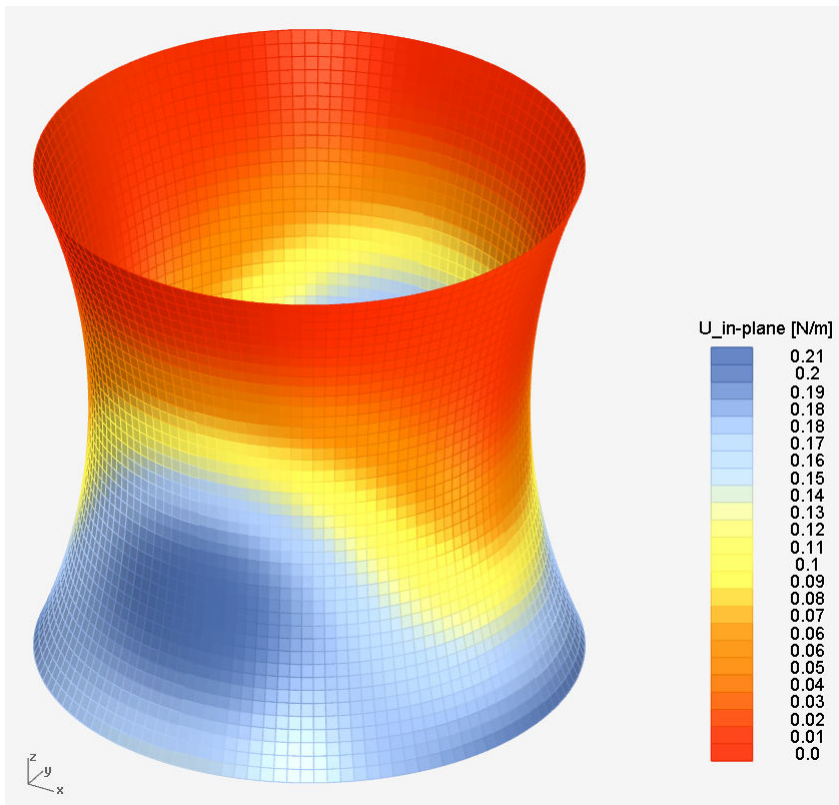
The total strain energy results for the ellipsoid for the loading condition wind.



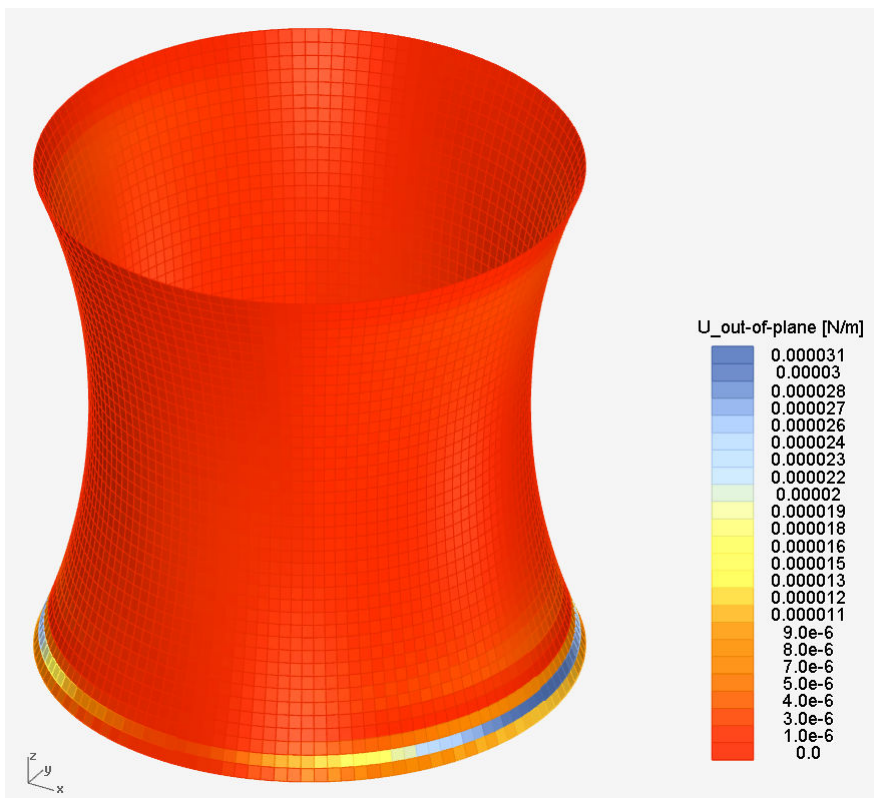
The strain energy results for  $U_{\alpha}$  for the ellipsoid for the loading condition wind.



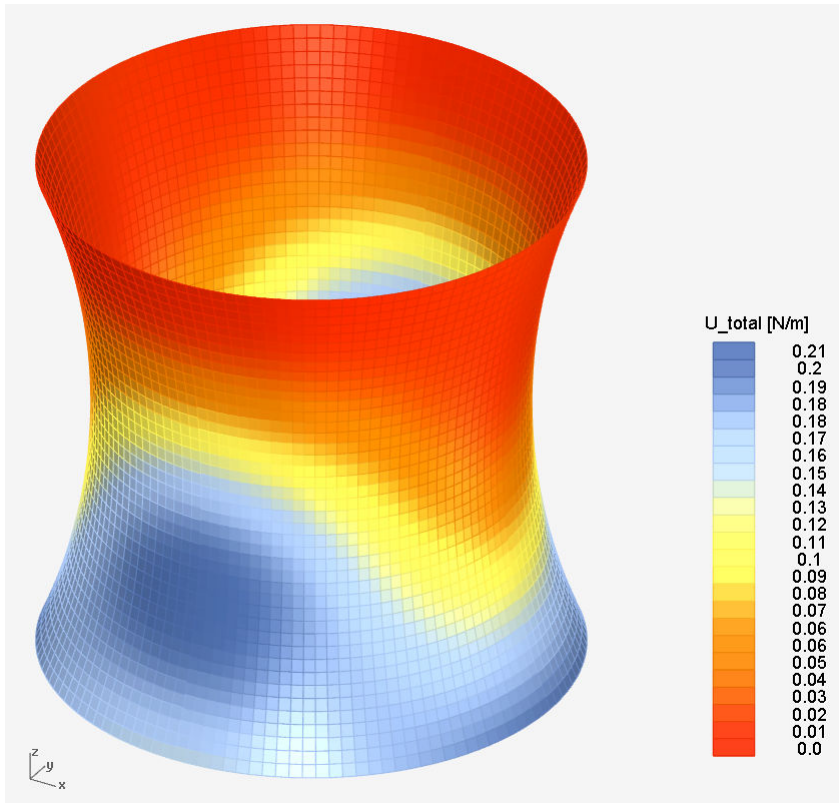
## Hyperboloid



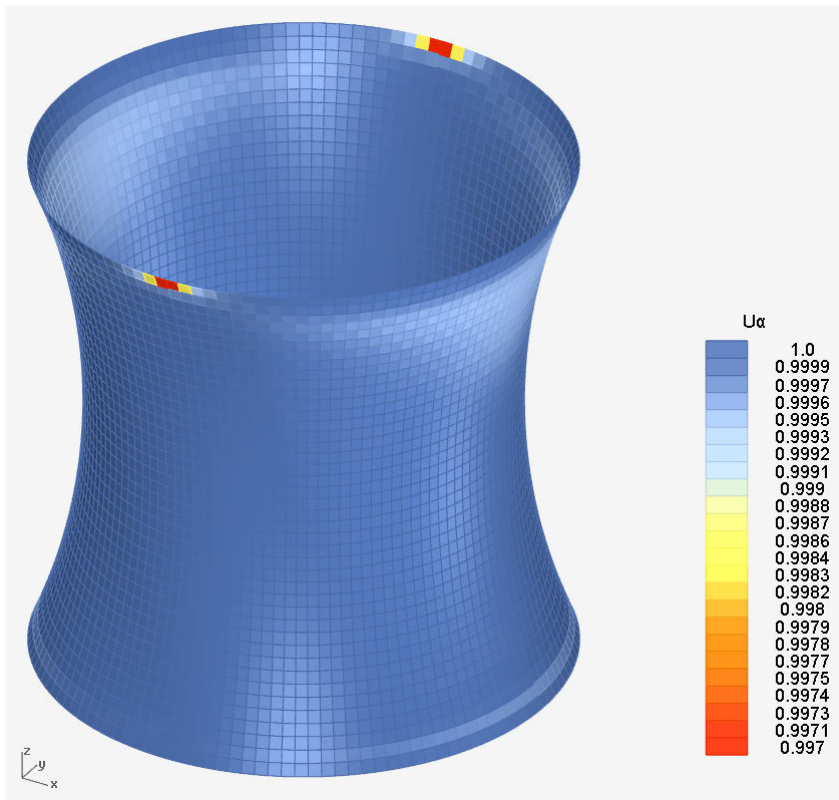
The in-plane strain energy results for the hyperboloid for the loading condition wind.



The out-of-plane strain energy results for the hyperboloid for the loading condition wind.

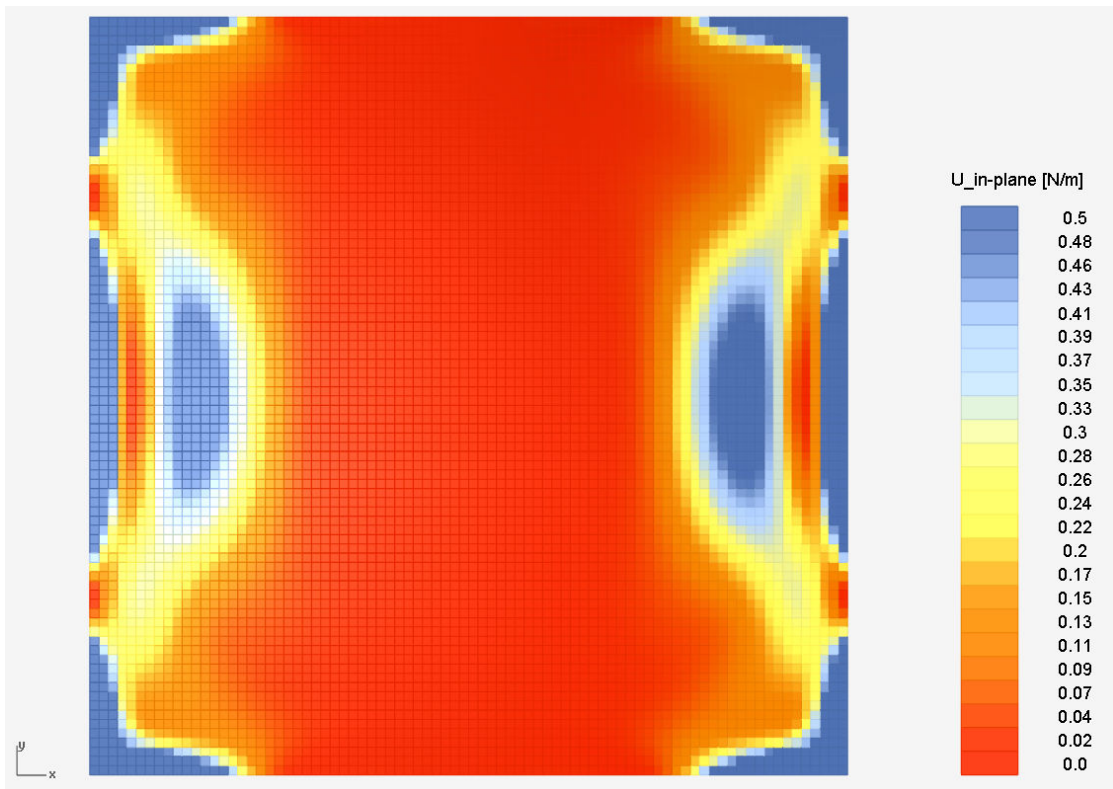


The total strain energy results for the hyperboloid for the loading condition wind.

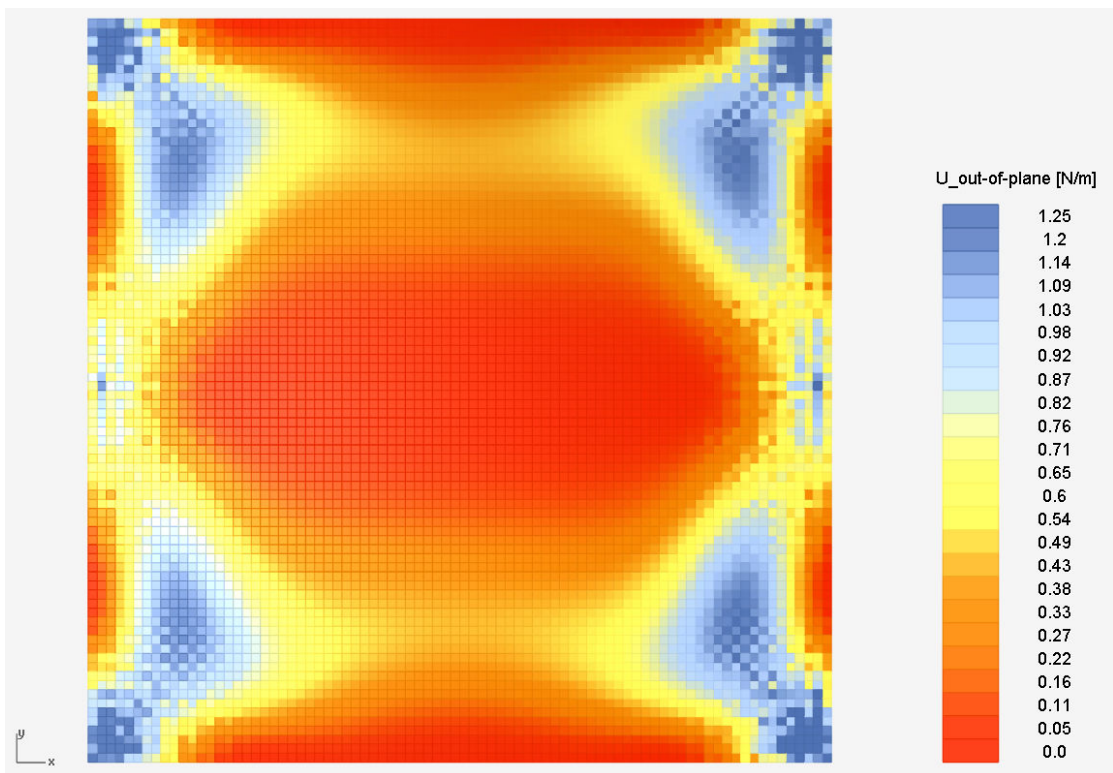


The strain energy results for  $U_\alpha$  for the hyperboloid for the loading condition wind.

## Hypar

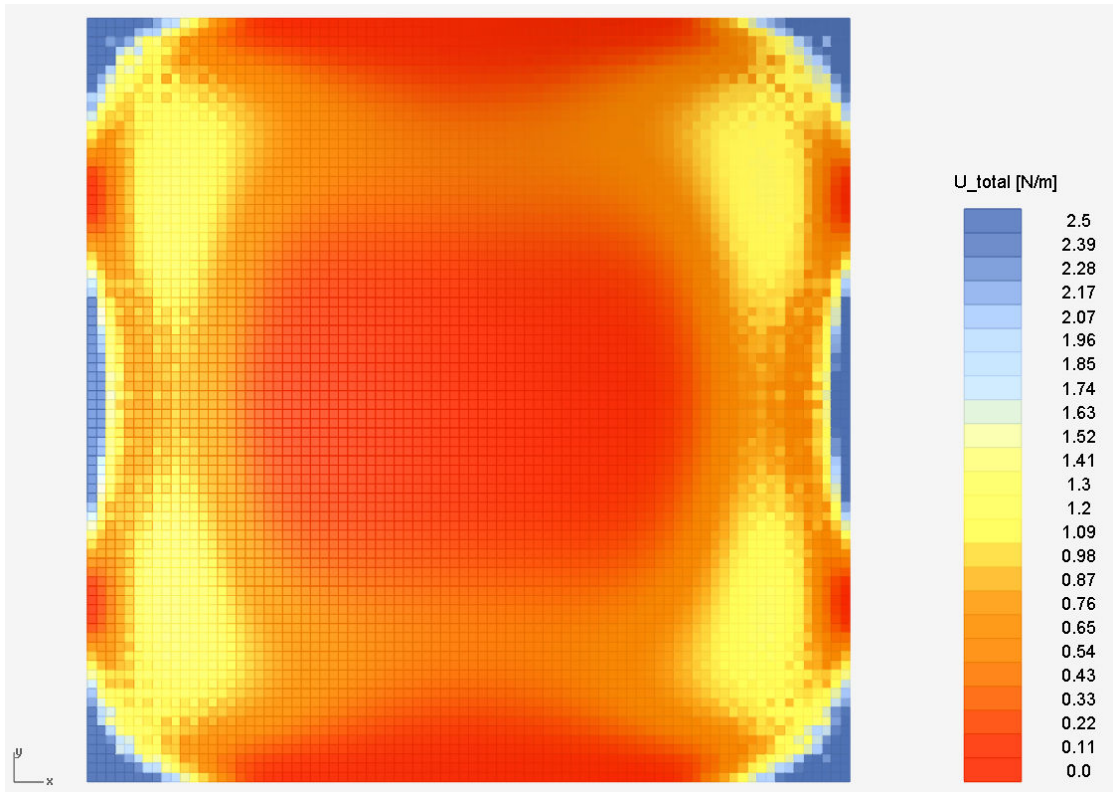


*The in-plane strain energy results for the hypar for the loading condition wind.*

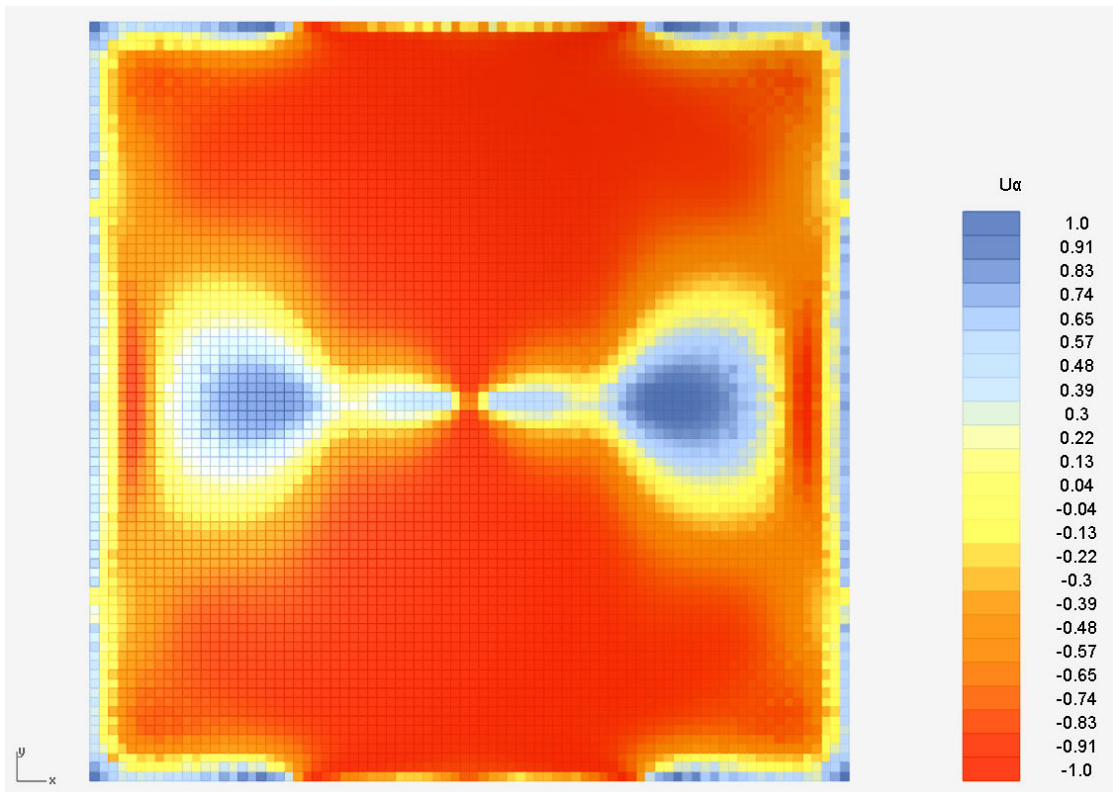


*The out-of-plane strain energy results for the hypar for the loading condition wind.*



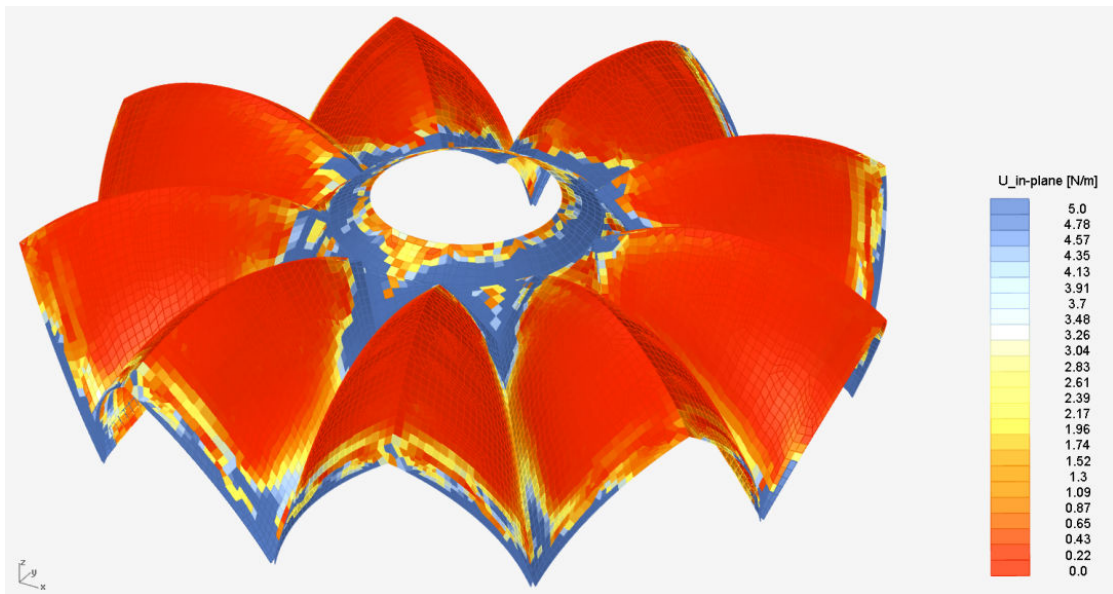


The total strain energy results for the hyperboloid for the loading condition wind.

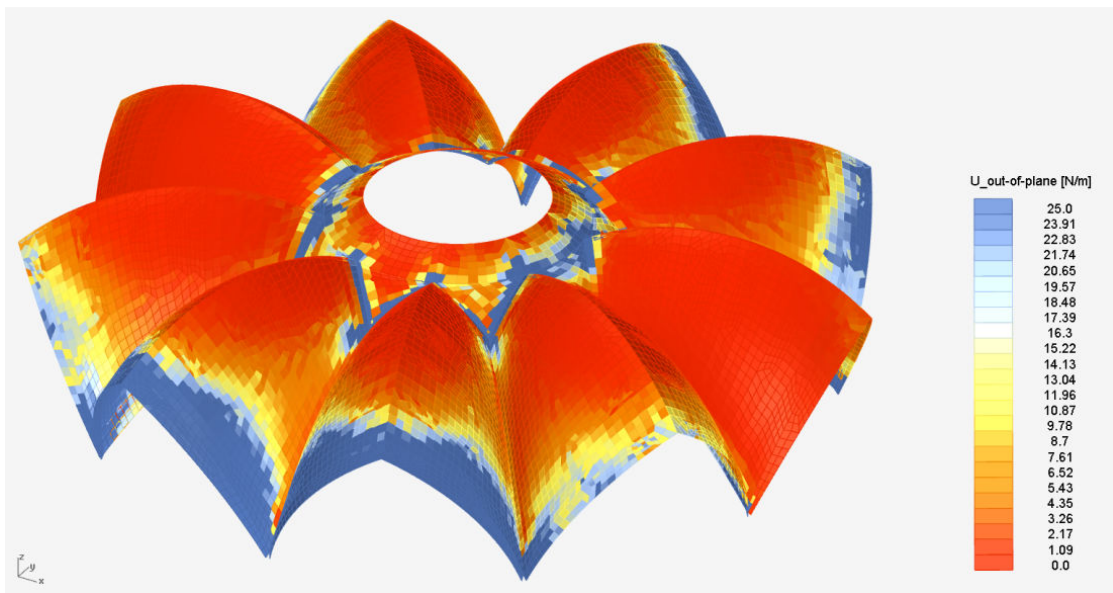


The strain energy results for  $U_\alpha$  for the hyperboloid for the loading condition wind.

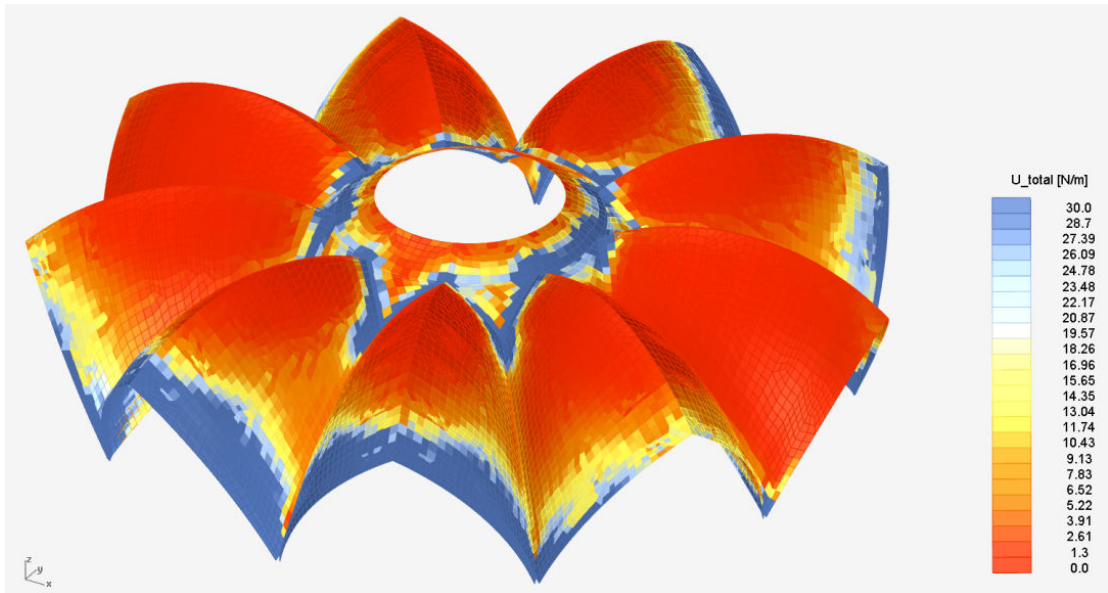
## Complex geometry



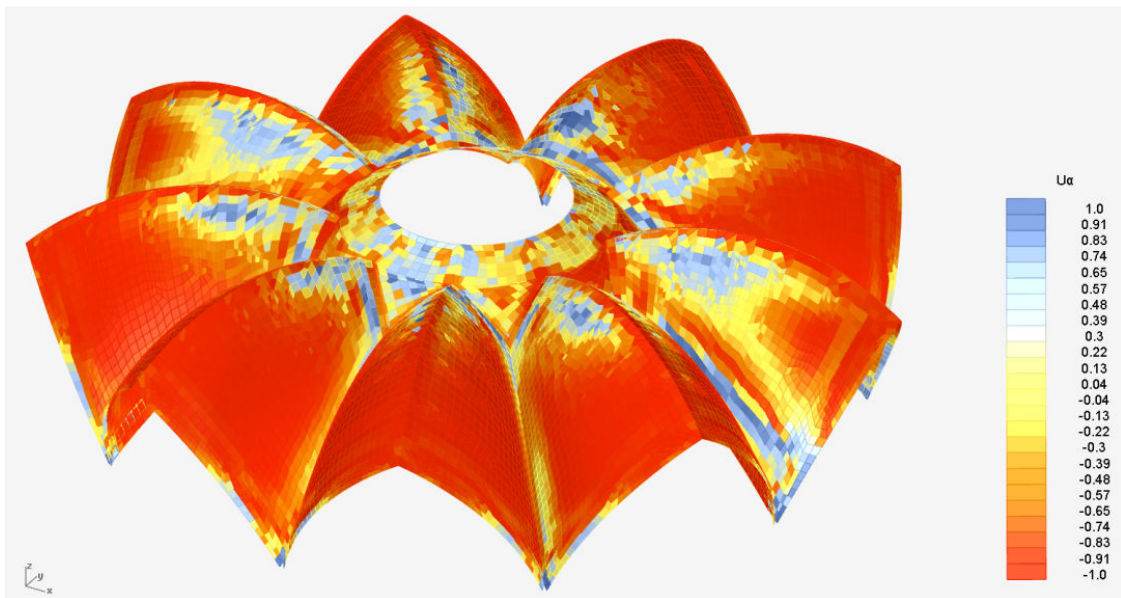
*The in-plane strain energy results for the complex geometry for the loading condition wind.*



*The out-of-plane strain energy results for the complex geometry for the loading condition wind.*



The total strain energy results for the complex geometry for the loading condition wind.



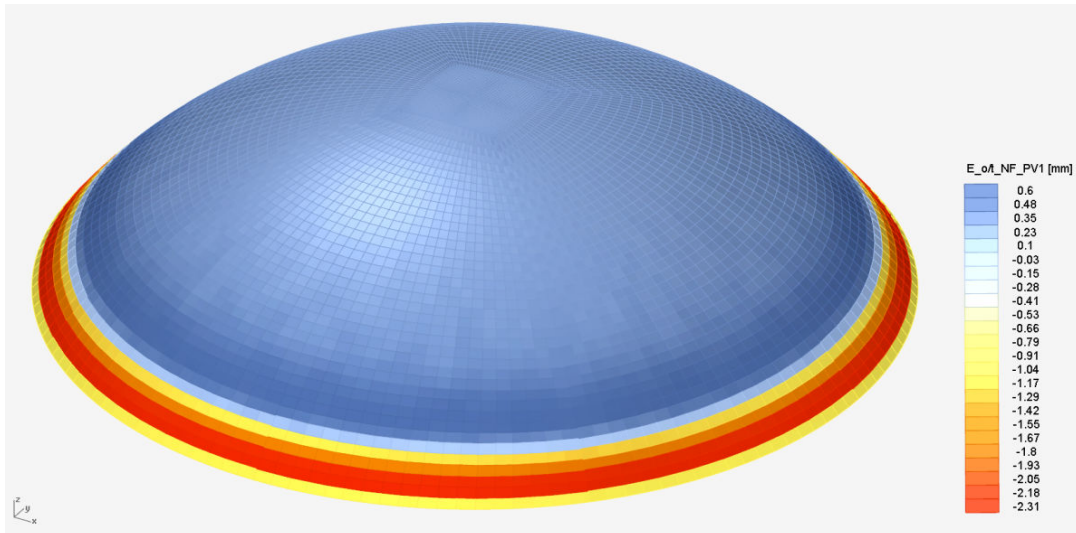
The strain energy results for  $U_{\alpha}$  for the complex geometry for the loading condition wind.



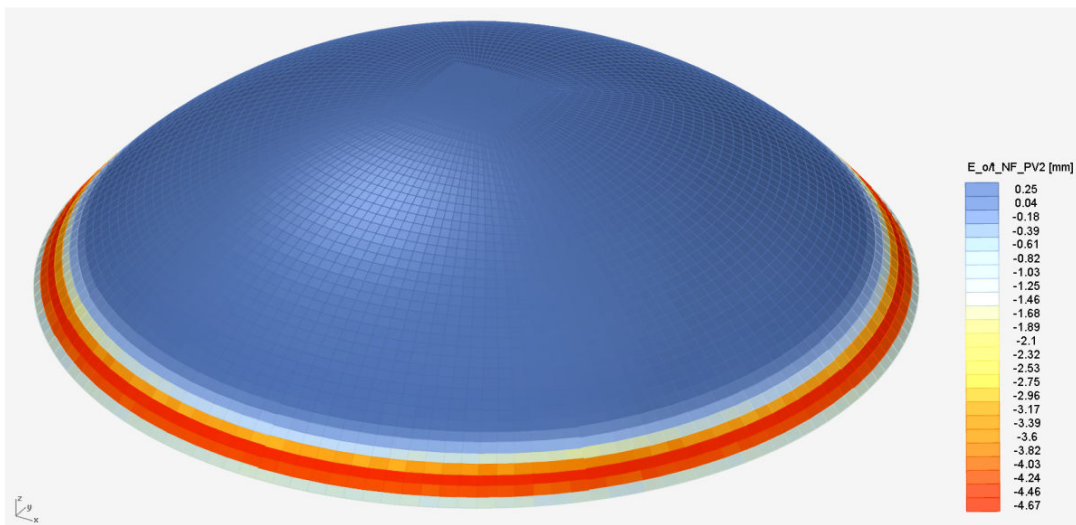
## Eccentricity of the Normal Force

### Self weight

#### Ellipsoid

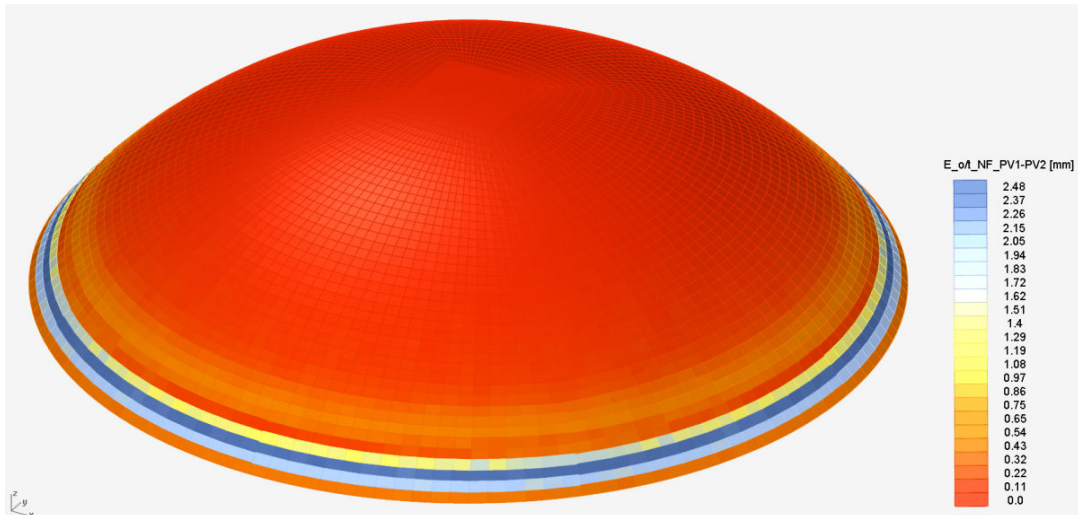


*The first principal values of the eccentricity of the normal force for the ellipsoid for the loading condition self weight.*

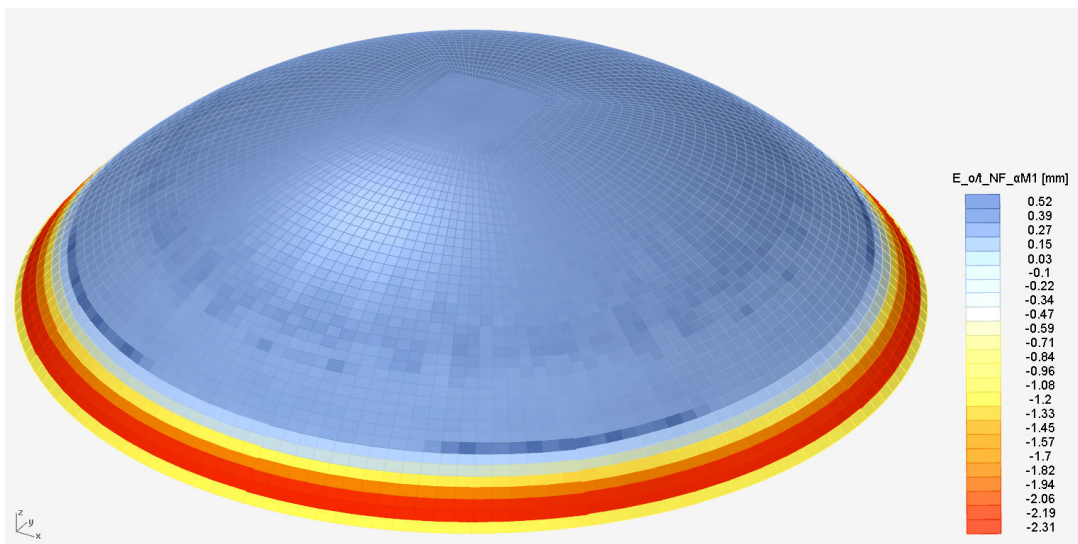


*The second principal values of the eccentricity of the normal force for the ellipsoid for the loading condition self weight.*

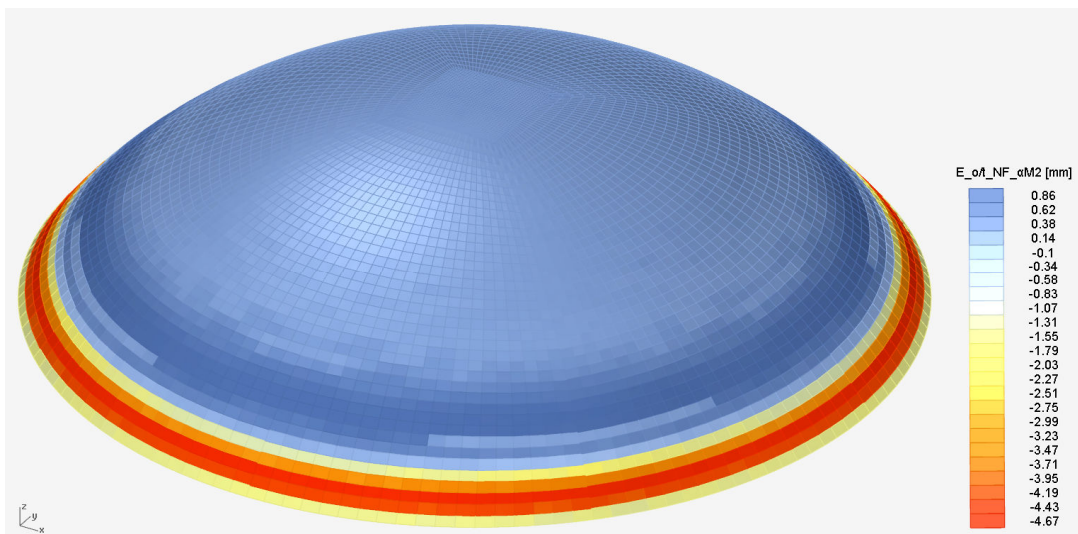




The difference between the first and second principal values of the eccentricity of the normal force for the ellipsoid for the loading condition self weight.

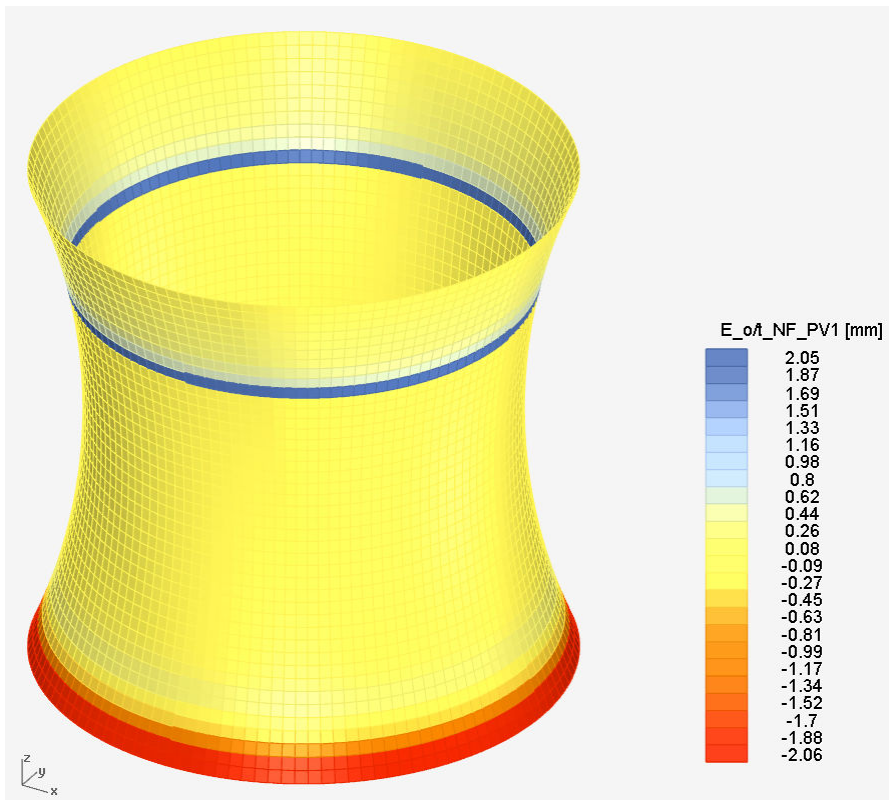


The values of the eccentricity of the normal force in the first principal directions of the distributed bending moments for the ellipsoid for the loading condition self weight.

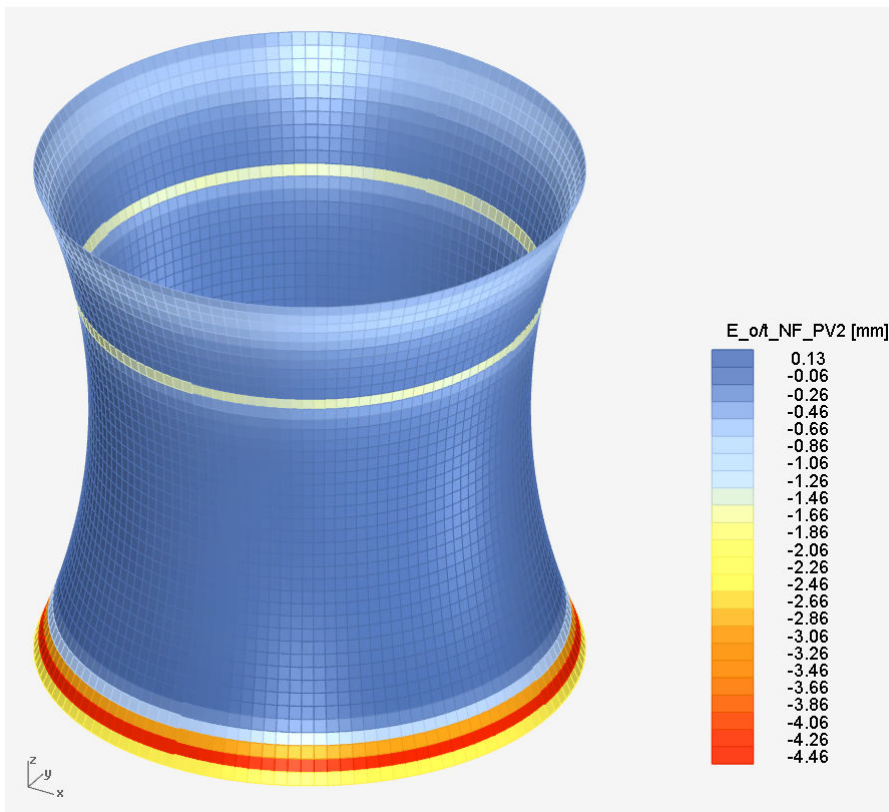


The values of the eccentricity of the normal force in the second principal directions of the distributed bending moments for the ellipsoid for the loading condition self weight.

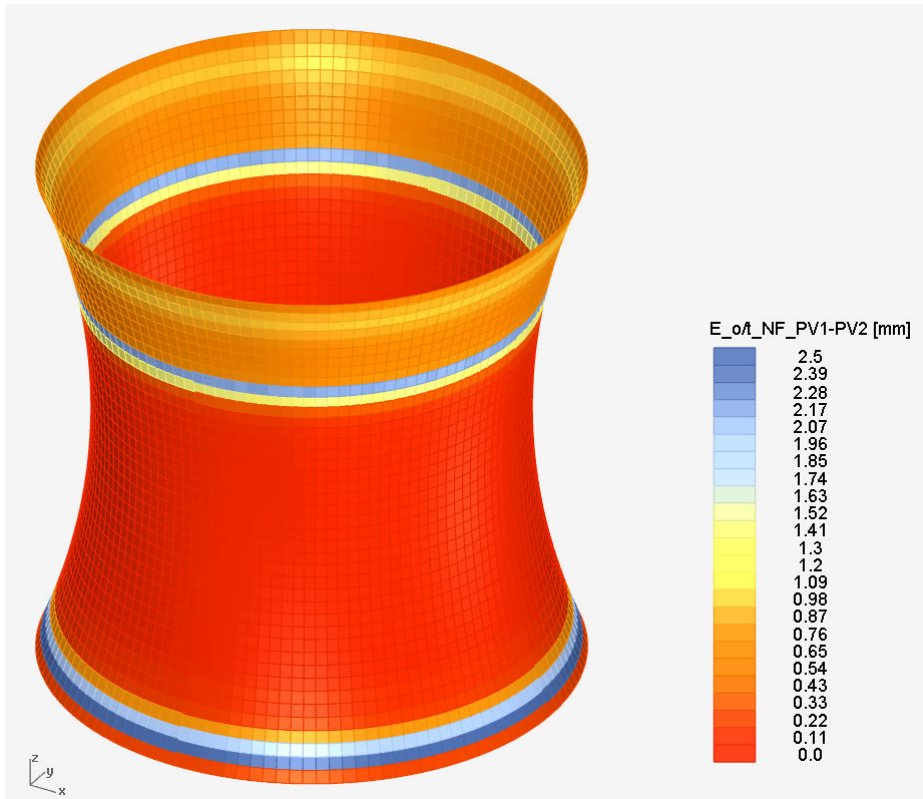
## Hyperboloid



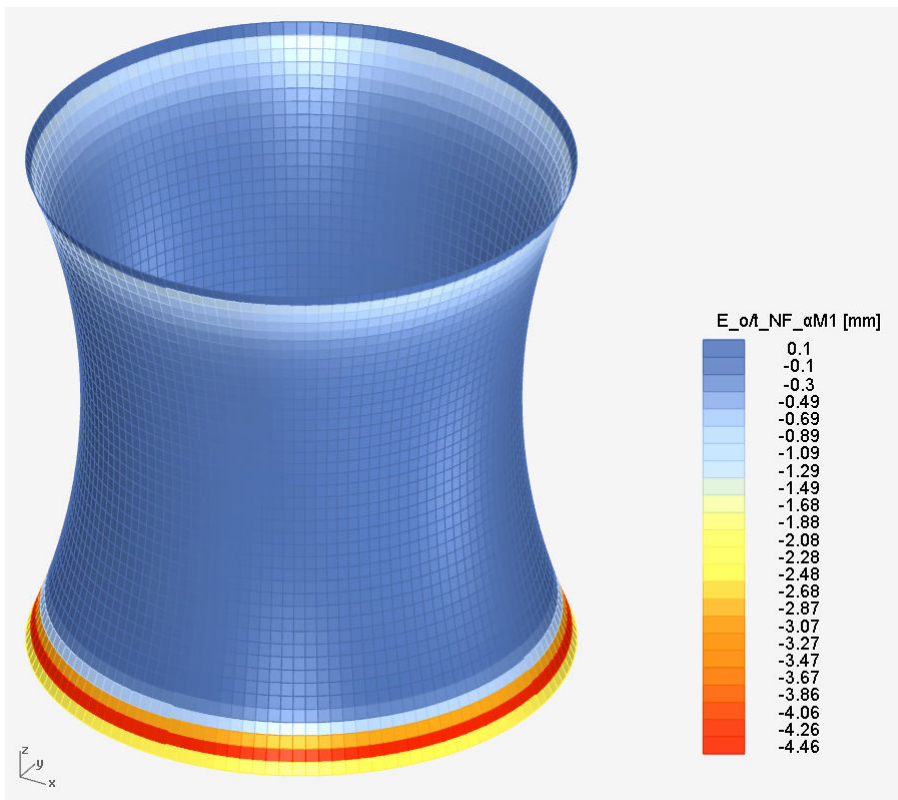
The first principal values of the eccentricity of the normal force for the hyperboloid for the loading condition self weight.



The second principal values of the eccentricity of the normal force for the hyperboloid for the loading condition self weight.

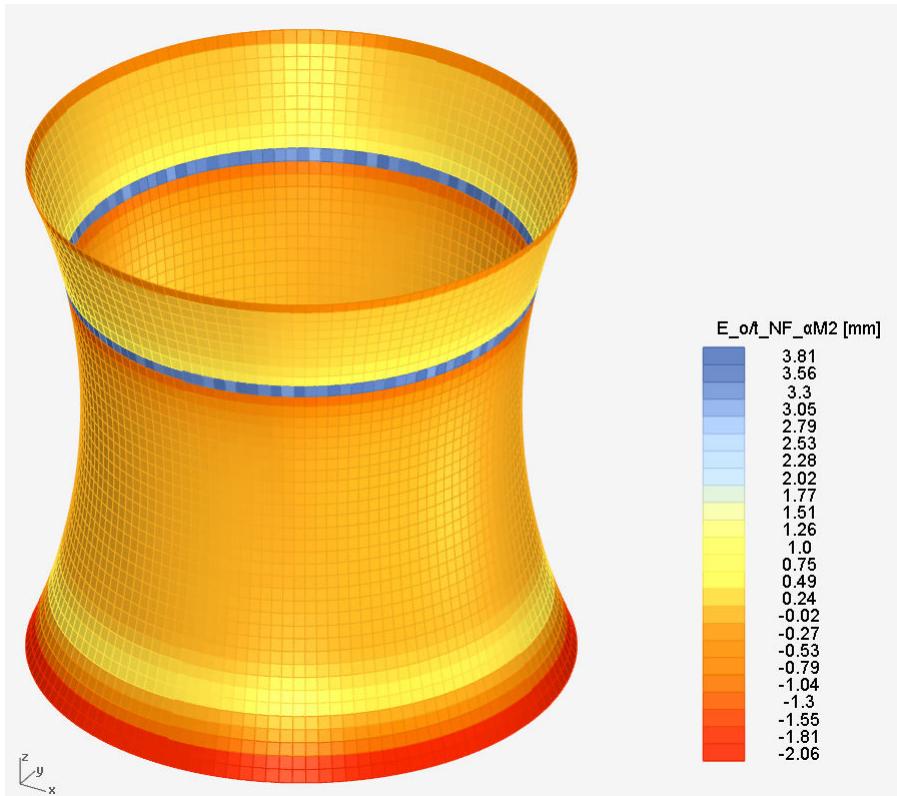


*The difference between the first and second principal values of the eccentricity of the normal force for the hyperboloid for the loading condition self weight.*



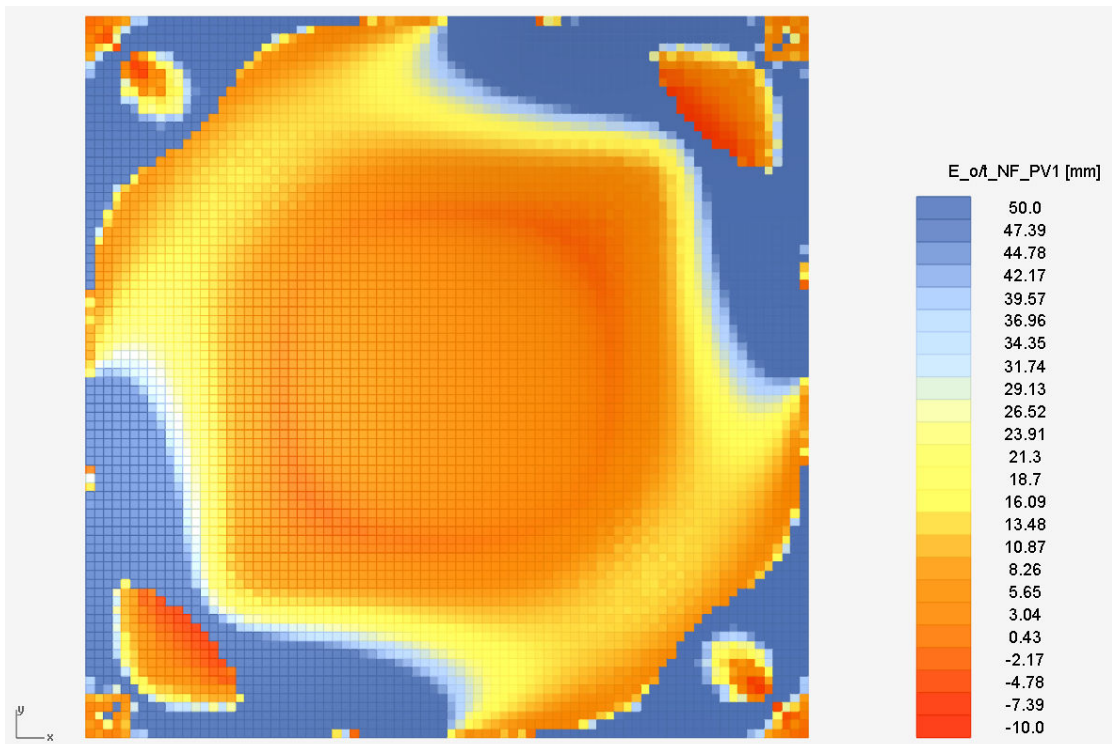
*The values of the eccentricity of the normal force in the first principal directions of the distributed bending moments for the hyperboloid for the loading condition self weight.*



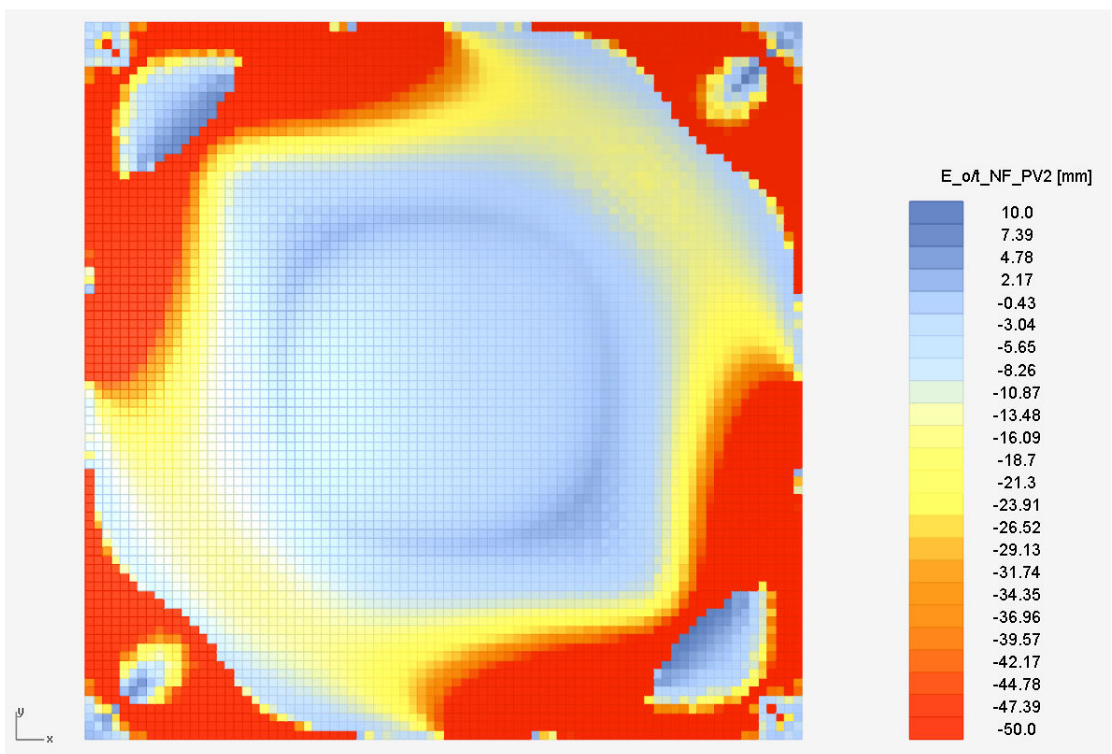


*The values of the eccentricity of the normal force in the second principal directions of the distributed bending moments for the hyperboloid for the loading condition self weight.*

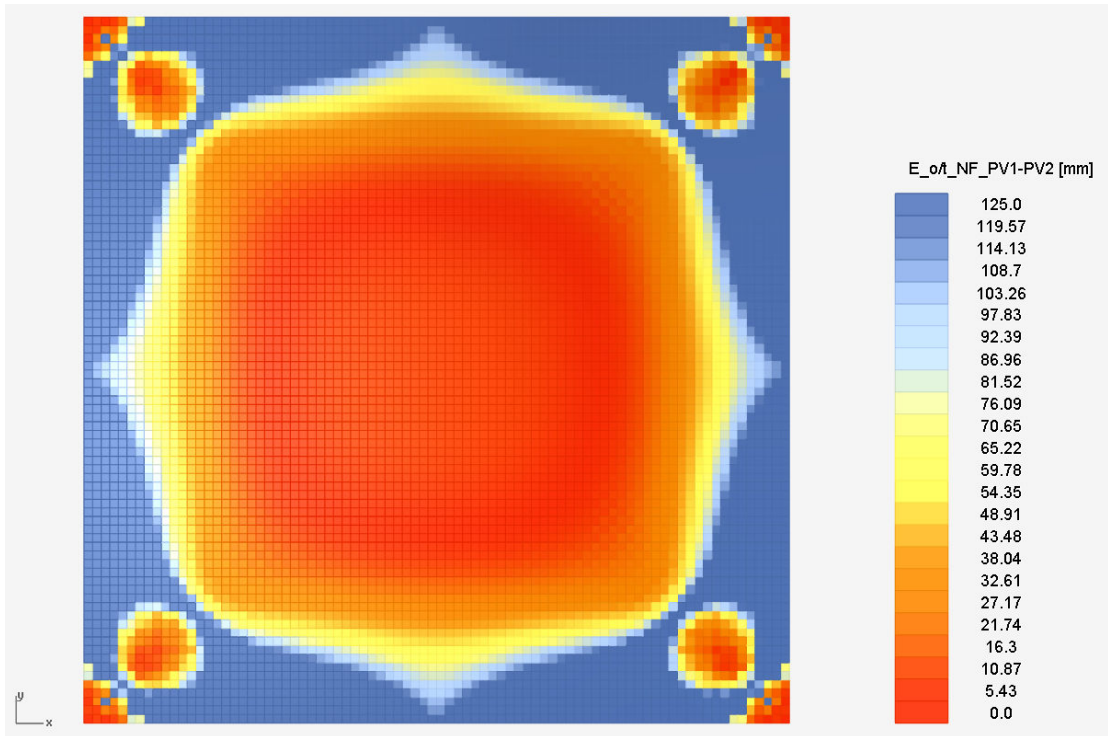
## Hypar



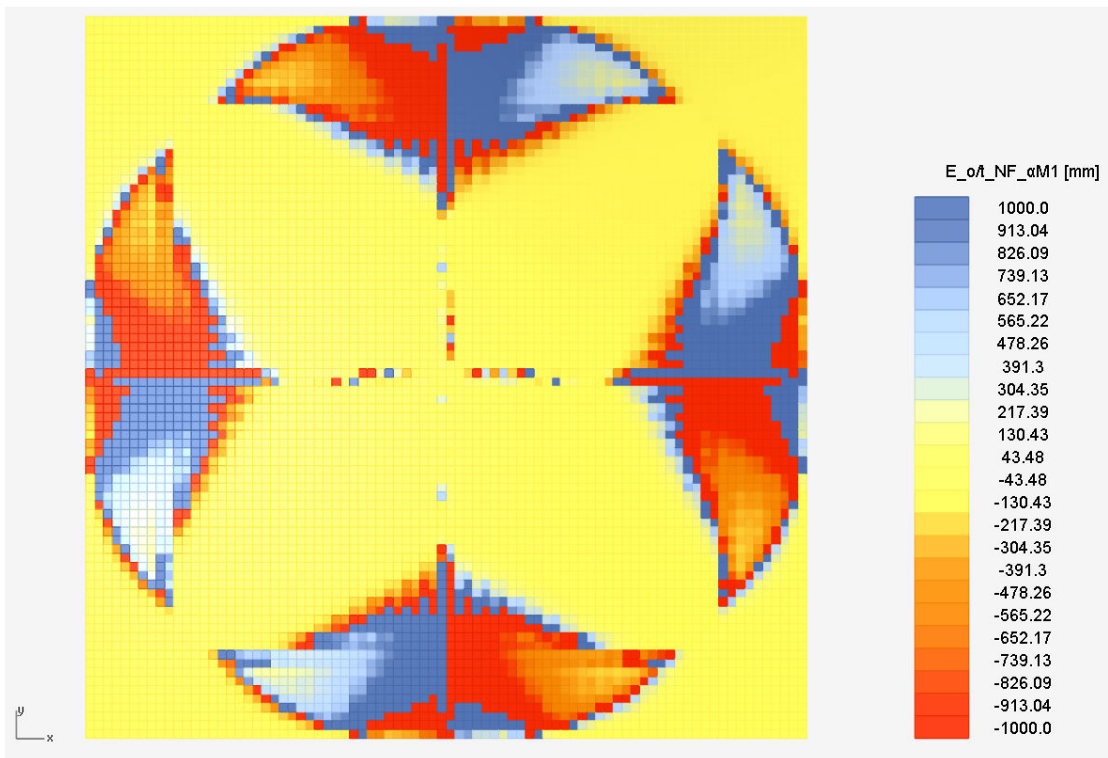
*The first principal values of the eccentricity of the normal force for the hypar for the loading condition self weight.*



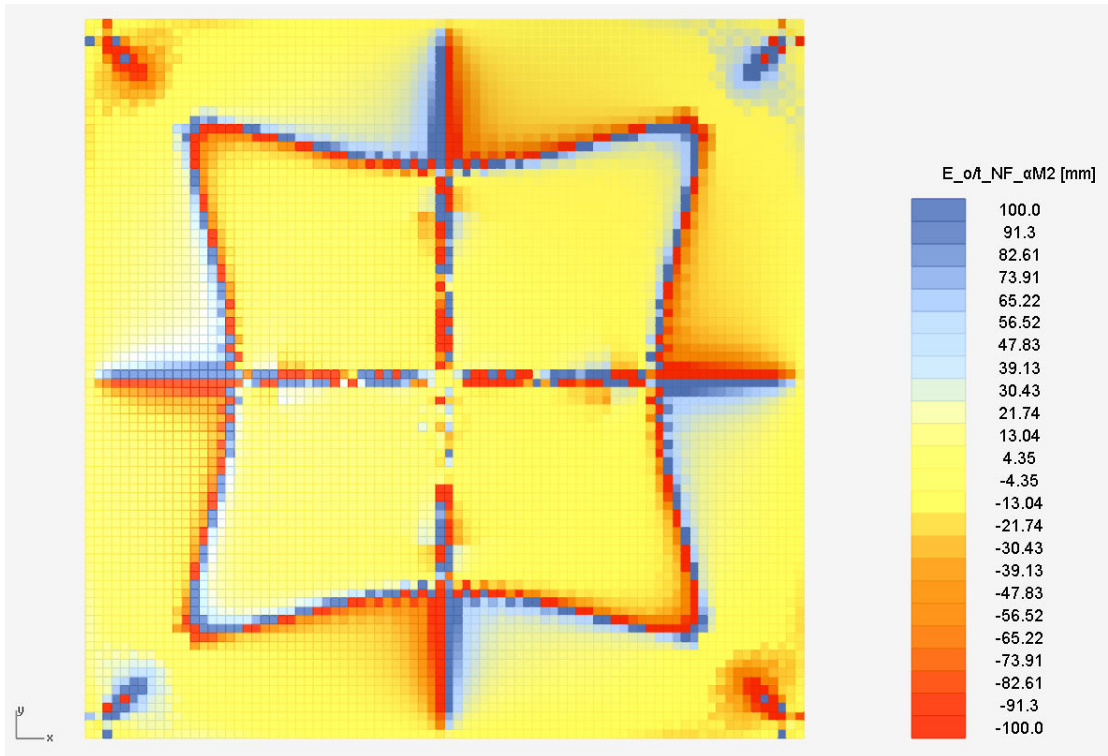
*The second principal values of the eccentricity of the normal force for the hypar for the loading condition self weight.*



*The difference between the first and second principal values of the eccentricity of the normal force for the hyper for the loading condition self weight.*



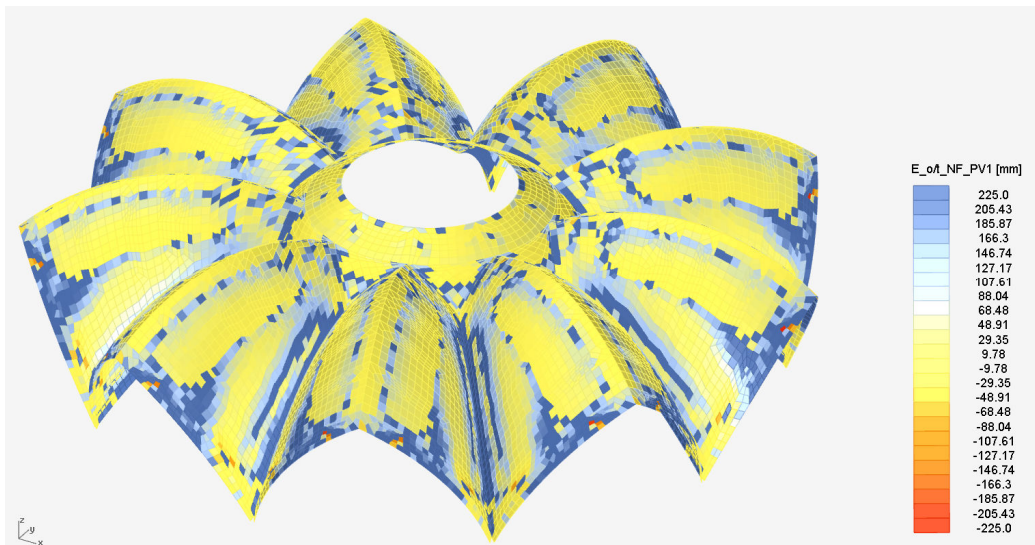
*The values of the eccentricity of the normal force in the first principal directions of the distributed bending moments for the hyper for the loading condition self weight.*



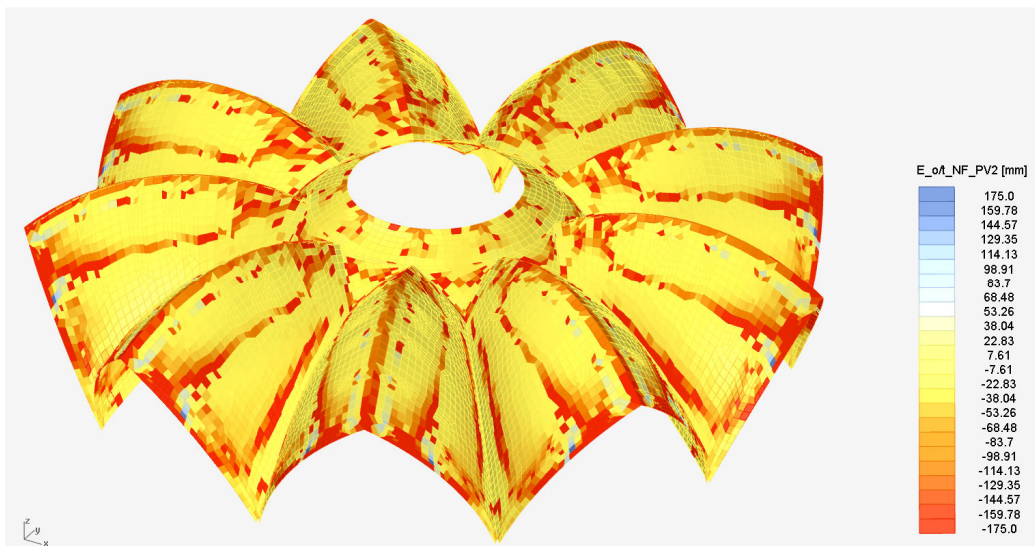
*The values of the eccentricity of the normal force in the second principal directions of the distributed bending moments for the hyperboloid for the loading condition self weight.*



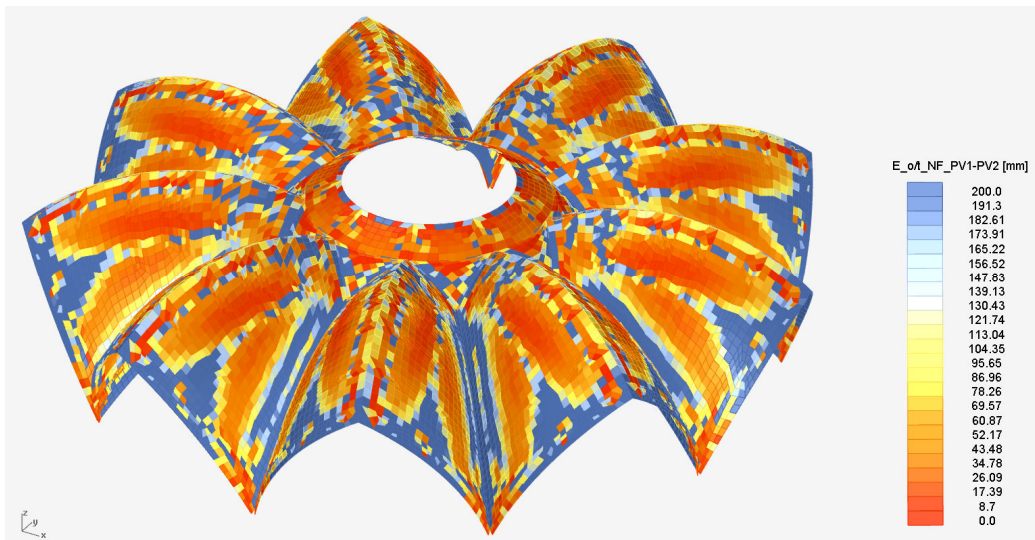
## Complex geometry



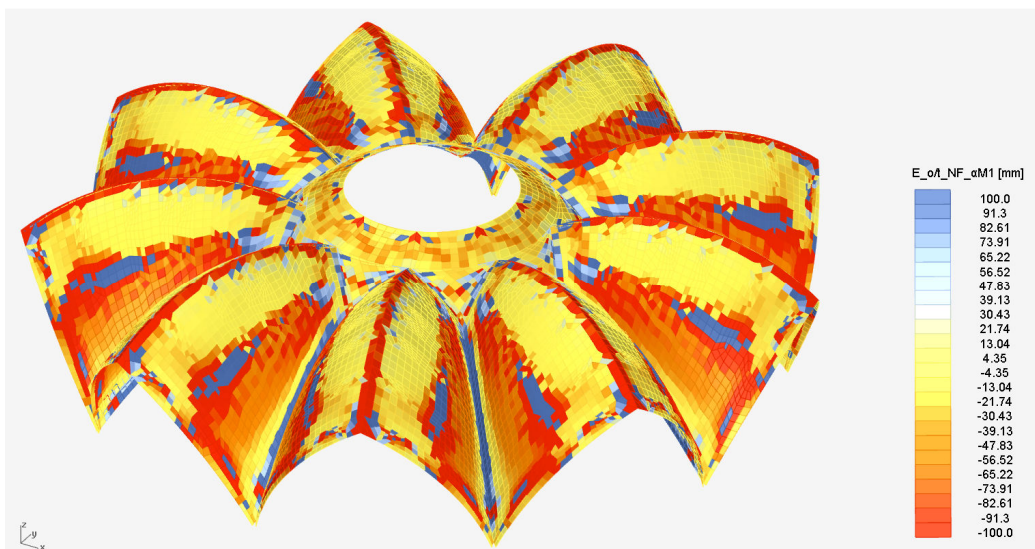
*The first principal values of the eccentricity of the normal force for the complex geometry for the loading condition self weight.*



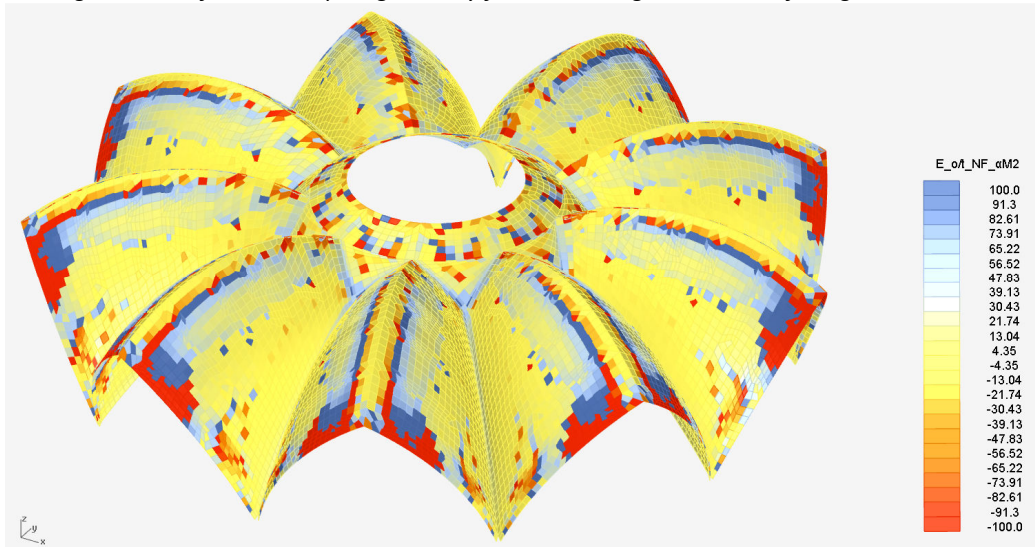
*The second principal values of the eccentricity of the normal force for the complex geometry for the loading condition self weight.*



*The difference between the first and second principal values of the eccentricity of the normal force for the complex geometry for the loading condition self weight.*



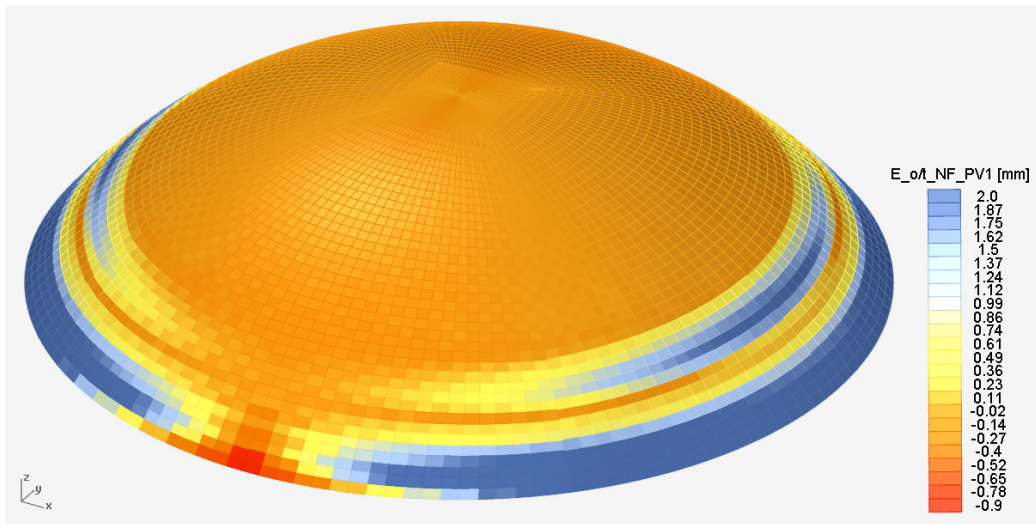
*The values of the eccentricity of the normal force in the first principal directions of the distributed bending moments for the complex geometry for the loading condition self weight.*



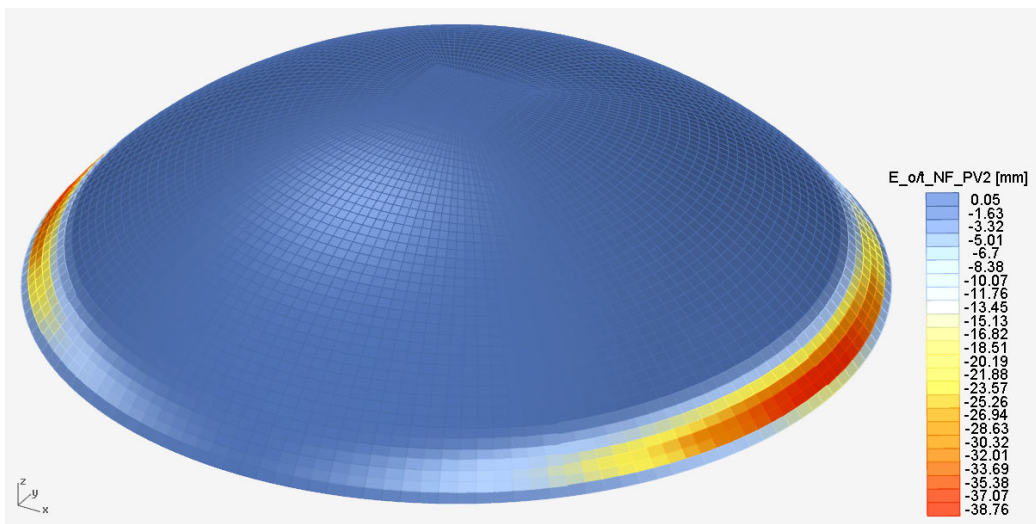
*The values of the eccentricity of the normal force in the second principal directions of the distributed bending moments for the complex geometry for the loading condition self weight.*

## Wind load

### Ellipsoid

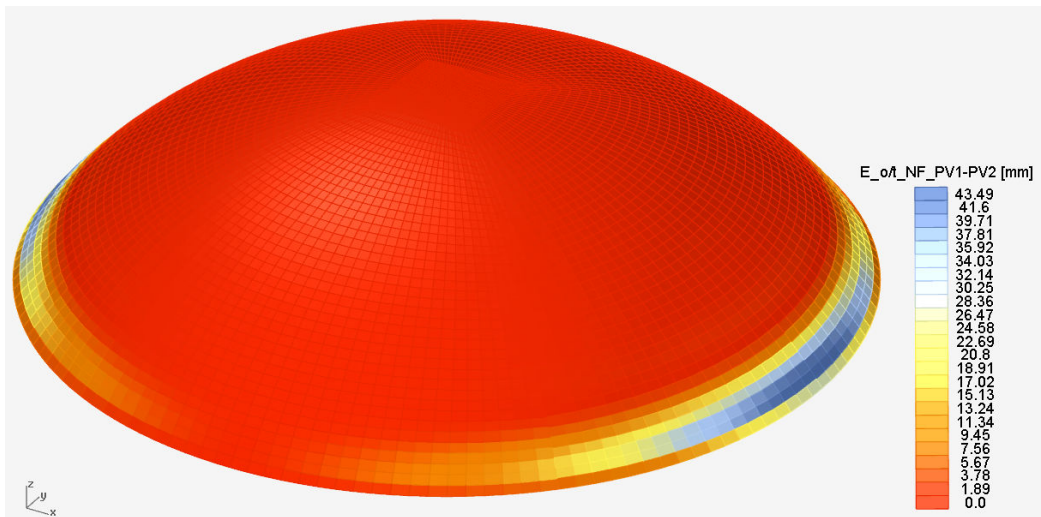


The first principal values of the eccentricity of the normal force for the ellipsoid for the loading condition self weight.

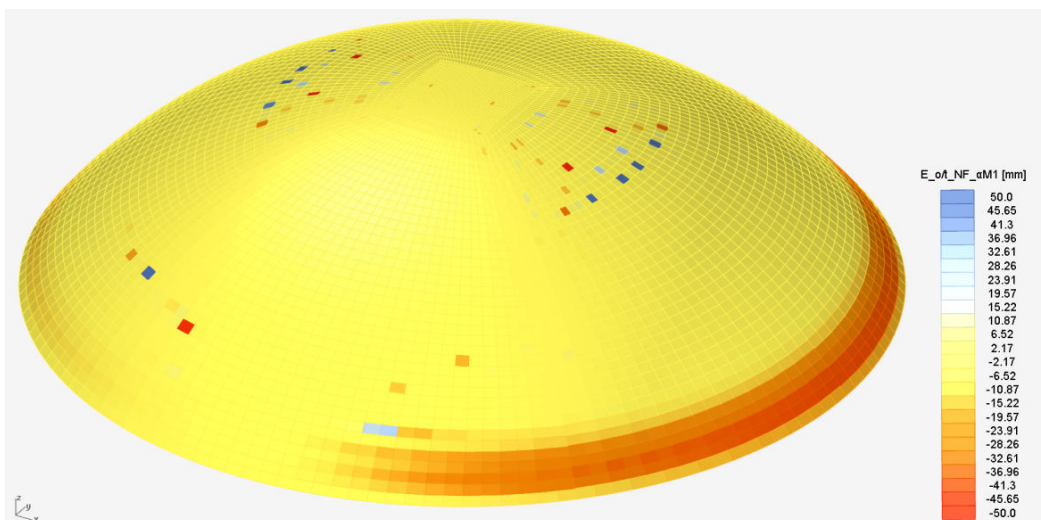


The second principal values of the eccentricity of the normal force for the ellipsoid for the loading condition self weight.

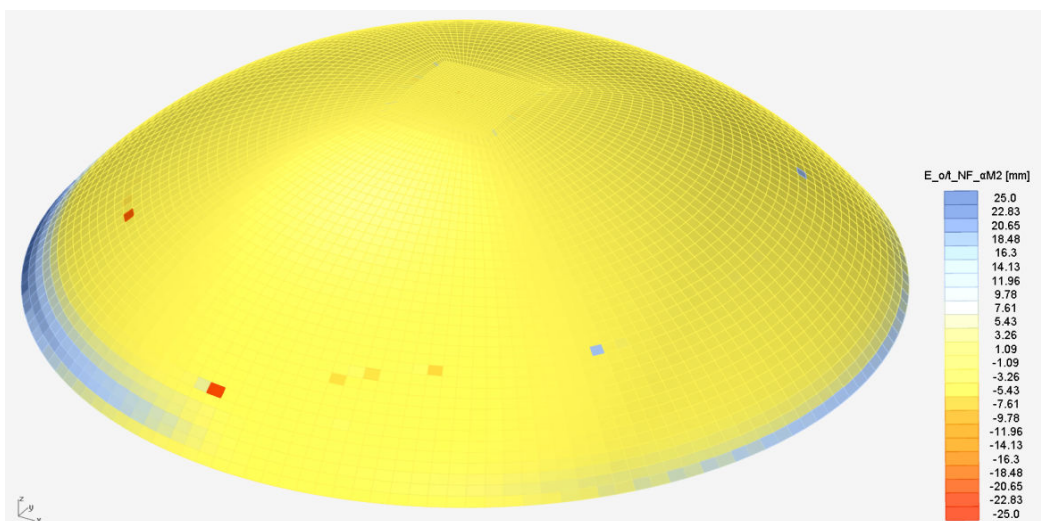




The difference between the first and second principal values of the eccentricity of the normal force for the ellipsoid for the loading condition self weight.

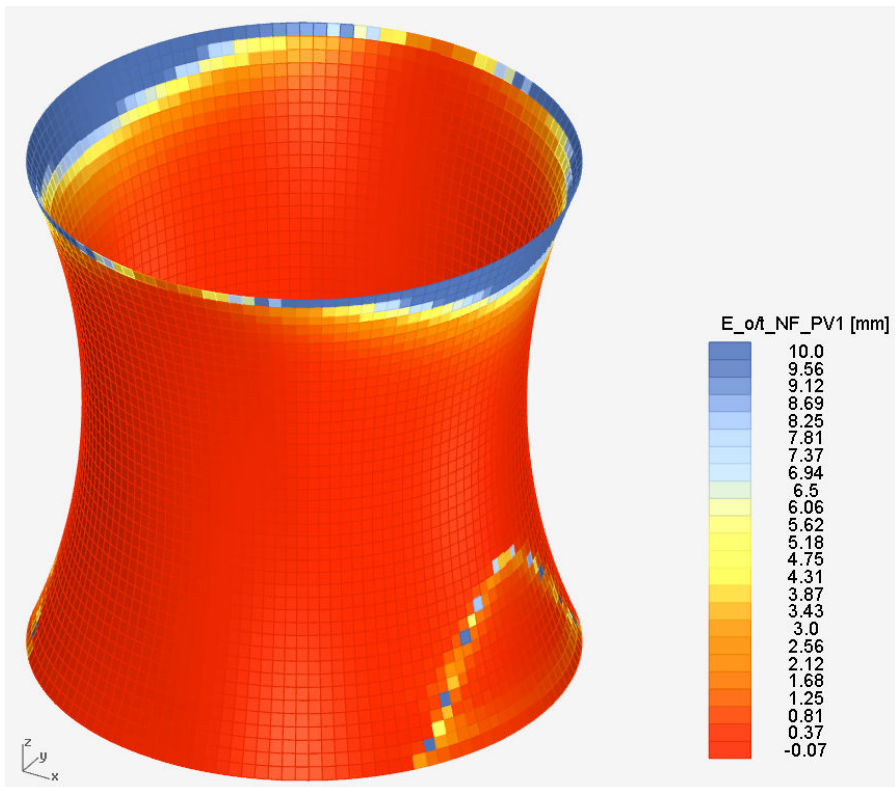


The values of the eccentricity of the normal force in the first principal directions of the distributed bending moments for the ellipsoid for the loading condition self weight.

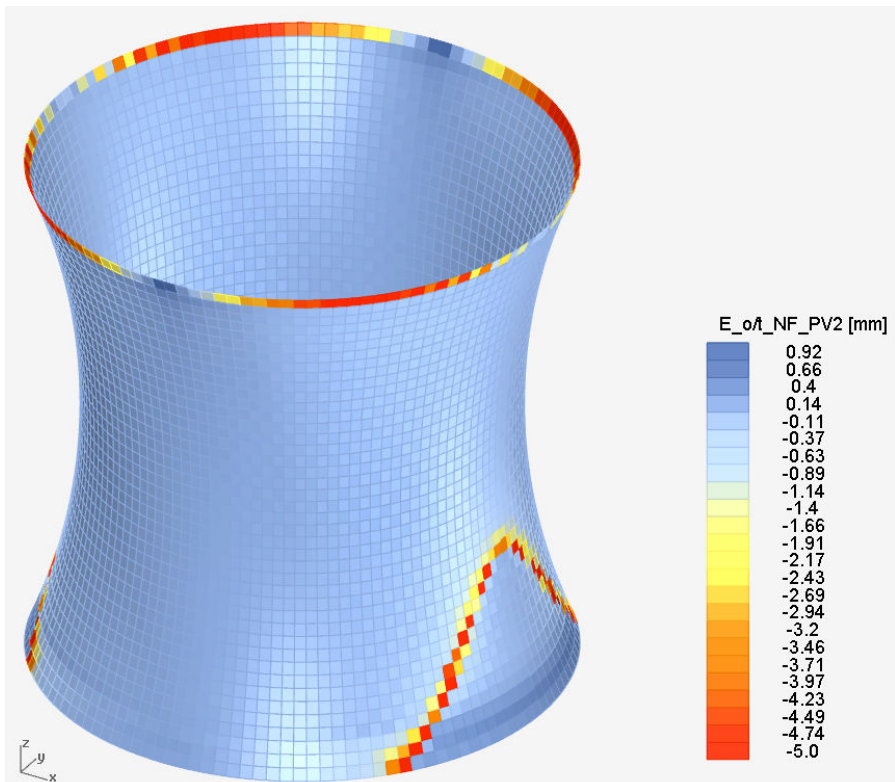


The values of the eccentricity of the normal force in the second principal directions of the distributed bending moments for the ellipsoid for the loading condition self weight.

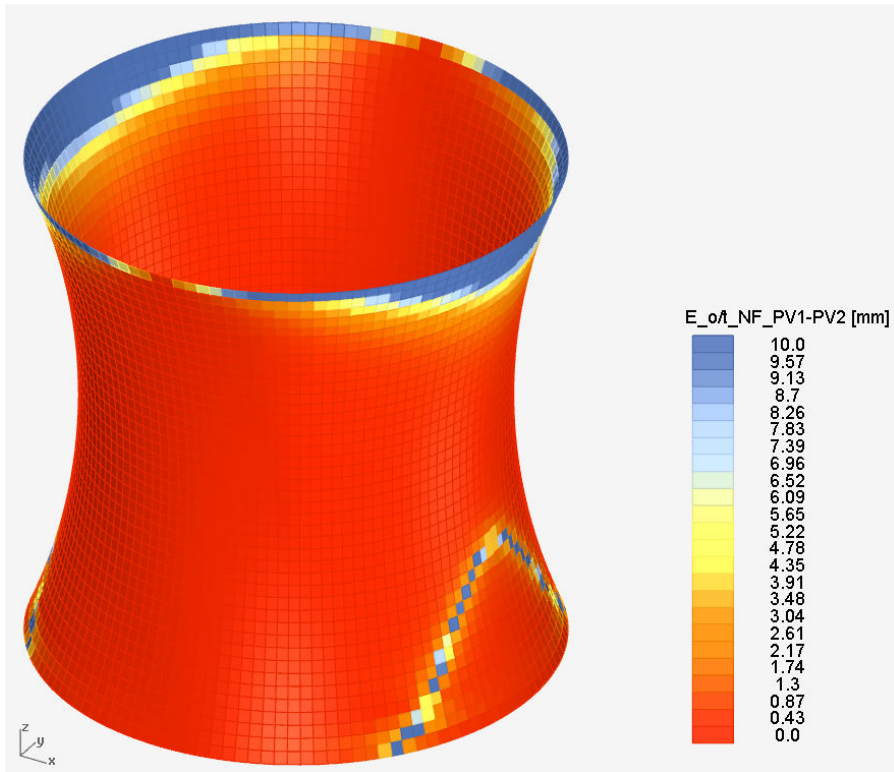
## Hyperboloid



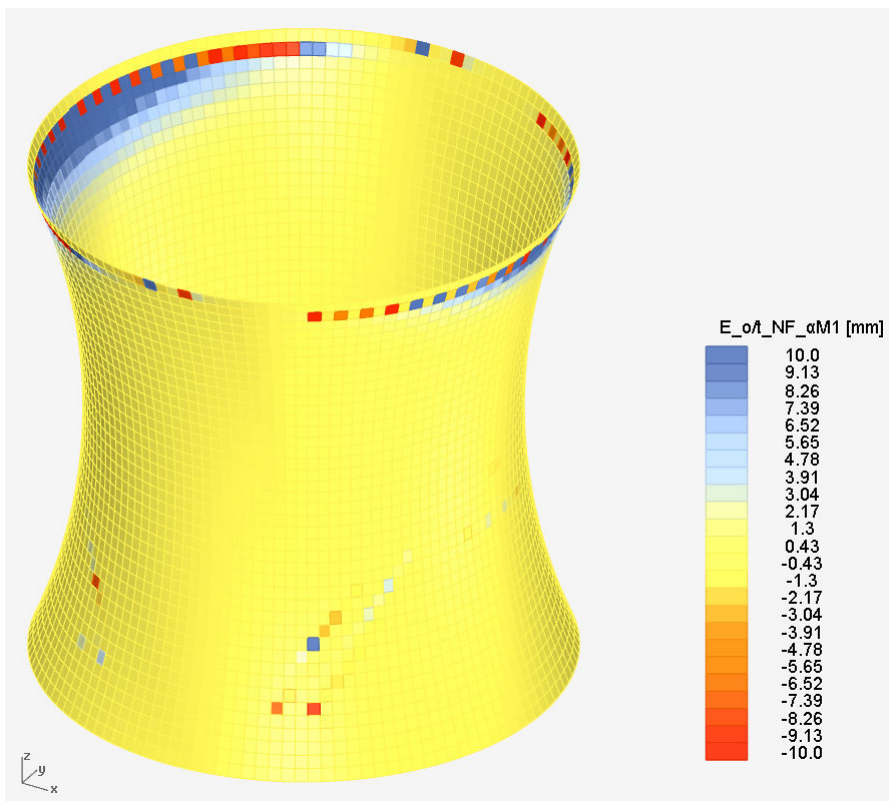
*The first principal values of the eccentricity of the normal force for the hyperboloid for the loading condition self weight.*



*The second principal values of the eccentricity of the normal force for the hyperboloid for the loading condition self weight.*

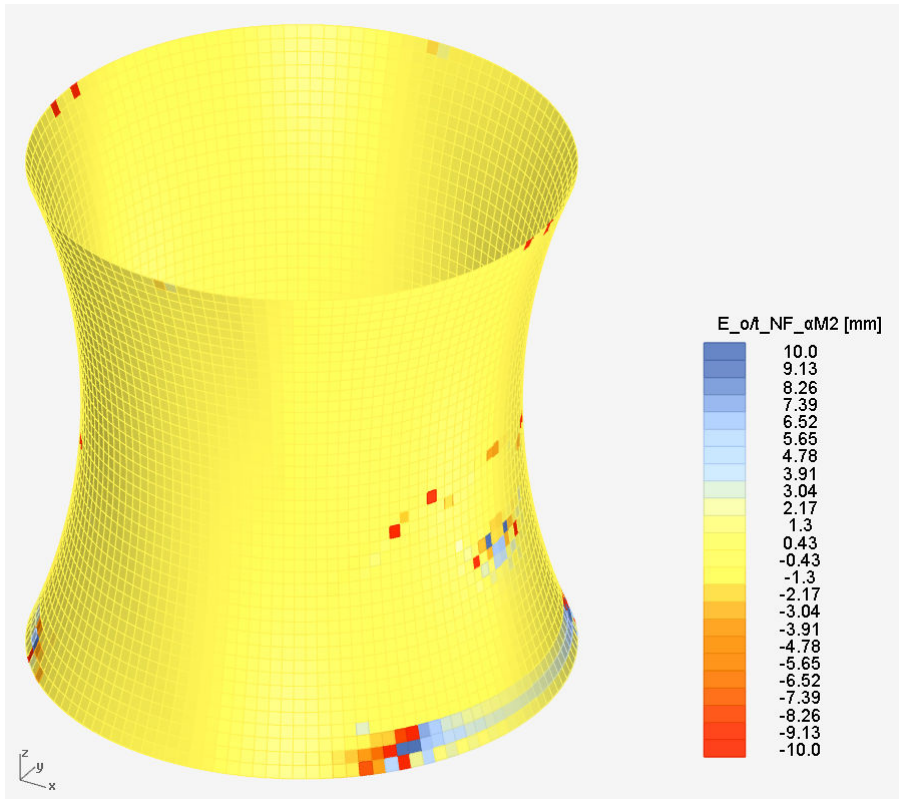


*The difference between the first and second principal values of the eccentricity of the normal force for the hyperboloid for the loading condition self weight.*



*The values of the eccentricity of the normal force in the first principal directions of the distributed bending moments for the hyperboloid for the loading condition self weight.*

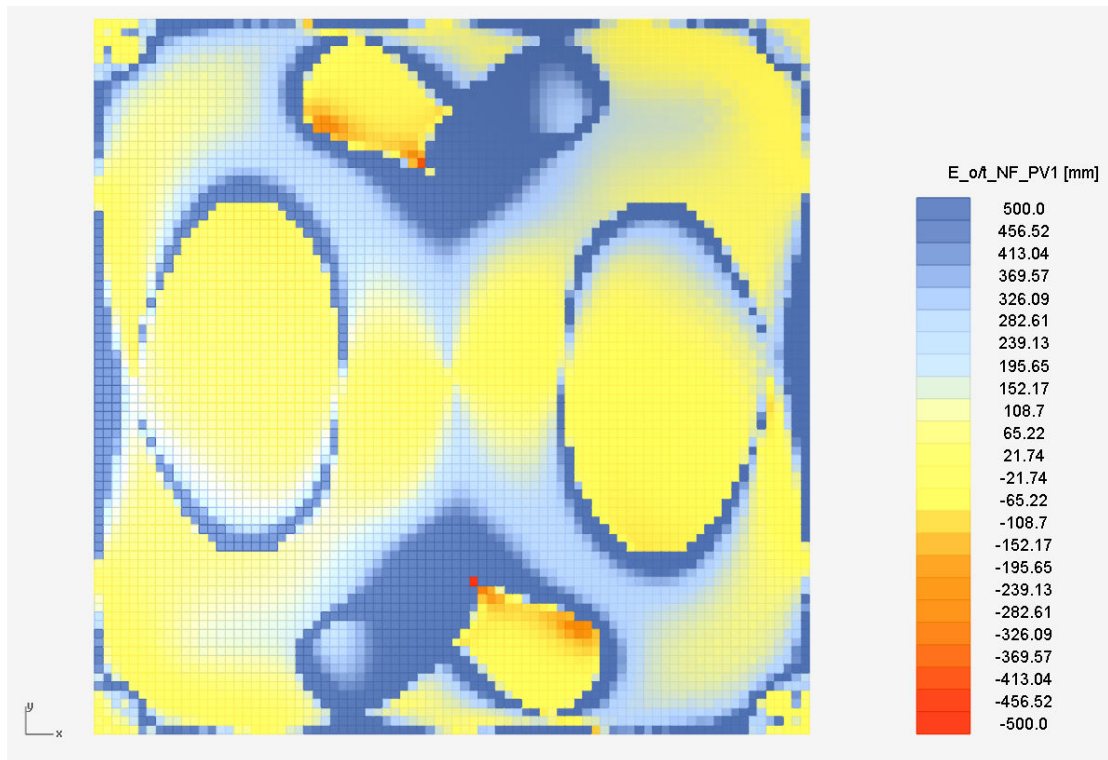




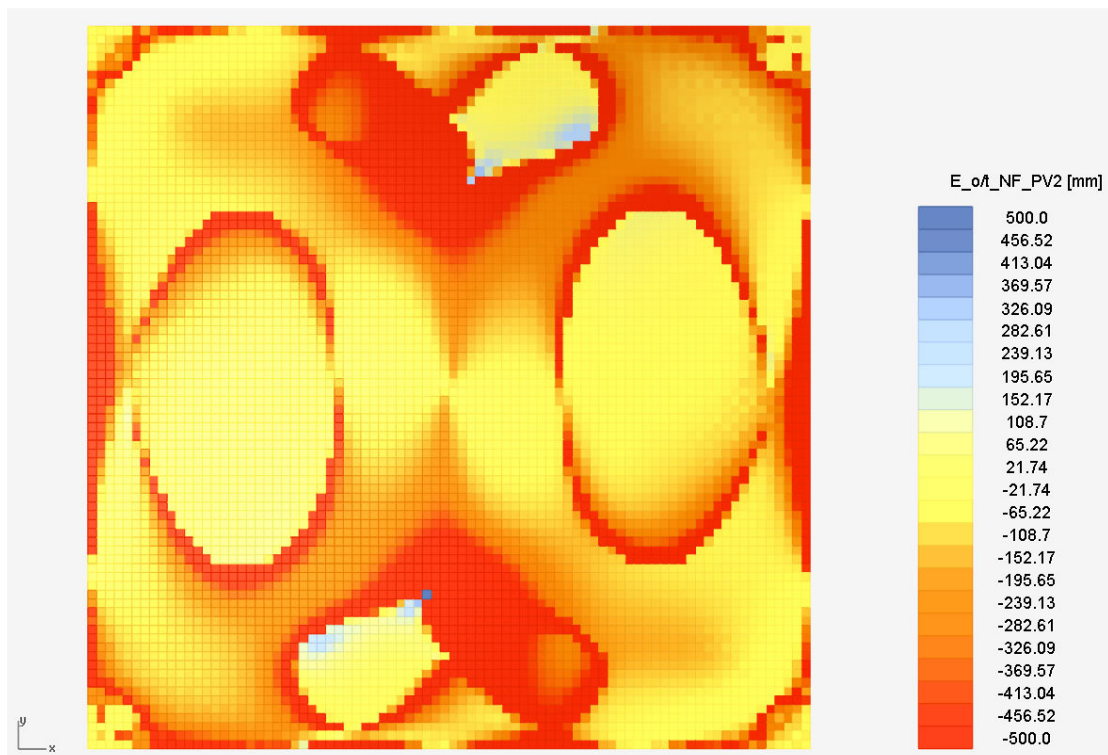
*The values of the eccentricity of the normal force in the second principal directions of the distributed bending moments for the hyperboloid for the loading condition self weight.*



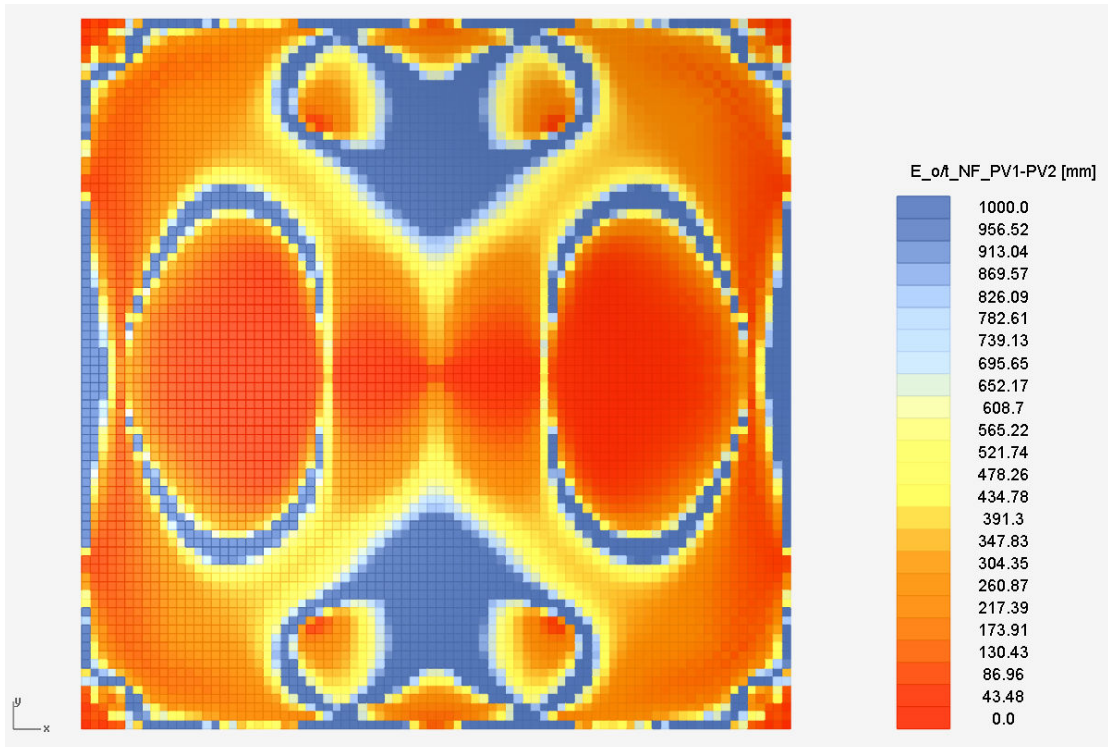
## Hypar



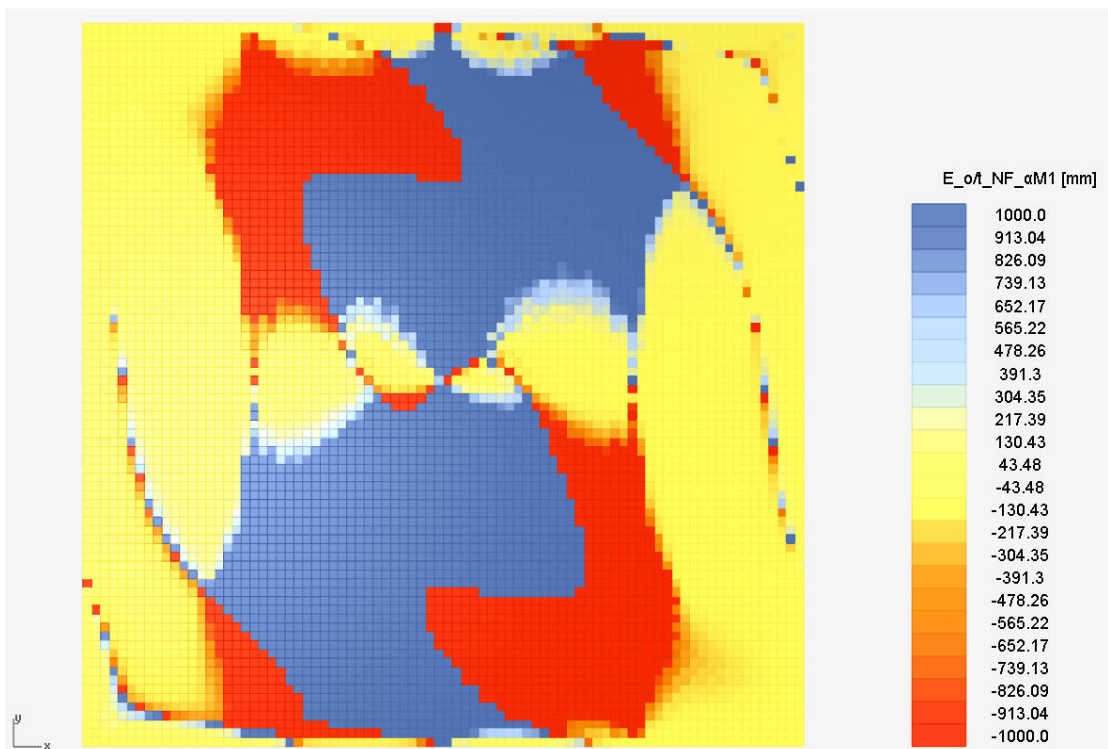
*The first principal values of the eccentricity of the normal force for the hypar for the loading condition self weight.*



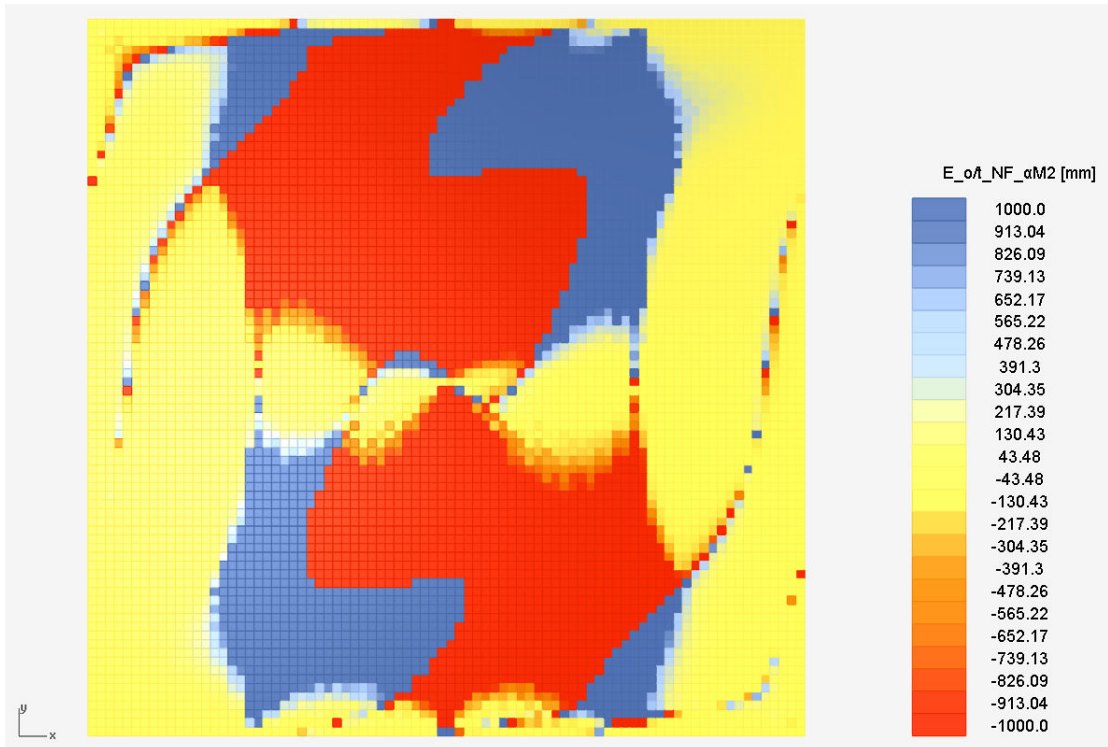
*The second principal values of the eccentricity of the normal force for the hypar for the loading condition self weight.*



The difference between the first and second principal values of the eccentricity of the normal force for the hyper for the loading condition self weight.



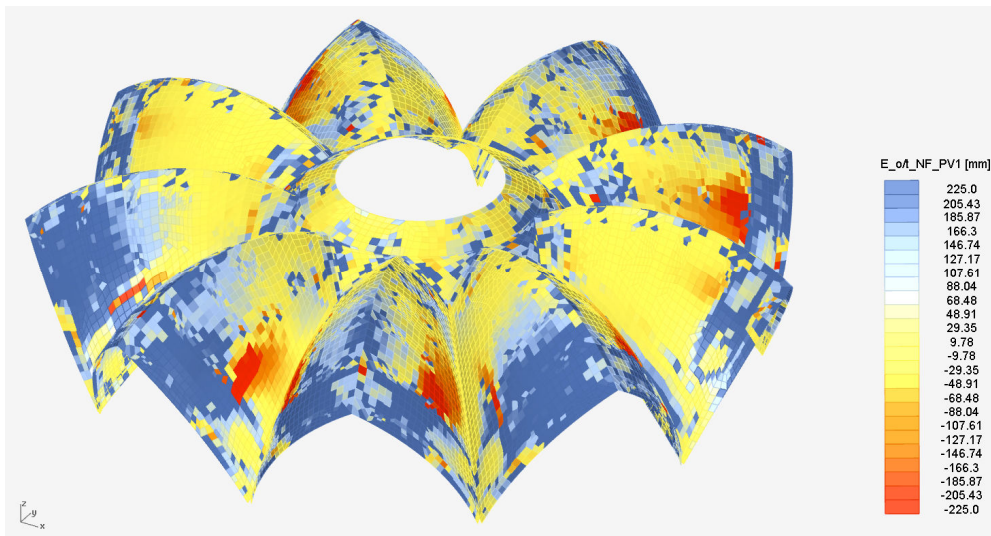
The values of the eccentricity of the normal force in the first principal directions of the distributed bending moments for the hyper for the loading condition self weight.



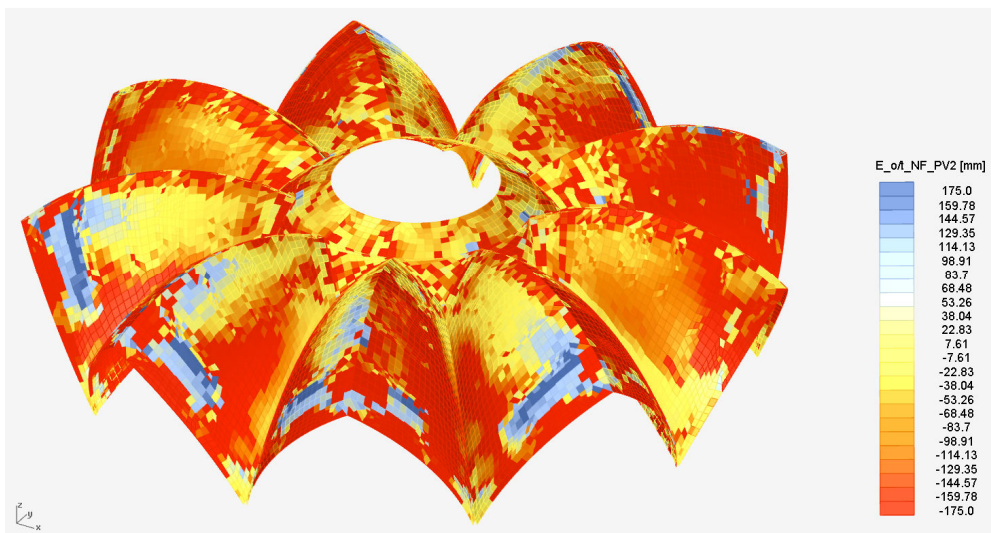
*The values of the eccentricity of the normal force in the second principal directions of the distributed bending moments for the hyperboloid for the loading condition self weight.*



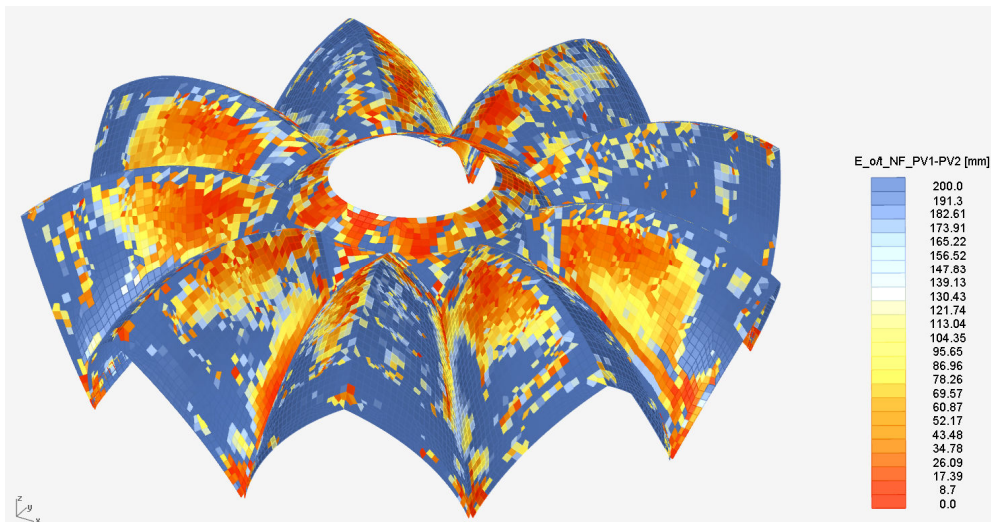
## Complex geometry



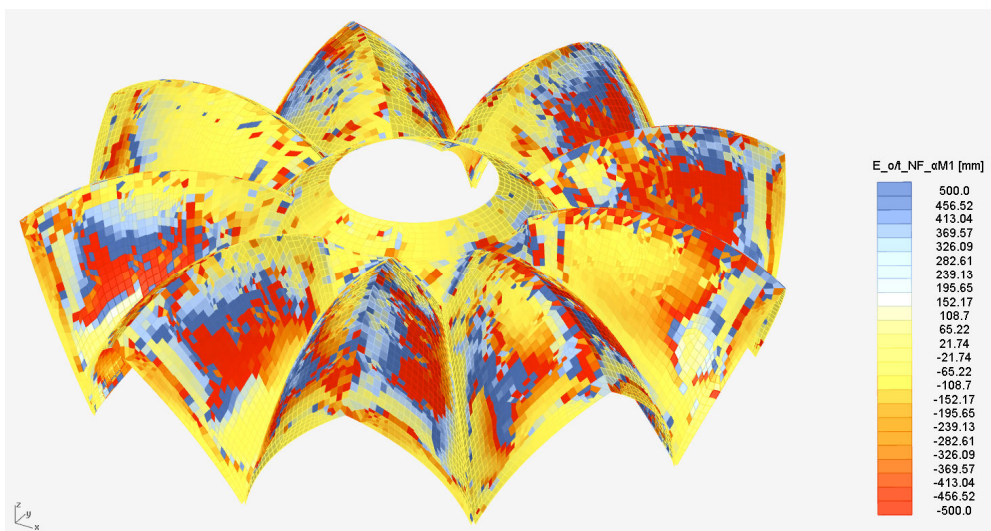
The first principal values of the eccentricity of the normal force for the complex geometry for the loading condition self weight.



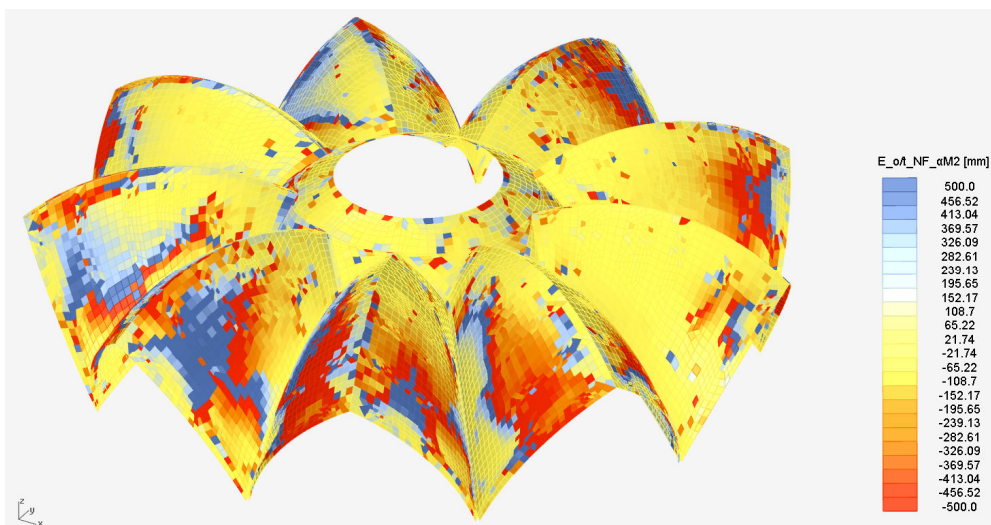
The second principal values of the eccentricity of the normal force for the complex geometry for the loading condition self weight.



*The difference between the first and second principal values of the eccentricity of the normal force for the complex geometry for the loading condition self weight.*



*The values of the eccentricity of the normal force in the first principal directions of the distributed bending moments for the complex geometry for the loading condition self weight.*

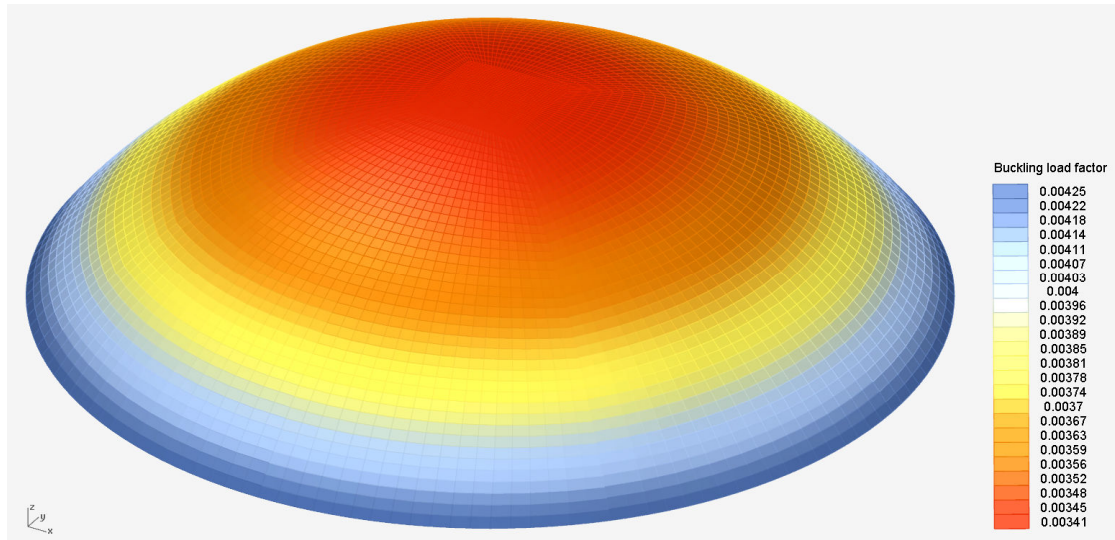


*The values of the eccentricity of the normal force in the second principal directions of the distributed bending moments for the complex geometry for the loading condition self weight.*

## Buckling Load Factor

Self weight

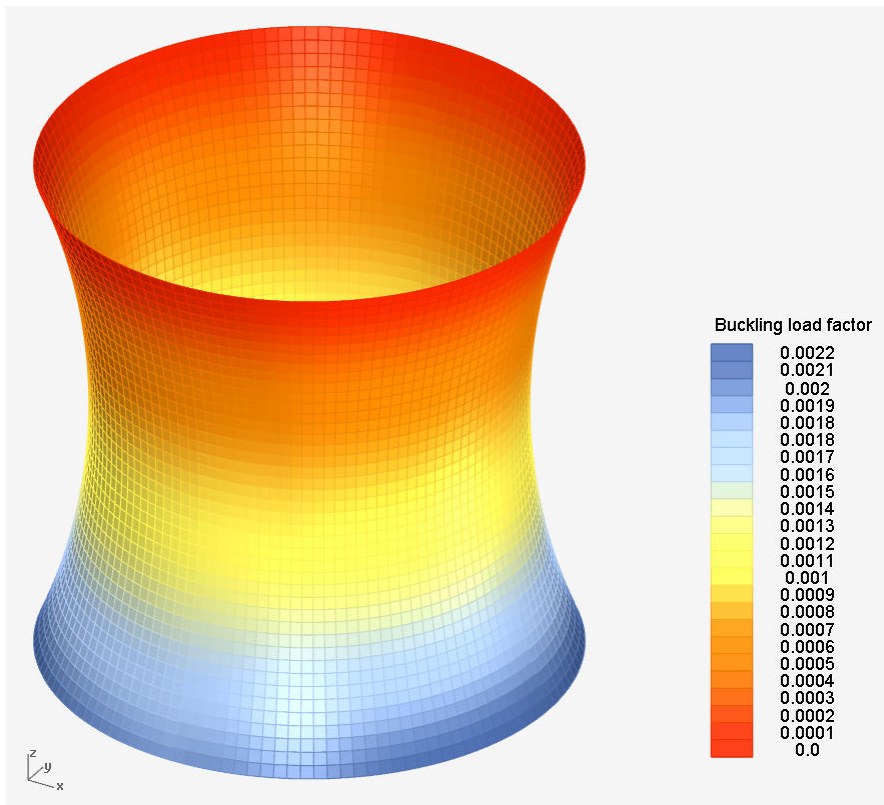
Ellipsoid



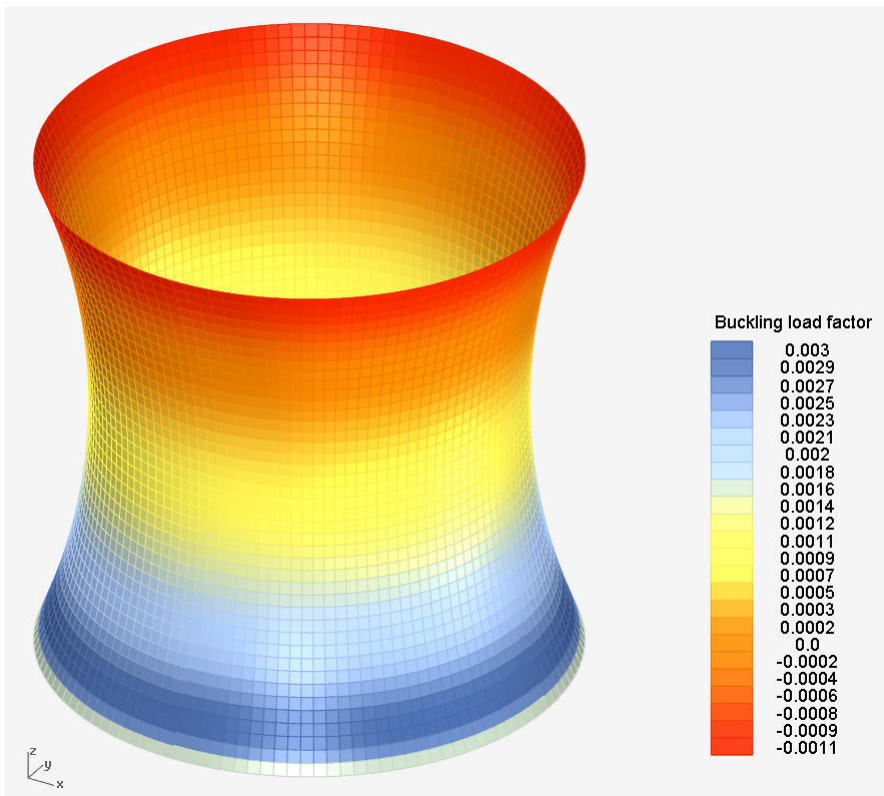
*The buckling load factor results for the ellipsoid for the loading condition self weight.*



## Hyperboloid

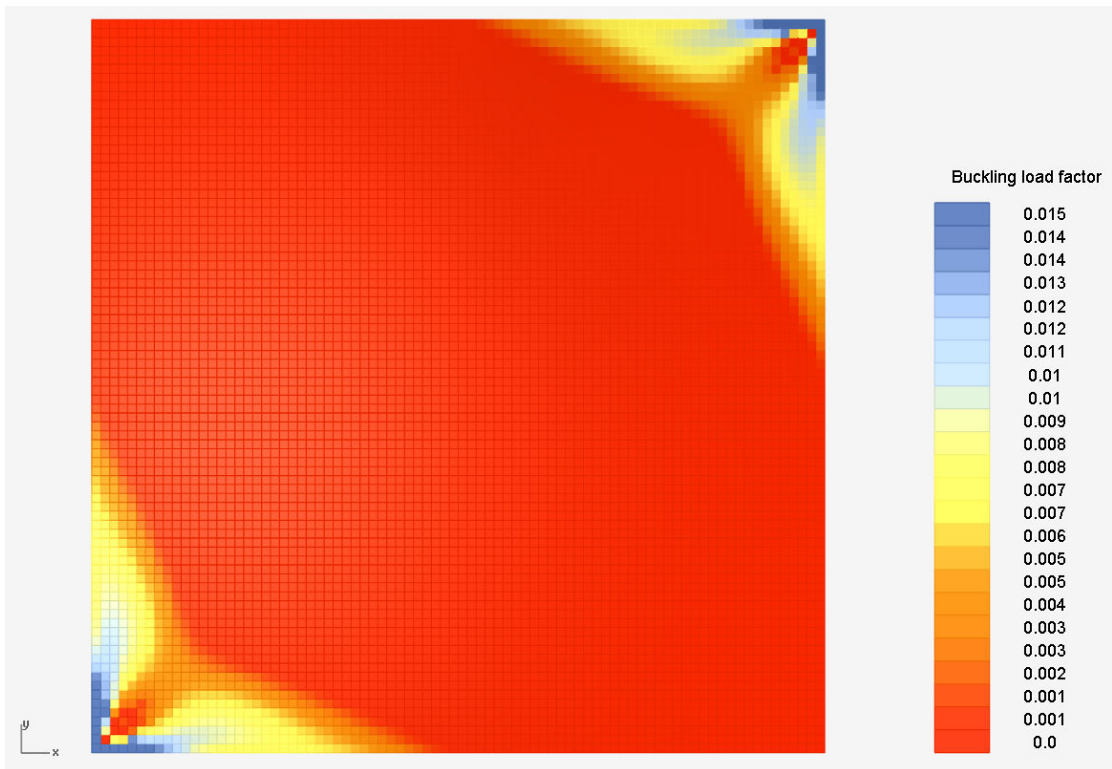


*The buckling load factor results in meridional (vertical) direction for the hyperboloid for the loading condition self weight.*

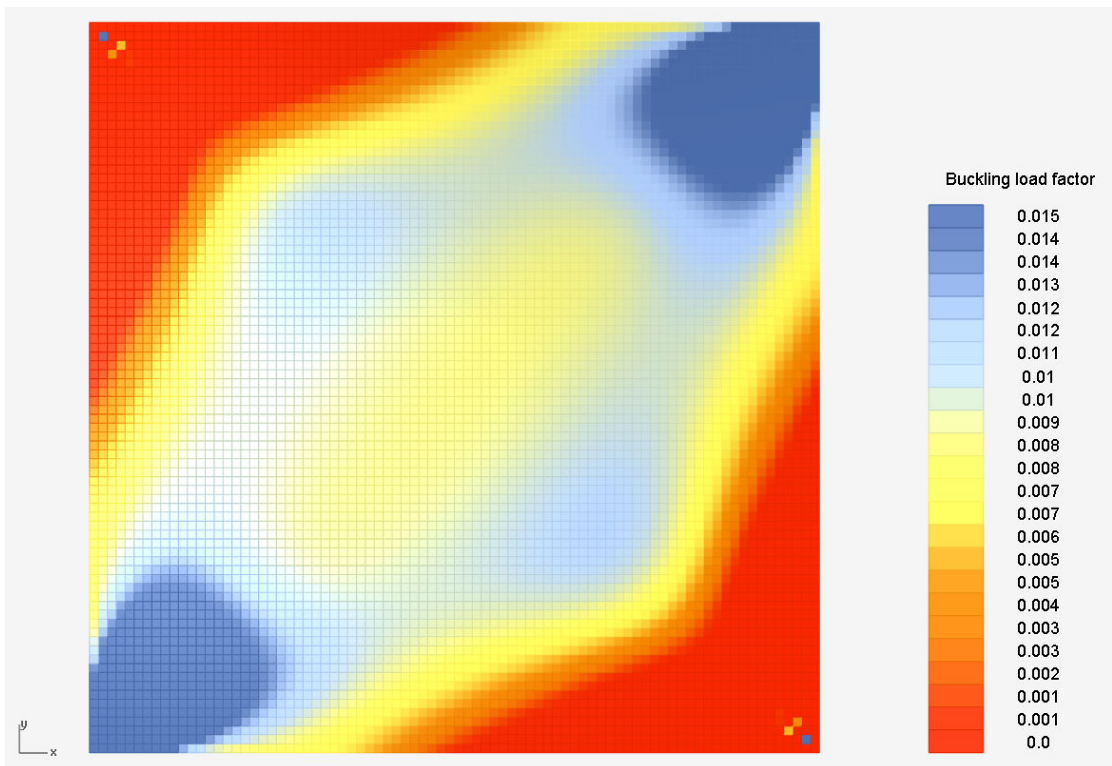


*The buckling load factor results in hoop force (horizontal) direction for the hyperboloid for the loading condition self weight.*

## Hypar

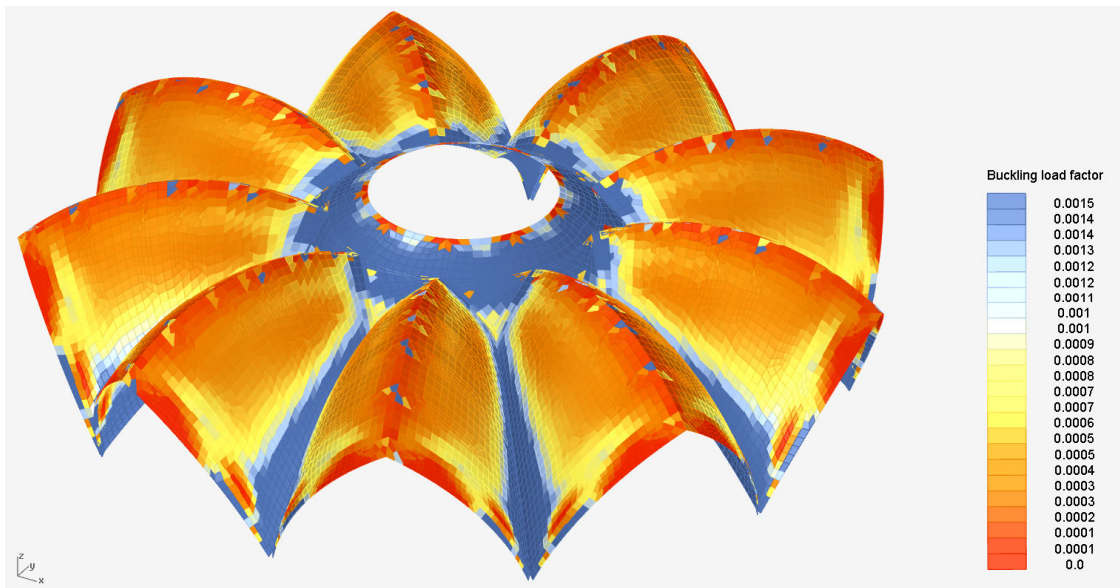


*The first buckling load factor results for the hypar for the loading condition self weight. Direction: from top left to bottom right.*

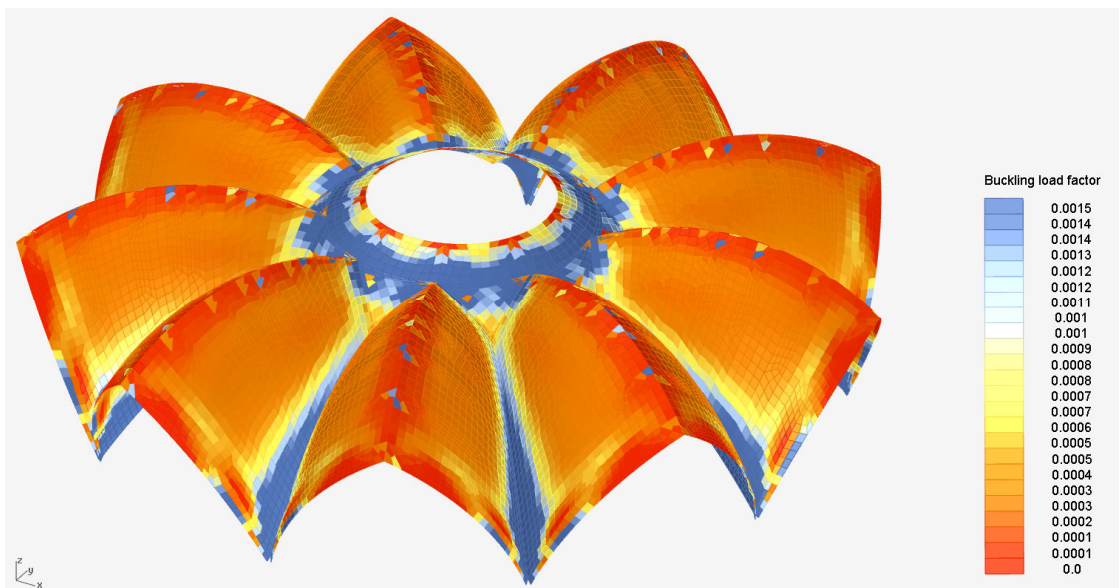


*The second buckling load factor results for the hypar for the loading condition self weight. Direction: from top right to bottom left.*

## Complex geometry



*The buckling load factor results for the complex geometry for the loading condition self weight. This image displays the correct values for the inner ring of elements.*

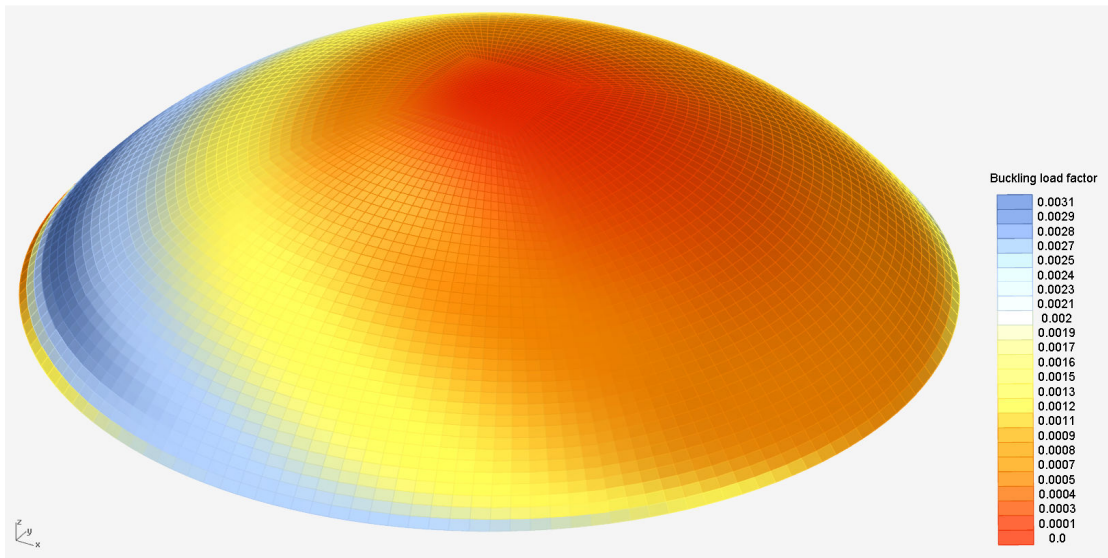


*The buckling load factor results for the complex geometry for the loading condition self weight. This image displays the correct values for the outer ring of elements.*



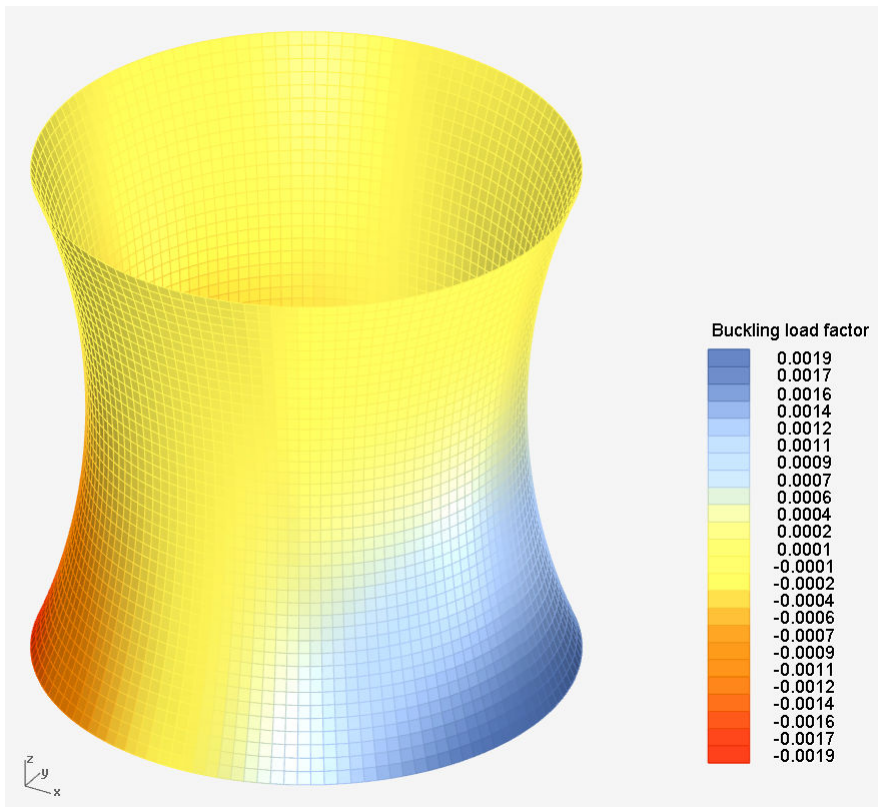
## Wind load

### Ellipsoid

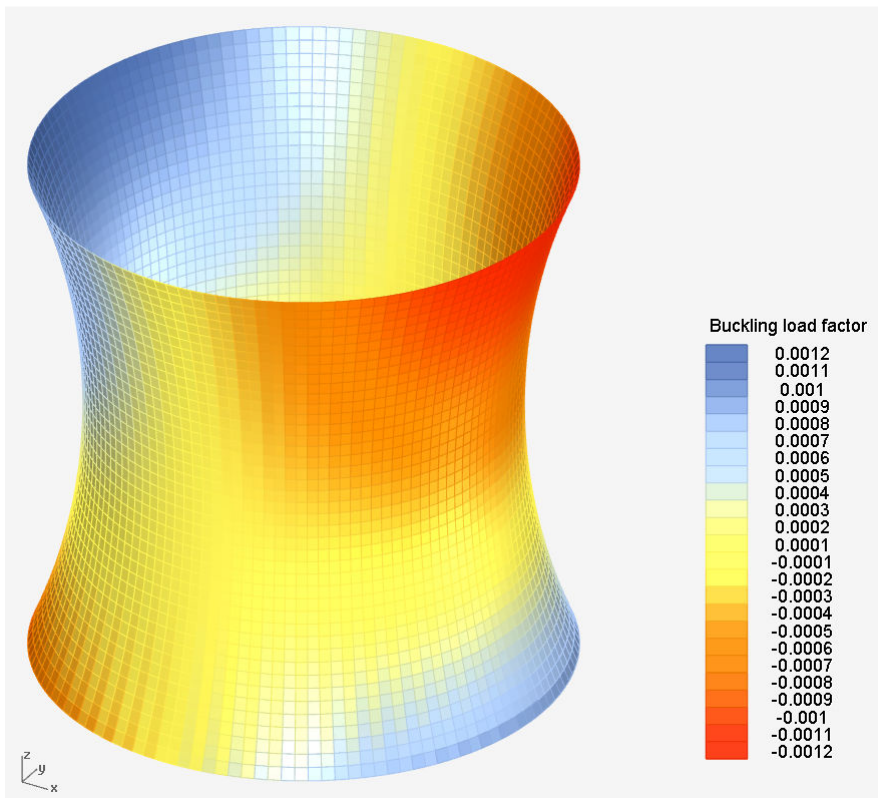


*The buckling load factor results for the ellipsoid for the loading condition wind.*

## Hyperboloid

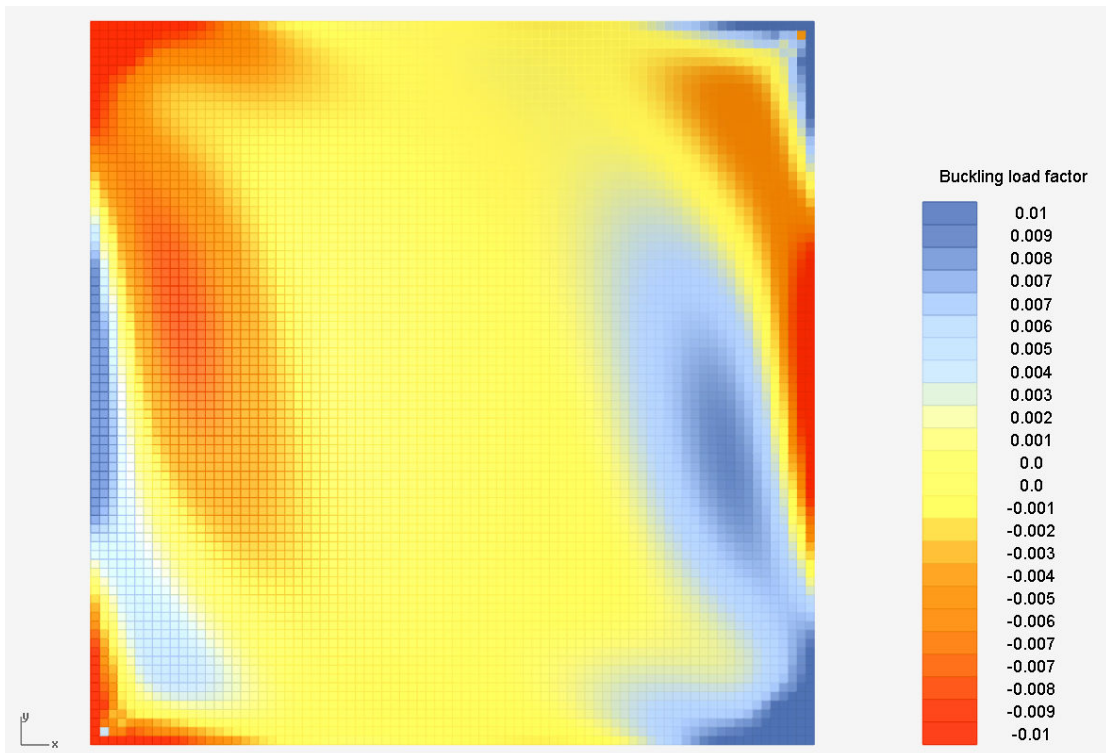


*The buckling load factor results in meridional (vertical) direction for the hyperboloid for the loading condition wind.*

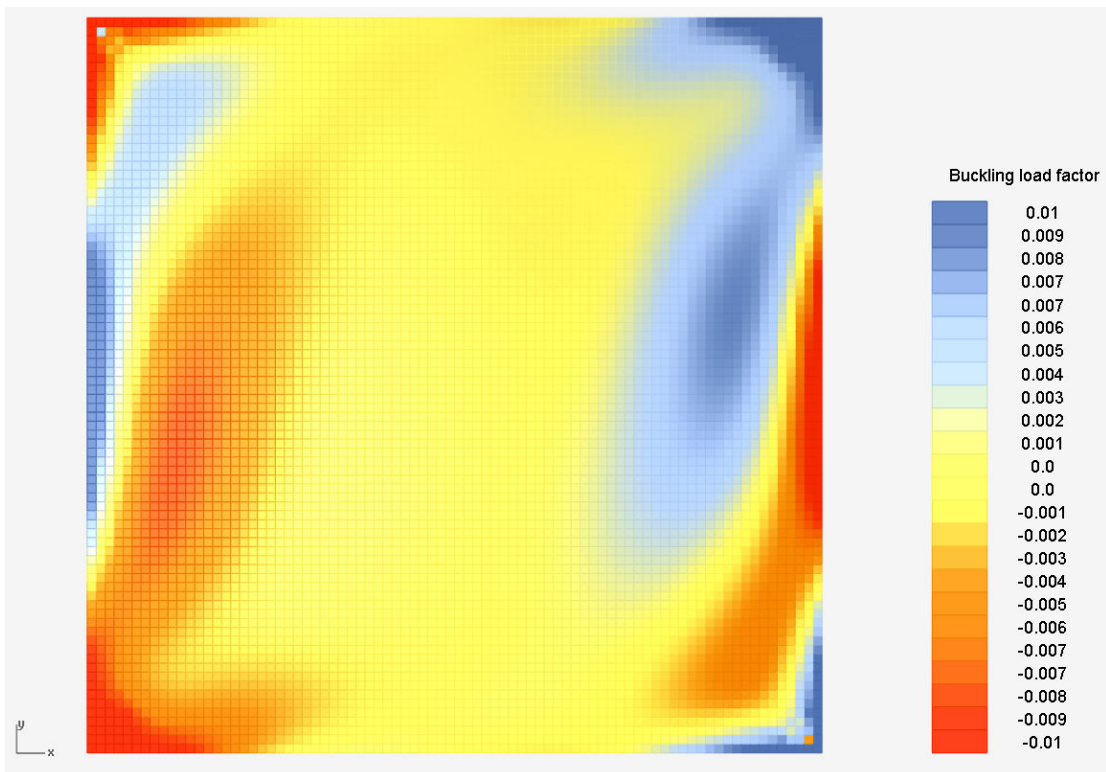


*The buckling load factor results in hoop force (horizontal) direction for the hyperboloid for the loading condition wind.*

## Hypar



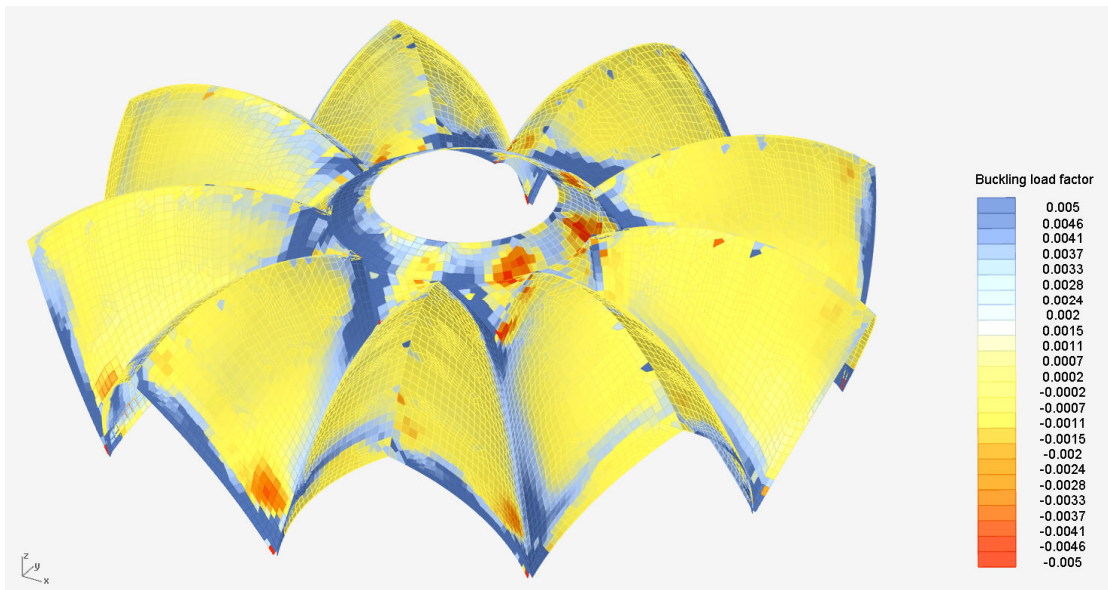
*The first buckling load factor results for the hypar for the loading condition wind. Direction: from top left to bottom right.*



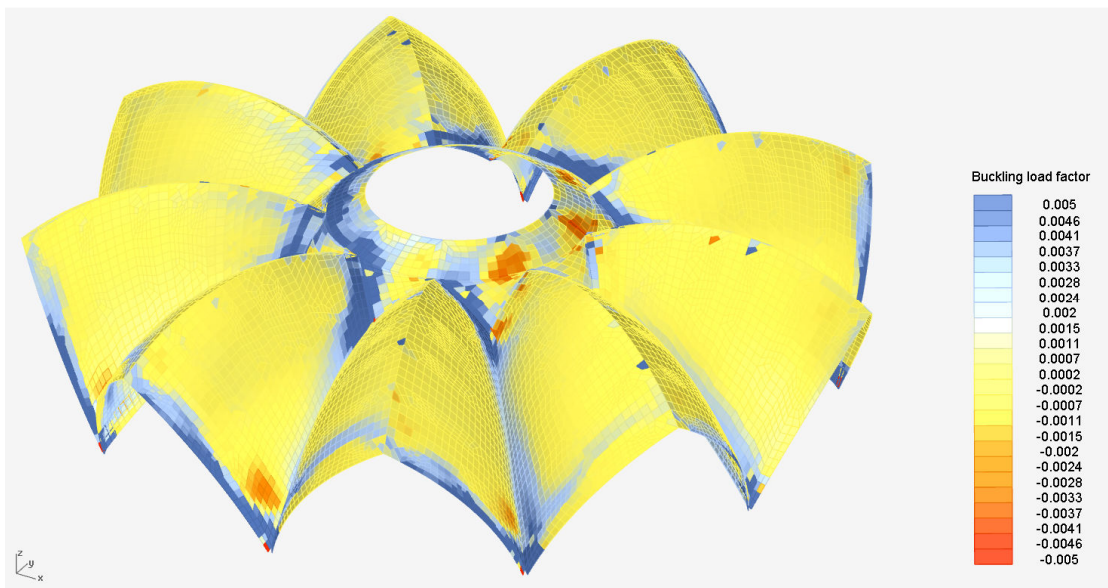
*The second buckling load factor results for the hypar for the loading condition wind. Direction: from top right to bottom left.*



## Complex geometry



*The buckling load factor results for the complex geometry for the loading condition wind. This image displays the correct values for the inner ring of elements.*

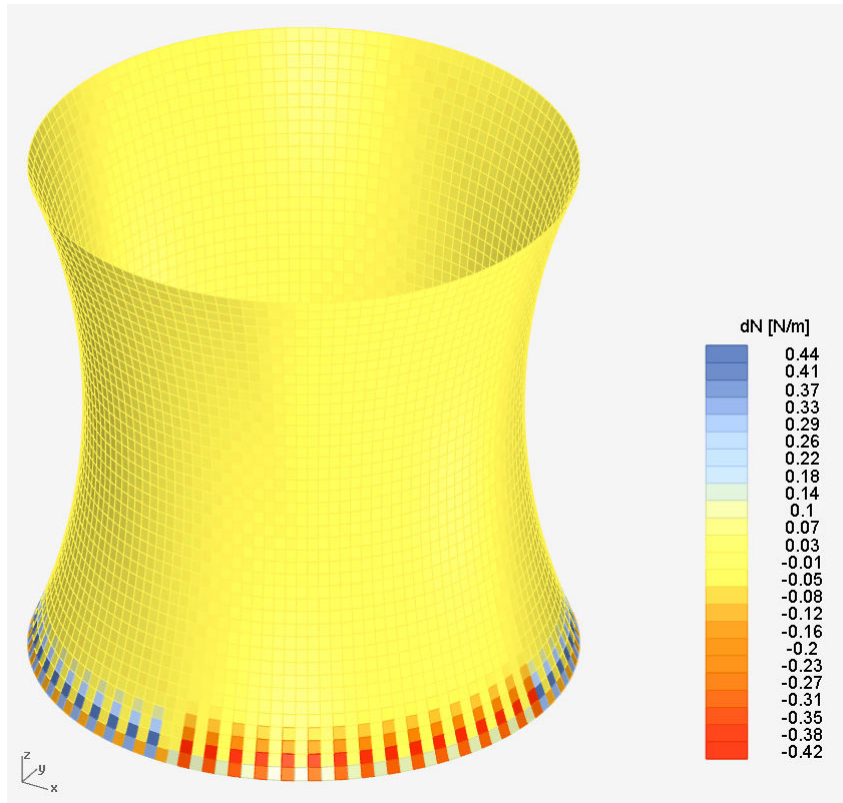


*The buckling load factor results for the complex geometry for the loading condition wind. This image displays the correct values for the outer ring of elements.*

## Out of balance of the in-plane shear force

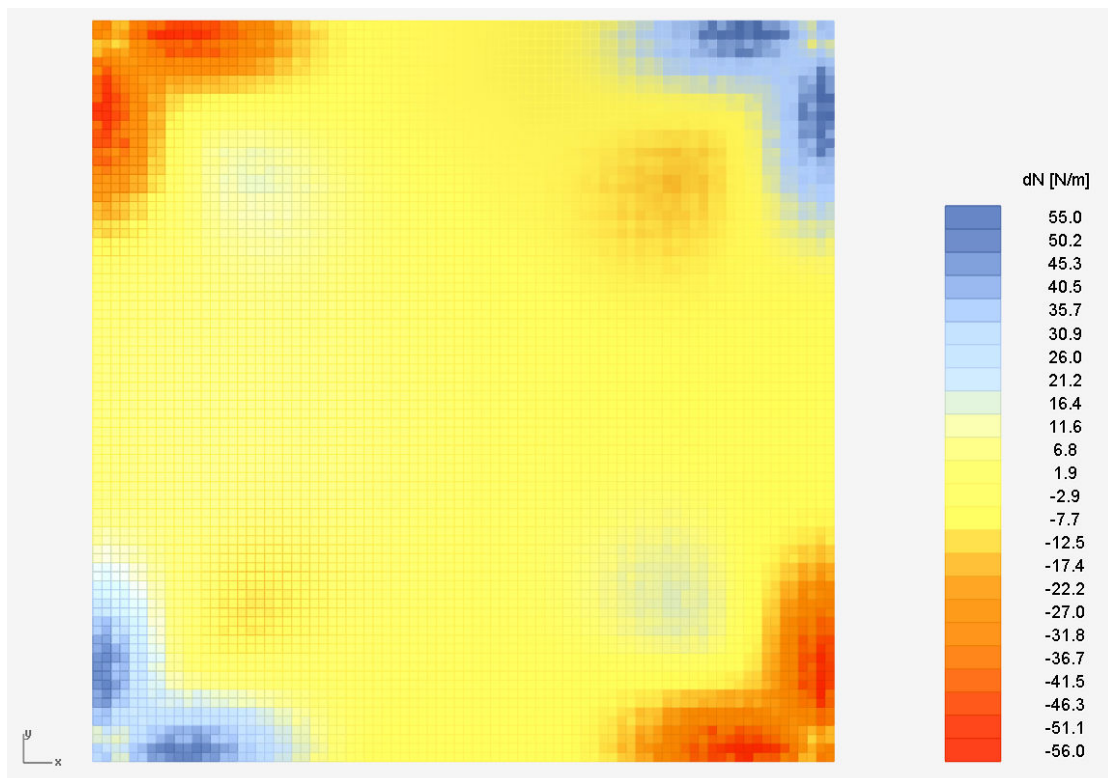
Self weight

Hyperboloid



*The out of balance of the in-plane shear force results for the hyperboloid for the loading condition self weight.*

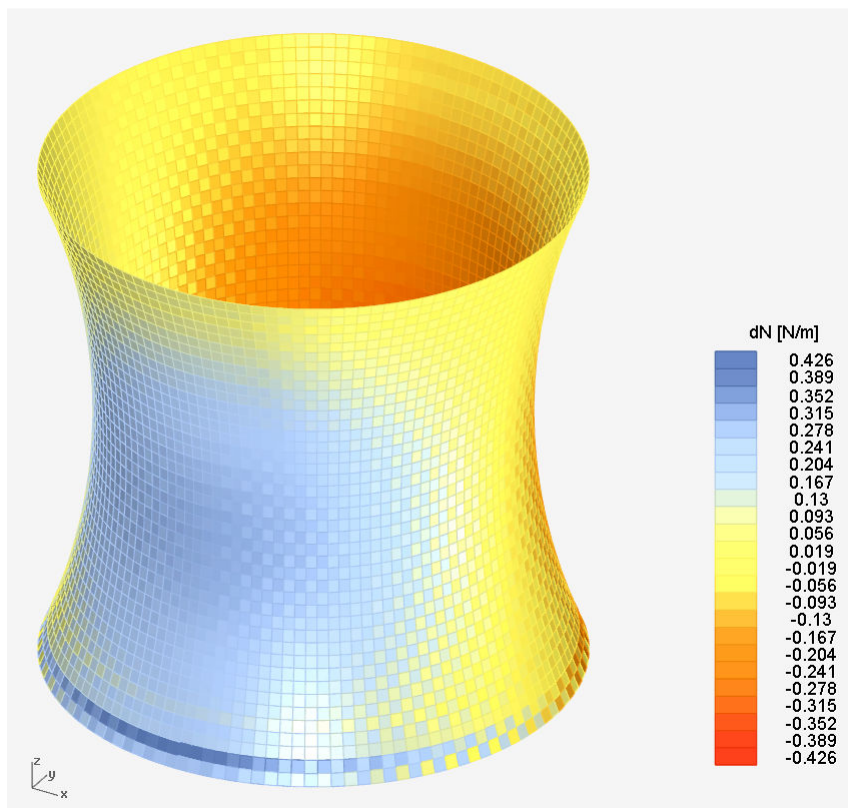
## Hypar



*The out of balance of the in-plane shear force results for the hypar for the loading condition self weight.*

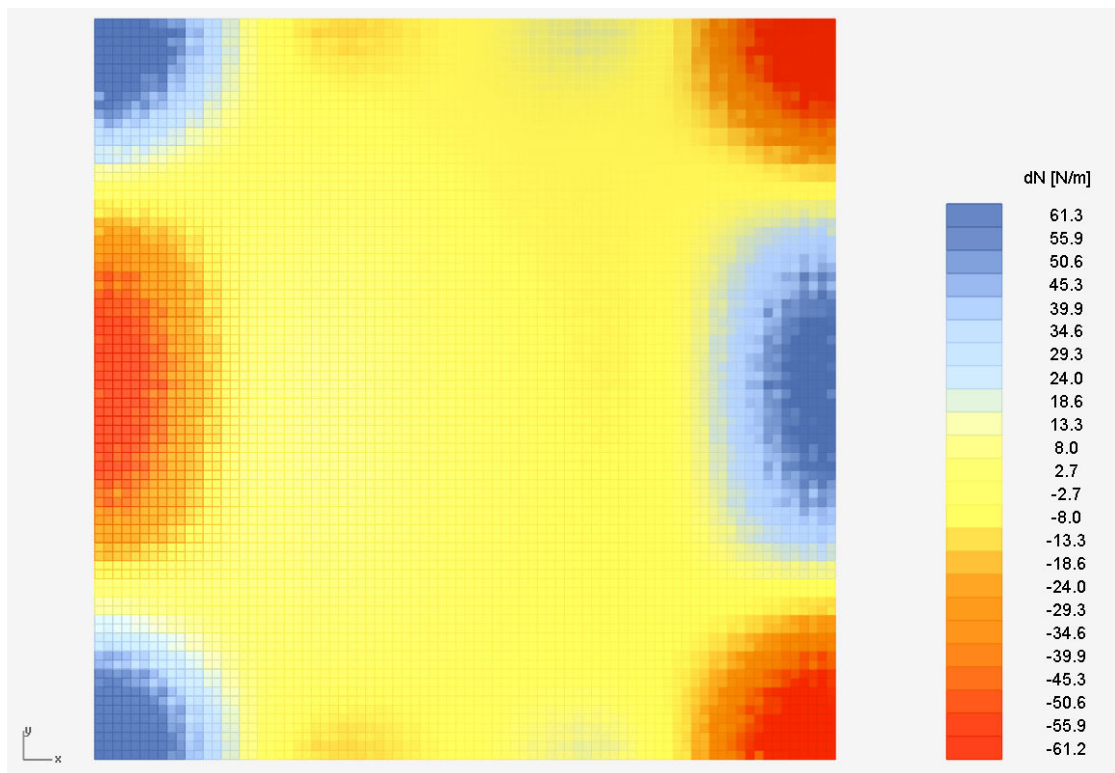
## Wind load

### Hyperboloid



*The out of balance of the in-plane shear force results for the hyperboloid for the loading condition wind.*

## Hypar



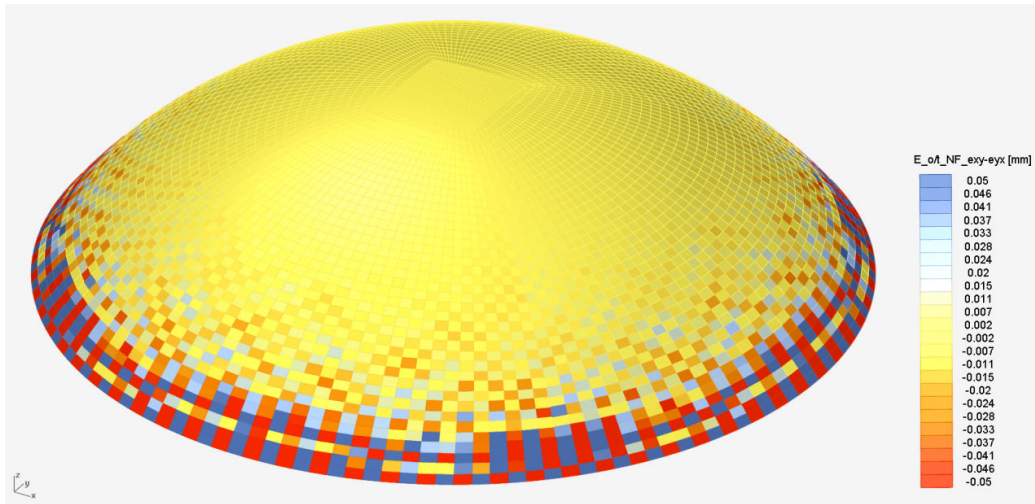
*The out of balance of the in-plane shear force results for the hypar for the loading condition wind.*



## Out of balance of the in-plane shear eccentricity of the normal force

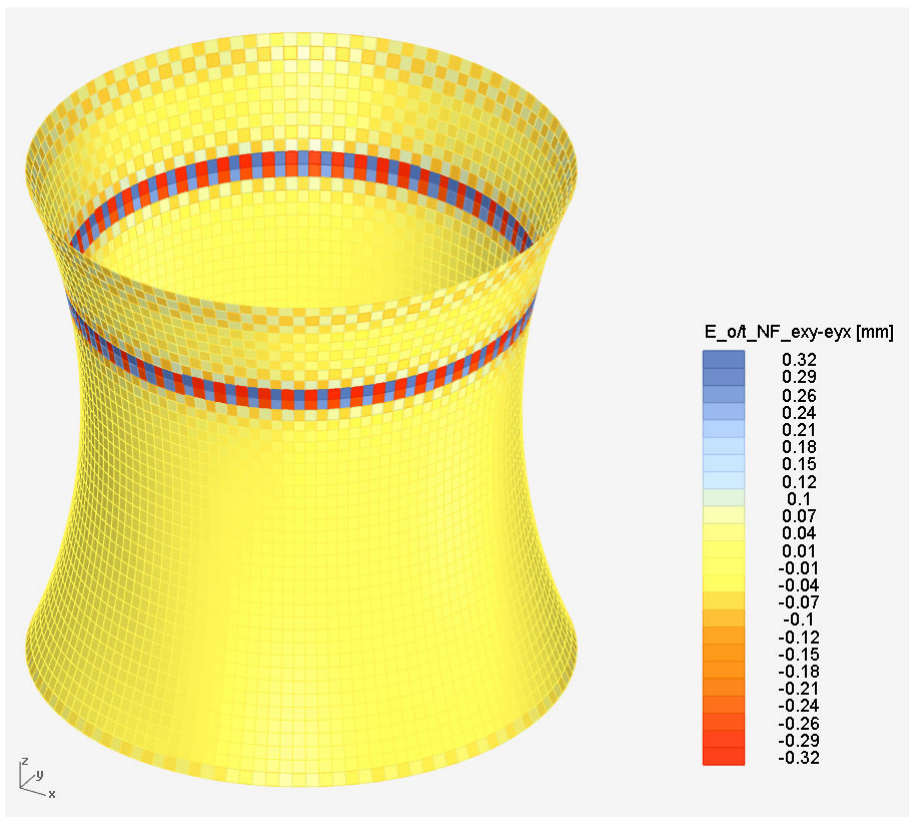
### Self weight

#### Ellipsoid



*The out of balance of the in-plane shear eccentricity of the normal force results for the ellipsoid for the loading condition self weight.*

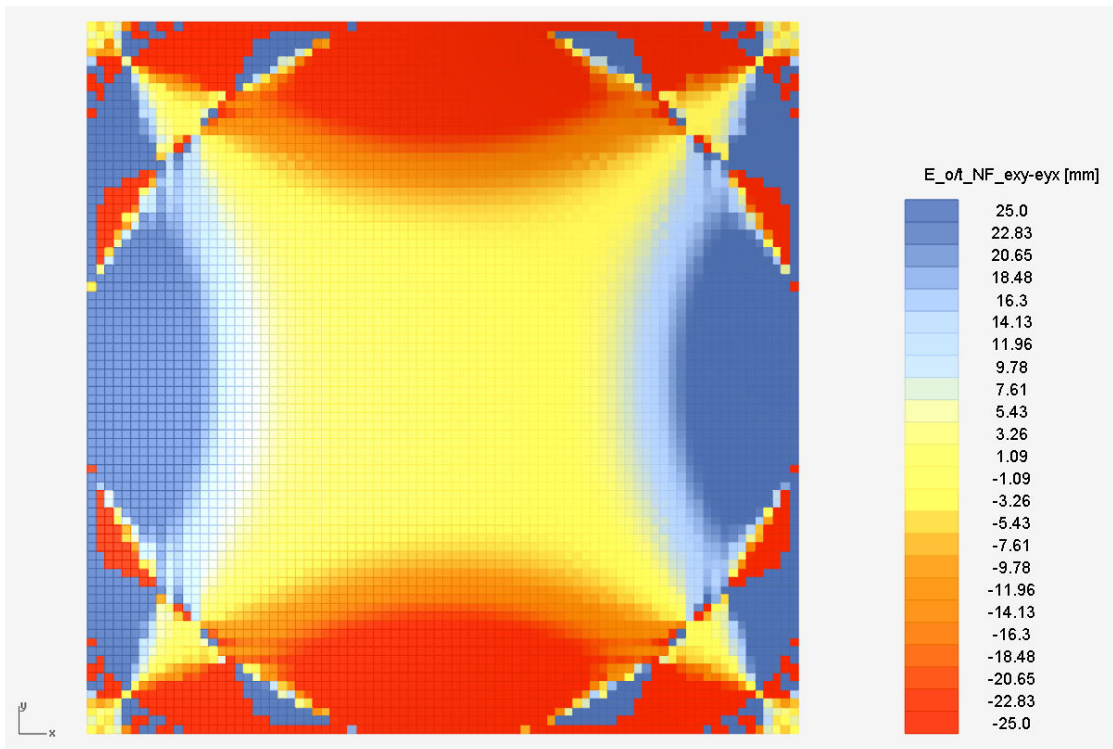
#### Hyperboloid



*The out of balance of the in-plane shear eccentricity of the normal force results for the hyperboloid for the loading condition self weight.*

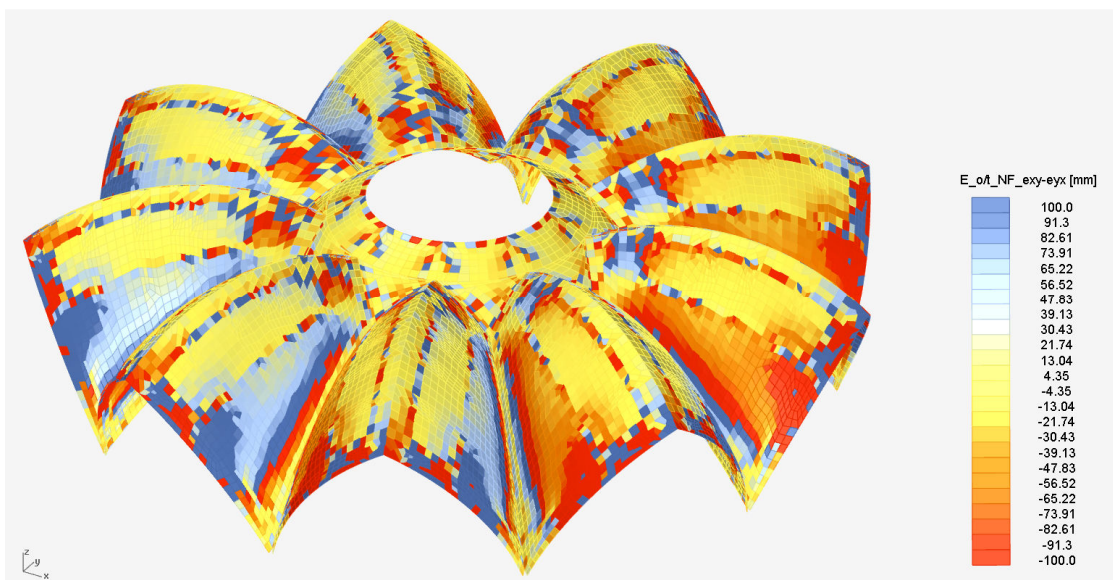


## Hypar



*The out of balance of the in-plane shear eccentricity of the normal force results for the hypar for the loading condition self weight.*

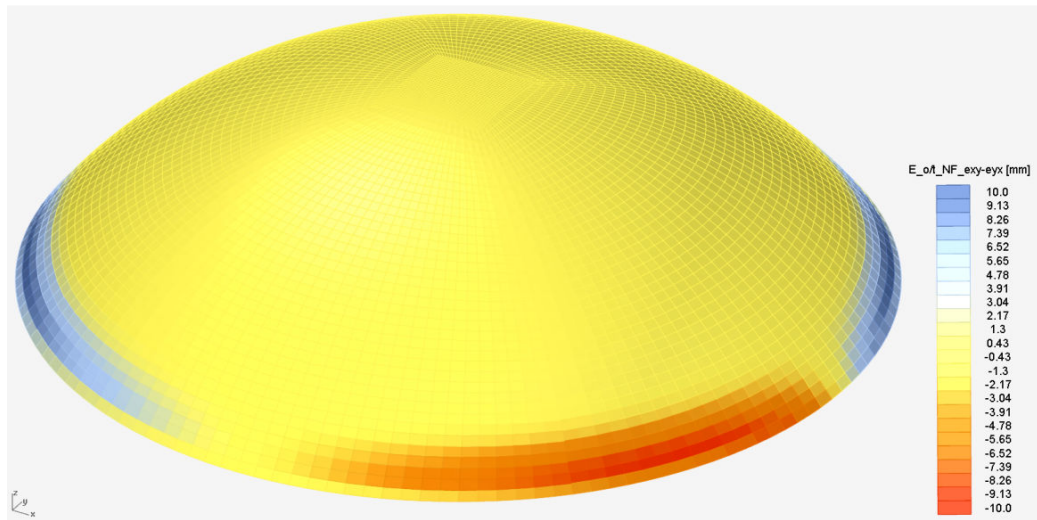
## Complex geometry



*The out of balance of the in-plane shear eccentricity of the normal force results for the complex geometry for the loading condition self weight.*

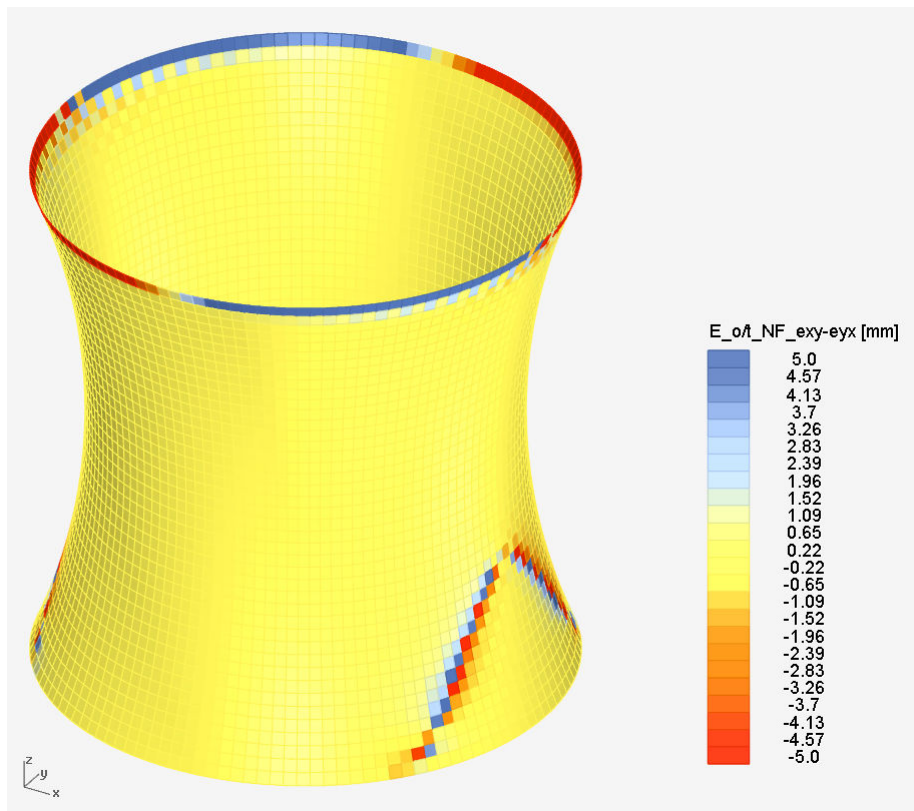
## Wind load

### Ellipsoid



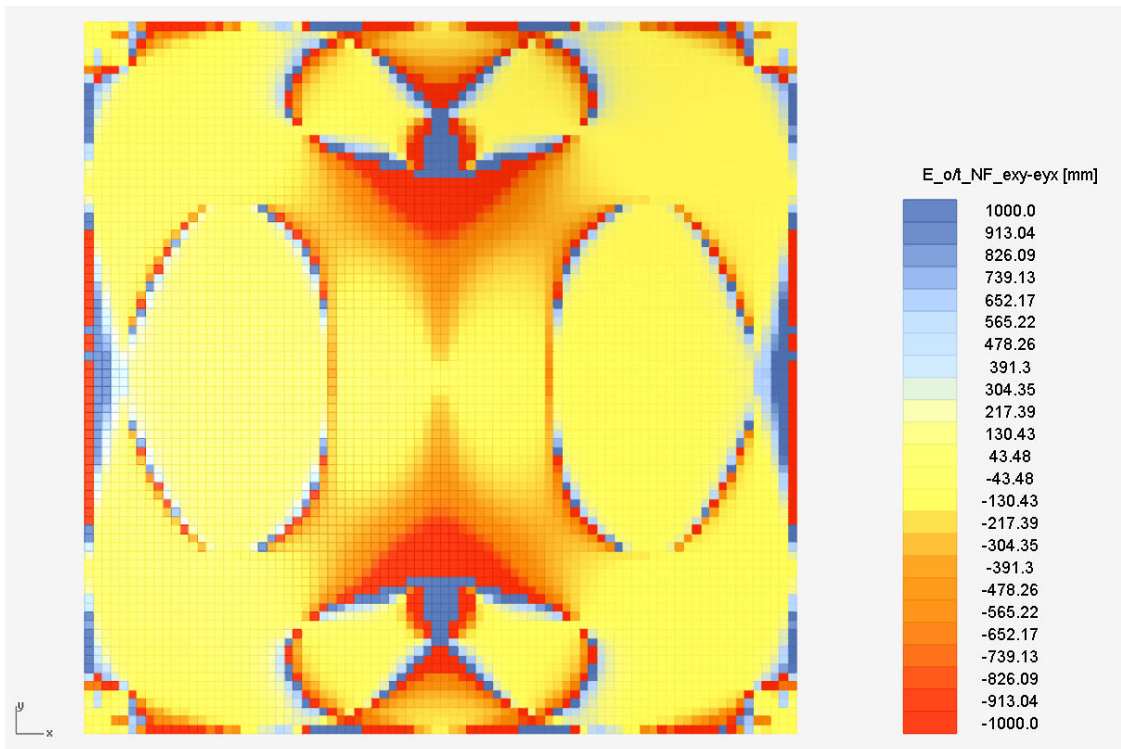
*The out of balance of the in-plane shear eccentricity of the normal force results for the ellipsoid for the loading condition wind.*

### Hyperboloid



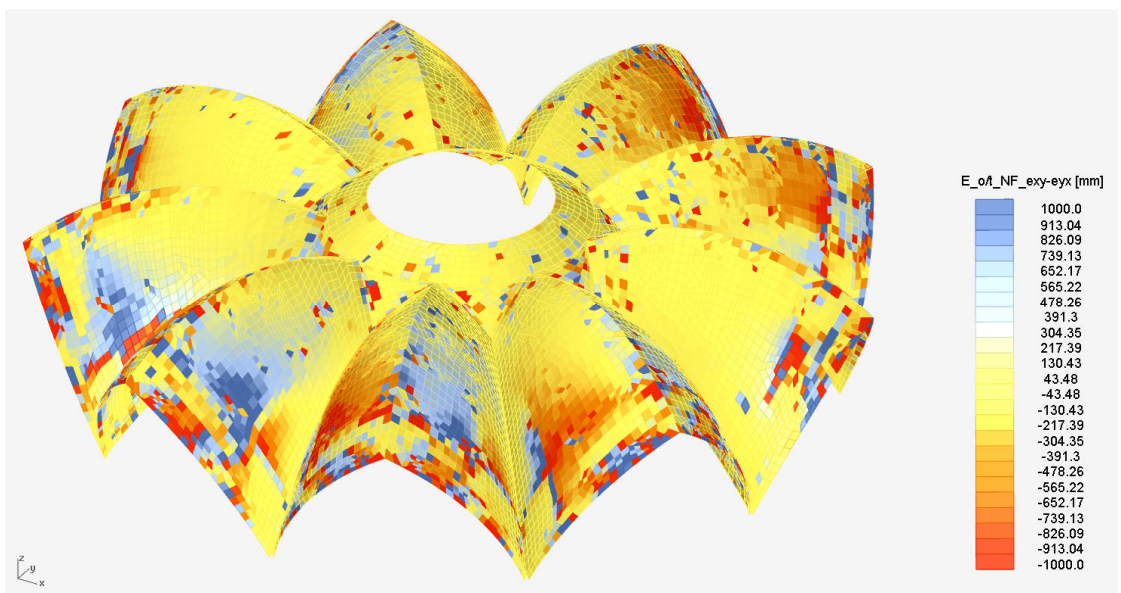
*The out of balance of the in-plane shear eccentricity of the normal force results for the hyperboloid for the loading condition wind.*

## Hypar



*The out of balance of the in-plane shear eccentricity of the normal force results for the hypar for the loading condition wind.*

## Complex geometry



*The out of balance of the in-plane shear eccentricity of the normal force results for the complex geometry for the loading condition wind.*

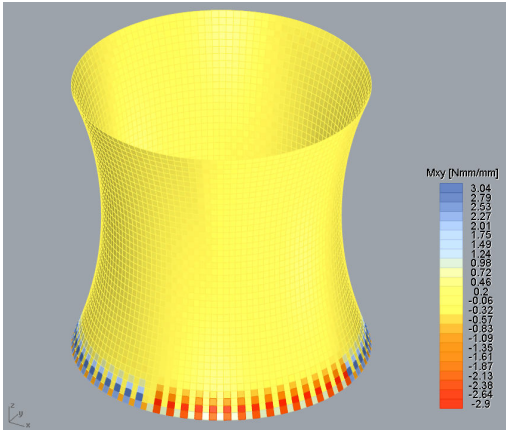
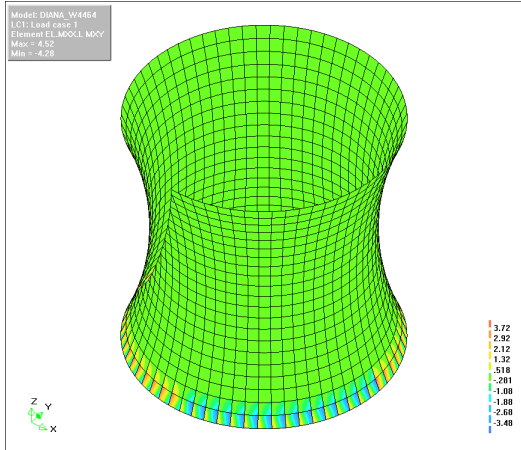




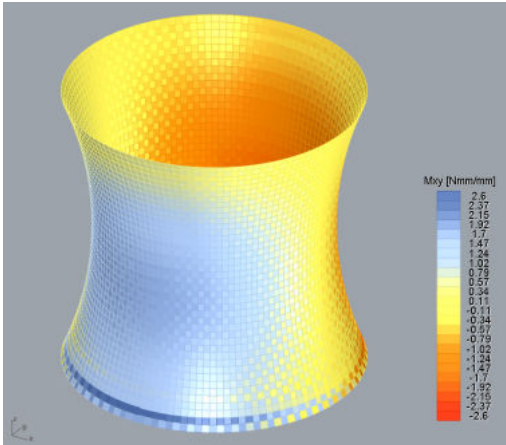
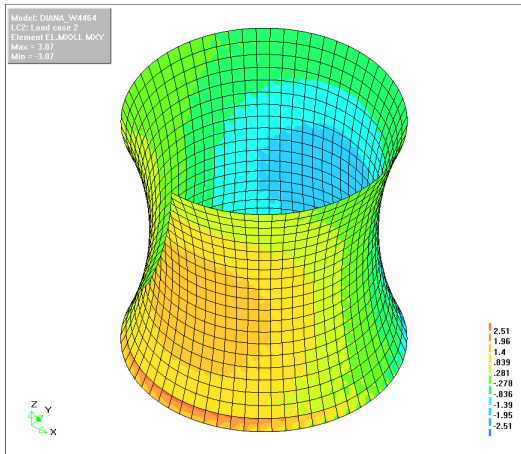


# APPENDIX E – COMPARISON DISTRIBUTED BENDING SHEAR MOMENT RESULTS

The blocky pattern in some of the Grasshopper model results mentioned in paragraph 3.3.5 is not the results of some kind of programming error. This same effect occurs also in the DIANA results, as can be seen in the figures below.

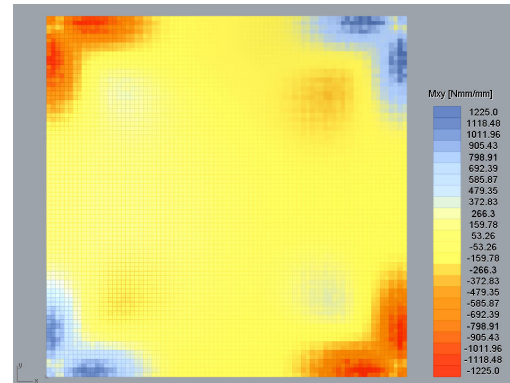
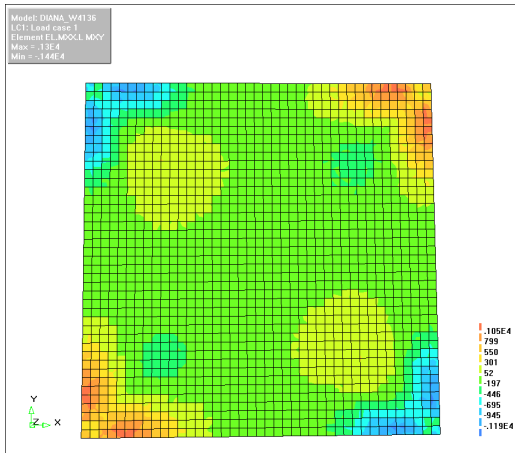


Comparison of the distributed shear bending moment for the load case self weight. On the left the contour plot of iDIANA, on the right the contour plot of the self-made post processor.

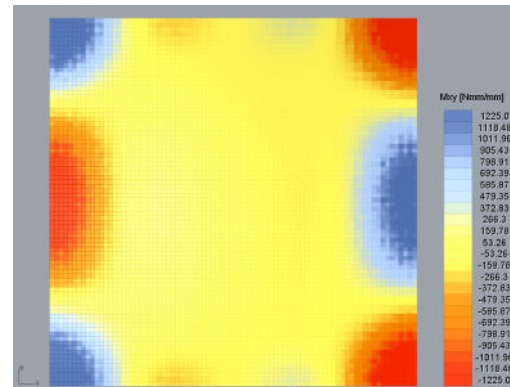
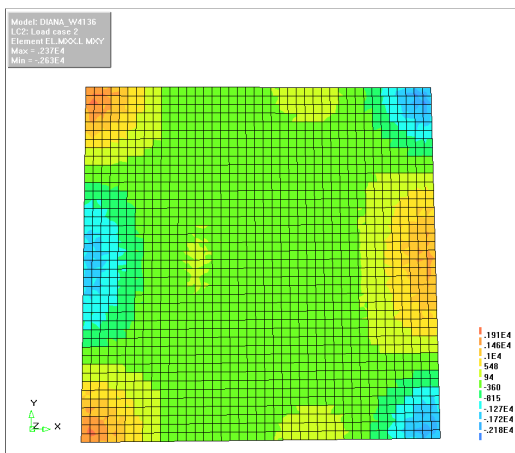


Comparison of the distributed shear bending moment for the load case wind load. On the left the contour plot of iDIANA, on the right the contour plot of the self-made post processor.





Comparison of the distributed shear bending moment for the load case self weight. On the left the contour plot of iDIANA, on the right the contour plot of the self-made post processor.



Comparison of the distributed shear bending moment for the load case wind load. On the left the contour plot of iDIANA, on the right the contour plot of the self-made post processor.



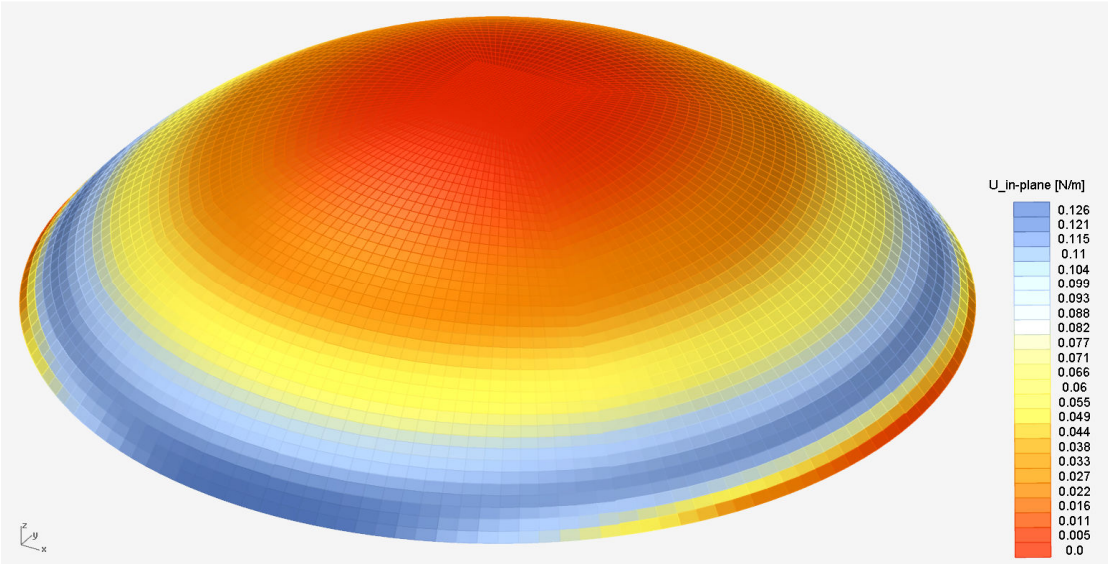


# APPENDIX F – EXAMPLE OF STRAIN ENERGY SUBDIVISION

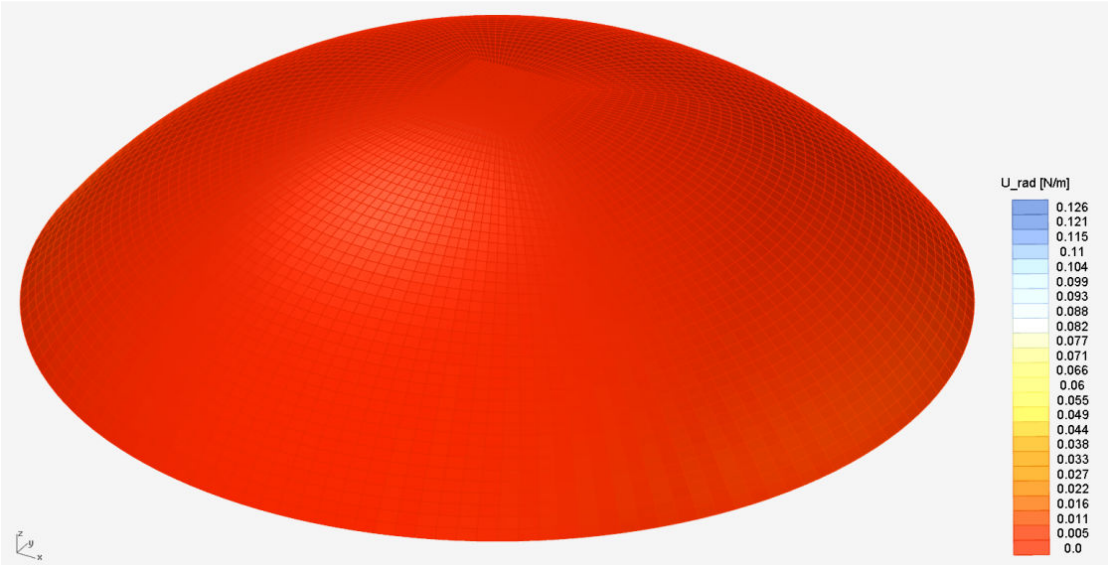
The in-plane strain energy consists of three parts, as can be seen in the following formula:

$$U_{in-plane} = \frac{1}{2} n_{xx} \epsilon_{xx} + \frac{1}{2} n_{xy} \gamma_{xy} + \frac{1}{2} n_{yy} \epsilon_{yy}$$

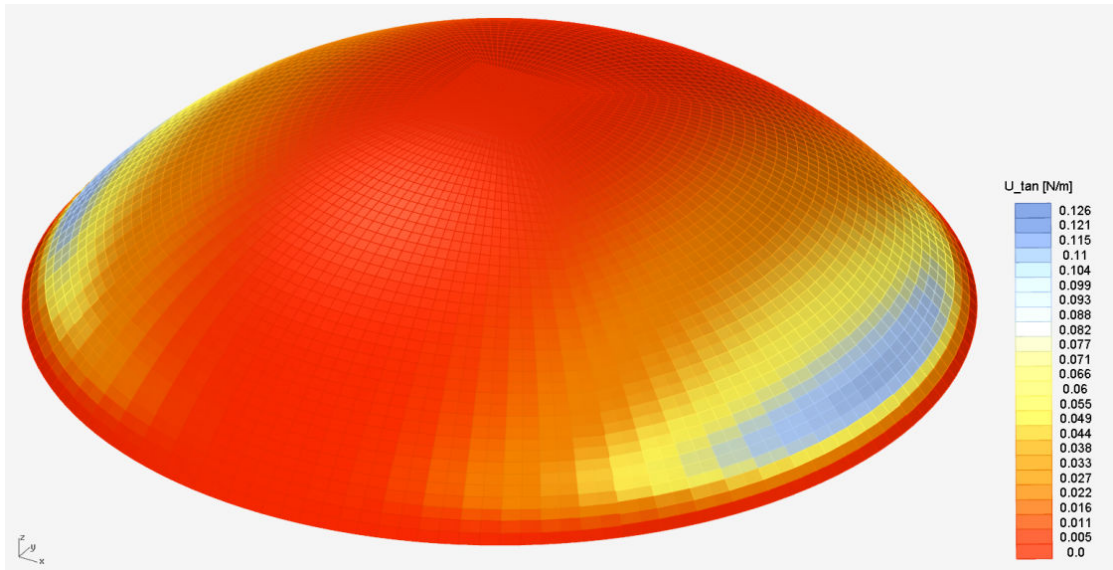
The figures below show the strain energy in the ellipsoid for the wind load. From the figure of the in-plane strain energy below it is not clear what structural mechanisms are operating. When each of the three parts that together comprise the in-plane strain energy is plotted in a separate figure, then it becomes clear that there actually are no meridional forces or deformations, that there occur hoop forces at both sides perpendicular to the wind load and that the majority of the forces is conveyed to the supports by shear forces in the sides parallel to the wind load direction.



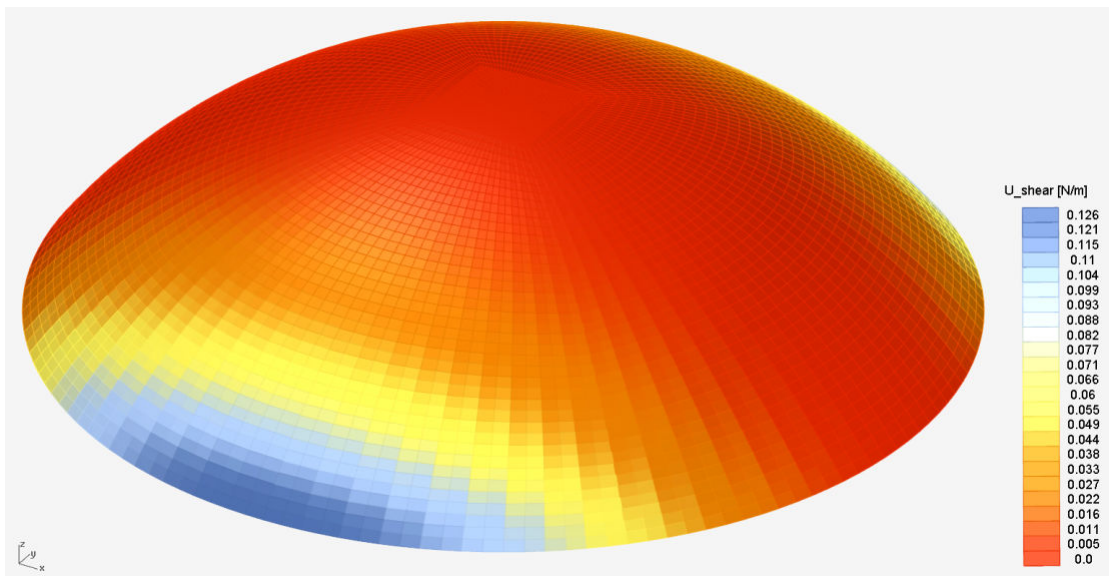
The in-plane strain energy.



Strain energy in meridional direction.



Strain energy in hoop force direction.



Shear strain energy.



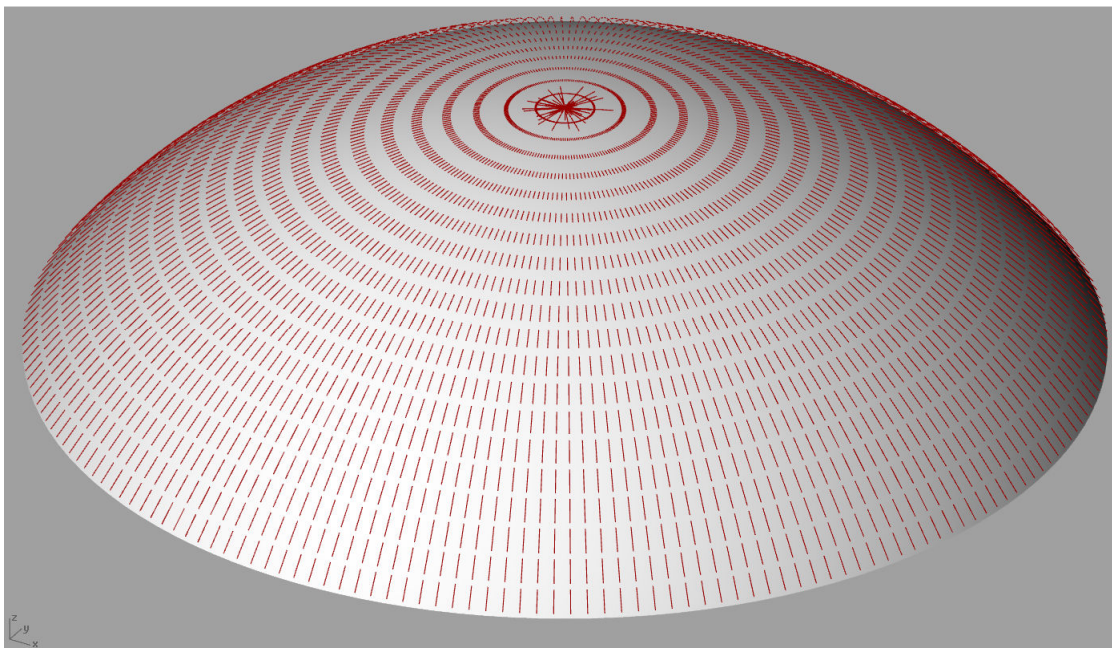




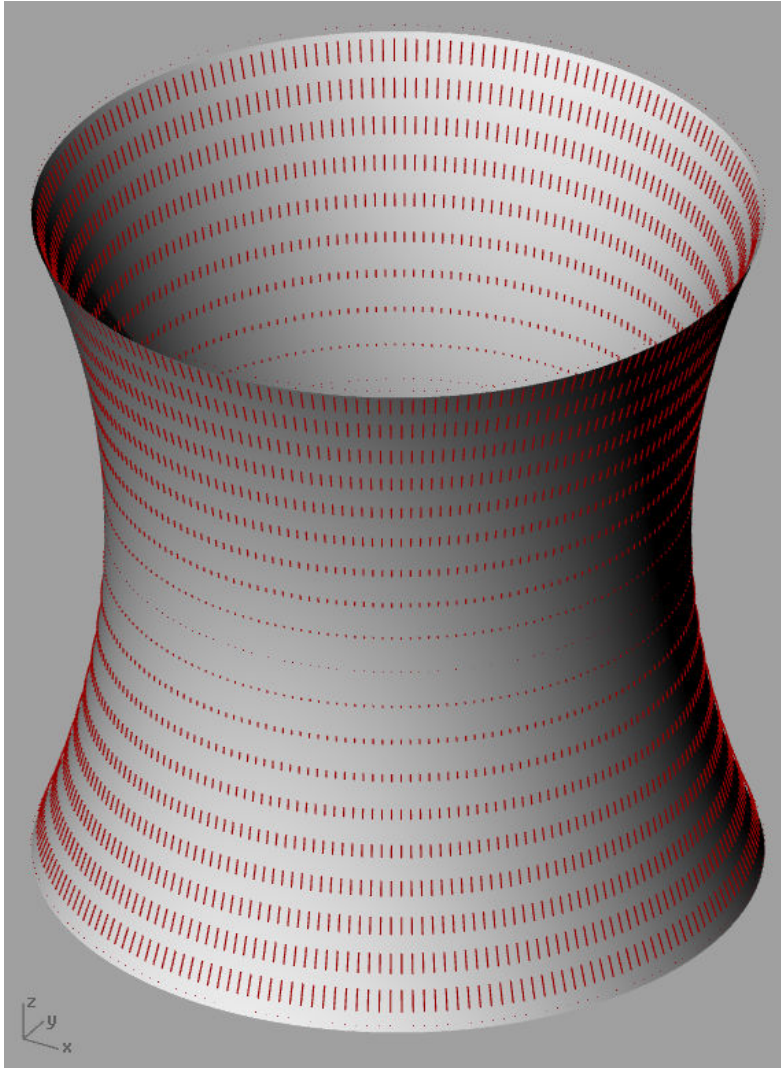
## APPENDIX G – RAIN FLOW ANALOY

With the development of the self-made post processor in Grasshopper it was quite simple to develop a RFA-tool as well with the curvature analysis components available in Grasshopper. The results can be seen in the figures below. Due to limitations of the curvature analysis component in Grasshopper the complex geometry could not be analysed. The red lines indicate the directions of the steepest descend and thus the directions of the rain flow. The length of the lines indicates the amount of descend. For the ellipsoid and the hyper, longer lines indicate a steeper descend, where this is the other way around for the hyperboloid. This is due to the way this tool is programmed in Grasshopper in combination with the geometry of the structures. Since this Rain Flow Analysis tool has only been developed as a proof of concept this difference has been left for what it is.

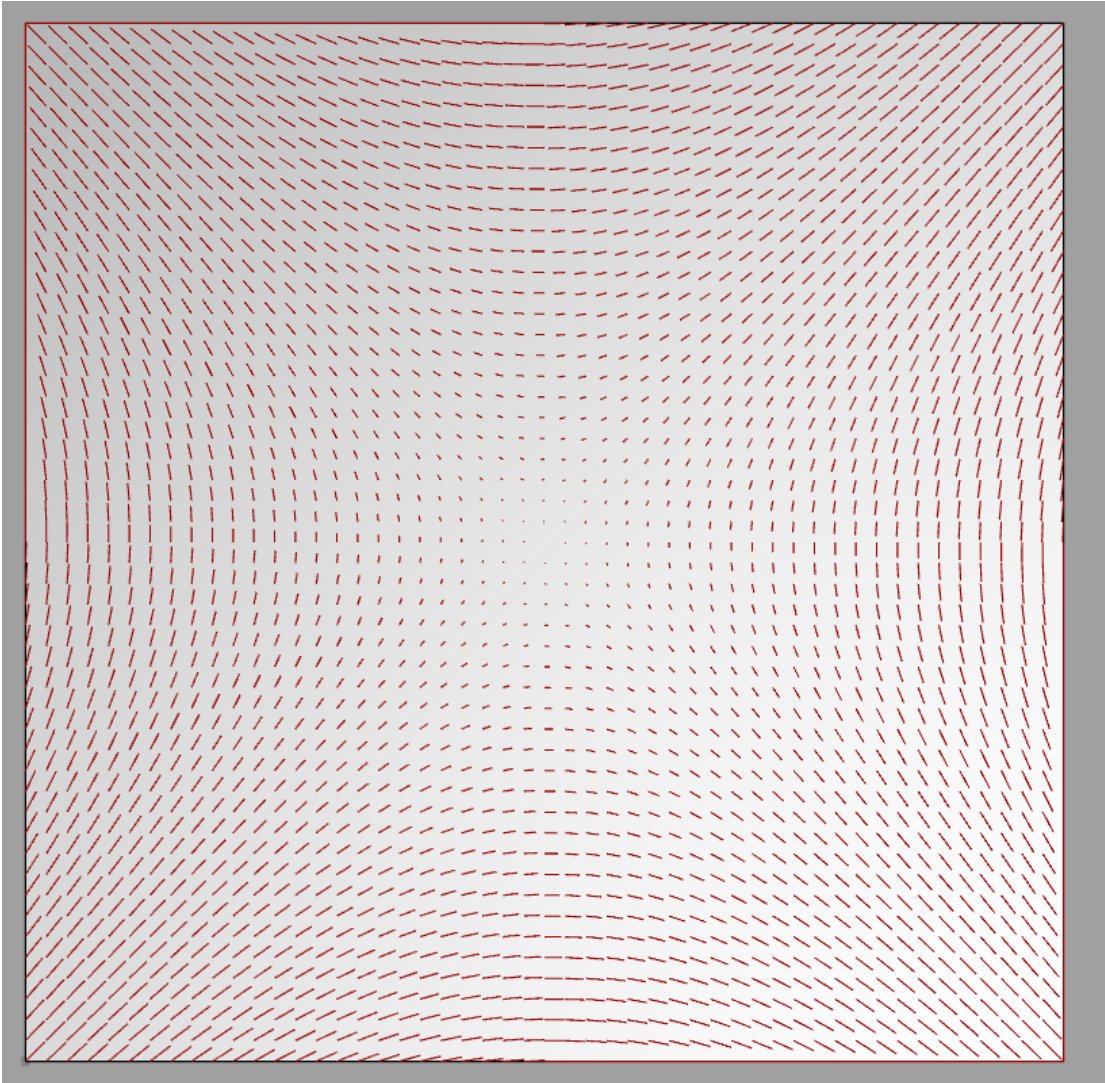
For these simple geometries the added value of the RFA-results seems to be limited as they provide little more mechanical insight than can be determined already by looking at the geometry of the structures. It might be possible that the added value of the rain flow analogy for more complex geometries is higher. For now these geometries need to consist of one or only a few surfaces in order to keep the analysis procedure in the Grasshopper tool perceptual. Maybe that someday an alteration of the curvature analysis components in Grasshopper leads to analysing multiple curved surfaces with only one component.



*Rain Flow Analogy for the ellipsoid.*



*Rain Flow Analysis for the hyperboloid.*



*Rain Flow Analogy for the hyper.*

